D-4

LA-2000
C/

LOS ALAMOS SCIENTIFIC LABORATORY
OF THE UNIVERSITY OF CALIFORNIA o LOS ALAMOS NEW MEXICO

✓ ① Blast (wave)
✓ ② Gasdynamics
✓ ③ Aerodynamics

BLAST WAVE

LEGAL NOTICE

This report was prepared as an account of Government sponsored work. Neither the United States, nor the Commission, nor any person acting on behalf of the Commission:

A. Makes any warranty or representation, express or implied, with respect to the accuracy, completeness, or usefulness of the information contained in this report, or that the use of any information, apparatus, method, or process disclosed in this report may not infringe privately owned rights; or

B. Assumes any liabilities with respect to the use of, or for damages resulting from the use of any information, apparatus, method, or process disclosed in this report.

As used in the above, "person acting on behalf of the Commission" includes any employee or contractor of the Commission to the extent that such employee or contractor prepares, handles or distributes, or provides access to, any information pursuant to his employment or contract with the Commission.

Printed in USA. [redacted] Available from the

Office of Technical Services
U. S. Department of Commerce
Washington 25, D. C.

LA-2000
PHYSICS AND MATHEMATICS
(TID-4500, 13th ed., Suppl.)

LOS ALAMOS SCIENTIFIC LABORATORY
OF THE UNIVERSITY OF CALIFORNIA LOS ALAMOS NEW MEXICO

REPORT WRITTEN: August 1947

REPORT DISTRIBUTED: March 27, 1958

BLAST WAVE*

by

Hans A. Bethe
Klaus Fuchs
Joseph O. Hirschfelder
John L. Magee
Rudolph E. Peierls
John von Neumann

*This report supersedes LA-1020 and part of LA-1021.

Contract W-7405-ENG. 36 with the U. S. Atomic Energy Commission

This report is a compilation of the declassified chapters of reports LA-1020 and LA-1021, which has been published because of the demand for the information. With the exception of Chapter 3, which was revised in 1953, it reports early work in the field of blast phenomena. Inasmuch as the authors had left the Los Alamos laboratory when this report was compiled, they have not had the opportunity to review their contributions and make modifications to reflect later thinking.

CONTENTS

		Page
Chapter 1	INTRODUCTION, by Hans A. Bethe	11
	1.1 Areas of Discussion	11
	1.2 Comparison of Nuclear and Ordinary Explosion	11
	1.3 The Sequence of Events in a Blast Wave Produced by a Nuclear Explosion	13
	1.4 Radiation	16
	1.5 Reflection of Blast Wave, Altitude Effect, etc.	21
	1.6 Damage	24
	1.7 Measurements of Blast	26
Chapter 2	THE POINT SOURCE SOLUTION, by John von Neumann	27
	2.1 Introduction	27
	2.2 Analytical Solution of the Problem	30
	2.3 Evaluation and Interpretation of the Results	46
Chapter 3	THERMAL RADIATION PHENOMENA, by John L. Magee and Joseph O. Hirschfelder	57
	3.1 Radiation Hydrodynamics: the Radiation Flux	59
	3.1.1 The Hydrodynamical Equations Including Radiation	60
	3.1.2 The Radiation Flux	61
	3.1.3 Steady State Smearing Out of a Shock Front by Radiation	66
	3.2 The Strong Blast Without Radiation	68
	3.3 The Opacity of Air	69

CONTENTS (Continued)

	3.3.1 High Temperature Opacity of Air	70
	3.3.2 Intermediate and Low Temperature Opacity of Air	74
	3.3.3 Absorption of Air at Normal Conditions	84
3.4	Radiation Expansion Period and the Formation of the Blast Wave	87
3.5	Radiative Effects in Strong Blast Period	90
	3.5.1 Qualitative Effects of Radiation in Strong Air Blast	90
	3.5.2 Diffusive Motion of the Internal Radiation Front	92
	3.5.3 Radiative Cooling of the Hot Core	95
3.6	The Ball of Fire	98
	3.6.1 Radiation Expansion Period	99
	3.6.2 Radiating Shock Front	103
	3.6.3 Expanded Ball of Fire	103
	3.6.4 Ball of Fire Radius	104
3.7	Scaling Laws	104
	3.7.1 Radiative Expansion Period	104
	3.7.2 Radiating Shock Front	105
	3.7.3 Strong Shock Period and the Total Radiation Yield	106
Chapter 4	APPROXIMATION FOR SMALL $\gamma - 1$, by Hans A. Bethe	107
4.1	General Procedure	107
4.2	General Equations	109
4.3	The Point Source	111
4.4	Comparison of the Point Source Results with the Exact Point Source Solution	116
4.5	The Case of the Isothermal Sphere	121
4.6	Variable Gamma	124
4.7	The Waste Energy	130

CONTENTS (Continued)

Chapter 5 ASYMPTOTIC THEORY FOR SMALL BLAST PRESSURE, by Hans A. Bethe and Klaus Fuchs 135

5.1 Introduction 135

5.2 Acoustic Theory 136

5.3 General Theory 137

5.4 Second Approximation 140

5.5 The Motion of the Shock Front 145

5.6 Results for Very Large Distances 146

5.7 The Energy 150

5.8 The Propagation of the Shock at Intermediate Distances 154

5.9 The Negative Phase. Development of the Back Shock 161

5.10 The Case of Two Pressure Pulses Catching Up with Each Other 166

5.11 The Continuation of the IBM Run 171

Chapter 6 THE IBM SOLUTION OF THE BLAST WAVE PROBLEM, by Klaus Fuchs 177

6.1 Introduction 177

6.2 The Initial Conditions of the IBM Run 179

6.2.1 The Isothermal Sphere 179

6.2.2 Initial Pressure and Density Distribution 180

6.3 The Total Energy 182

6.4 The IBM Run 182

6.5 Results 183

6.6 Comparison with TNT Explosion. Efficiency of Nuclear Explosion 184

6.7 Scaling Laws 202

CONTENTS (Continued)

Chapter 7 THE EQUATION OF STATE OF AIR, by Klaus Fuchs and Rudolph E. Peierls 205

7.1 Equation of State of Air Between 2×10^4 and 2×10^6 Degrees 205

7.1.1 Outline of Method 205
7.1.2 The Partition Function of the Ions 208
7.1.3 The Partition Function of Free Electrons 211
7.1.4 Degree of Ionization 219
7.1.5 The Free Energy, Thermal Energy, Entropy, and Pressure 221
7.1.6 The Hugoniot Curve 234

7.2 The Equation of State of Air Below 25,000°K 237

7.2.1 The Range from 12,000 to 25,000°K 237
7.2.2 The Range from 300 to 12,000°K 239

7.3 The Equation of State of Air at Low Pressures 240

7.3.1 Introduction 240
7.3.2 The Composition of Air 240
7.3.3 The Thermodynamical Quantities 247

7.4 Collected Results 253

7.5 Approximate Form of Adiabatics for IBM Run of Nuclear Explosion 253

7.6 Approximate Form Used for IBM Run of HE Explosion 297

ILLUSTRATIONS

Chapter 1 INTRODUCTION

1.1 Path of Acoustic Waves Starting from the Center "0" 23

Chapter 3 THERMAL RADIATION PHENOMENA

3.1 Rosseland Mean Free Path 72
3.2 Rosseland Mean Free Path 73

ILLUSTRATIONS (Continued)

3.3	Mean Free Path for Absorption of Radiation by O^- and O_2^-	80
3.4	Absorption Coefficient of NO_2 for T $\cong$ 300°K	81
3.5	Mean Free Path of Radiation in NO_2	82
3.6	Mean Free Path of Radiation in NO_2; Radiation the Same Temperature as the NO_2	83
3.7	Mean Free Path of Radiation in NO_2; the Radiation Temperature Above 10,000°K	85
3.8	Absorption of Air; T = 300°K; p = 1 atm	86
3.9	Radius of Internal Radiation Front vs Shock Radius	93
3.10	Over-all Time History of the Blast Wave	96
3.11	Shock Temperature vs Shock Radius	102

Chapter 5 ASYMPTOTIC THEORY FOR SMALL BLAST PRESSURE

5.1	Symmetrical Equal Shock Waves	151
5.2	Initial Pressure Pulse	158
5.3	Three Shocks Where the Reflected Shock Will Sometime Catch Up with the Rear of the First Pulse	166
5.4	Plot of g(s) vs s	172
5.5	Overpressure vs Shock Radius	176

Chapter 6 THE IBM SOLUTION OF THE BLAST WAVE SOLUTION

6.1	Shock Pressure vs Distance for Nuclear Explosion	185
6.2	Pressure vs Time	186
6.3	Pressure vs Time	187
6.4	Pressure vs Time	188
6.5	Pressure vs Distance at a Fixed Time	189
6.6	Pressure vs Distance at a Fixed Time	190
6.7	Pressure vs Distance at a Fixed Time	191
6.8	Pressure vs Distance at a Fixed Time	192
6.9	Pressure vs Distance at a Fixed Time	193
6.10	Pressure vs Distance at a Fixed Time	194
6.11	Pressure vs Distance at a Fixed Time	195
6.12	Pressure vs Distance at a Fixed Time	196

ILLUSTRATIONS (Continued)

6.13 Pressure vs Distance at a Fixed Time 197
6.14 Deviation of the Positive Phase of a Pulse at a Fixed Distance 198
6.15 The Positive Impulse and the Energy in the Blast 199
6.16 Efficiency of Nuclear Bomb as Compared to an Equivalent Charge of TNT 201

Chapter 7 THE EQUATION OF STATE OF AIR

7.1 Degree of Ionization 229
7.2 Hugoniot Curve; Density vs Pressure 236
7.3 Hugoniot Curve; Temperature as a Function of Shock Pressure 238

TABLES

Chapter 2 THE POINT SOURCE SOLUTION

2.1 x/x_{shock} 51
2.2 X/X_{shock} 52
2.3 ρ/ρ_{shock} 53
2.4 u/u_{shock} 53
2.5 p/p_{shock} 54
2.6 $\epsilon_i/\epsilon_{i\ shock} = T/T_{shock}$ 54
2.7 $\epsilon_c/\epsilon_{c\ shock}$ 55
2.8 Some Other Useful Quantities 55

Chapter 3 THERMAL RADIATION PHENOMENA

3.1 Data for Opacity Calculation 75
3.2 Values of Number of Electrons per Cubic Centimeter in Air 79
3.3 Some Properties of the Blast Wave During Radiation Expansion Period 89
3.4 Some Properties of the Blast Wave During Radiation Expansion Period 90

TABLES (Continued)

	3.5 Effect of Shielding	101
Chapter 4	APPROXIMATION FOR SMALL $\gamma - 1$	
	4.1 Variation of Ratio of Internal Pressure to Shock Pressure with Gamma	112
Chapter 7	THE EQUATION OF STATE OF AIR	
	7.1 Ionization Energies	212
	7.2 Energy Levels of Nigrogen and Oxygen Ions	213
	7.3 The Integrals $I(\alpha)$ and $J(\alpha)$	217
	7.4 The Integrals L_ν	218
	7.5 The Degrees of Ionization and Number of Free Electrons	222
	7.6 Pressure, Energy, and Entropy	232
	7.7 The Adiabatics	233
	7.8 The Shock Wave Curve	235
	7.9 Partition Functions of Molecules and Atoms	244
	7.10 Low-Density Equation-of-State Data	251
	7.11 Pressure vs Temperature for Various Compressions	254
	7.12 Properties of Air Along the Hugoniot Curve	261
	7.13 Thermodynamic Properties of Air at a Pressure of 1 bar	262
	7.14 Properties of Air Along the Adiabatics Terminating in the Hugoniot Curve	263
	7.15 Thermodynamic Properties of Air	273
	7.16 Properties of Air Along the Adiabatics	284
	7.17 Rate of Change of Shock Pressure with Entropy	288
	7.18 Smoothed Equation of State of Air	291
	7.19 Values of V_s, V_o, α, and β as Functions of p_s/p_o	300

Chapter 1

INTRODUCTION

by Hans A. Bethe

1.1 Areas of Discussion

In this report the general phenomena connected with a blast wave in air will be discussed. The particular features of the blast wave produced by a nuclear explosion will be emphasized, but many of the developments in this volume will apply generally to blast waves produced by any type of explosion.

In this introductory chapter we shall try to give a general idea of the various phenomena occurring in a blast wave in air, of their interrelation and their time sequence. In the following chapters the details of the theory will be given, including curves showing the pressure distribution as a function of time and position.

We have not included any detailed discussion of the effects of an atomic bomb other than the blast effect. Only a short discussion of other effects is given in Chapter 3. For further discussion, especially on flash burn and radioactivity, reports on the experience in Japan should be consulted.

1.2 Comparison of Nuclear and Ordinary Explosion

The main difference between a nuclear explosion and that of an ordinary explosive (denoted here by HE) is that in the first case the energy is developed in a very much smaller space. The temperatures reached are consequently very much higher, namely of the order of fifty million degrees inside the active material, as compared with about five thousand degrees inside the HE. This has several consequences in making the two types of explosion differ.

The most important of these is that a nuclear explosion can be considered more nearly as a point source of energy than an HE explosion. The solution for the blast wave originating from a point source is particularly simple (see Section 1.3 and Chapter 2), so that the blast wave from a nuclear explosion is simpler to treat than that from an HE explosion. In the case of an HE explosion it takes a considerable time until the energy is transferred from the HE to the surrounding air, owing to the great difference in density between these two media. During all this period the pressure in the air shock wave is less than it would be for a point source explosion liberating the same energy. This phenomenon was already pointed out by G. I. Taylor in his first treatment of the shock wave produced by a point source explosion. He found that the experimental pressures at small distances were lower, and decreased more slowly with increasing distance, than his theory indicated.

The effect discussed in the last paragraph is reversed when the overpressure in the blast wave has decreased to the order of an atmosphere or less. This is due to the irreversible dissipation of energy (increase of entropy) at the shock front. This dissipation is greater the higher the shock pressure. As we have seen, in the initial phase, at a given radius and at a given energy release, the shock pressure is lower in the HE explosion than in the nuclear explosion. Therefore, less energy is dissipated in the blast caused by HE and, therefore, more energy is left in the blast by the time the blast pressure has become small. In other words, the energy released by HE is transformed into blast more efficiently than that released by a nuclear explosion. The latter, on the other hand, should be just the efficiency calculated theoretically for a point source explosion.

A further point of difference, again connected with the concentration of the nuclear explosion, is the appearance of large amounts of electromagnetic radiation in a nuclear explosion. Air temperatures of the order of a million degrees can be expected. In the case of an HE explosion, even with a bare charge, the highest temperature reached in the air is about three thousand degrees. At a million degrees, radiation is very powerful and will transport energy through the air very easily, while at three thousand radiation plays only a minor role.

It is, therefore, not surprising that a much larger fraction of the energy is emitted in the form of visible, or ultra-violet, radiation if we have a nuclear explosion. In the Trinity test it was measured that about 15 to 20 per cent of the total energy was emitted in the form of radiation which could penetrate the air to a distance of several miles. This radiation has appreciable heating effects which manifested themselves in the melting of the sand near the Trinity explosion to a distance of about three hundred meters. In Japan the radiation caused intense heat over a large area and caused many

deaths and injuries due to flash burn up to distances of nearly one kilometer. Also, up to considerable distances the effect of radiation was observed in the charring of wood and other combustible material.

The difference in blast pressure as a function of distance between nuclear and HE explosions makes it difficult to use measurements made with HE bombs for the purpose of deducing the effectiveness of an atomic bomb from its energy release, or of deducing the energy release from measurements of the pressure. For this reason a special calculation was made of the pressure obtainable from a point source explosion as a function of the distance (Chapters 5 and 6).

To summarize, a nuclear explosion differs from an HE explosion of the same energy release in the following points:

(1) The pressure at small distances is higher.

(2) The pressure at large distances is smaller.

(3) The radiation emitted is greater and, therefore, the heating effects are greater.

Other differences, of course, are due to the much greater yield of a nuclear explosion as compared to common HE explosions. This difference in size actually makes a qualitative difference in the effects; for instance, the duration of the blast produced by an atomic bomb is longer than the characteristic vibration periods of most structures which can be destroyed. Therefore, the criterion for estimating the damage to structures by nuclear bombs is the peak pressure in the blast wave, rather than the impulse, which is the commonly used criterion for ordinary bombs. As a consequence of this, the area of damage by nuclear bombs increases only as the two-thirds power of the energy release, since the distance at which a given pressure is obtained goes as the one-third power of the energy release. In the region of ordinary bombs the damage area is proportional to the four-thirds power of the energy release because the distance at which a certain impulse is found goes as the two-thirds power of the energy.

1.3 The Sequence of Events in a Blast Wave Produced by a Nuclear Explosion

The nuclear explosion will produce a shock wave going out through the material comprising the bomb. After a certain time this shock wave will reach the outer surface of the bomb and will then be transmitted to the surrounding air. This will start a shock wave in air which will spread spherically into the undisturbed air.

The transmission of impulse from the solid material of the bomb to the air is closely analagous to the corresponding phenomenon with ordinary

HE. However, the amount of solid material is much smaller in comparison with the energy release than it is in an ordinary HE bomb. Therefore, the transmission of energy to the air will be completed at relatively high pressures and from then on the blast wave will have in effect the same shape as for a point source explosion.

Calculations have been made showing the influence of the heavy material in the bomb upon the structure of the shock wave in the initial stages. It has been shown that the shock pressure is first somewhat lower, and later somewhat higher, than it would be for a point source. This effect makes it rather difficult to obtain the energy release from measurements of the shock pressure at very early stages. These calculations show also how the solution for the shock wave approaches the point source solution when the mass of air in the shock wave exceeds the mass of the bomb. This proves the essential stability of the point source solution of Taylor and von Neumann.

Our considerations so far have not taken into account the existence of radiation. However, we have mentioned earlier that the air may be heated to as much as a million degrees or more by an atomic bomb. At such high temperatures the effect of radiation is very great; in particular, radiation can transport energy from one piece of material to another very effectively. It is not yet clear to what extent this transport of radiation will actually determine the transport of energy in the air surrounding a nuclear bomb. In Section 1.4 and in Chapter 3, we shall describe the phenomena which will occur if the radiation is effective.

Fortunately, it can be shown that, whether or not the propagation of energy by radiation is important, after a certain time the properties of the air shock wave become very similar to the point source solution. This point source solution will, therefore, determine the further development of the shock wave as its radius increases and its pressure decreases. Methods were evolved to study the further development of the point source solution at lower pressures than are covered by the Taylor-von Neumann theory. The first correction which has to be applied to that theory is due to the fact that the equation of state air cannot be described by adiabatics of the form

$$p = A\rho^{\gamma} \tag{1.1}$$

with constant γ and A another constant. The assumption of constant γ is essential in the point source solution of Taylor and von Neumann. It is possible, however, to take into account variations of γ as long as γ itself does not deviate much from unity. In this case most of the material behind the shock wave is concentrated immediately behind the wave front and the

problem of finding the pressure distribution can, therefore, be reduced essentially to a one-dimensional problem which can be solved. This method is developed in Chapter 4.

New phenomena will occur when the pressure behind the shock front ceases to be very large compared to atmospheric pressure. In this case the limiting form of the Hugoniot equations is no longer valid. The density behind the shock is no longer constant and similarity no longer holds for the solution. In principle, it is possible to continue calculations into this region, using the method developed in Chapter 4. However, this is quite cumbersome and it is not clear at what shock pressure the approximation will break down. It was, therefore, decided to make a complete numerical calculation for these lower pressures.

A similar numerical calculation had previously been done by Penney. The present calculation was facilitated by several circumstances:

(1) It was possible to use IBM computers for the integration, which reduced tedious computing work to a minimum and increased the speed of operations very greatly.

(2) The calculation was done with an isothermal sphere at the center such as is expected due to the effect of radiation (see Section 1.4); therefore, from the beginning, temperature, pressure, and material velocity were smooth functions of the distance from the origin, and none of these quantities reached unduly high values near the center. In this way erratic fluctuations in the early values of physical quantities were avoided.

(3) The use of mechanical devices for the integration made it possible to use fine intervals in the coordinate and in the time.

(4) New data on the equation of state for air were available (see Chapter 7).

The numerical calculation of the blast wave was begun at a pressure of 80 atm and continued to a pressure of 1.025 atm in the shock. Details and results are reported in Chapter 6. The results show clearly the formation of a negative phase (pressure below atmospheric) in the shock wave. The shape of the pressure wave is very similar to the observed shape.

As the overpressure in the shock wave decreases to a small fraction of 1 atm, it is possible to use more approximate methods to describe the further development of the shock wave. This theory is a correction of ordinary acoustic theory and is described in Chapter 5. From this theory it is possible to calculate the asymptotic behavior of a shock wave at very large distances. As in all calculations on shock waves it is assumed that the shock front is infinitely sharp, i.e., that the viscosity of the air is very small. When the pressure decreases to very small values, viscosity and turbulence effects will occur which will change the shape and size of the pressure pulse.

We have described the history of the blast wave from high to low pressures without making reference to radiation except at the beginning. Actually radiation will continue to play an important role which will be discussed in the next section.

1.4 Radiation

The theory developed in the last section is based on the assumption that any material element of the air retains the energy it is first given. Its internal energy changes only by doing work on neighboring material elements, but there is no transport of energy from one element to another.

Such transport of energy can actually occur in various ways. One possibility is ordinary heat conduction; however, this is quite small under the circumstances considered. Another possibility is convection by turbulent motion; very little is known about this mechanism, but it is likely that it does not play any major role. The most effective transport of energy is probably by radiation.

At the high temperatures which exist in the air in the neighborhood of a nuclear bomb, let us say a million degrees, a considerable fraction of the energy is contained in radiation rather than in kinetic energy of the particles in the air. The radiation has a very high mobility since it moves with the velocity of light. The transport of energy by radiation will be determined by the opacity of the air under the given conditions. This opacity is very small for radiation of high frequency, especially if the air itself is at high temperature (see Chapter 3).

It must be expected, therefore, that considerable radiative transport of energy will take place in the air shock wave produced by the nuclear explosion. With decreasing pressure and temperature in the shock wave, the influence of energy transport will at first decrease. This is due to two causes:

(1) The fraction of the energy contained in radiation decreases with the temperature, and

(2) The opacity of the air becomes greater as the temperature of radiation and air decreases.

The greatest effects of radiation will, therefore, occur at the very beginning of the process. It is conceivable that there is, in the very beginning, a stage in which the propagation of radiation is faster than the motion of the shock wave. However, whether such a stage occurs in an actual nuclear explosion has not been decided as yet. The uncertainty is due to the fact that it is very difficult to calculate, theoretically, the transmission of energy from the heavy material of the bomb to the air in detail.

Another difficulty is due to the very fact that radiation transport may be important in the air and may lead to an immediate loss of energy by those parts of the air which have been heated by the shock coming from the atomic bomb. Fortunately it makes very little difference to the later stages of the blast wave whether or not there is a radiative stage.

If there is, initially, a radiative stage, the phenomena are as follows: The radiation will spread very quickly and will heat surrounding air. The heated air is practically transparent to radiation of high energy, at least as long as the air temperature is sufficiently high to remove the K-electrons from the air atoms. With normal density the temperature required for removal of half the K-electrons is about a million degrees; therefore, this figure was mentioned above as the critical temperature. The ionization is a very sensitive function of the temperature so that an increase in temperature by 20 per cent will make the ionization nearly complete.

The radiation will therefore continue to spread rapidly into new material, and this process will stop only when the air temperature decreases to 1,000,000 degrees. In other words, the radiative stage will continue until the radiation has spread over an air volume of such size that it can just be heated by the available energy of the explosion to a temperature of 1,000,000 degrees. This volume is clearly proportional to the energy released. For an energy release of 10,000 tons of TNT equivalent[1] and with air initially at atmospheric pressure and 0°C, the radius of this hot sphere will be about 10 meters.

At such a small distance of only 10 meters, the air shock and the radiation will still be affected by the details of the transmission of the shock from the bomb into air. Delay in transmission will reduce the importance of radiation in transporting energy.

Further spread of the radiation would lead to a decrease of the temperature below the critical value of about one million degrees and, therefore, to considerably higher opacity of the air. The further spread of the radiation becomes very much slower and will, in general, be slower than the motion of the shock wave. From now on the shock front will move ahead of the radiation. We shall have a comparatively large sphere which has been swept by the shock wave, and inside of this a smaller sphere which has been affected by the radiation.

The rate of spreading of the radiation decreases quite rapidly with temperature. It is a good approximation to assume that from a certain point on, the radiation does not spread at all. In this case we have a

---

1. A "ton of TNT" by definition releases an amount of energy equal to 4.185×10^{16} ergs (a million kilocalories).

sphere in which radiation has effectively equalized the temperature (isothermal sphere). This sphere contains a fixed amount of air, but its volume continues to increase as the shock wave propagates. It is again a good approximation to assume that the temperature, the density, and the pressure are uniform in this sphere. In Chapter 4 a theory of the blast wave, including such an isothermal sphere, is developed. The isothermal sphere has also been taken into account in the numerical calculations at lower pressure (Chapter 6); actually these calculations are greatly facilitated by the existence of the isothermal sphere.

In reality, of course, the radiation will continue to spread into new material all the time. To follow this process it is necessary to know the opacity of air as a function of temperature and density. Calculations of the opacity are reported in Chapter 3. Our present knowledge of the opacity is still very incomplete because the calculations are extremely complicated. However, we have attempted to obtain at least an approximate theory of the propagation of radiation, which is also reported in Chapter 3. This theory is in qualitative agreement with our previous assumption that the spread of the radiation sphere is slow compared with that of the shock wave after the temperature falls below about one million degrees.

The phenomena so far described determine the distribution of temperature and density inside the shock wave. From the practical point of view, however, the most important radiation problem is the emission of radiation which can penetrate to large distances. In order to penetrate through ordinary cold air, i.e., through the air outside the shock wave, radiation has to be of long wave length. Nearly all radiation up to an energy $h\nu = 7$ ev is transmitted by air without absorption. Between 7 ev and the ionization potential of about 15 ev there are many absorption bands which absorb very effectively. There are some gaps of low absorption so that the effective limit of transmission of air lies between 7 and 15 ev, but closer to the lower limit.

All radiation of higher energy than 15 ev is absorbed by air sufficiently effectively to prevent transmission over distances of more than a few centimeters. Therefore, even though the temperature of the hot air near the atomic explosion is extremely high, corresponding to a spectrum predominantly in the X-ray region, the radiation going out to a distance will still be confined to the visible and the near ultraviolet.

This feature of the absorption by cold air reduces enormously the total amount of radiation which can be emitted by the hot air. If all types of radiation could be transmitted, the energy radiated would be proportional to the fourth power of the temperature, and the energy loss by radiation would soon exhaust the energy supplied to the air by the explosion. In this sense the high opacity of cold air for high frequency radiation is a necessary

condition for the production of an effective blast wave by a nuclear explosion.

Since transmission is possible only for radiation up to a certain limiting energy, of the order of 10 ev, the emission from a hot sphere of air will be proportional only to the first power of the temperature. This is because the radiation energy in each "normal mode" of black body radiation is given by the Planck distribution

$$\frac{h\nu}{e^{h\nu/kT} - 1} \tag{1.2}$$

which, for $h\nu \ll kT$, reduces to kT. The number of effective normal modes into which radiation can be emitted is determined by the effective limiting energy and is independent of temperature. Even so, the fraction of the energy which is radiated to large distances is appreciable, about 15 to 20 per cent according to the measurements made at the Trinity test. This will give rise to considerable heat effects.

The radiated energy is not necessarily lost to the blast wave. Only a few per cent of the total energy is radiated very early. The bulk of the radiation is emitted at a fairly late stage and from some distance behind the shock. The energy loss will set up a rarefaction wave, but it is probable that this rarefaction wave will reach the shock front only when the pressure has already decreased to very low values. Hence the "radiative loss of blast energy" is only a few per cent.

This brings us to the question of where the radiation visible at large distances comes from. This problem is also of importance for optical observations of the explosion. In particular, it is an interesting question whether the shock front itself appears luminous or whether the luminosity originates from a smaller sphere. This depends on the temperature of the shock front. If that temperature is sufficiently high, the opacity of the air behind the shock front for visible light will be large. In this case any light coming from the very hot gases near the center will be absorbed by the gas near the shock front and will be re-emitted in the form of radiation characteristic of the temperature near the shock front. If, on the other hand, the temperature behind the shock becomes relatively low, the gas becomes practically transparent for visible and near ultraviolet radiation, just like cold air. In this case the radiation emitted by the hotter layers nearer the center of the explosion will be transmitted by the region directly behind the shock front without being appreciably absorbed. Therefore, the radiation will then appear to come from a sphere smaller than the shock front.

The criterion for luminosity of the shock front is that the mean free path of radiation be small compared to a length of the order of the radius

of the shock. This criterion is fulfilled for shock temperature above about 5,000 degrees. The main factor which determines the opacity in this temperature region is the number of free electrons and ions. This number increases exponentially with temperature; at the critical temperature of 5,000 degrees the fraction of atoms ionized is about 10^{-6}. Only the free electrons can absorb light of long wave length when they pass through the electric field of the atoms. The neutral atoms themselves are, as we know, incapable of absorbing or emitting any long wave length radiation.

The luminosity of the shock wave is important for the problem of measuring the energy release in a nuclear explosion. It is possible to deduce the energy release from a measurement of the radius of the shock wave as a function of time at early times. One very convenient way of doing this is by optical observation. This observation is easy as long as the shock wave itself is luminous, because then the radius of the shock wave is equal to that of the luminous region. At later times the luminous region is smaller than the shock wave. The measurement is, therefore, easiest until the shock temperature has dropped to 5,000 degrees, which corresponds to a shock pressure of about 200 atm.

In Chapter 3 calculations are reported giving the radius of the luminous region when it becomes smaller than the shock wave. The light seen at large distances comes then from behind the shock front but still from regions much farther from the center than the isothermal sphere. The effective temperature of the radiation, accordingly, is higher than the shock temperature but much lower than that of the isothermal sphere. The correctness of this statement depends on the fact that there is a region of high opacity between the isothermal sphere and the apparent luminous sphere. This region must be interposed between two regions of low opacity, namely the inner isothermal sphere and the region between the luminous sphere and the shock front.

Present indications are that, at a certain stage[2] in the development of the blast wave, the transparent region near the center and that near the shock front will join if the air has its normal composition. This would lead to an emission of a very large amount of radiation, which might easily reduce the energy available to the shock by a factor of 2 or more.

Fortunately, this energy loss seems to be prevented by the formation of a layer of NO_2 behind the shock front which is opaque for radiation. This layer is formed in two stages: at certain temperatures around 5,000 degrees air in equilibrium will contain about 1 per cent NO. This substance, upon

---

2. This occurs when the shock radius is about 100 meters for an explosion of 10,000 tons.

cooling, reacts quickly with oxygen to form NO_2. The details of this process are discussed in Chapter 3. The NO_2 is opaque to visible and ultraviolet radiation up to temperatures of about 5,000 degrees, at which NO_2 dissociates. The analysis of the opacity indicates that radiation will be emitted by the hot sphere near the center and will go almost unimpeded through the air layer of intermediate temperature, let us say between 5,000 degrees and 20,000 degrees, which is highly transparent. It will then be absorbed further out in the NO_2 layer and will serve to heat this layer and finally to dissociate the NO_2. The radiation which goes to large distances is emitted from the outside of the NO_2 layer.

Owing to the considerable difficulties in calculating the opacity of air, these calculations can be taken only as indications and should not be considered as firm predictions; however, they appear to be confirmed qualitatively by the results of the Trinity test and we conclude, therefore, that the radiative loss of blast energy is only a few per cent.

When the pressure in the blast wave falls to very low values, let us say, to overpressures below 1 atm, the blast wave becomes entirely separated from the hot gases which remain at the center. These hot gases will still be able to emit radiation and will do so to a considerable extent. They will also have a tendency to rise in the atmosphere. As they rise they become mixed with the surrounding cold air and are thereby cooled. There is, therefore, competition between the cooling of the gases by radiation and by mixing. After a few seconds the latter mechanism will predominate and the temperature of the hot sphere will fall sufficiently to make the emission of light unimportant from then on.

For the spectrum of the radiation visible at large distances, an important factor seems to be the absorption of light by molecules formed in the air by the shock wave itself. The most important absorbers of this type seem to be NO_2 and O_3. These gases seem to be responsible for the absorption of all light beyond the near ultraviolet.

1.5 Reflection of Blast Wave, Altitude Effect, Etc.

Until now we have considered the properties of a spherical blast wave which would exist if the explosion took place in an infinite homogeneous atmosphere. Important modifications are necessary to take into account the reflection from the ground and the variation of the air density with altitude.

Much experimental and theoretical work has been done on the reflection of blast waves from solid surfaces. The theoretical work was initiated and largely carried out by von Neumann; the experimental work is due mostly to the laboratories at Woods Hole and Princeton. All this work

shows that the pressure is considerably increased by reflection from the ground. If the blast wave falls on the ground vertically, or at a moderate angle with the vertical, then regular reflection is obtained which can be treated theoretically in an elementary way. In the case of more glancing incidence, a Mach wave is formed which appears to have a very complicated structure and which involves particularly high reflected pressures, if the incident shock is weak.

Most of the experimental work was done at overpressures of a fraction of an atmosphere. Very little is known, both theoretically and experimentally, about the case of high overpressures. This case is naturally quite important for a nuclear explosion and the lack of information makes it difficult to interpret the moving pictures of the test explosion at Trinity after the shock wave has touched the ground.

The effect of reflection is of considerable practical importance since it can be predicted that a given bomb will be more effective in causing damage when detonated appreciably above ground level than when detonated on the ground. For this reason, the actual atomic bombs were detonated at considerable height. The height of detonation was determined from the expected energy release and from the available experimental information on the reflected pressures as a function of the angle of incidence of the shock wave.

Another important consideration in determining the most advantageous height of detonation is the height of the stem of the Mach wave. Only behind this stem can the high reflection pressure be expected. It is therefore desirable that the Mach stem be high enough compared with the height of the objects to be destroyed.

Another problem which becomes increasingly important with increasing energy release is the density variation of the atmosphere with altitude. This density variation has two different effects. The first is that the pressure in the shock at a given distance from a given explosion will depend on the direction, i.e., it will be different vertically above the explosion and in a horizontal direction, for the same distance. This effect can be treated rather simply by using the obvious assumption that the energy emitted into a unit solid angle is the same for all directions, and that the duration of the pressure pulse will also be independent of direction. However, this simple treatment omits consideration of the fact that the dissipation of energy at the shock front will also depend on the barometric pressure of the air into which the shock propagates. This dissipation will, therefore, be different in a vertical and a horizontal direction, and the theory has to be modified accordingly.

The second effect of the stratification of the atmosphere is refraction. This effect has not yet received theoretical treatment. The temperature

generally decreases with increasing height; therefore, the velocity of sound decreases. Accordingly the atmosphere acts like a medium whose refractive index increases with altitude. This gives the possibility of total reflection of any wave which goes downward at a sufficiently small angle with the horizontal. Such a wave meets layers of air of decreasing refractive index and therefore will be bent upward and may never reach the ground. Figure 1.1 illustrates the path of acoustic waves starting from the center 0 in various directions. It is seen that there is a maximum horizontal distance on the ground at which a signal from the point 0 can still be received. Any point beyond the point A on the ground will not receive any acoustic signal; a zone of silence exists starting at the point A.

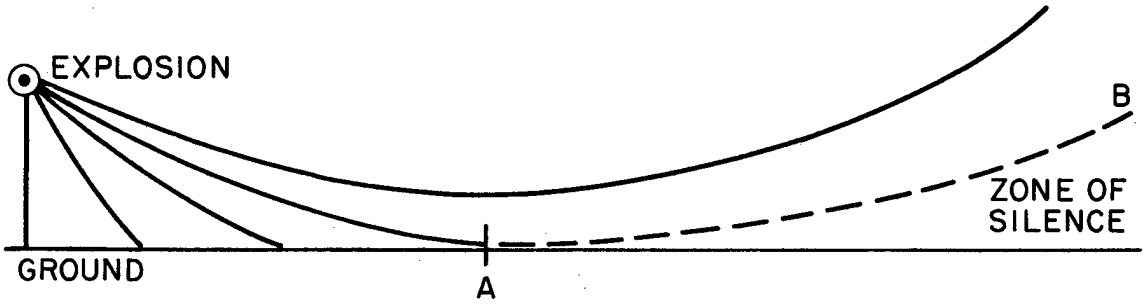

Fig. 1.1 Path of acoustic waves starting from the center "0"

In the case of shock waves the situation is slightly different. In this case the velocity of propagation depends, not only on the temperature of the air into which the shock propagates, but also on the shock pressure. The shock velocity increases with increasing shock pressure. Now, referring to Fig. 1.1, the shock wave exists and therefore a high pressure prevails above the line AB, but not below that line. This means that the propagation velocity above the line AB is higher than below that line, which reverses the dependence of the refractive index on altitude. Consequently, a shock wave will actually not be able to leave the ground; there will always be a finite pressure on the ground, although this pressure may be somewhat smaller than the pressure at slightly greater altitude. This pressure difference will partly, or completely, compensate the difference in sound velocity between different layers of air.

No calculations have been made to determine the actual pressure profile in a shock wave moving along the ground. Moreover, it is not known what the minimum overpressure is which will keep the shock wave on the ground. It is fairly certain that any shock wave which has sufficient pressure

to cause damage will show the phenomenon outlined, i.e., will stay on the ground in spite of the refractive properties of the air.

Further effects have to do with the humidity of air. If the air has high humidity but no condensed water droplets, it is possible that condensation occurs after the shock wave, owing to the adiabatic expansion of the air behind the shock wave. This effect is analagous to the basic principle of the Wilson Cloud Chamber. It gives a very spectacular look to a shock wave if it occurs.

If there are condensed water droplets in the air, i.e., in a fog or heavy rain, the opposite phenomenon may take place. The water droplets may be evaporated by the high temperature in the shock wave. This evaporation is facilitated by a tearing up of the water droplets due to the strong air motion in the shock. This effect may reduce the energy available in the shock wave.

1.6 Damage

The aim of the theory of the blast wave is, of course, to predict the extent of damage which can be caused by a nuclear bomb. The damage radius will depend on the type of structure against which the bomb is used and the kind of damage which is considered significant.

It is well known that the criterion for damage depends on the duration of the pressure wave. For waves whose duration is short compared with the natural period of the structures to be affected, the impulse in the blast wave matters, i.e., the integral of the pressure over the time. On the other hand, for pressure waves of long duration, the duration becomes immaterial and only the initial peak pressure matters. Evidence from ordinary HE bombs points to the conclusion that, in that case, the impulse criterion is valid as would be expected from the short duration of the shock wave produced by such bombs. For the largest bombs used in World War II, from 2 to 5 tons, there is some evidence that the impulse criterion begins to break down. There is no doubt that for nuclear explosions the simple pressure criterion is valid.

There is some question as to what pressures are necessary to destroy a given structure. According to the last paragraph, these pressures cannot be deduced from observations with ordinary HE bombs because those bombs act according to the impulse criterion. In most cases the static strength of the buildings is the best indication of the required peak pressure. It is possible, of course, that a peak pressure smaller than the static strength may suffice to destroy a structure because dynamic loading can be approximately twice as effective as static loading.

The limiting pressure for damage from a nuclear bomb has been estimated to lie between 3 and 8 psi, the lower figures holding for Japanese houses and the higher ones for continental European and United States city apartment houses. Industrial buildings, and especially concrete structures, may have still greater strength.

It was mentioned in Section 1.2 that the damage radius is proportional to the cube root of the energy release if the pressure determines the damage. The damage area is, therefore, proportional to the two-thirds power of the energy release.

Although blast damage is the most important, there are also other causes of damage which should not be neglected. These are discussed in Chapter 3. The most important of these is due to the heat generated by the nuclear explosion, which may act against buildings and especially against personnel. The intensity of radiation is

$$I = E/L^2 \tag{1.3}$$

where L is a given distance and E is the energy release. The distance at which a given radiation intensity is found is proportional to the square root of the energy release, as compared with the cube root for the distance at which a given blast pressure is obtained. Therefore, for very large energy release, damage by the heat of radiation may become more important than the blast.

Further types of damage affecting only personnel are those due to neutrons, gamma rays, and fission product fall-out. The neutron intensity decreases very rapidly with distance, owing to the diffusion and absorption of the neutrons in air. This type of damage is effectively limited to distances up to 600 or 1,000 meters and is very little dependent on the energy release. Damage by gamma rays behaves similarly, but its range may be slightly greater.

The deposition of radioactivity depends on the height at which the nuclear bomb is released. If it is released on the ground a large fraction of the fission products is likely to fall out in the immediate neighborhood or at relatively small distances from the point of explosion. If the release is made at an appreciable altitude, as is usually preferable for obtaining maximum blast damage, most of the radioactivity is taken high up in the air with the rising hot gases from the explosion. The ball of fire is discussed in Section 3.6. After they have risen to great height, the fission products are likely to be distributed over a very large area by the wind. When they are subsequently deposited, the activity at any particular place is much diluted and also reduced by radioactive decay, and is likely to be harmless.

1.7 Measurements of Blast

Extensive measurements were made of the blast pressures at the first test of the atomic bomb at Trinity. Many different methods were used for the measurement of blast, including standard types, such as piezo-electric crystals, and newly developed methods, such as the condenser gauge. The measurements are compared with the theoretical relation between distance and pressure. They are used for an evaluation of the energy release in the explosion.

For the Trinity test the various methods of measurement gave concordant results. Probably the most reliable of all the blast measurements was that of the excess velocity of the shock wave over the sound velocity.

Another method of determining the energy release is from the shock pressure in the early stages of the blast wave. In an ideal case, the energy could be evaluated from the simultaneous knowledge of shock pressure and radius by using the point source theory (Chapter 2). The shock pressure can be deduced from the shock velocity, i.e., from a knowledge of the shock radius as a function of time. In the case of the Trinity test, evaluation was made difficult by the fact that the explosion took place only 30 meters from the ground. For shock radii as small as this, the existence of heavy material near the center of the shock wave causes perturbations which can be evaluated only approximately. The evaluation gives a result in sufficient agreement with other evidence on the energy release.

Several other methods have been used for measuring the blast pressures. One of these is to measure the pressures in the immediate vicinity of the explosion by the use of such instruments as crusher gauges or simply strong bars which may be bent by the pressure. Over Japan, on the other hand, the only obvious way of measurement was by airborne instruments at a considerable distance from the explosion; condenser gauges were used for this purpose.

It must be evident that, in spite of intensive work on the theory and the measurement of blast, this problem is far from solved, especially if it comes to questions like the reflection from an irregular surface, the shielding of buildings by each other or by intervening hills, or the dissipation of energy by obstacles. Our information is still very meager. It is only possible to give approximate values for damage areas under average conditions.

Chapter 2

THE POINT SOURCE SOLUTION

by John von Neumann

2.1 Introduction

The conventional picture of a blast wave is this: In a homogeneous atmosphere a certain sphere around the origin is suddenly replaced by homogeneous gas of much higher pressure. The high pressure area will immediately begin to expand against the surrounding low pressure atmosphere and send a pressure wave into it. As the high pressure area expands, its density decreases and with it the pressure; hence the effects it causes in the surrounding atmosphere weaken. As the pressure wave expands spherically through the atmosphere it is diluted over spherical shells of ever-increasing radii, and hence its intensity (the density of energy, and with it the overpressure) decreases continuously also. This pressure wave is known (both theoretically and experimentally) to consist at all times of a discontinuous shock wave at the head, and to weaken gradually as one goes backward from that head.

This description of the blast wave caused by an explosion is somewhat schematic, since the high pressure area caused by an explosion is not produced instantaneously, nor is its interior homogeneous, nor is it in general exactly spherical. Nevertheless, it seems to represent a reasonable approximation of reality.

Mathematically, however, this approximate description offers very great difficulties. To determine the details of the history of the blast, that is, of its decay, the following things must be computed: (I) The trajectory of the shock wave, that is, of the head of the blast wave, and (II) the continuous flow of air behind the shock (ahead of the shock the air is unperturbed and at rest). This requires the solution of a partial differential equation bounded by the unknown trajectory (I). Along this trajectory the theory of shocks

imposes more boundary conditions than are appropriate for a differential equation of the type (II), and this overdetermination produces a linkage between (I) and (II) which should permit one to determine the trajectory of (I) and to solve (II). To this extent the problem is a so-called "free boundary" partial differential equation problem. However, the situation is further complicated by the fact that at each point (II) the local entropy is determined by the entropy change the corresponding gas underwent when it crossed the shock (I), that is, by the shock strength at a certain point of (I). The latter depends on the shape of the trajectory (I), and the entropy in question influences the coefficients of the differential equation (II). Hence the differential equation (II) itself depends on the shape of the unknown trajectory (I). This dependence cannot be neglected as long as the entropy change caused by the shock is important, that is, as long as the shock is strong (in air a shock can be considered "strong" if the shock pressure exceeds 3 atm). Mathematically such problems are altogether inaccessible to our present analytical techniques. For this reason the general problem of the decay of blast has been treated only by approximate analytical methods, or numerically, or by combinations of these.

For very violent explosions a further simplification suggests itself, which changes the mathematical situation very radically. For such an explosion it may be justified to treat the original, central, high pressure area as a point. Clearly, the blast coming from a point, or rather from a negligible volume, can have appreciable effects in the outside atmosphere only if the original pressure is very high. One will expect that, as the original high pressure sphere shrinks to a point, the original pressure will have to rise to infinity. It is easy to see, indeed, how these two are connected. One will want the energy of the original high pressure area to have a fixed value E_0, and as the original volume containing E_0 shrinks to zero, the pressure in it will have to rise to infinity. It is clear that of all known phenomena nuclear explosions come nearest to realizing these conditions.

We will therefore investigate the laws of the decay of blast wave[1] due to a point explosion of energy E_0.

---

1. The main facts in the discussion which follows were presented by G. I. Taylor, British Report RC-210, June 27, 1941; and John von Neumann, NDRC, Div. B, Report AM-9, June 30, 1941. Important simplifications (in particular, the use of the variable θ of Eq. 2.44) are due to G. Y. Kynch, British Report BM-82, MS-69, Sept. 18, 1943. The results were generalized by J. H. Van Vleck, NDRC, Div. B, Report AM-11, Sept. 15, 1942. Compare also the later work of G. I. Taylor, Proc. Roy. Soc. (London), A201, 159 (1950).

The essential simplification permitted by this model is the so-called "similarity property" of the solution. This property can be explained in the following manner:

Denote pressure, density, and temperature in the atmosphere by p, ρ, T. The significant data of the situation are these: The original (ball of fire) values of p, ρ, T in undisturbed air, p_0, ρ_0, T_0; the equation of state of the atmosphere, $p = c\rho T$; the caloric equation of state, $E_i = [c/(\gamma - 1)]T$; and the original (explosive) release of energy, E_0. The mass and the characteristics of the point explosive are to be neglected, in the same sense in which a genuine point source is being assumed. Also, since the pressures which we propose to consider are to be very high, that is, very high compared to p_0, we will usually neglect p_0. (However, ρ_0 is not neglected!)

Put, accordingly, $p_0 = 0$ for the time being. Furthermore, let $t = 0$ be the time of the original energy release (explosion). Since the constant c is needed to connect the dimension of T to the "cgs" system, and since the constant γ is dimensionless, the only dimensioned quantities which appear among the data of the problem are $E_0 \sim ml^2t^{-2}$ and $\rho_0 \sim ml^{-3}$. Hence, the only combinations of the units of mass, length, and time (m, l, t) which can be significant in this problem are ml^{-3} and l^2t^{-2}.

Now let $t = ct'$, a lines change of time-scale. Then if our problem as stated possesses a well-defined and unique solution, this solution must be unaffected by the above change in time-scale. This means

$$ml^2t^{-2} = m'l'^2t'^{-2} = ml^2c^{-2}t'^{-2}$$

$$ml^{-3} = m'l'^{-3}$$

From this it follows that

$$1 = l'c^{2/5}; \quad m = m'c^{6/5}$$

This will indeed be the case providing that

$$\text{lengths} \propto t^{2/5}$$

$$\text{mass} \propto t^{6/5}$$

To put it more precisely, denote the distances from the site of the original energy release (explosion by the letters x, X, Ξ. Let the trajectory of the shock wave (blast head) be

$$\Xi = \Xi(t) \tag{2.1}$$

If a gas element had originally (at t = 0) the (unperturbed) position x, then let its position at the time t be

$$X = X(x, t) \tag{2.2}$$

(x is the Lagrangian, X the Eulerian coordinate.) Now by the above Eq. 2.1 must have the form

$$\Xi = at^{2/5} \tag{2.1'}$$

and Eq. 2.2 must have the form

$$\frac{X}{t^{2/5}} = f\left(\frac{x}{t^{2/5}}\right) \tag{2.2'}$$

It is evident that these relations will greatly simplify the entire problem. Only a one-variable function, f(z), is unknown; the partial differential equations must become ordinary ones and the unknown trajectory of the shock is replaced by one unknown parameter a. As will appear below, the situation is even more favorable. Everything can be determined by means of explicit quadratures.

2.2 Analytical Solution of the Problem

We must now set up the equations controlling the two phenomena referred to in Section 2.1: (I) the trajectory of the shock wave; (II) the continuous airflow behind the shock. These are to be formulated with the help of Eqs. 2.1' and 2.2' of Section 2.1. We rewrite 2.1' unchanged: $\Xi = at^{2/5}$; but in 2.2' we replace $t^{2/5}$ by $at^{2/5}$

$$X = at^{2/5}\, F\left(\frac{x}{at^{2/5}}\right) \tag{2.2''}$$

and also introduce

$$z = \frac{X}{\Xi} = \frac{x}{at^{2/5}} \tag{2.3}$$

Ahead of the shock lies the unperturbed atmosphere in the state $p_0 = 0$ (cf. Section 2.1) ρ_0, T_0 and with the mass velocity 0; behind the shock lies the shocked (compressed and heated) and then more or less re-expanded atmosphere in the state $p, \rho = \rho_0[\partial(x^3)/\partial(X^3)]_t, T$, and with the mass velocity $u = (\partial X/\partial t)_x$. The shock itself has the velocity $U = d\Xi/dt$. Thus

$$\rho = \rho_0 \left[\frac{\partial(x^3)}{\partial(X^3)}\right]_t = \rho_0 \frac{x^2}{X^2}\left(\frac{1}{\frac{\partial X}{\partial x}}\right)_t = \rho_0 \frac{z^2}{F(z)^2}\frac{1}{F'(z)} \tag{2.4}$$

$$u = \left(\frac{\partial X}{\partial t}\right)_x = \frac{2}{5} a t^{-3/5} [F(z) - z\, F'(z)] \tag{2.5}$$

$$U = \frac{d\Xi}{dt} = \frac{2}{5} a t^{-3/5} \tag{2.6}$$

Let us now consider the conditions immediately behind the shock; that is, at $X = \Xi$ (precisely: $X = \Xi - 0$). Immediately before the shock got there, this gas was in its original state of rest, i.e., it had $X = x$. Since the shock causes no discontinuous changes in position (but only in pressure, density, mass velocity), hence $X = x$ remains true immediately behind the shock. Thus, $X = x = \Xi$, i.e., $F(z) = z = 1$. In other words, the shock occurs at $z = (1)$ (immediately behind it: $z = 1 - 0$), and it imposes upon F the boundary condition

$$F(z) = 1 \qquad \text{at } z = 1 \tag{2.7}$$

We note that for reasons of symmetry the origin can never be displaced; i.e., $x = 0$ goes at all times with $X = 0$. This gives for F the further boundary condition

$$F(z) = 0 \qquad \text{at } z = 0 \tag{2.8}$$

Returning to the shock, Eqs. 2.4 to 2.6 above, with $z = 1$, give the conditions immediately behind it. The Hugoniot shock conditions express all that must be required at this point. They can be stated as follows:

$$\frac{\rho}{\rho_0} = \frac{(\gamma + 1)p + (\gamma - 1)p_0}{(\gamma - 1)p + (\gamma + 1)p_0} \tag{2.9}$$

$$u = \frac{2(p - p_0)}{\sqrt{2\rho_0\,[(\gamma + 1)p + (\gamma - 1)p_0]}} \tag{2.10}$$

$$U = \sqrt{\frac{(\gamma + 1)p + (\gamma - 1)p_0}{2\rho_0}} \tag{2.11}$$

Considering $p_0 = 0$ (cf. above), these become

$$\rho = \frac{\gamma + 1}{\gamma - 1}\,\rho_0 \tag{2.9'}$$

$$u = \sqrt{\frac{2}{\gamma + 1}\,\frac{p}{\rho_0}} \tag{2.10'}$$

$$U = \sqrt{\frac{\gamma + 1}{2}\,\frac{p}{\rho_0}} \tag{2.11'}$$

We rewrite Eqs. 2.10' and 2.11' to express p and u in terms of U.

$$u = \frac{2}{\gamma + 1}\,U \tag{2.10''}$$

$$p = \frac{2}{\gamma + 1}\,\rho_0\,U^2 \tag{2.11''}$$

Equation 2.11'' cannot be compared with 2.4 to 2.6, since it contains p, which does not occur there. Equations 2.9' and 2.10'' can be compared, putting $z = 1$ in 2.4 to 2.6 and using 2.7. Both give the same thing:

$$F'(z) = \frac{\gamma - 1}{\gamma + 1} \quad \text{at } z = 1 \tag{2.12}$$

Thus we have exhausted the discussion of the physical problem in Section 2.1, that is, essentially of the shock conditions. This turned out to be equivalent to the boundary conditions given by Eqs. 2.7 and 2.12 at $z = 1$; Eq. 2.8 at $z = 0$ is self evident.

The flow of the gas behind the shock is expected to be shock-free and hence adiabatic. That is, every particle x of the gas has the same entropy $p\rho^{-\gamma}$ at all times after it crossed the shock. We can therefore take for it

the value of $p\rho^{-\gamma}$ immediately behind the shock, with the same x. Given z,t for a particle, and using Eqs. 2.1' and 2.3, its x is $at^{2/5}z$; hence the t' at which it crossed the shock is defined by $at'^{2/5}z = at^{2/5}z$, i.e., $t' = tz^{5/2}$. Hence by Eqs. 2.9' and 2.11' we have immediately behind the shock

$$p\rho^{-\gamma} = \frac{2}{\gamma+1}\rho_0 U^2 \left(\frac{\gamma+1}{\gamma-1}\rho_0\right)^{-\gamma}$$

$$= \frac{2(\gamma-1)^{\gamma}}{(\gamma+1)^{\gamma+1}} \rho_0^{-(\gamma-1)} U^2$$

Using Eqs. 2.4 and 2.6 this gives

$$p = \frac{8(\gamma-1)^{\gamma}}{25(\gamma+1)^{\gamma+1}} \rho_0 a^2 t'^{-6/5} \frac{z^{2\gamma}}{[F(z)]^{2\gamma}} \frac{1}{[F'(z)]^{\gamma}}$$

that is, by the above,

$$p = \frac{4}{25} \Phi \rho_0 a^2 t^{-6/5} \frac{z^{2\gamma-3}}{[F(z)]^{2\gamma}} \frac{1}{[F'(z)]^{\gamma}} \tag{2.13}$$

where

$$\Phi = \frac{2}{\gamma+1}\left(\frac{\gamma-1}{\gamma+1}\right)^{\gamma} \tag{2.14}$$

We now pass to the consideration of (II) in Section 2.1, that is, of the continuous flow of air behind the shock. As we saw above, this region is defined by $0 < x < \Xi$, i.e., by $0 < z < 1$, and in it z,t,x,X are connected by Eqs. 2.2'' and 2.3, and p,ρ,u are given by Eqs. 2.13, 2.4 and 2.5.

With the help of these relations one can set up the equation of motion and thereby achieve a complete formulation of our problem. It turns out, however, that it is preferable to work with the energy principle instead. Since only one Lagrangian coordinate is involved (x), it is indeed adequate to consider the energy principle only. And by virtue of unusually favorable special circumstances, the energy principle leads to a differential equation of order 1, whereas the equation of motion would lead to one of order 2. A reduction of the order by another unit is possible in either case for reasons of symmetry, and therefore the former procedure permits the

reduction of the entire problem to quadrature. This situation is mathematically of some interest and not at all trivial, but we do not propose to pursue this aspect here any further. At any rate we are going to use the energy principle, since it leads to an easier solution.

Consider the energy contained in the gas behind the shock. It is made up of the inner (thermic) energy $1/(\gamma-1)\ p/\rho$ and the kinetic energy $1/2\ u^2$ (both per unit mass); hence, the total energy per unit mass is

$$\epsilon = \frac{1}{\gamma - 1}\frac{p}{\rho} + \frac{1}{2}u^2$$

The amount of gas in the spherical shell reaching from the particles x to the particles x + dx is the same for all t, and hence we may use its value for t = 0, which is clearly $4\pi\rho_0\ x^2\ dx$. Hence the total energy inside the sphere of the particles x is

$$\epsilon_1(x) = 4\pi\rho_0 \int_0^x \epsilon\ x^2\ dx$$

$$= 4\pi\rho_0 \int_0^x \left(\frac{1}{\gamma - 1}\frac{p}{\rho} + \frac{1}{2}u^2\right) x^2\ dx$$

or upon introducing z, and using Eqs. 2.3 to 2.5 and 2.13

$$(1) \qquad \epsilon_2(z) = 4\pi\rho_0 \int_0^z \left\{ \frac{1}{\gamma-1} \frac{\frac{4}{25}\ \Phi\rho_0\ a^2 t^{-6/5}\ \frac{z^{2\gamma-3}}{[F(z)]^{2\gamma}}\ \frac{1}{[F'(z)]^{\gamma}}}{\rho_0\ \frac{z^2}{[F(z)]^2}\ \frac{1}{F'(z)}} + \frac{1}{2}\ \frac{4}{25}\ a^2 t^{-6/5}\ [F(z) - z\,F'(z)]^2 \right\} a^3 t^{6/5}\ z^2\ dz$$

that is,

$$(2) \qquad \epsilon_2(z) = \frac{8\pi}{25}\ \rho_0\ a^5 \int_0^z \left\{ \frac{2}{\gamma - 1}\ \Phi\ \frac{z^{2(\gamma-1)-3}}{[F(z)]^{2(\gamma-1)}}\ \frac{1}{[F'(z)]^{\gamma-1}} + [F(z) - z\,F'(z)]^2 \right\} t^2\ dz \qquad (2.15)$$

From Eq. 2.15 we can draw two conclusions.

The first conclusion obtains by putting $z = 1$. Then Eq. 2.15 represents the entire energy within the shocked region. Outside the shocked region the energy of the gas is 0 (since $\rho_0 = 0$, $u = 0$), and at $t = 0$ this (energy = 0) would apply to the entire gas. Hence $\epsilon_2(1)$ is the total energy acquired by the gas between $t = 0$ and present $t > 0$. This quantity is the same for all $t > 0$, and clearly positive. It is obvious that it must be identified with the explosion energy E_0 of Section 2.1. So we have

$$E_0 = \frac{8\pi}{25} \rho_0 a^5 \int_0^1 \left\{ \frac{2}{\gamma - 1} \Phi \frac{z^{2(\gamma-1)-3}}{[F(z)]^{2(\gamma-1)}} \frac{1}{[F'(z)]^{\gamma-1}} + [F(z) - z F'(z)]^2 \right\} z^2 \, dz \qquad (2.16)$$

The second conclusion obtains by considering a general z (> 0, < 1). It is clear from Eq. 2.15 that the energy within the z-sphere is constant. This was a physical necessity for $z = 1$, i.e., for the entire shock zone, but for general z it is a new fact with considerable consequences.

Indeed, let such a z (> 0, < 1) be given. This z-sphere contains the gas within the x-sphere, $x = at^{2/5}z$; i.e., its material content changes with t. The constancy of its energy amounts to stating that the energy flowing into it with the new material that enters is exactly compensated by the work which its original surface does by expanding against the surrounding pressure. It should be noted that in making this last statement we are stating the energy principle, that is, the equivalent of the equation of motion.

Let us therefore express the two energy changes referred to above and state their equality.

The energy of the material entering the z-sphere, i.e., the x-sphere $x = at^{2/5}z$, in the time between t and $t + dt$ is

$$4\pi\rho_0 x^2 (dx)_t \, \epsilon = 4\pi\rho_0 \left(\frac{1}{\gamma - 1} \frac{p}{\rho} + \frac{1}{2} u^2 \right) x^2 (dx)_t$$

and using the form of the integrand in the first expression (1), $\epsilon_2(z)$ of Eq. 2.15, the right hand side becomes

$$4\pi\rho_0 \left\{ \frac{1}{\gamma-1} \frac{\frac{4}{25}\,\Phi\rho_0\, a^2 t^{-6/5}\, \frac{z^{2\gamma-3}}{[F(z)]^{2\gamma}}\, \frac{1}{[F'(z)]^{\gamma}}}{\rho_0 \frac{z^2}{[F(z)]^2}\, \frac{1}{F'(z)}} + \frac{1}{2}\,\frac{4}{25}\, a^2 t^{-6/5}\, [F(z) - z\,F'(z)]^2 \right\} a^2 t^{4/5}\, z^2\, \frac{2}{5}\, at^{-3/5}\, dt\, z$$

that is,

$$\frac{16\pi}{125}\,\rho_0\, a^5 t^{-1} \left\{ \frac{2}{\gamma-1}\,\Phi\, \frac{z^{2(\gamma-1)-3}}{[F(z)]^{2(\gamma-1)}}\, \frac{1}{[F'(z)]^{\gamma-1}} + [F(z) - z\,F'(z)]^2 \right\} z^3\, dt \qquad (2.17)$$

The work done by the original surface by expanding against the surrounding pressure is

$$4\pi p X^2\, u\, dt$$

and using Eqs. 2.2", 2.3, 2.5, and 2.13, this becomes

$$4\pi\,\frac{4}{25}\,\Phi\,\rho_0\, a^2 t^{-6/5}\, \frac{z^{2\gamma-3}}{[F(z)]^{2\gamma}}\, \frac{1}{[F'(z)]^{\gamma}}\, a^2 t^{4/5}\, [F(z)]^2\, \frac{2}{5}\, at^{-3/5}\, [F(z) - z\,F'(z)]\, dt$$

that is,

$$\frac{32\pi}{125}\,\rho_0\, a^5 t^{-1}\,\Phi\, \frac{z^{2\gamma-3}}{[F(z)]^{2(\gamma-1)}}\, \frac{1}{[F'(z)]^{\gamma}}\, [F(z) - z\,F'(z)]\, dt \qquad (2.18)$$

Equating 2.17 and 2.18 gives

$$\frac{2}{\gamma-1}\,\Phi\,\frac{z^{2(\gamma-1)}}{[F(z)]^{2(\gamma-1)}}\,\frac{1}{[F'(z)]^{\gamma-1}}+z^3\,[F(z)-z\,F'(z)]^2$$

$$=2\,\Phi\,\frac{z^{2\gamma-3}}{[F(z)]^{2(\gamma-1)}\,[F'(z)]^{\gamma}}\,[F(z)-z\,F'(z)] \qquad (2.19)$$

This equation is equivalent to the equation of motion, as pointed out earlier in this section. Together with the boundary conditions (Eqs. 2.7, 2.12, and 2.8) it contains the full statement of our problem while the connection with the given explosion energy E_0 is given by Eq. 2.16.

We now proceed to the integration of the differential equation, 2.19. Put

$$z = e^s \qquad (2.20)$$

$$F(z) = e^{\nu s}\,\Phi(s) \qquad (2.21)$$

the constant ν to be determined later. Then Eq. 2.19 becomes

$$\frac{2}{\gamma-1}\,\Phi\,\exp[2(\gamma-1)-2(\gamma-1)\nu-(\gamma-1)(\nu-1)]s\,\frac{1}{\Phi^{2(\gamma-1)}\left(\frac{d\Phi}{ds}+\nu\Phi\right)^{\gamma-1}}$$

$$+\exp(3+2\nu)s\left[\frac{d\Phi}{ds}+(\nu-1)\Phi\right]^2$$

$$=-2\Phi\,\exp[2\gamma-3-2(\gamma-1)\nu-\gamma(\nu-1)+\nu]s\,\frac{\frac{d\Phi}{ds}+(\nu-1)\Phi}{\Phi^{2(\gamma-1)}\left(\frac{d\Phi}{ds}+\nu\Phi\right)^{\gamma}}$$

Each of these three terms contains a factor e^{As}, the values of A being

(1) $2(\gamma-1)-2(\gamma-1)\nu-(\gamma-1)(\nu-1)$

(2) $3+2\nu$,

(3) $2\gamma-3-2(\gamma-1)\nu-\gamma(\nu-1)+\nu$

The first and the third are clearly equal, and they differ from the second by $(3\gamma-1)\nu-3(\gamma-2)$. Hence all three are equal, and thereby s no longer appears explicitly in the differential equation, if

$$\nu = \frac{3(\gamma - 2)}{3\gamma - 1} \tag{2.22}$$

So we have

$$\frac{2}{\gamma - 1}\,\Phi\,\frac{1}{\Phi^{2(\gamma-1)}\left(\frac{d\Phi}{ds} + \nu\Phi\right)^{\gamma-1}} + \left[\frac{d\Phi}{ds} + (\nu - 1)\,\Phi\right]^2$$

$$= -2\Phi\,\frac{\frac{d\Phi}{ds} + (\nu - 1)\Phi}{\Phi^{2(\gamma-1)}\left(\frac{d\Phi}{ds} + \nu\Phi\right)^{\gamma}} \tag{2.23}$$

Now put

$$\Psi = \frac{d\Phi}{ds} + \nu\Phi \tag{2.24}$$

that is,

$$zF'(z) = e^{\nu s}\,\Psi(s) \tag{2.24'}$$

Then Eq. 2.23 becomes

$$\frac{2}{\gamma - 1}\,\Phi\,\frac{1}{\Phi^{2(\gamma-1)}\,\Psi^{\gamma-1}} + (\Psi - \Phi)^2 = -2\Phi\,\frac{\Psi - \Phi}{\Phi^{2(\gamma-1)}\,\Psi^{\gamma}}$$

that is,

$$(\Psi - \Phi)^2 + 2\Phi\,\frac{\Psi - \Phi}{\Phi^{2(\gamma-1)}\,\Psi^{\gamma}} + \frac{2}{\gamma - 1}\,\Phi\,\frac{1}{\Phi^{2(\gamma-1)}\,\Psi^{\gamma-1}} = 0 \tag{2.25}$$

Thus $\Phi\Psi$ are functions of each other by Eq. 2.25, and then Eqs. 2.22, 2.23, and 2.24' permit determination of $z, F(z), F'(z)$ by one quadrature.

We first solve Eq. 2.25 explicitly by parametrisation. Recall

$$\Phi = \frac{2}{\gamma + 1}\left(\frac{\gamma - 1}{\gamma + 1}\right)^{\gamma} \tag{2.14}$$

Put

$$D = \frac{\gamma - 1}{\gamma + 1} \tag{2.26}$$

Then

$$\Phi = (1 - D)D^{\gamma}, \quad \frac{2}{\gamma - 1} = \frac{1 - D}{D} \tag{2.14'}$$

Now Eq. 2.25 may be written

$$\left(\frac{\Phi}{\Psi} - 1\right)^2 - 2\Phi \frac{\frac{\Phi}{\Psi} - 1}{\Phi^{2(\gamma-1)}\,\Psi^{(\gamma+1)}} + \frac{2}{\gamma - 1}\,\Phi \frac{1}{\Phi^{2(\gamma-1)}\,\Psi^{\gamma+1}} = 0$$

that is,

$$\left(\frac{\Phi}{\Psi} - 1\right)^2 - 2\,\frac{1 - D}{D} \quad \frac{\frac{\Phi}{\Psi} - 1}{\Phi^{2(\gamma-1)}\left(\frac{\Psi}{D}\right)^{\gamma+1}} + \left(\frac{1 - D}{D}\right)^2 \frac{1}{\Phi^{2(\gamma-1)}\left(\frac{\Psi}{D}\right)^{\gamma+1}} = 0$$

or equivalently,

$$\left(\frac{\frac{\Phi}{\Psi} - 1}{\frac{1}{D} - 1}\right)^2 - 2\,\frac{1}{\Phi^{2(\gamma-1)}\left(\frac{\Psi}{D}\right)^{\gamma+1}}\,\frac{\frac{\Phi}{\Psi} - 1}{\frac{1}{D} - 1} + \frac{1}{\Phi^{2(\gamma-1)}\left(\frac{\Psi}{D}\right)^{\gamma+1}} = 0$$

Now put

$$\xi = \frac{\frac{\Phi}{\Psi} - 1}{\frac{1}{D} - 1} \tag{2.27}$$

$$\eta = \Phi^{2(\gamma-1)}\left(\frac{\Psi}{D}\right)^{\gamma+1} \tag{2.28}$$

Then the above equation becomes

$$\xi^2 - 2\frac{\xi}{\eta} + \frac{1}{\eta} = 0$$

that is,

$$\eta = \frac{2\xi - 1}{\xi^2}$$

It is convenient to define a new quantity θ by

$$\xi = \frac{1 + \theta}{2} \tag{2.29}$$

We can now express s explicitly in terms of θ, and then z, F(z), F'(z) also. To do this, we first note that according to Eq. 2.29

$$\eta = \frac{4\theta}{(1 + \theta)^2} \tag{2.30}$$

Next Eq. 2.27 gives

$$\frac{\Phi}{\Psi/D} = D\frac{\Phi}{\Psi} = D\left[\left(\frac{1}{D} - 1\right)\xi + 1\right] = (1 - D)\xi + D$$

and then this relation and Eq. 2.28 give

$$\Phi = \eta^{\frac{1}{3\gamma-1}}\,[(1 - D)\xi + D]^{\frac{\gamma+1}{3\gamma-1}}$$

$$\Psi = D\eta^{\frac{1}{3\gamma-1}}\,[(1 - D)\xi + D]^{-\frac{2(\gamma-1)}{3\gamma-1}}$$

Substituting from Eqs. 2.26, 2.29, and 2.30, we get

$$\Phi = \theta^{\frac{1}{3\gamma-1}}\left(\frac{\theta + 1}{2}\right)^{-\frac{2}{3\gamma-1}}\left(\frac{\theta + \gamma}{\gamma + 1}\right)^{\frac{\gamma+1}{3\gamma-1}} \tag{2.31}$$

$$\Psi = \frac{\gamma - 1}{\gamma + 1}\,\theta^{\frac{1}{3\gamma-1}}\left(\frac{\theta + 1}{2}\right)^{-\frac{2}{3\gamma-1}}\left(\frac{\theta + \gamma}{\gamma + 1}\right)^{-\frac{2(\gamma-1)}{3\gamma-1}} \tag{2.32}$$

Note that θ must be positive: Φ is intrinsically positive by Eqs. 2.21 and 2.2" along with F'(z) and X; Ψ is intrinsically positive by Eqs. 2.24' and 2.4 along with F'(z) and ρ_i; the positivity of Φ and Ψ implies the positivity of η by Eq. 2.28 and the positivity of θ by Eq. 2.30. Thus we require

$$\theta > 0 \tag{2.33}$$

By the definition of Ψ in Eq. 2.24,

$$\frac{d\Phi}{ds} = \Psi - \nu\Phi$$

Hence,

$$s = \int \frac{d\Phi}{\Psi - \nu\Phi} = \int \frac{\frac{d\Phi}{\Phi}}{\frac{\Psi}{\Phi} - \nu}$$

The integrand is easily rewritten with the help of Eqs. 2.27, 2.29, and 2.31, yielding

$$s = \int \frac{\frac{1}{3\gamma - 1}\frac{d\theta}{\theta} - \frac{2}{3\gamma - 1}\frac{d\theta}{\theta + 1} + \frac{\gamma + 1}{3\gamma - 1}\frac{d\theta}{\theta + \gamma}}{\frac{\gamma - 1}{\theta + \gamma} + \frac{3(2 - \gamma)}{3\gamma - 1}}$$

$$= \int \frac{(\theta + \gamma)\left(\frac{d\theta}{\theta} - 2\frac{d\theta}{\theta + 1}\right) + (\gamma + 1)\,d\theta}{3(2 - \gamma)\theta + 2\gamma + 1}$$

$$= \int \frac{\theta + \gamma}{\theta[3(2 - \gamma)\theta + 2\gamma + 1]}d\theta - \int \frac{2(\theta + \gamma)}{(\theta + 1)[3(2 - \gamma)\theta + 2\gamma + 1]}d\theta + \int \frac{\gamma + 1}{3(2 - \gamma)\theta + 2\gamma + 1}\,d\theta$$

Carrying out the integration we get

$$s = c_1 + \frac{\gamma}{2\gamma + 1} \ln\theta - \frac{2}{5} \ln(\theta + 1)$$

$$+ \frac{13\gamma^2 - 7\gamma + 12}{15(2 - \gamma)(2\gamma + 1)} \ln[3(2 - \gamma)\theta + (2\gamma + 1)] \qquad (2.34)$$

Before we go further, let us express the boundary conditions, Eqs. 2.7, 2.12, in the new parameters.

Equations 2.7 and 2.12 require that at $z = 1$, $F(z) = 1$ and $F'(z) = (\gamma - 1)/(\gamma + 1)$. By Eqs. 2.20, 2.21 and 2.24' this means that at $s = 0$, we must have $\Phi = 1$, and $\Psi = (\gamma - 1)/(\gamma + 1)$. By Eqs. 2.31 and 2.32 this means that at $s = 0$, we have $\theta = 1$. [$\theta = 1$ clearly implies $\Phi = 1$, $\Psi = (\gamma - 1)/(\gamma + 1)$, and it is implied by them since $\Psi/\Phi = (\gamma - 1)/(\theta + \gamma)$.]

Hence Eqs. 2.7 and 2.12 are just sufficient to determine the constant of integration c_1 in Eq. 2.34, and they are satisfied if we rewrite 2.34 in the following form:

$$s = \frac{\gamma}{2\gamma + 1} \ln\theta - \frac{2}{5} \ln \frac{\theta + 1}{2}$$

$$+ \frac{13\gamma^2 - 7\gamma + 12}{15(2 - \gamma)(2\gamma + 1)} \ln \frac{3(2 - \gamma)\theta + (2\gamma + 1)}{7 - \gamma} \qquad (2.34')$$

Now we express the original similarity variable z in terms of θ:

$$z = e^s = \theta^{\frac{\gamma}{2\gamma+1}} \left(\frac{\theta + 1}{2} \right)^{-2/5} \left[\frac{3(2 - \gamma)\theta + (2\gamma + 1)}{7 - \gamma} \right]^{\frac{13\gamma^2-7\gamma+12}{15(2-\gamma)(2\gamma+1)}} \qquad (2.34'')$$

Next, using Eqs. 2.31 and 2.22 we obtain

$$F(z) = e^{\nu s} \Phi(s) = \theta^{\frac{\gamma-1}{2\gamma+1}} \left(\frac{\theta + 1}{2} \right)^{-2/5} \left(\frac{\theta + \gamma}{\gamma + 1} \right)^{\frac{\gamma+1}{3\gamma-1}}$$

$$\left[\frac{3(2 - \gamma)\theta + (2\gamma + 1)}{7 - \gamma} \right]^{-\frac{13\gamma^2-7\gamma+12}{5(2\gamma+1)(3\gamma-1)}} \qquad (2.35)$$

These equations show that the boundary condition, Eq. 2.8 is automatically satisfied: Eq. 2.34" (with Eq. 2.33) shows that $z \to 0$ corresponds to $\theta \to 0$, and Eq. 2.35 shows that this implies $F(z) \to 0$.

Hence Eqs. 2.34" and 2.35 contain the complete solution of our problem in parametric form [2.34" (with 2.33)] and show that the interval

$$0 < z \leqq 1 \quad (0 < \times \leqq \text{日}) \tag{2.36}$$

corresponds to the interval $0 < \theta \leqq 1$.

It is convenient to express $F'(z)$ and $F(z) - zF'(z)$, too, in terms of θ. We find using Eqs. 2.34", 2.32, and 2.22 that

$$F'(z) = e^{(\nu-1)s}\,\Psi = \frac{\gamma-1}{\gamma+1}\,\theta^{-\frac{1}{2\gamma+1}}\left(\frac{\theta+\gamma}{\gamma+1}\right)^{-\frac{2(\gamma-1)}{3\gamma-1}}$$

$$\left[\frac{3(2-\gamma)\theta+(2\gamma+1)}{7-\gamma}\right]^{-\frac{13\gamma^2-7\gamma+12}{3(2-\gamma)(2\gamma+1)(3\gamma-1)}} \tag{2.37}$$

On the other hand, Eqs. 2.31 and 2.32 give

$$\frac{F(z)}{zF'(z)} = \frac{\Phi}{\Psi} = \frac{\gamma+1}{\gamma-1}\,\frac{\theta+\gamma}{\gamma+1} = \frac{\theta+\gamma}{\gamma-1}$$

$$\frac{F(z)}{zF'(z)} - 1 = \frac{\theta+1}{\gamma-1} = \frac{2}{\gamma-1}\,\frac{\theta+1}{2}$$

Using these relations together with Eqs. 2.34" and 2.37 we have

$$F(z) - zF'(z) = e^{\nu s}(\Phi - \Psi) = \frac{2}{\gamma+1}\,\theta^{\frac{\gamma-1}{2\gamma\ 1}}\left(\frac{\theta+1}{2}\right)^{3/5}\left(\frac{\theta+\gamma}{\gamma+1}\right)^{-\frac{2(\gamma-1)}{3\gamma-1}}$$

$$\left[\frac{3(2-\gamma)\theta+(2\gamma+1)}{7-\gamma}\right]^{-\frac{13\gamma^2-7\gamma+12}{5(2\gamma+1)(3\gamma-1)}} \tag{2.38}$$

We can now use Eqs. 2.3, 2.2", 2.13, 2.4 and 2.5 to express x, X, p, ρ, u in terms of θ. The results are

$$x = at^{2/5} \cdot \theta^{\frac{\gamma}{2\gamma+1}} \left(\frac{\theta + 1}{2}\right)^{-2/5} \left[\frac{3(2 - \gamma)\theta + (2\gamma + 1)}{7 - \gamma}\right]^{\frac{13\gamma^2-7\gamma+12}{15(2-\gamma)(2\gamma+1)}} \tag{2.39}$$

$$X = at^{2/5} \cdot \theta^{\frac{\gamma-1}{2\gamma+1}} \left(\frac{\theta + 1}{2}\right)^{-2/5} \left(\frac{\theta + \gamma}{\gamma + 1}\right)^{\frac{\gamma+1}{3\gamma-1}}$$

$$\left[\frac{3(2 - \gamma)\theta + (2\gamma + 1)}{7 - \gamma}\right]^{-\frac{13\gamma^2-7\gamma+12}{5(2\gamma+1)(3\gamma-1)}} \tag{2.40}$$

$$\rho = \frac{\gamma + 1}{\gamma - 1} \rho_0 \cdot \theta^{\frac{3}{2\gamma+1}} \left(\frac{\theta + \gamma}{\gamma + 1}\right)^{-\frac{4}{3\gamma-1}}$$

$$\left[\frac{3(2 - \gamma)\theta + (2\gamma + 1)}{7 - \gamma}\right]^{\frac{13\gamma^2-7\gamma+12}{(2-\gamma)(2\gamma+1)(3\gamma-1)}} \tag{2.41}$$

$$u = \frac{4}{5(\gamma + 1)} at^{-3/5} \cdot \theta^{\frac{\gamma-1}{2\gamma+1}} \left(\frac{\theta + 1}{2}\right)^{3/5} \left(\frac{\theta + \gamma}{\gamma + 1}\right)^{-\frac{2(\gamma-1)}{3\gamma-1}}$$

$$\left[\frac{3(2 - \gamma)\theta + (2\gamma + 1)}{7 - \gamma}\right]^{-\frac{13\gamma^2-7\gamma+12}{5(2\gamma+1)(3\gamma-1)}} \tag{2.42}$$

$$p = \frac{8}{25(\gamma + 1)} \rho_0 a^2 t^{-6/5} \cdot \left(\frac{\theta + 1}{2}\right)^{6/5} \left(\frac{\theta + \gamma}{\gamma + 1}\right)^{-\frac{4\gamma}{3\gamma-1}}$$

$$\left[\frac{3(2 - \gamma)\theta + (2\gamma + 1)}{7 - \gamma}\right]^{\frac{13\gamma^2-7\gamma+12}{5(2-\gamma)(3\gamma-1)}} \tag{2.43}$$

We express the internal (thermal) energy $1/(\gamma - 1)\ p/\rho$ and the kinetic energy $1/2\ u^2$ per unit mass

$$\epsilon_i = \frac{1}{\gamma - 1}\frac{p}{\rho} = \frac{8}{25(\gamma + 1)^2}\, a^2 t^{-6/5} \cdot \theta^{-\frac{3}{2\gamma+1}} \left(\frac{\theta + 1}{2}\right)^{6/5} \left(\frac{\theta + \gamma}{\gamma + 1}\right)^{-\frac{4(\gamma-1)}{3\gamma-1}}$$

$$\left[\frac{3(2 - \gamma)\theta + (2\gamma + 1)}{7 - \gamma}\right]^{-\frac{2(13\gamma^2-7\gamma+12)}{5(2\gamma+1)(3\gamma-1)}} \tag{2.44}$$

$$\epsilon_c = \frac{1}{2}u^2 = \frac{8}{25(\gamma + 1)^2}\, a^2 t^{-6/5} \cdot \theta^{\frac{2(\gamma-1)}{2\gamma+1}} \left(\frac{\theta + 1}{2}\right)^{6/5} \left(\frac{\theta + \gamma}{\gamma + 1}\right)^{-\frac{4(\gamma-1)}{3\gamma-1}}$$

$$\left[\frac{3(2 - \gamma)\theta + (2\gamma + 1)}{7 - \gamma}\right]^{-\frac{2(13\gamma^2-7\gamma+12)}{5(2\gamma+1)(3\gamma-1)}} \tag{2.45}$$

Hence,

$$\frac{\epsilon_c}{\epsilon_i} = \theta \tag{2.46}$$

giving an immediate physical interpretation of the parameter θ.

We need finally the expression for the total energy E_0. Instead of calculating it using Eq. 2.16, it is now preferable to use a different procedure.

We replace the inner and kinetic energies ϵ_c, ϵ_i per unit mass by those ϵ_c', ϵ_i' per unit volume.

Equation 2.46 gives again

$$\frac{\epsilon_c'}{\epsilon_i'} = \theta$$

and now

$$E_0 = \int_0^{\Xi} (\epsilon_i' + \epsilon_c') 4\pi X^2 \, dX$$

$$= 4\pi \int_0^{\Xi} (\theta + 1)\epsilon_i' X^2 \, dX$$

$$= 8\pi \Xi^3 \int_0^1 \frac{\theta + 1}{2} \epsilon_i' [F(z)]^2 \, dF(z)$$

Now $\epsilon_i' = \rho\epsilon_i = 1/(\gamma - 1)p$; hence Eq. 2.43 gives

$$E_0 = K\rho_0 a^5 \tag{2.47}$$

where

$$K = \frac{64\pi}{75(\gamma^2 - 1)} \int_0^1 \left(\frac{\theta + 1}{2}\right)^{11/5} \left(\frac{\theta + \gamma}{\gamma + 1}\right)^{-\frac{4\gamma}{3\gamma-1}}$$

$$\left[\frac{3(2 - \gamma)\theta + (2\gamma + 1)}{7 - \gamma}\right]^{\frac{13\gamma^2-7\gamma+12}{5(2-\gamma)(3\gamma-1)}} d(F)^3 \tag{2.47'}$$

F^3 being obtainable from Eq. 2.35.

2.3 Evaluation and Interpretation of the Results

The formulae 2.39 to 2.46 give a complete description of the physical situation, while, 2.47 and 2.47' connect the necessary constant a with the physically given constants E_0, ρ_0. We will now formulate verbally some of the main qualitative features expressed by Eqs. 2.39 to 2.46.

The center is at $\theta = 0$: $x = X = 0$. The shock is at $\theta = 1$: $x = X = \Xi = at^{2/5}$. The ratio kinetic energy/internal energy is θ; hence it varies from the value $\theta = 0$ at the center to the value $\theta = 1$ at the shock.

In all formulae 2.39 to 2.45 the θ-dependent terms are 1 for $\theta = 1$, that is, at the shock. In other words: the first factor gives the value of the corresponding quantity at the shock.

The formulae are valid[2] for $1 < \gamma < 2$.

These formulae are regular in the limit $\gamma \to 1, \theta \to 0$ except for the powers of θ, and the factor $(\gamma + 1)/(\gamma - 1)$ in ρ. It should be noted that the three other factors become all $(\theta + 1)/2$, and hence can give rise to no singularities. We restate these formulae in their limiting form for $\gamma = 1$ except that we conserve terms of order $(\gamma - 1)$[but not $(\gamma - 1)^2$ and higher terms] in the θ exponent and the leading $1/(\gamma - 1)$ term (but no other terms) in ρ. This gives:

$$x = at^{2/5} \cdot \theta^{1/3 + \frac{1(\gamma-1)}{9}} \tag{2.39'}$$

$$X = at^{2/5} \cdot \theta^{\frac{\gamma-1}{3}} \tag{2.40'}$$

$$\rho = \frac{2}{\gamma - 1} \rho_0 \cdot \theta^{1-\frac{2(\gamma-1)}{3}} \cdot \frac{\theta + 1}{2} \tag{2.41'}$$

$$u = \frac{2}{5} at^{-3/5} \cdot \theta^{\frac{\gamma-1}{3}} \tag{2.42'}$$

$$p = \frac{4}{25} \rho_0 a^2 t^{-6/5} \cdot \frac{\theta + 1}{2} \tag{2.43'}$$

$$\epsilon_i = \frac{2}{25} a^2 t^{-6/5} \cdot \theta^{-1+\frac{2(\gamma-1)}{3}} \tag{2.44'}$$

$$\epsilon_c = \frac{2}{25} a^2 t^{-6/5} \cdot \theta^{\frac{2(\gamma-1)}{3}} \tag{2.45'}$$

---

2. At this point it should be mentioned that one reason for developing the theory in the present form was to facilitate application of the small $\gamma - 1$ theory of Bethe in Chap. 4.

For $\gamma \to 2$ the last factor has to be considered separately, since its basis, $[3(2-\gamma)\theta + (2\gamma+1)]/(7-\gamma)$ becomes 1, while the exponent becomes infinite in some cases (x, ρ, p). Where the exponent stays finite $(X, u, \epsilon_i, \epsilon_c)$, this factor is simply 1, but for the others (x, ρ, p as above) it assumes the indefinite form 1^{∞}. These cases may be discussed on the basis of the expression

$$\left[\frac{3(2-\gamma)\theta + (2\gamma+1)}{7-\gamma}\right]^{\frac{1}{2-\gamma}}$$

This can be written

$$\left[1 - (2-\gamma)\frac{3}{7-\gamma}(1-\theta)\right]^{\frac{1}{2-\gamma}}$$

This has the same $\gamma \to 2$ limit as

$$e^{-\frac{3}{7-\gamma}(1-\theta)}$$

that is

$$e^{-3/5\ (1-\theta)}$$

Hence the last factors in Eqs. 2.39 to 2.45 become

$$e^{-2/5\ (1-\theta)} \qquad (2.39'')$$

$$1 \qquad (2.40'')$$

$$e^{-6/5\ (1-\theta)} \qquad (2.41'')$$

$$1 \qquad (2.42'')$$

$$e^{-6/5\ (1-\theta)} \qquad (2.43'')$$

$$1 \qquad (2.44'')$$

1 (2.45")

respectively. The other factors offer no difficulties at all.

The formulae which have been derived so far permit us to make some general qualitative remarks about the nature of the point source solution. These are the following:

1. Equation 2.41 shows that the density vanishes at the center. Table 2.3 shows in more detail that the density increases from 0 to its maximum value as one moves from the center to the shock. Table 2.1, referred to spacial positions with the help of Table 2.2, shows even more: most material is situated near the shock, and as γ approaches 1 all material gets asymptotically into positions near the shock.

2. By Eqs. 2.39 and 2.40, $x \propto X^{\gamma/(\gamma-1)}$ for $X \to 0$; and by Eqs. 2.39' and 2.40' even $X \to 0$ can be omitted if $\gamma \to 1$. That is, the amount of material within the sphere of radius X ($4\pi/3\ x^3$) decreases with a high power $[\gamma/(\gamma - 1)]$ of the volume of that sphere ($4\pi/3\ X^3$), and this tendency goes to complete degeneration as $\gamma \to 1$ $[\gamma/(\gamma - 1) \to \infty]$. Indeed, for any fixed volume, except the total one (that is, whenever $\theta^{(\gamma-1)/(2\gamma+1)}$ fixed = $\omega_0 < 1$), the mass in the sphere tends to 0 as $\gamma \to 1$ (that is, with the above assumption $\theta^{\gamma/(2\gamma+1)} = \omega_0{}^{\gamma/(\gamma-1)} \to 0$).

3. Near the center $\rho = 0$, as we saw in paragraphs 1 and 2 above, but $p \to p_0$ where $0 < p_0 < \infty$. Indeed, Table 2.5 shows that p_0/p_{shock} has very moderate values: As γ varies from 1 to 2, this ratio varies from 1/2 to about 1/4. Table 2.5, referred to spacial positions with the help of Table 2.2, and to the quantities of matter affected with the help of Table 2.1, also shows that p varies mostly near the shock, and only little in the region which contains little material. It shows also that this tendency, too, goes to complete degeneration as $\gamma \to 1$.

4. Since $\rho \to 0$ and $p \to p_0$, $0 < p_0 < \infty$ near the center, temperature $T \propto \epsilon_i \propto p/\rho \to \infty$ near the center. This is also clear from Eq. 2.44. Equations 2.44 and 2.45 show, furthermore, that $\epsilon_i \to \infty$, $\epsilon_c \to 0$ near the center.

5. Already Eqs. 2.1', 2.6, and 2.11" show that $p_{shock} \propto \Xi^{-3}$. Equation 2.43 (with $\theta = 1$), 2.47, and 2.47' show more specifically that

$$p_{shock} = \lambda \frac{E_0}{\Xi^3} \qquad (2.48)$$

where

$$\lambda = \frac{8}{25(\gamma + 1)} \frac{1}{K} = \frac{3(\gamma - 1)}{8\pi} \frac{1}{\int \text{as in } 2.47'} \qquad (2.48')$$

To sum up: The point source blows all material away from the center. The gradually emptying region around the center has ρ degenerating to 0, $T \propto \epsilon_i$ degenerating to ∞, while p tends to constancy, with moderate values of p/p_{shock}. As $\gamma \to 1$, these tendencies accentuate more and more, they go finally to complete degeneracy, and all material concentrates in the immediate vicinity of the shock.

Tables 2.1 to 2.8 give numerical values of some relations discussed in this chapter.

Table 2.1

$$\frac{x}{x_{shock}} = \frac{x}{\Xi} = \left(\frac{\text{mass within } \theta \text{ sphere}}{\text{mass within shock}}\right)^{1/3} = z$$

where x is the Lagrangian label; value of z is in upper left corner and z^3 in lower right corner.

γ	θ					
	0	0.2	0.4	0.6	0.8	1
1	0 0	0.5848 0.2	0.7368 0.4	0.8434 0.6	0.9283 0.8	1 1
1.2	0 0	0.5579 0.1736	0.7140 0.3640	0.8269 0.5655	0.9196 0.7775	1 1
1.4	0 0	0.5330 0.1514	0.6919 0.3312	0.8103 0.5321	0.9104 0.7546	1 1
1.667	0 0	0.5026 0.1269	0.6633 0.2919	0.7879 0.4892	0.8977 0.7233	1 1
2	0 0	0.4679 0.1025	0.6289 0.2487	0.7595 0.4381	0.8806 0.6829	1 1

Table 2.2

$$\frac{X}{X_{shock}} = \frac{X}{\Xi} = \left(\frac{\text{volume within } \theta \text{ sphere}}{\text{volume within shock}} \right)^{1/3} = F(z)$$

where X is the Eulerian position; value of F(z) is in upper left corner and $F(z)^3$ in lower right corner.

γ	θ					
	0	0.2	0.4	0.6	0.8	1
1	0 0	1 1	1 1	1 1	1 1	1 1
1.2	0 0	0.9326 0.8111	0.9641 0.8961	0.9810 0.9440	0.9920 0.9763	1 1
1.4	0 0	0.8747 0.6693	0.9305 0.8057	0.9621 0.8907	0.9838 0.9521	1 1
1.667	0 0	0.8084 0.5283	0.8887 0.7018	0.9372 0.8231	0.9723 0.9192	1 1
2	0 0	0.7381 0.4021	0.8399 0.5925	0.9060 0.7436	0.9571 0.8767	1 1

Table 2.3

$\frac{\rho}{\rho_{shock}}$

	θ					
γ	0	0.2	0.4	0.6	0.8	1
1	0	0.1200	0.2800	0.4800	0.7200	1
1.2	0	0.1362	0.2954	0.4901	0.7240	1
1.4	0	0.1508	0.3083	0.4978	0.7265	1
1.667	0	0.1682	0.3223	0.5052	0.7279	1
2	0	0.1868	0.3358	0.5107	0.7271	1

Table 2.4

$\frac{u}{u_{shock}}$

	θ					
γ	0	0.2	0.4	0.6	0.8	1
1	0	0.1	1	1	1	1
1.2	0	0.8793	0.9279	0.9592	0.9821	1
1.4	0	0.7872	0.8685	0.9236	0.9659	1
1.667	0	0.6929	0.8027	0.8820	0.9460	1
2	0	0.6039	0.7349	0.8363	0.9229	1

Table 2.5

$$\frac{p}{p_{shock}}$$

	θ					
γ	0	0.2	0.4	0.6	0.8	1
1	0.5	0.6	0.7	0.8	0.9	1
1.2	0.4235	0.5266	0.6360	0.7515	0.8730	1
1.4	0.3656	0.4674	0.5814	0.7079	0.8473	1
1.667	0.3062	0.4037	0.5191	0.6550	0.8143	1
2	0.2508	0.3407	0.4534	0.5952	0.7741	1

Table 2.6

$$\frac{\epsilon_i}{\epsilon_{i_{shock}}} = \frac{T}{T_{shock}}$$

	θ					
γ	0	0.2	0.4	0.6	0.8	1
1	∞	5	2.5	1.6667	1.2500	1
1.2	∞	3.8659	2.1526	1.5333	1.2057	1
1.4	∞	3.0988	1.8857	1.4219	1.1662	1
1.667	∞	2.4006	1.6107	1.2967	1.1187	1
2	∞	1.8236	1.3502	1.1656	1.0646	1

Table 2.7

$$\frac{\epsilon_c}{\epsilon_{c_{shock}}}$$

	θ					
γ	0	0.2	0.4	0.6	0.8	1
1	0	1	1	1	1	1
1.2	0	0.7732	0.8611	0.9200	0.9645	1
1.4	0	0.6198	0.7543	0.8531	0.9330	1
1.667	0	0.4801	0.6443	0.7780	0.8950	1
2	0	0.3647	0.5401	0.6993	0.8517	1

Table 2.8

SOME OTHER USEFUL QUANTITIES

γ	$\int$ of Eq. 2.47'	K of Eq. 2.47'	λ of Eq. 2.48'
1	0.250	$_{\infty}$(1)	$_{0}$(2)
1.2	0.289	1.764	0.0825
1.4	0.308	0.8510	0.155
1.667	0.329	0.4928	0.242
2	0.350	0.312	0.341

(1) The significant quantity is $(\gamma - 1)K$; see Eq. 2.47'.

(2) The significant quantity is $\lambda/(\gamma - 1)$; see Eq. 2.48'.

Chapter 3

THERMAL RADIATION PHENOMENA (Revised 1953)

by John L. Magee and Joseph O. Hirschfelder

The most profound difference between a nuclear and a chemical explosion is that the former liberates its energy in a much smaller volume. This has the consequence that the temperature created in a nuclear explosion is much higher, about a million degrees at the time a typical nuclear bomb bursts its case, as compared with five thousand degrees inside an ordinary high explosive. This means that a nuclear bomb will release a significant fraction, actually about one-third, of its total energy in the form of thermal radiation.

Thermal radiation plays a dual role in atomic explosions. First of all it is intimately associated with the formation and the development of the shock wave. Secondly, the thermal radiation emitted to large distances is responsible for a great many personnel casualties by skin burns and is responsible for damage to structures by incendiary action.

For definiteness, we shall generally refer to a nuclear explosion releasing energy equivalent to 10,000 tons of TNT.[1] When the effects of such an explosion reach the case of the bomb, the temperature is so high that radiation presents the most rapid mechanism for energy transfer. Consequently, there follows a period of "radiation expansion" which lasts throughout the first 10 meters or so. This period is characterized by having the air heated to a high temperature by radiation before it is set in motion by hydrodynamic effects.

A strong air shock wave develops when the radiation front is about 10 meters out and the air temperature has dropped to about 300,000°K. After this time, the shock wave runs ahead and the radiation front moves

1. A "ton of TNT" by definition releases an amount of energy equal to 4.185×10^{16} ergs.

more slowly. The motion of the radiation behind the shock is probably of minor importance to the behavior of the blast. It has been neglected altogether in the other blast treatments in this volume.

It is convenient to introduce at this point two terms which will later prove useful. The ball of fire is defined, for this discussion, as the total mass of air which is hot enough to radiate visible light. The hot inner core from which the blast originates will be called the isothermal sphere. The material enclosed in this sphere, bounded by the "internal radiation front," is so hot that it is transparent to its own radiation. Because of the ease with which radiation can travel between any two points within this sphere, thermal gradients cannot exist; the term isothermal sphere is therefore appropriate.

Throughout the history of the air expansion, by radiation and shock energy is being lost in the wave lengths which cold air transmits. At first the front is hot enough to radiate as a black body. Finally, the shock front cools down and becomes transparent; radiation now comes from the higher temperatures behind. The shock front stops radiating at about 100 meter radius, and up to this time a rather negligible amount of radiation has been lost, approximately 0.3 per cent of the total yield. The formation of molecular absorbing materials, for example NO_2, at temperatures between 2000 and 5000°K forms a protective shell to prevent radiation from the higher temperature interior from escaping. For a while this shell absorbs energy from the hot core and transmits it to the shock front, adding strength to the blast. Finally, radiation from the core is transmitted through the fringe of surrounding air which is also hot enough (~5000°K) to radiate. The radius of the ball of fire is about 200 meters at this time. This body of hot gas radiates strongly, and most of the observed radiation energy comes out in a few seconds (three or so) after the formation of this sphere. This energy loss does not weaken the shock, however, since the blast wave out-distances hydrodynamical signals from the ball of fire at this stage.

The first three sections in this chapter deal with the laws of radiation and hydrodynamics divorced from atomic bomb considerations. The next two sections consider the role thermal radiation plays in the formation and subsequent development of the shock wave. Finally in the last section, the radiation emitted from the ball of fire as a function of time is considered. The radiation phenomena in the air blast are thus described only in the last three sections and some readers may prefer starting with Section 3.4 for the first reading.

It should be emphasized, perhaps, that this description of radiation phenomena in the air blast is rough and largely qualitative. It might be more satisfactory to include radiation in the hydrodynamical treatment of the blast problem at the start, rather than to attempt to describe the effects

as perturbations as we have done in this chapter.

There are also influences of gamma radiation, bomb materials, and turbulence on the radiation effects which are neglected here. The principal thermal radiation effects, however, are believed to be correctly described.

3.1 Radiation Hydrodynamics: the Radiation Flux

In general hydrodynamics there are two ways for radiation to play a role: (a) radiation is a means for transporting energy, and (b) radiation exerts pressure. At the time that the explosion of a 10,000 ton nuclear explosion bursts into the air, the temperature ($\sim 10^6$ °K) is sufficiently low so that radiation pressure is negligible compared with material pressure. Consequently, it is the transportation of energy by radiation which is of most interest here and we consider the radiation flux in some detail.

Under equilibrium conditions, radiation pressure is given by

$$P_{rad} = \frac{1}{3} aT^4 = \frac{7.67 \times 10^{-15} \; T^4}{3 \times 1.0132 \times 10^6} = (2.523 \times 10^{-21}) \, T^4 \text{ atm} \qquad (3.1)$$

Here a is the Stefan-Boltzmann radiation constant, 7.67×10^{-15} erg/cm^{3}deg^4, and T is the temperature in degrees Kelvin. If T were 1,000,000°K, the radiation pressure would only be 2,523 atm and negligible compared to the material pressure (which would be considerably greater than 100,000 atm at such a time). When the temperature has dropped to 100,000°K, the radiation pressure is only one-fourth of an atmosphere.

Similarly the radiation energy, E(rad) per cubic centimeter, is negligible compared to the material internal energy, E(int) per cubic centimeter, since

$$E_{rad}(\text{per cm}^3) = aT^4 = 7.67 \times 10^{-15} \; T^4 \text{ erg/cm}^3 \qquad (3.2)$$

$$E_{int}(\text{per cm}^3) = \frac{p(\text{atm}) \times 1.0132 \times 10^6}{(\gamma - 1)} \text{ ergs/cm}^3 \qquad (3.3)$$

Here γ is the specific heat ratio which might have a value ranging from $\gamma = 1.1$ to 1.2. If T were 1,000,000°K, E(rad) per cubic centimeter would be 8×10^9 ergs/cm^3. In order for the material internal energy to exceed this it would only be necessary for the pressure to exceed 1000 or 2000 atm (in place of the hundreds of thousands of atmospheres it would have at such a time).

Now let us consider the effects of radiation on the general hydrodynamical equations. The existence of thermal radiation does not effect the equation of continuity (since radiation has no mass), nor the equation of motion (since we can neglect radiation pressure), and it only modifies the equation of energy conservation through the flux of energy in the form of radiation, $\vec{F}$.

Let E be the total energy (per cm^3); then

$$E = \frac{p}{\gamma - 1} + \frac{1}{2}\rho u^2 + E_{rad} \tag{3.4}$$

where ρ is the density of the matter (gm/cm^3) and u is its velocity (cm/sec). Then the time rate of change of E (at a fixed location) can be written

$$\frac{\partial E}{\partial t} = \left(\frac{\partial E}{\partial t}\right)_1 + \left(\frac{\partial E}{\partial t}\right)_{rad} \tag{3.5}$$

Here $(\partial E/\partial t)_1$ is the rate of change of energy due to the mechanical, viscous, thermal effects, etc., and $(\partial E/\partial t)(rad)$ is the net increase in E per second due to radiation. If A is the radiation energy absorbed per second per cubic centimeter, and B is the radiation energy emitted per second per cubic centimeter, it follows that

$$\left(\frac{\partial E}{\partial t}\right)_{rad} = A - B \tag{3.6}$$

Or, since A − B is the negative of the divergence of the radiation flux, we can write

$$\frac{\partial E}{\partial t} = \left(\frac{\partial E}{\partial t}\right)_1 + A - B = \left(\frac{\partial E}{\partial t}\right)_1 - \text{div } \vec{F} \tag{3.7}$$

Equation 3.7 makes it possible to introduce the effect of radiation flux in the equation for conservation of energy where it was previously neglected.

3.1.1 The Hydrodynamical Equations[2] Including Radiation

For the case of radial symmetry (where r is the distance from the

2. The hydrodynamical equations are discussed in Chapter 2.

center and t is the time), neglecting P(rad), E(rad), viscosity, and thermal conductivity but including radiation flux, the hydrodynamic equations become

(1) Equation of Continuity

$$\frac{d\rho}{dt} = -\frac{\rho}{r^2}\frac{\partial}{\partial r}(r^2 u) \tag{3.8}$$

(2) Equation of Motion

$$\frac{du}{dt} = -\frac{1}{\rho}\frac{\partial p}{\partial r} \tag{3.9}$$

(3) Equation of Energy Balance

$$\frac{d}{dt}\left[\frac{1}{2}u^2 + \frac{p}{\rho(\gamma - 1)}\right] = -\frac{1}{\rho r^2}\frac{\partial}{\partial r}(r^2 F) \tag{3.10}$$

By algebraic manipulations of these relations it is possible to obtain an equation for the rate of change of entropy. This can be written in the form

$$\frac{d}{dt}\ln(p\rho^{-\gamma}) = \frac{(\gamma - 1)}{pr^2}\frac{\partial}{\partial r}(r^2 F) \tag{3.11}$$

In these equations, the symbol d/dt represents the substantial derivative

$$\frac{d}{dt} = \frac{\partial}{\partial t} + u\frac{\partial}{\partial r} \tag{3.12}$$

The radiation flux, F, in Eqs. 3.10 and 3.11 is the radial component of the vector quantity.

3.1.2 The Radiation Flux[3]

From very simple elementary considerations it is clear that the flux

---

3. Some useful references on radiative transfer are S. Chandrasekhar, Radiative Transfer, Clarendon Press, Oxford, 1950; S. Chandrasekhar, Introduction to the Study of Stellar Structure, University of Chicago Press, 1939; and S. Rosseland, Theoretical Astrophysics, Clarendon Press, Oxford, 1936.

of radiation can be expressed at any point in space as an integral over all space. Radiation which reaches the point in question, S or (x, y, z), must have been emitted by the matter at some other point, (x', y', z'); there are two possibilities: (a) the ray came directly from the point of emission, or (b) it was scattered once or more before reaching the point S. A great deal of the complication in radiative transfer problems comes from scattering. Fortunately, scattering cannot have an appreciable effect in our problems of interest and so we completely neglect it from the start. Our equations are, therefore, not in their most general form but should be satisfactory for treating the radiation phenomena resulting from a nuclear explosion.

Let us suppose that the material has a coefficient of absorption, μ_ν (cm^{-1}) for the frequency ν. Also, $B_\nu(x', y', z')$ is the energy emitted per cubic centimeter per second from the point (x', y', z') in this frequency range per unit frequency interval. Then it is desirable to define the radiation flux, $\vec{F}_\nu$, for this frequency range so that

$$\vec{F}(x, y, z) = \int_0^\infty \vec{F}_\nu(x, y, z)\, d\nu \tag{3.13}$$

and

$$B(x', y', z') = \int_0^\infty B_\nu(x', y', z')\, d\nu \tag{3.14}$$

From geometrical considerations it follows that the component of $\vec{F}_\nu(x, y, z)$ in the x direction, $\vec{F}_{x\nu}(x, y, z)$, can be expressed in terms of μ_ν and $B_\nu(x', y', z')$ by the integral

$$\vec{F}_{x\nu}(x, y, z) = -\iiint_{-\infty}^{\infty} B_\nu(x', y', z') \frac{\cos(x, L)}{4\pi L^2} \exp\left(-\int_0^L \mu_\nu dL'\right) dx'dy'dz' \tag{3.15}$$

Here L is the distance between (x', y', z') and (x, y, z), and $\cos(x, L)$ is the cosine of the angle that this line makes with the x axis. The integral, $\int_0^L \mu_\nu dL'$, is to be taken along the line joining the two points. Clearly

$\cos(x, L) = (x' - x)/L$. The validity of Eq. 3.15 depends upon the fact that scattering has been neglected. There are three conditions under which the radiation flux can be further simplified: (1) uniform distribution of matter at constant temperature over some part of space; (2) any one-dimensional problem; and (3) any system having very intense absorption. The first case corresponds to the penetration of radiation through the cold air to points far ahead of the shock wave. The second case represents an approximation to the spherical geometry when the radius of the point in question is large compared to the mean free path of the radiation. The third case leads to Rosseland's mean free path treatment for the diffusion of radiation.

One-Dimensional Radiation Flux Problem. Suppose that conditions only vary in one direction and the x axis is taken to be perpendicular to the plane of stratification. It is clear that F_y and F_z must vanish. The integral, Eq. 3.15, for $F_{x\nu}$ can be simplified by replacing the cartesian coordinates by the cylindrical coordinates, (ϕ', ρ', x'). The integration over ϕ' can be made immediately giving a factor of 2π. Now eliminating the variable ρ' in terms of the new variable, $s = (x'^2 + \rho'^2)^{1/2}$,

$$F_{x\nu} = -\frac{1}{2}\int_{-\infty}^{\infty} dx' \int_0^{\infty} B_\nu(x') \frac{x'}{s^2} \exp\left[-\tau_\nu(x, x') \frac{s}{x'}\right] ds \tag{3.16}$$

And integrating over s, we have finally

$$F_{x\nu}(x) = \frac{1}{2}\int_{-\infty}^{x} G_\nu(x')\, dx' - \frac{1}{2}\int_x^{\infty} G_\nu(x')\, dx \tag{3.17}$$

Here

$$G_\nu(x') = B_\nu(x') \{\exp[-|\tau_\nu(x', x)|] + |\tau_\nu(x', x)|\ \mathrm{Ei}[-|\tau_\nu(x', x)|]\} \tag{3.18}$$

where

$$\tau_\nu(x', x) = \int_{x'}^{x} \mu_\nu(x'')\, dx'' \tag{3.19}$$

and $\mathrm{Ei}[-|\tau_\nu(x', x)|]$ is the exponential integral. Equation 3.17 makes it comparatively easy to determine the radiation flux for any one-dimensional problem where the coefficient of absorption and the rate of emission are

known as a function of distance.

Intense Absorption of Radiation and the Method of Rosseland. The radiative flux can be expressed in a simple form if the absorption of radiation is so intense that the radiation is in local thermodynamic equilibrium with the matter.

If the medium were of infinite size and at constant temperature, the energy density, u_ν, of the radiation (in unit frequency range) would be characteristic of a black body at the temperature, T, of the matter

$$u_\nu = \frac{8\pi h\nu^3}{c^3} \frac{1}{e^{h\nu/kT} - 1} \tag{3.20}$$

If the matter has a coefficient of absorbtion, μ_ν, the energy absorbed in this frequency range per cubic centimeter per second would be $cu_\nu\mu_\nu$. The radiation emitted per cubic centimeter per second would be equal to this since a radiative equilibrium would exist

$$B_\nu = cu_\nu\mu_\nu \tag{3.21}$$

Now consider a situation in which the temperature varies so slowly that in a distance of $1/\mu_\nu$ very little change has taken place in $u_\nu\mu_\nu$ for all frequencies. Then to a first approximation, B_ν is given by Eq. 3.21 where u_ν is characteristic of the local temperature, $T(x', y', z')$. To the first approximation μ_ν varies sufficiently slowly with distance that it may be taken locally to be constant. Then if we make a Taylor's series expansion of u_ν in the neighborhood of (x, y, z), Eq. 3.15 becomes to the first approximation

$$F_{x\nu}(x,y,z) = -c\mu_\nu \int_{-\infty}^{\infty}\int\int \left[u_\nu(x,y,z) + \left(\frac{\partial u_\nu}{\partial x}\right)_{x,y,z}(x'-x) + \left(\frac{\partial u_\nu}{\partial y}\right)_{x,y,z}(y'-y) + \left(\frac{\partial u_\nu}{\partial z}\right)_{x,y,z}(z'-z)\right] \frac{(x'-x)}{L} \frac{\exp[-L\mu_\nu(x,y,z)]}{4\pi L^2} dx'dy'dz' \tag{3.22}$$

Integration of the terms involving u_ν, $\partial u_\nu/\partial y$, and $\partial u_\nu/\partial z$ gives zero since the integrand is antisymmetrical with respect to the term, $(x' - x)$. The remaining contribution can be integrated immediately in terms of spherical coordinates to give

$$F_{x\nu}(x, y, z) = -\frac{c}{3\mu_\nu}\frac{\partial u_\nu}{\partial x} \tag{3.23}$$

But since u is a function only of the local temperature, we can express this relation in the form

$$F_{x\nu}(x, y, z) = -\frac{c}{3\mu_\nu}\frac{du_\nu}{dT}\frac{\partial T}{\partial x} \tag{3.24}$$

Then according to Eq. 3.13 the total flux is given by

$$F_x = \int_0^\infty F_{x\nu}\,d\nu = -\frac{c}{3}\left[\int_0^\infty \frac{1}{\mu_\nu}\frac{du_\nu}{dT}\,d\nu\right]\frac{\partial T}{\partial x} \tag{3.25}$$

Rosseland[3] defined a mean free path, λ_R, for the thermal radiation such that

$$F_x = -\frac{c\lambda_R}{3}\frac{\partial E_{rad}}{\partial x} = -\frac{c\lambda_R}{3}\frac{d(aT^4)}{dT}\frac{\partial T}{\partial x} \tag{3.26}$$

And since

$$E_{rad} = aT^4 = \int_0^\infty u_\nu\,d\nu$$

a comparison of Eqs. 3.25 and 3.26 shows that[4]

$$\lambda_R = \frac{\displaystyle\int_0^\infty \frac{1}{\mu_\nu}\frac{du_\nu}{dT}\,d\nu}{\displaystyle\int_0^\infty \frac{du_\nu}{dT}\,d\nu} \tag{3.27}$$

4. Discussion of induced emission has been neglected in this treatment. The only result of the inclusion of this effect is to multiply the absorption coefficient by the factor $[1 - \exp(-h\nu/kT)]$. See any text mentioned in Ref. 3.

The Rosseland definition of the mean free path corresponds to simple kinetic theory of gas arguments. Light travels with the velocity c. At any one time 1/6 of the photons are moving in the x direction and 1/6 are moving in the opposite direction. If the mean free path is λ_R, the flux for radiation is given by Eq. 3.26.

3.1.3 Steady State Smearing Out of a Shock Front by Radiation

Because of radiation, the temperature and pressure at a shock front are smeared out so that there is no longer a mathematical discontinuity. Taylor and Maccoll[5] showed that this smearing out does not affect the shock velocity or pressure, but of course it does have a very profound effect on the radiation emitted by a shock wave.

Let us idealize the situation by assuming that the shock velocity, $\dot{R}$, and the shock temperature, T_s, do not vary with time; the temperature of the shocked material is T_s quite independent of r; and the shock radius, R, is so large compared to the zone of radiation smearing that we can neglect the effects of curvature. Consider a coordinate system moving in the z direction with the velocity $\dot{R}$. In this coordinate system, the position of the shock front remains constant and the velocity of the material entering the shock zone is $u = -\dot{R}$. Let z be the distance in front of the shock. The material in front of the shock front has the density ρ_0. The energy equation, Eq. 3.10, becomes for the material in front of the shock

$$\left(\frac{\partial}{\partial t} - \dot{R}\frac{\partial}{\partial z}\right)\left(\frac{1}{2}\dot{R}^2 + C_v T\right) = -\frac{1}{\rho_0}\frac{\partial F}{\partial z} \tag{3.28}$$

Here the internal energy per gram has been written in the form $C_v T$ [rather than the equivalent form $p/\rho(\gamma - 1)$ as given in Eq. 3.10], where C_v is the specific heat per gram of the material at constant volume. Once the steady state has been established,

$$\frac{\partial \dot{R}}{\partial t} = \frac{\partial (C_v T)}{\partial t} = 0$$

and Eq. 3.28 can be integrated to give

---

5. G. I. Taylor and J. W. Maccoll in W. F. Durand, Editor-in-Chief, Aerodynamic Theory, Vol. III, Div. H, J. Springer, Berlin, 1934-1936.

$$\frac{1}{2}\dot{R}^3\rho_0 + \rho_0\dot{R}\,C_vT - F = \text{constant} \tag{3.29}$$

The term $1/2\,\dot{R}^3\rho_0$ is itself constant, so that it can be subtracted from both sides of this equation to give a new constant. The new constant must be zero since the radiation flux a long way in front of the shock zone is essentially zero, the initial temperature of the cold air being so low that it can be neglected. Let us assume that the radiation flux can be expressed in the form

$$F = -\frac{c\lambda}{3}\,\frac{d(aT^4)}{dT}\,\frac{\partial T}{\partial z} \tag{3.30}$$

Here λ is "the radiation mean free path." For example, λ might be taken to be λ_R, the Rosseland mean free path, Eq. 3.27. Equation 3.29 then becomes

$$\rho_0\dot{R}\,C_vT + \frac{4}{3}\lambda\,caT^3\,\frac{dT}{dz} = 0 \tag{3.31}$$

If the mean free path varies with the nth power of the temperature,

$$\lambda = \lambda_0T^n \tag{3.32}$$

Equation 3.31 can be integrated to give

$$T^{n+3} + \frac{3(n+3)}{4}\,\frac{\rho_0\dot{R}\,C_v}{\lambda_0 ca}\,z = \text{constant} \tag{3.33}$$

When $z = 0$, $T = T_s$, so that the constant must be equal to T_s^{n+3}. If we let z_0 be the distance in front of the shock at which the temperature becomes zero,

$$z_0 = \frac{4\lambda_0\,caT_s^{n+3}}{3(n+3)\,\rho_0\dot{R}\,C_v} \tag{3.34}$$

so that Eq. 3.33 can be written in the form

$$\frac{z}{z_0} = 1 - \left(\frac{T}{T_s}\right)^{n+3} \tag{3.35}$$

or

$$T = T_s \left(1 - \frac{z}{z_0}\right)^{\frac{1}{n+3}} \tag{3.36}$$

For the cases in which we are interested, n is close to 3.

3.2 The Strong Blast Without Radiation

A treatment of strong blast waves with neglect of radiation has been given in some detail in Chapter 2. A second treatment due to Taylor[6] has actually been used in some of our later considerations, and so we shall summarize the results here.

If radiation is neglected, the explosion of an atomic bomb can be idealized by supposing that all of the energy is released at a mathematical point. G. I. Taylor showed that for this case (as long as the shock pressure, p_s, is large compared to the initial pressure of the cold air, p_0) the hydrodynamical solutions have a simple form. If R is the radius of the shock front,

$$p = p_0 R^{-3} f_1(r/R) \tag{3.37}$$

$$\rho = \rho_0 \psi(r/R) \tag{3.38}$$

$$u = R^{-3/2} \phi_1(r/R) \tag{3.39}$$

Here ρ_0 is the initial density of the cold air. The functions $f_1(r/R)$, $\psi(r/R)$, and $\phi_1(r/R)$ are obtained by direct substitution of p, ρ, and u into Eqs. 3.8, 3.9, and 3.10, taking the radiation flux to be zero. In general these functions depend upon the value of γ and must be obtained by numerical integration.

---

6. G. I. Taylor, Proc. Roy. Soc. (London), A201, 159 (1950).

The variation of the shock radius is obtained by satisfying the equations of conservation of mass, momentum, and energy at the discontinuity (shock front). It is found that

$$R = s(\gamma)t^{2/5}E_{tot}^{1/5}\rho_0^{-1/5} \tag{3.40}$$

Thus

$$\dot{R}^2R^3 = \text{constant} = \frac{4}{25}s(\gamma)^5 E_{tot}/\rho_0 \tag{3.41}$$

Here $s(\gamma)$ is a calculated function of γ; t is the time after the explosion, and E_{tot} is the total energy released by the explosion.

3.3 The Opacity of Air

Problems involving radiative effects in air can be divided roughly into four temperature regions. At very high temperatures (above 20,000°K) the absorption of air is due to bound-free and free-free transitions of atoms and positive atomic ions. In this temperature region we are interested in radiation diffusion and thus the Rosseland mean opacity, which has been calculated and is discussed in Section 3.3.1.

In the intermediate temperature region, between 5000°K and 20,000°K, the absorption is due to bound-free transitions of the negative ions O^- and N^- as well as bound-free transitions of the neutral atom and free-free transitions. Over much of this region the effect of the O^- ion is most likely dominant. The Rosseland approximation is not of interest to us in this region and we only consider the direct average of the absorption coefficient which gives the rate of emission of thermal radiation (see Eq. 3.21).

In the low intermediate temperature region between 2000°K and 5000°K, most of the air is present in molecular form and the absorption of its own thermal radiation is most likely dominated by the small amounts of NO_2 present. We are interested in two properties of this air: (a) the rate at which it radiates its own thermal radiation, since this property determines the length of time the shock front radiates; and (b) the absorption of higher temperature radiation which comes from the hot core (see Section 3.5.3). The absorption of very high energy radiation ($h\nu \geq 6.6$ ev) is by O_2 principally, but NO_2 absorbs strongly in the visible region and thus is important when the radiation temperature falls below 20,000°K.

In the low temperature region, below 2000°K, air is almost completely

transparent to low temperature radiation, since no NO_2 can be formed (see Section 3.5.3). It transmits all frequencies from λ = 1860 A ($h\nu$ = 6.6 ev) through the visible and its infrared transmission depends upon the moisture content.

3.3.1 High Temperature Opacity of Air (above 20,000°K)

The Rosseland mean free path, Eq. 3.27, can be expressed in the form[7]

$$\lambda_R = 8.5 \times 10^{-18} \frac{\rho\, T^2\, Mt}{g\, \bar{Z}^2} \exp\left(\frac{\psi}{kT}\right) \tag{3.42}$$

The function ψ is known as the "Fermi energy" and

$$\exp\left(\frac{\psi}{kT}\right) = \frac{2\,(2\pi m_e kT)^{3/2}}{N_e h^3} \tag{3.43}$$

Here N_e is the number of free electrons per unit volume, and m_e is the electron mass. $\bar{Z}^2$ is the square of the effective nuclear charge for the free-free scattering. It has been taken to be that for 3s,p electrons as determined by Slater screening constants. M is the average atomic weight, 14.42. The Gaunt factor,[7] g, actually varies slightly with temperature and density, but for these calculations it was taken as 0.875. It is probably within 10 per cent of this value throughout the range of interest.

Most of the calculation centers about the "guillotine factor," t.

$$t = \frac{S(W_i\ T_a)}{F_0} + \sum_{s=1}^{n} \frac{S(W_\sigma + 1/T_a) - S(W_\sigma/T_a)}{F_0 + F_s} \tag{3.44}$$

Here, the W_i's are the ionization energies of the various electrons in the mixture arranged in order of increasing magnitude, expressed in Rydberg units; T_a is the temperature in units of 157,800°C; $S(W_i/T_a)$ is the Strömgren function;[7] for all conditions of interest here $F_0 = 1$.

---

7. P. M. Morse, Astrophys. J., 92, 27 (1940); the factor $\exp(\psi/kT)$ is designated as $1/\eta$ by Morse.

$$F_s = \frac{2\ \exp(\psi/kT)}{\overline{Z}^2 T_a} \sum_{\sigma=1}^{s} \frac{Z_\sigma^4\ P(W_\sigma/T_a)\ \alpha_\sigma}{n_\sigma} \tag{3.45}$$

Here $\overline{Z}^2$ is the same factor appearing in Eq. 3.42. Z_σ is the effective nuclear charge on the electron having the ionization potential W_σ and principal quantum number n_σ. Z_σ was calculated from Slater screening constants for the various states of ionization. The factor α_σ is the fractional occupation of the shell in which the electron has the ionization potential W_σ. The factor $P(W_\sigma/T_a)$ is the probability of occurrence of the state σ; i.e., it is the fraction of atoms in the mixture having an electron in the state σ.

From the above discussion it is evident that the high temperature opacity problem consists principally in obtaining the composition of air under the conditions of interest. The probabilities of occurrence of each ionic species must be known and also the excited states of each of these. The compositions which were used are given in Chapter 7. The roughest feature of the opacity calculations was the neglect of excited states of the various ionic species. This was done because part of the composition calculations themselves were made treating all species as in their ground states. This method of treatment is more satisfactory for thermodynamic properties than for opacity. At some temperatures the opacity will be too large and at others it will be too small. Since opacity is a complicated function of relative positions of all the ionization and excitation potentials, it is difficult to put limits on the errors. However, in most of the region of interest practically all of absorption is due to L electrons and it is probable that the neglect of the line absorption is a more serious error.

The results of the calculations are given in Figs. 3.1 and 3.2. The calculations were made at several densities at each temperature, usually not the even densities which are shown in the figures; the values were obtained by graphical interpolation.

Calculation Procedure for High Temperature Opacity. Let x_0 be the fraction of original air atoms which are neutral oxygen atoms, and x_i be the fraction which is ionized i times. Let the corresponding quantities for nitrogen be $y_0, y_i, \ldots$. Then:

$$\sum_{i=0}^{8} x_i + \sum_{i=0}^{8} y_i = 1 \tag{3.46}$$

At the high temperatures of the calculation there are no molecules. The x_i's and y_i's corresponding to a given condition (temperature and density)

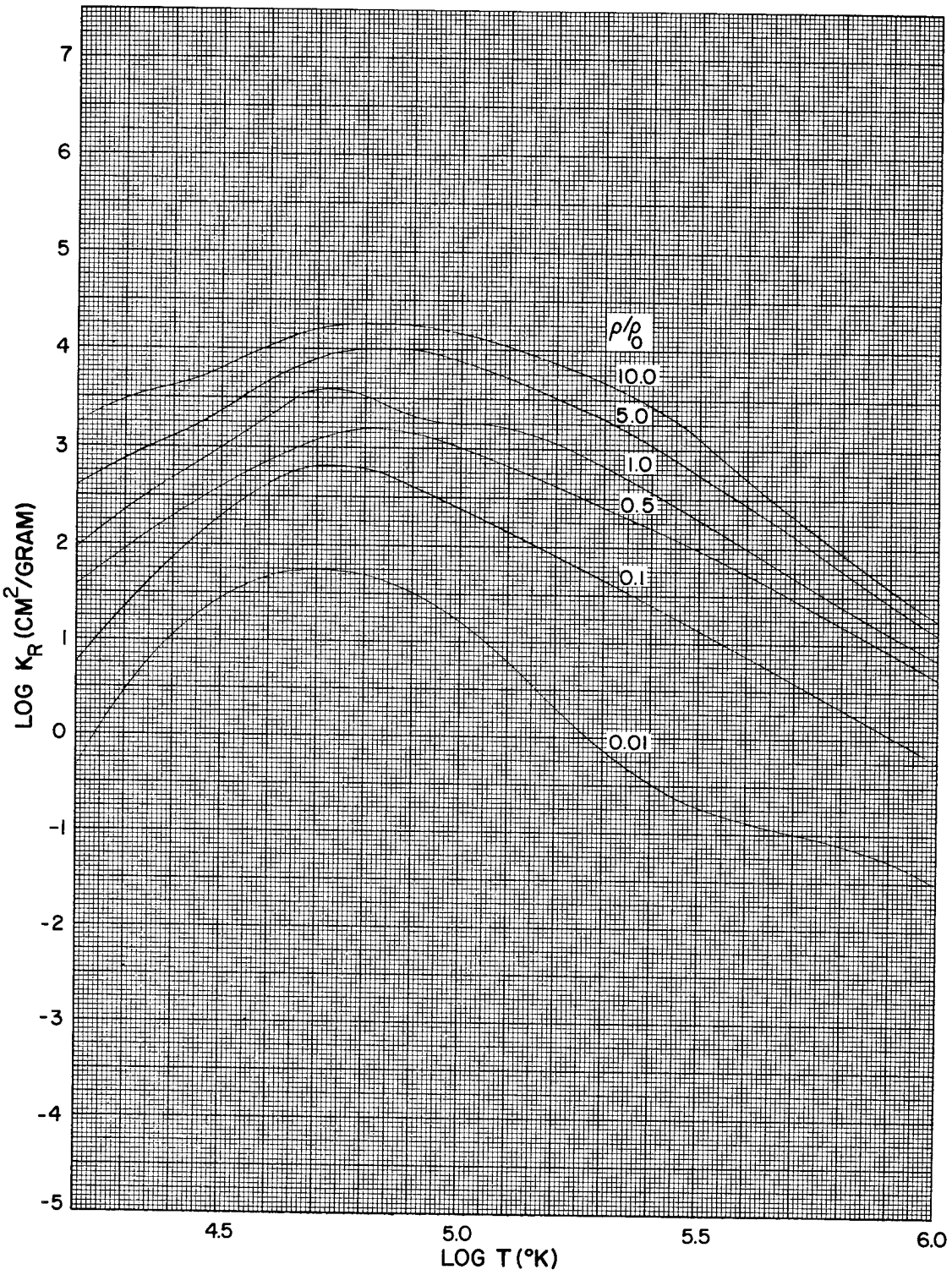

Fig. 3.1 Rosseland mean free path; $K_R = 1/(\rho\lambda R)$

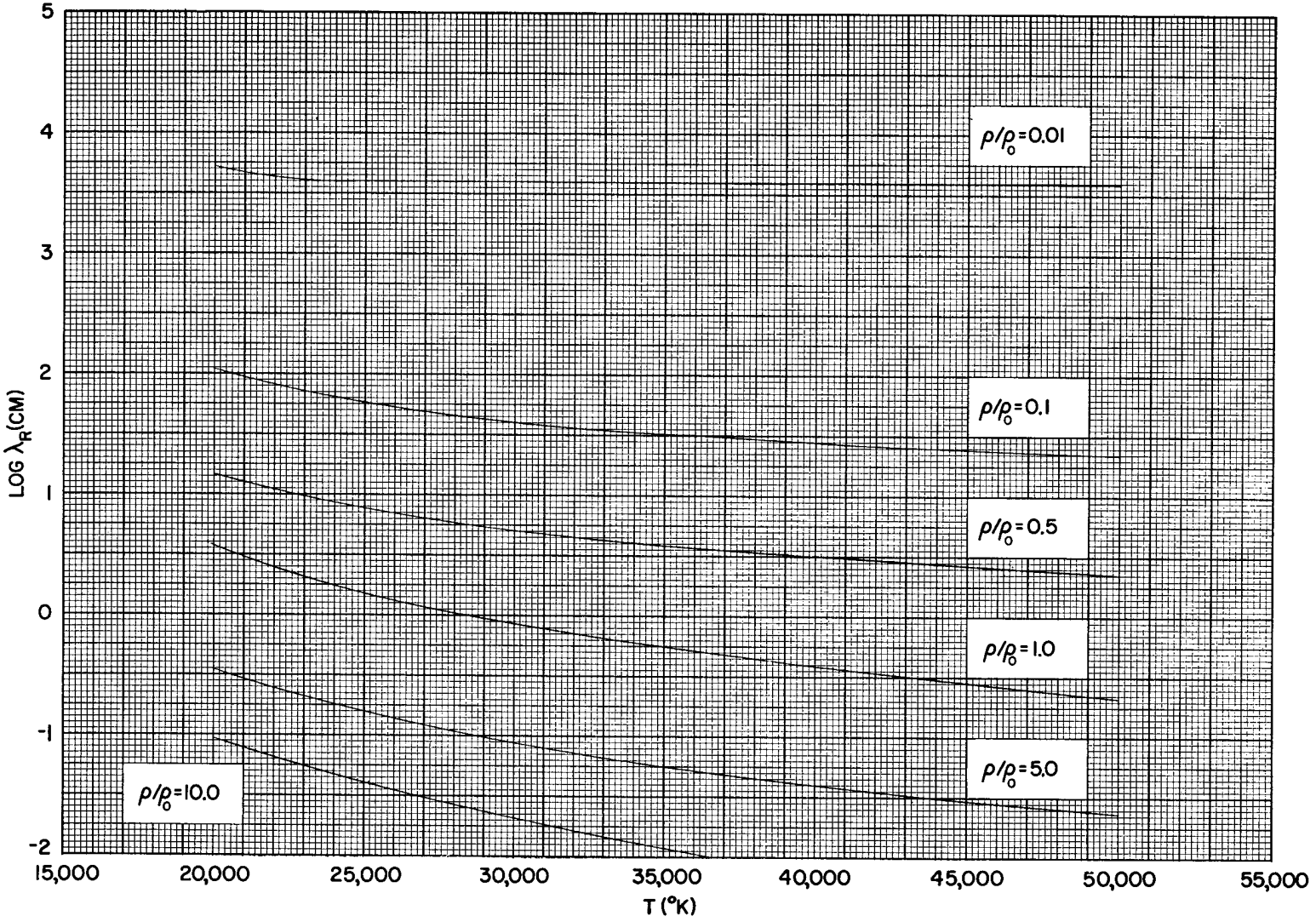

Fig. 3.2 Rosseland mean free path

were obtained from equation-of-state data. The various quantities necessary for the calculation are given in Table 3.1. Also,

$$\overline{Z}^2 = \sum x_i \, Z_{x_i}^2 + \sum y_i \, Z_{y_i}^2 \tag{3.47}$$

The charges for free-free absorption Z_{x_i}, Z_{y_i} were calculated for 3s,p electrons using Slater's screening constants. Most of the absorption is due to the photo-electric effect and so the calculation is not at all sensitive to this charge.

The values of F_s were then calculated, assuming that all of the ions were in their ground states. Pressure ionization was completely ignored. Finally, values of the factor t were obtained with the help of Morse's tables of the Strömgren function.[7]

3.3.2 Intermediate and Low Temperature Opacity of Air (20,000°K to 2,000°K

In this temperature region we are most interested in a frequency averaged absorption coefficient of radiation of temperature T_2 passing through matter at temperature T_1,

$$\overline{K'}(T_1, T_2) = \frac{\int_0^\infty K'_\nu(T_1)\, u_\nu(T_2)\, d\nu}{\int_0^\infty u_\nu(T_2)\, d\nu} \tag{3.48}$$

where $K'_\nu(T_1) = K_\nu(T_1)(1 - e^{-h\nu/kT_1})$; $K_\nu(T_1)$ is the mass absorption coefficient in square centimeters per gram for matter at the temperature T_1; $u_\nu(T_2)$ is the energy in black body radiation per unit frequency range at T_2. Such a frequency averaged absorption coefficient is useful in determining the transmission of thermal radiation of temperature T_2 through a region in which the temperature is T_1 (see Section 3.5.2). The coefficient $K'(T_1, T_1)$ gives the rate of emission of radiation, since according to Eq. 3.21[8]

8. The factor $(1 - e^{-h\nu/kT_1})$ due to induced emission was omitted from Eq. 3.21. We are also using K for the mass absorption coefficient (cm^2/gram) whereas before we used μ for absorption coefficient (cm); thus the factor ρ must be included in Eq. 3.49.

Table 3.1

DATA FOR OPACITY CALCULATION

Nitrogen

Degree Ionized	Spectroscopic Notation	Ionization Potential, ev*	α	Z_σ, photo-electric effect	Z_i, free-free effect
0	N I	14.54	5/8	3.90	0.75
1	N II	29.59	4/8	4.25	1.60
2	N III	47.39	3/8	4.60	2.45
3	N IV	78.42	2/8	4.95	3.30
4	N V	98.14	1/8	5.30	4.15
5	N VI	491.18	1	6.70	5.00

Oxygen

0	O I	13.598	6/8	4.55	0.90
1	O II	35.07	5/8	4.90	1.75
2	O III	54.84	4/8	5.25	2.60
3	O IV	77.38	3/8	5.60	3.45
4	O V	113.83	2/8	5.95	4.30
5	O VI	138.48	1/8	6.30	5.15
6	O VII	667.83	1	7.70	6.00
7	O VIII	870.59	1/2	7.00	7.00
8	O IX	--	0	--	8.00

*K. Fuchs, G. J. Kynch and R. Peierls, The Equation of State of Air at High Temperatures, Report MS-61, Dec. 1942.

$$B_\nu(T_1) = c\rho K'_\nu(T_1)\, u_\nu(T_1) \tag{3.49}$$

Here ρ is the density.

The total amount of energy radiated per unit time per unit volume is

$$\int_0^\infty B_\nu(T_1)\, d\nu = c\rho u(T_1) \frac{\int_0^\infty K'_\nu(T_1)\, u_\nu(T_1)\, d\nu}{\int_0^\infty u_\nu(T_1)\, d\nu} = c\rho K'(T_1)\, u(T_1) \tag{3.50}$$

where, of course,

$$u(T_1) = \int_0^\infty u_\nu(T_1)\, d\nu$$

Thus it is this average which is of interest in the determination of the rate of radiation from a region which absorbs only weakly.

Opacity due to O^- and O_2^-. A rough calculation of the absorption in the 5000°K to 10,000°K region has been made by consideration of the effect of O^- and O_2^- alone. Bates and Massey[9] have calculated the absorption coefficient of O^-. They use 2.2 ev for the ionization potential, whereas a more recent determination by Vier and Mayer[10] gave 3.07 ev. Wildt and Chandrasekhar[11] have reconsidered the absorption based on the new ionization potential, but in this section we shall use the values given by Bates and Massey. The absorption cross section appears to be rather sensitive to the actual position of the excited state of O^-; and for low velocities of the ejected electron (i.e., radiation of rather low temperatures, ≈1500°K), the absolute value of the cross section is uncertain to a factor of about 10. At higher temperatures (6000°K to 12,000°K for the radiation temperature), there is less uncertainty and the cross section seems to be almost constant, independent of the polarizability. (See Fig. 5 of paper by Bates and Massey.[9]) For the averaged absorption cross section

---

9. D. R. Bates and H. S. W. Massey, Phil. Trans. Roy. Soc. (London), Series A-239, 269-304 (1943).

10. D. T. Vier and J. E. Mayer, J. Chem. Phys. 12, 28 (1944).

11. R. Wildt and S. Chandrasekhar, Astrophys. J. 100, 87 (1944).

$$\overline{Q_D} = \frac{\int_0^\infty Q_D(\nu) \frac{u_\nu}{h\nu} d\nu}{\int_0^\infty \frac{u_\nu}{h\nu} d\nu} \tag{3.51}$$

we shall take $\overline{Q_D} = 0.7 \times 10^{-17}$ cm^2 per ion, independent of the temperature. The cross section in Eq. 3.51 is averaged over the number of photons per frequency range instead of over the energy as we have done in Eq. 3.48. In view of the other uncertainties, however, it would seem legitimate to use this average. With this procedure, the opacity only depends on the number of ions present.

Above about 5000°K, all O_2 is dissociated into atoms, and the opacity calculation is rather simple. Bates and Massey do not estimate the cross section for the molecular ion, but merely say that its effect should be of similar order of magnitude as for the O^- ion. We shall say that the effect per atom of O is independent of whether the molecules are dissociated or not.

Taking

$$\frac{N_{O^-}}{N_O} = 1.38 \times 10^{-16} N_e \frac{10}{T^{3/2}} \exp(11{,}090/T) \tag{3.52}$$

when N_{O^-}, N_O, and N_e are the number of O^- ions, O atoms and electrons per cubic centimeter, respectively; and

$$N_O = 0.4 \times 2.445 \times 10^{19} \left(\frac{\rho}{\rho_0}\right) \tag{3.53}$$

along with

$$\overline{Q_D} = 0.7 \times 10^{-17} \text{ cm}^2 \tag{3.54}$$

we get

$$K \frac{(\text{cm}^2)}{g} = 7.49 \times 10^{-12} N_e \frac{10}{T^{3/2}} \exp(11{,}090/T) \tag{3.55}$$

A convenient form for use is

$$\rho\bar{K}\left(\frac{cm^2}{cm^3}\right) = 9.66 \times 10^{-15} \left(\frac{\rho}{\rho_0}\right) N_e \frac{10}{T^{3/2}} \exp(11{,}090/T) \tag{3.56}$$

Some values of N_e for air are given in Table 3.2.

Graphs of the mean free path

$$\lambda = \frac{1}{\rho\bar{K}} \tag{3.57}$$

are given in Fig. 3.3.

Absorption of NO_2. An absorption coefficient for NO_2 throughout the range λ = 40,000 A to λ = 2500 A has been pieced together from data in the literature.[12]

In Fig. 3.4 are given data taken in the vicinity of normal temperature, 300°K, and it has been assumed in our rough calculations that this coefficient will be independent of temperature. In the vicinity of any one frequency, this is undoubtedly a very poor assumption, but the integrated effects should be much better. Again we are simplifying Eq. 3.48 since only the temperature of the radiation matters.

Values of $\bar{K}'$ averaged according to Eq. 3.48 are shown in Fig. 3.5. For NO_2 it is more convenient to define the absorption coefficient in terms of square centimeters per atmosphere instead of square centimeters per gram.

In Figs. 3.5 and 3.6 we have values of the mean free path

$$\lambda = \frac{1}{\bar{K}' \, P(NO_2)}$$

for air of various densities and temperatures. The values of ρ/ρ_0 and T refer to the condition of the air; the amount of NO_2 present is the equilibrium amount and has been obtained from Curtiss and Hirschfelder.[13] $P(NO_2)$ is

---

12. Louis Harris and G. W. King, J. Chem. Phys. 2, 51 (1934), λ = 40,000 to 15,000 A; J. K. Dixon, ibid. 8, 157 (1940), λ = 7000 to 4500 A; A. Farkas and H. W. Melville, Experimental Methods in Gas Reactions, London, Macmillan, 1939, λ = 4360 to 2650 A.

13. C. F. Curtiss and J. O. Hirschfelder, Thermodynamic Properties of Air, Vol. II, Report CM-472 University of Wisconsin Naval Research Laboratory, 1948.

Table 3.2

VALUES OF NUMBER OF ELECTRONS PER CUBIC CENTIMETER (N_e) IN AIR

ρ/ρ_0	T, °K					
	4000	6000	8000	10,000	15,000	20,000
0.01		3.72×10^{13}	1.51×10^{15}	1.38×10^{16}	2.11×10^{17}	4.35×10^{17}
0.1	1.78×10^{11}	1.10×10^{14}	4.79×10^{15}	4.37×10^{16}	8.86×10^{17}	2.9×10^{18}
0.5	4.79×10^{11}	2.24×10^{14}	1.05×10^{16}	1.02×10^{17}	1.94×10^{18}	3.14×10^{18}
1.0	7.24×10^{11}	3.24×10^{14}	1.38×10^{16}	1.38×10^{17}	2.85×10^{18}	1.22×10^{19}
5.0	2.09×10^{12}	8.63×10^{14}	2.87×10^{16}	3.07×10^{17}	6.48×10^{18}	2.86×10^{19}
10.0	3.02×10^{12}	1.41×10^{15}	3.89×10^{16}	4.22×10^{17}	9.11×10^{18}	4.13×10^{19}

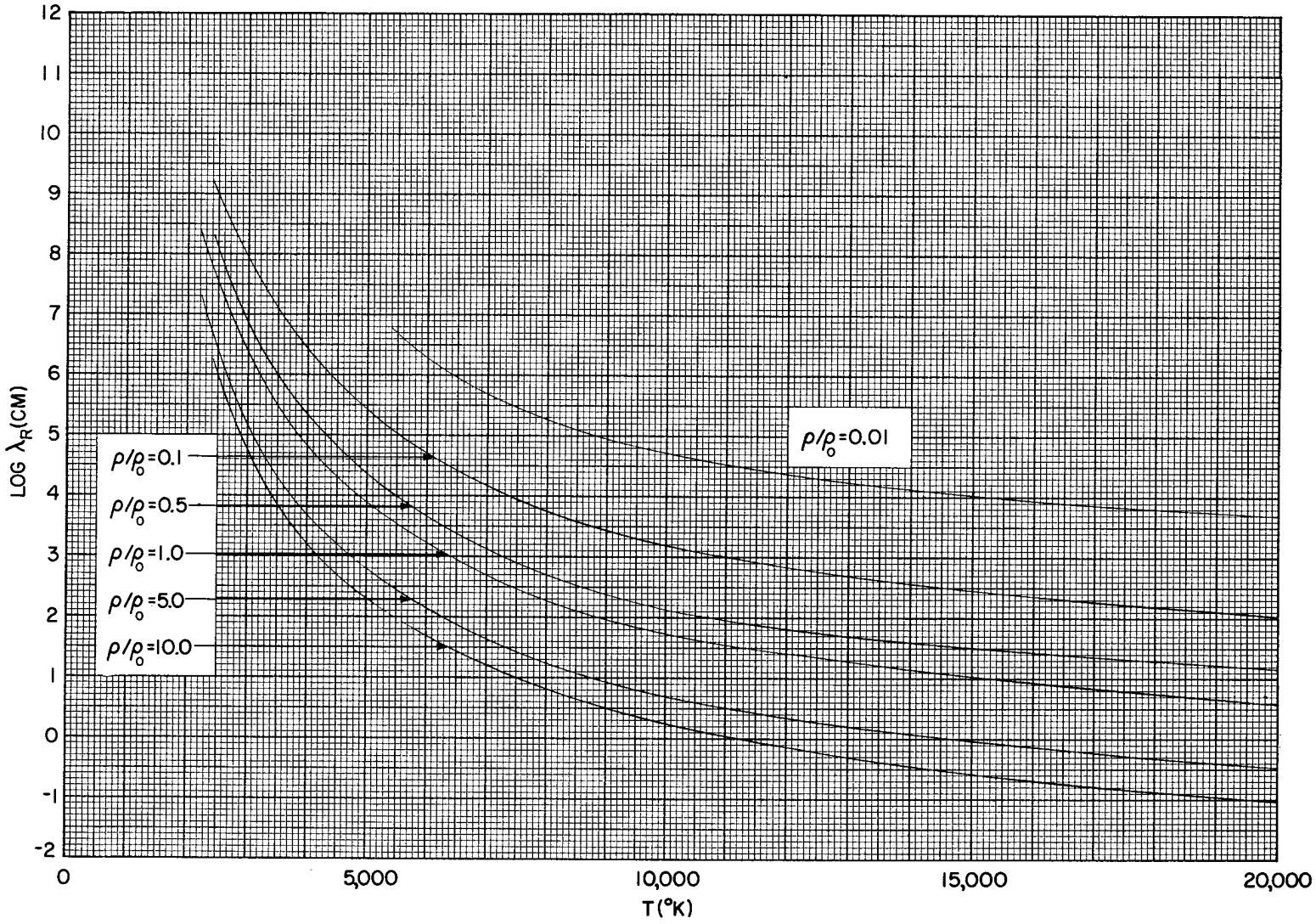

Fig. 3.3 Mean free path for absorption of radiation by O^- and O_2^-; $\lambda = 1/\rho\overline{K}$

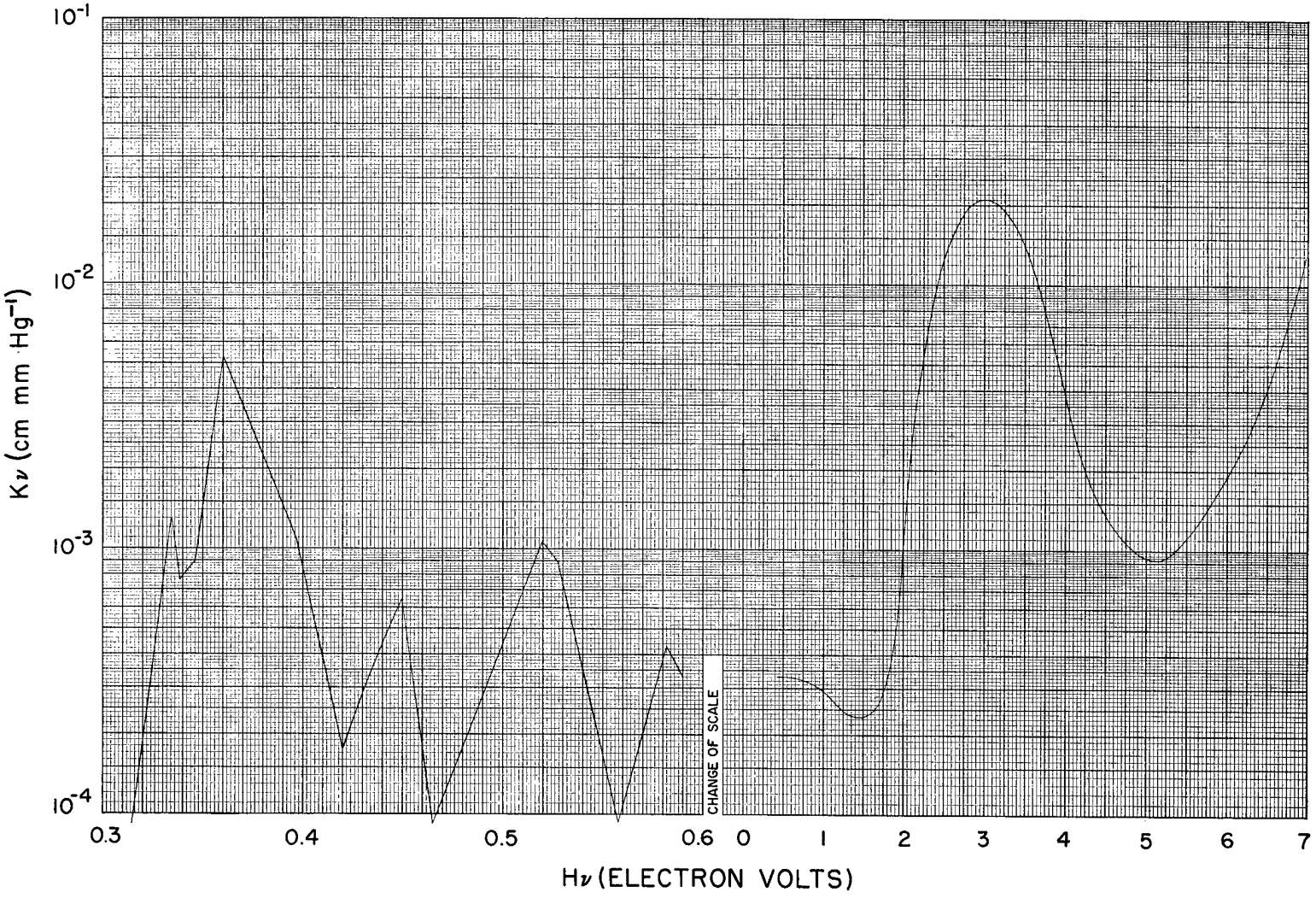

Fig. 3.4 Absorption coefficient of NO_2 for T ≅ 300°K

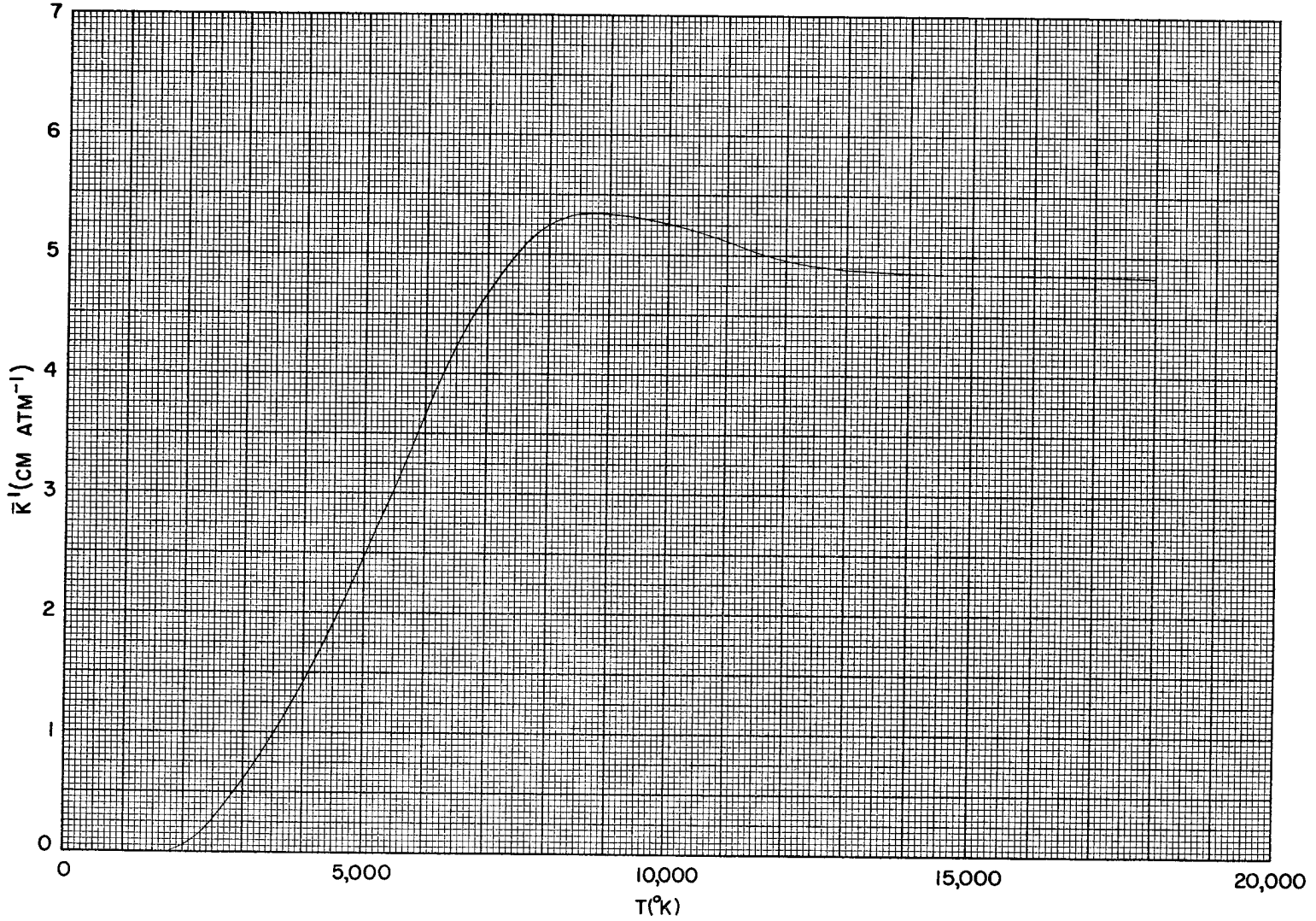

Fig. 3.5 Mean free path of radiation in NO_2, $\lambda = 1/\overline{K'}\ P(NO_2)$

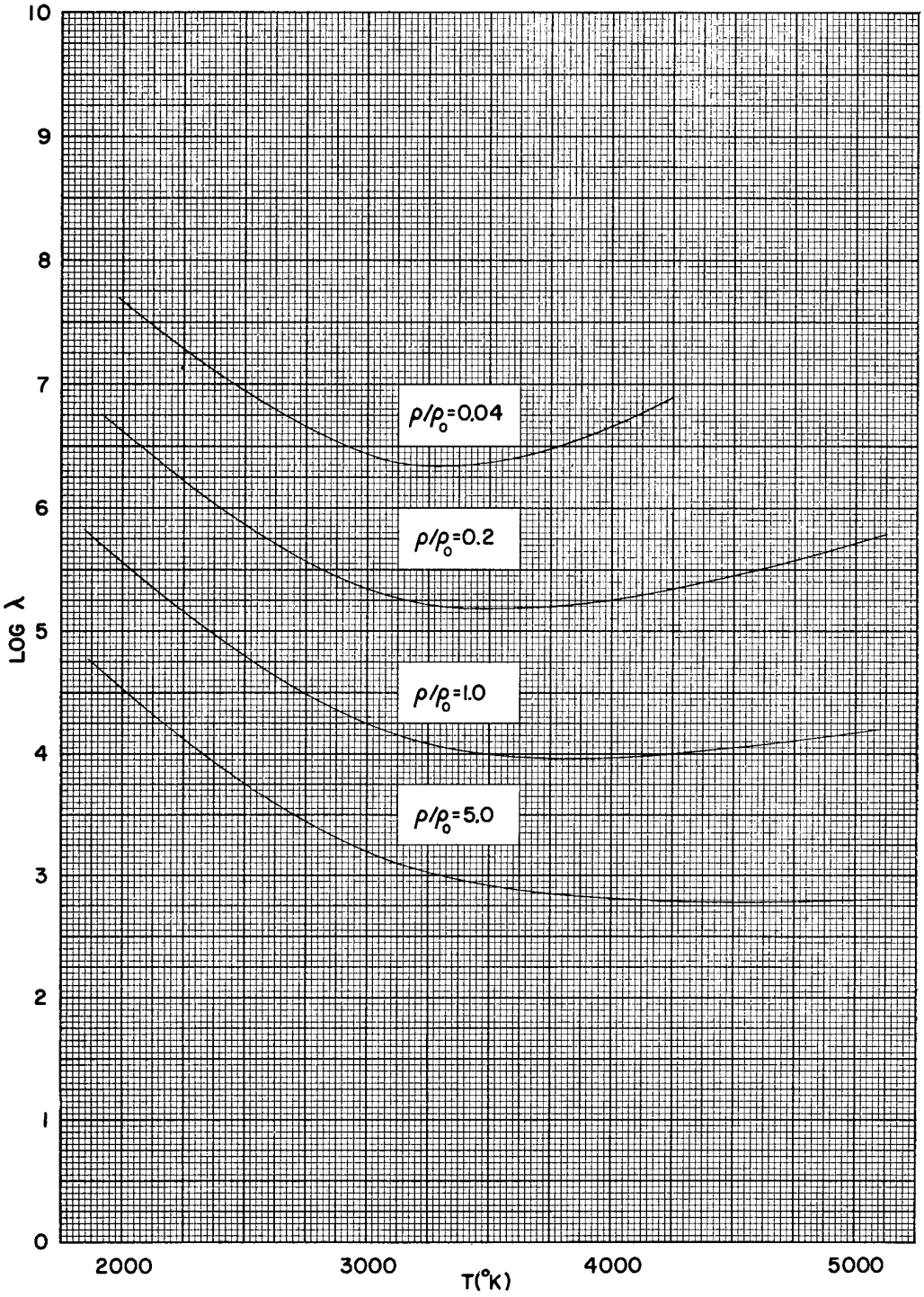

Fig. 3.6 Mean free path of radiation in NO_2; radiation the same temperature as the NO_2. $\lambda = 1/\bar{K}' \; P(NO_2)$

the partial pressure in atmospheres which the NO_2 would exert at 0°C. In Fig. 3.6 the values of λ are for black body radiation of the same temperature of the matter. In Fig. 3.7 the radiation is above 10,000°K; it is seen in Fig. 3.5 that the average absorption coefficient is approximately constant for radiation of all temperatures above 10,000°K. According to the theory presented in Section 3.5 it is the vanishing of the absorption coefficient of NO_2 at about 2000° that causes the ball of fire to darken suddenly as this temperature is reached.

Transient Effect in Opacity. The above considerations were made for air completely at equilibrium at the various indicated temperatures. It is well known that oxygen and nitrogen molecules transfer energy between vibrational and translational energy very slowly, and so a lag is expected in the establishment of complete equilibrium in the temperature region 5000°K and below. Thus, air cooling down into this temperature region is expected to contain vibrationally excited molecules for some rather long time period, probably many milliseconds. This condition will be particularly significant for air in which molecules have formed in three-body collision processes from atoms.

Another mechanism for creation of vibrationally excited molecules is from ultraviolet absorption; on re-emission of radiation to return to the ground electronic state of the molecule, the Franck-Condon principle insures that some of the molecules will obtain vibrational excitation.

The principal interest in vibrationally excited air molecules is in their transmission of high-energy ultraviolet radiation from the hot core. The absorption threshold for electronic absorption is reduced from 6.6 ev to a lower value depending upon the vibrational excitation, and thus the opacity is correspondingly higher.

No quantitative estimates have been made of this effect, but it is believed to be of importance.

3.3.3 Absorption of Air at Normal Conditions

The absorption of air in the ultraviolet at 300°K and 1 atm pressure has been reported.[14] These measurements cover the range from 792.5 A (15.64 ev) to 1860 A (6.66 ev). These are shown in Fig. 3.8. The absorption from 1860 A through the visible is essentially zero; also the absorption of air in the infrared is negligible.

---

14. E. G. Schneider, J. Opt. Soc. Amer. 30, 128 (1940).

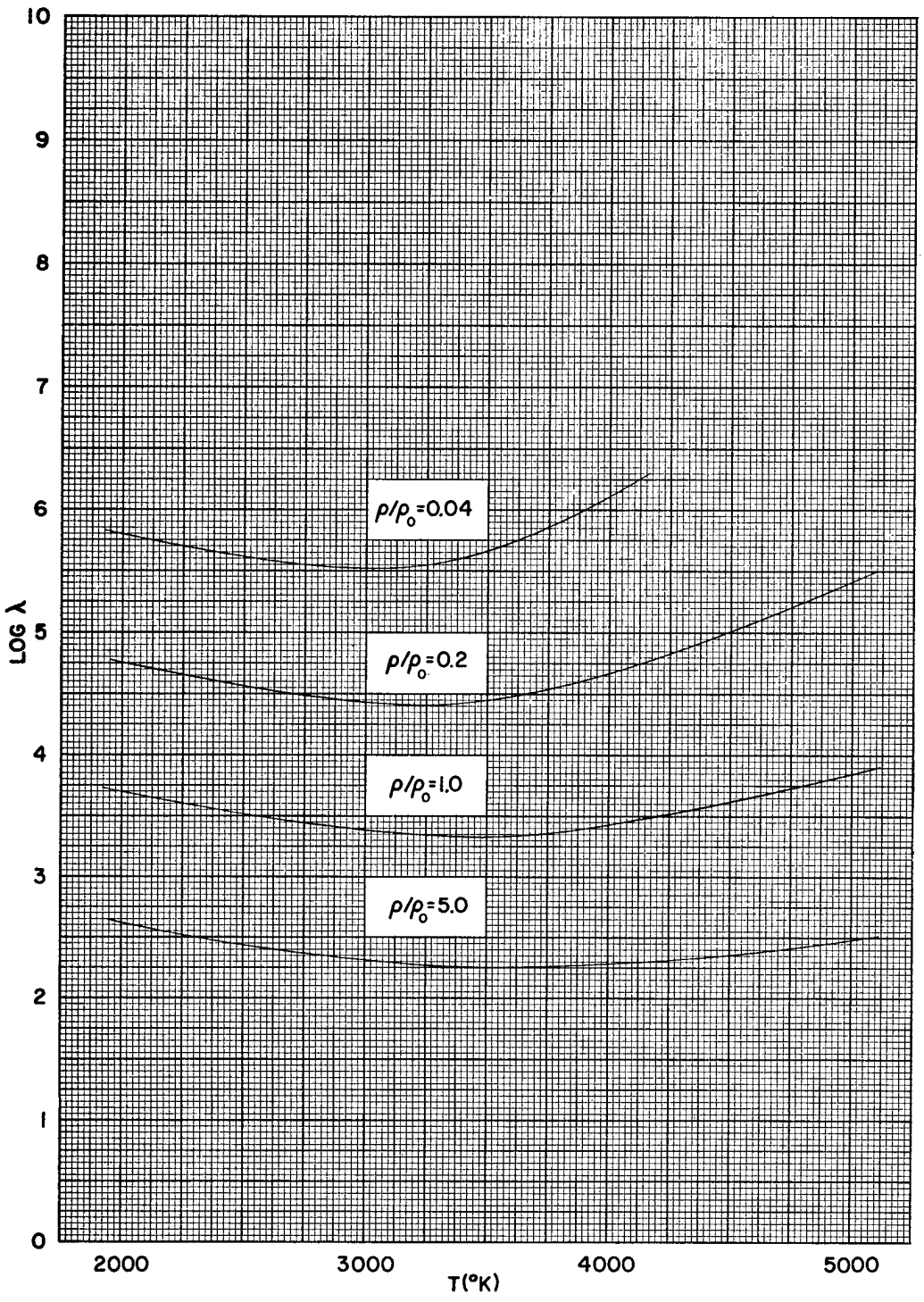

Fig. 3.7 Mean free path of radiation in NO_2; the radiation temperature above 10,000°K

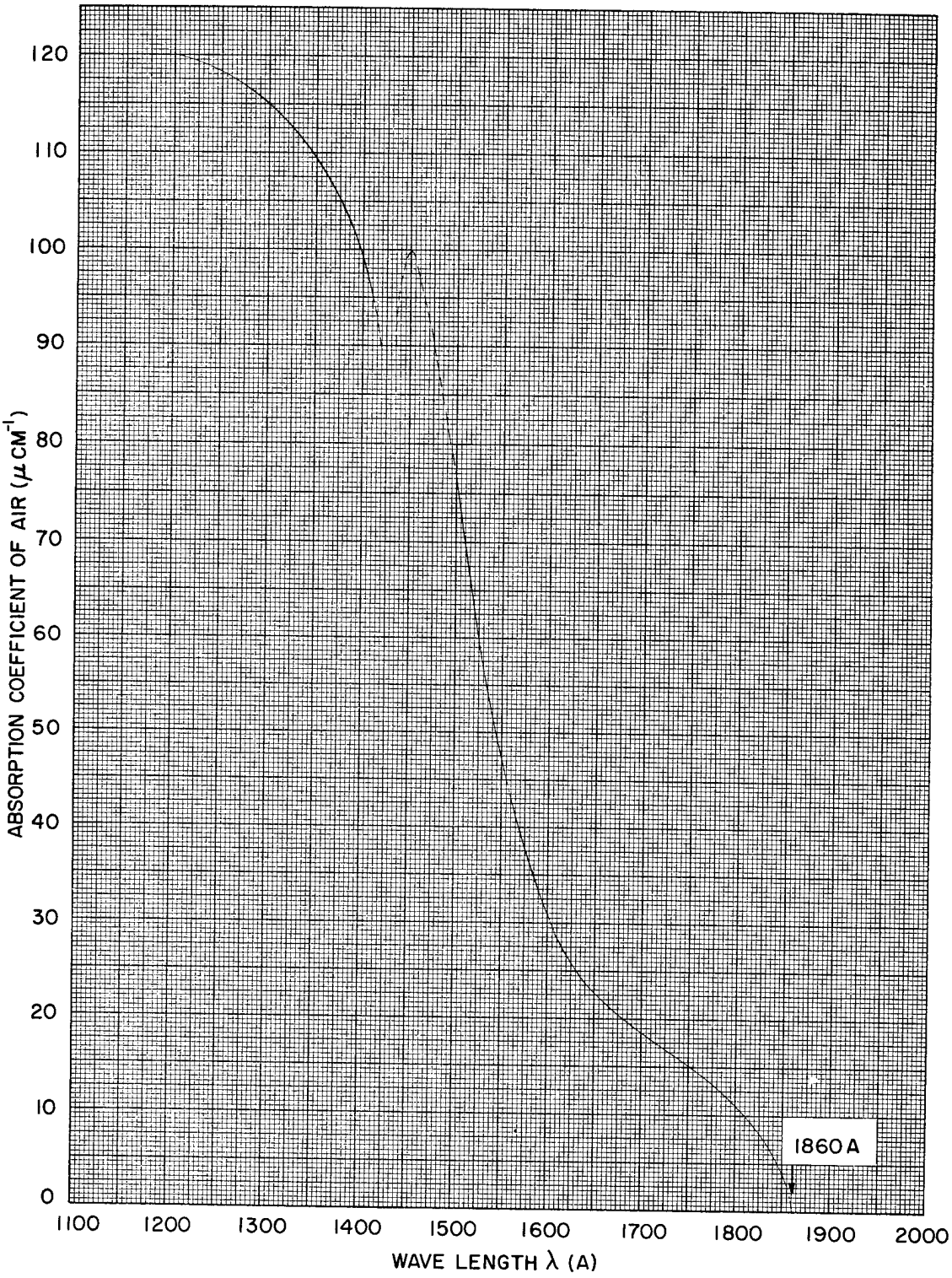

Fig. 3.8 Absorption of air; T = 300°K; p = 1 atm

3.4 Radiation Expansion Period and the Formation of the Blast Wave

We shall now consider the initial period of radiation expansion before a true strong air shock is formed at about 10 meter radius. This period is characterized by having the air first heated to a high temperature by radiation before it is set into motion by hydrodynamical signals from the explosion. The description offered here is qualitative.

We shall find that there is a very well defined point at which energy transfer by radiation becomes unimportant compared with work done by mechanical accelerations. In order to investigate the problem, let us consider the expansion of a parcel of air which has been affected during this period, and let us say that the expansion occurs in a pseudo adiabatic manner, with an effective specific heat ratio $\overline{\gamma}$. The equation

$$\frac{d}{dt} \ln (p\rho^{-\overline{\gamma}}) = 0 \tag{3.58}$$

describes this process. Now subtract this equation from Eq. 3.11, which describes the process when radiation is considered explicitly.

$$(\overline{\gamma} - \gamma) \frac{d}{dt} \ln V = -\frac{(\gamma - 1)}{pr^2} \frac{\partial}{\partial r} (r^2 F) \tag{3.59}$$

where $V = 1/\rho$. Using the equation of continuity (3.8), we can write

$$(\overline{\gamma} - \gamma) \frac{\partial}{\partial r} (r^2 u) = \frac{(\gamma - 1)}{p} \frac{\partial}{\partial r} (r^2 F) \tag{3.60}$$

The conditions in the body of the fluid then obey the usual hydrodynamical relations, neglecting radiation, but replacing γ by $\overline{\gamma}$. However, if a shock front exists, γ rather than $\overline{\gamma}$ appears in the Hugoniot relations:

$$\frac{\rho_s}{\rho_0} = \frac{\gamma + 1}{\gamma - 1} \tag{3.61}$$

$$\frac{p_s(R)}{\rho_s} = \left(\frac{2}{\gamma + 1}\right) \dot{R}^2 \tag{3.62}$$

Fortunately, an appreciable era does not exist in which both radiation and shock are of equal importance for the hydrodynamics. We shall now show that the value of $\bar{\gamma} - \gamma$ varies as $R^{-16.5}$. This means that when an air shock forms, it very quickly becomes dominating. To show this dependence on radius, we can examine the Taylor similarity solution for strong shock waves (Section 3.2).

$$p \sim R^{-3}$$

$$T \sim p/\rho \sim R^{-3}$$

$$u \sim R^{-3/2}$$

If we assume that

$$\lambda_R \sim T^3 \, (\rho_0/\rho)$$

then according to Eq. 3.26

$$F = -\frac{4c\lambda_R}{3} aT^3 \frac{\partial T}{\partial r} \sim R^{-21}$$

Therefore, from Eq. 3.60

$$\bar{\gamma} - \gamma = -\frac{(\gamma - 1)\frac{\partial}{\partial r}(r^2 F)}{p\frac{\partial}{\partial r}(r^2 u)} \sim \frac{R^{-21}}{R^{-3} R^{-3/2}} = R^{-16.5} \qquad (3.63)$$

Of course a strong shock formed in the manner just described would not immediately have a good Taylor similarity, but the conclusion that the shock forms suddenly is not very dependent on this detail. Although the radius at which the shock forms is not explicitly given by this treatment, it is determined within rather narrow limits in any particular case. The following figures (Table 3.3) for a 10,000 ton explosion illustrate the use of this treatment.

Table 3.3

SOME PROPERTIES OF THE BLAST WAVE
DURING RADIATION EXPANSION PERIOD

R, cm	E_{rad}/E_{int}	$\dot{R}$, cm/sec	T, °K	$\bar{\gamma} - \gamma$
841	0.0035	4.8×10^6	492,500	0.28
1015	0.00123	3.8×10^6	328,300	0.032
1122	0.00052	3.3×10^6	246,250	0.0058
1271	0.00022	2.6×10^6	180,000	0.0011

The internal energy (E_{int}) and temperature relation was calculated with a hypothetical bomb model using the equation of state for air due to Fuchs, Kynch and Peierls (see Table 3.1 reference). $\dot{R}$ was calculated with use of Eq. 3.62 and the assumption that the pressure, p_s, corresponds to an isothermal distribution of the matter within the radius R. One can be sure that the radiation is important as long as $\bar{\gamma} - \gamma$ is of the order of $\gamma - 1$ or greater. The exact place is not easy to determine, but in view of the very rapid variation of $\bar{\gamma} - \gamma$ with R, it is really not important that one locate the initial air shock radius exactly. It seems reasonable to say that the air shock forms at between 10 and 12 meters for a 10,000 ton explosion, probably more nearly 10 meters. This consideration suggests that the temperature has a unique role and a criterion may be stated that an air shock will form when the isothermal sphere temperature drops to approximately 300,000°K.

It is to be noted that the fraction of energy in the form of radiation (column 2 of Table 3.3) is very small, even in the radiation expansion phase.

At this point we shall make a second consideration which also gives an indication of the radius at which the air shock forms. Let us consider propagation of energy from an explosion with a constant velocity, which, of course, is only an approximate description of the actual situation. There is always radiation heating preceding a shock: if the radiation front is far ahead of the shock, we have the initial radiative phase. If the two fronts are close together, we get a good description of the structure of the shock front at later times.

The mathematical details of this model are considered in Section 3.1.3

above. For the same 10,000 ton explosion, values of z_0 calculated with Eq. 3.34 are shown in Table 3.4. As before, there is no definitely indicated value of R at which the radiative phase has ended. However, when z_0 becomes much less than R, it is clear that radiative transport of energy is much less important than hydrodynamical transport. For R = 8.41 meters, $z_0/R = 0.12$; and at R = 10.15, $z_0/R = 0.013$. Radiation is certainly important in the first case, and of little importance in the latter.

The differential treatment of Section 3.1.3 breaks down when λ_0 is comparable with z_0, and an integral method should really be used. However, the conclusions drawn above would not be changed by such an improved treatment.

Table 3.4

SOME PROPERTIES OF THE BLAST WAVE
DURING RADIATION EXPANSION PERIOD

R, meters	$\dot{R}$, cm/sec	E_{rad}/E_{int}	λ_0, cm	z_0, cm
5.07	5.98×10^6	3.38×10^{-3}	61	226
8.41	4.75×10^6	3.53×10^{-3}	20	98
10.15	3.77×10^6	1.23×10^{-3}	6	13
11.22	3.28×10^6	5.24×10^{-4}	2.5	2.6
12.71	2.59×10^6	2.17×10^{-5}	1.1	0.54

3.5 Radiative Effects in Strong Blast Period

In this section we shall describe the effects of radiation during the strong blast period as perturbations on the radiationless strong blast, which has been treated in Chapters 2, 4, and 6.

3.5.1 Qualitative Effects of Radiation in Strong Air Blast

In the last section we saw that the strong air shock formed when shock transmission became faster than radiative transmission of energy into the

cold air. During the initial phase of the strong shock, the radiation front continues to exist, behind the shock front, and carries the high temperatures of the core outward, by radiation diffusion, into the air through which the shock has already passed. The motion of this "internal radiation front" is considered in more detail in Section 3.5.2.

It might be well to point out that the hot core bounded by the internal radiation front is the same as the isothermal sphere of the small $(\gamma - 1)$ theory of Chapter 4. In the radiationless theory presented in Chapter 4, the amount of air contained in the isothermal sphere does not change at all as it expands to atmospheric pressure.

The motion of the internal radiation front is understood qualitatively in terms of the dependence of the opacity of air on temperature. The Rosseland mean opacity, which controls the diffusive transport of radiation, decreases with temperature above 50,000°K (see Fig. 3.1). The internal radiation front is, of course, formed at a temperature of about 300,000°K and thus as it diffuses out (through the air already affected by the shock) the radiation mean free path decreases at first as the temperature drops. Thus for a while there remains a well-defined radiation front moving more slowly as time increases. As the temperature of the core approaches 50,000°, however, the diffusion mechanism breaks down since the mean free path increases as the temperature drops. The energy from the hot core is now radiated very strongly into the colder air ahead.

The energy radiated at this time by the 50,000° core is not lost to the blast. Most of it ($h\nu \geq 6.6$ ev) is absorbed strongly in O_2 molecules and these exist in large numbers in air below 5000°K. At the time the core reaches 50,000°, the shock radius is about 80 meters and the shock temperature is 3000°K. As the temperature of the core falls, the absorption of NO_2, which is present in the air between 2000° and 5000°, becomes more important. This compound absorbs most of the visible spectrum. As noted in Section 3.3.2, there will also be absorption due to vibrationally excited air molecules, particularly O_2, present in excess of their equilibrium concentration. During this period the radiation flux actually strengthens the blast since it transports energy closer to the front, which of course tends to increase the pressure.

Although at the time the core starts radiating strongly the cold air ahead is so opaque that essentially none of the radiation is transmitted through the shock front, this situation starts changing immediately. Three circumstances increase the transmission of the air ahead of the core as the time progresses: (a) as the temperature of the core drops due to radiation and expansion, a larger fraction of its emitted radiation is below $h\nu \geq 6.6$ ev and is therefore transmitted by O_2; (b) the amount of NO_2 and vibrational excitation formed in the air is limited to the region in which the

shock temperature was 2000°K or higher (see Section 3.5.3); (c) the absorbing zone expands with time so that it becomes too tenuous to absorb a significant fraction of the radiation.

Soon after the shock front stops radiating, at about 80 to 100 meter radius, radiation from the hot core is transmitted and the brightness of the ball of fire reaches a second maximum. Thereafter, the ball of fire cools itself, by loss of radiation, in about 3 sec; very little energy is radiated at later times.

3.5.2 Diffusive Motion of the Internal Radiation Front

After the strong shock forms, for a while we know that the shock front moves much faster than the internal radiation front. At this time the mean free path of the radiation is falling with the temperature (see Fig. 3.1). From the approximate solutions for strong shocks (with neglect of radiation) we know the variation of pressure and density behind the shock as a function of the time. An approximate treatment of the internal radiation front can be made by calculating the transmission of radiation through a region which has these properties. The ambient temperature of this region is (inconsistently) taken as zero, which is permissible if T_0 is much larger than T_s.

A similarity solution for the motion of the internal radiation front can be found under these conditions. The result can be given as

$$r_0 = \left[1.916 \times 10^4 \, E^{0.698} \, R^{0.733} - 6.015 \times 10^8\right]^{1/3} \tag{3.64}$$

Here r_0 is the Lagrangian coordinate of the radiation front, the original position in centimeters of the matter which is at the radiation front when the shock front is at R. The yield of the explosion in tons of TNT equivalent is given by E. For 10,000 tons of TNT yield this relation of r_0 vs R is shown graphically in Fig. 3.9. Also the actual radius of the radiation sphere, R_0, is given; R_0 and r_0 are related by the continuity equation.

$$\rho_0 dr_0^3 = \rho dR_0^3 \tag{3.65}$$

The relation between shock radius, R, and pressure, p_s, is given by the Taylor theory; and the relation between the shock pressure, p_s, and internal pressure, p_i, is taken from the small $(\gamma - 1)$ theory (Chapter 4)

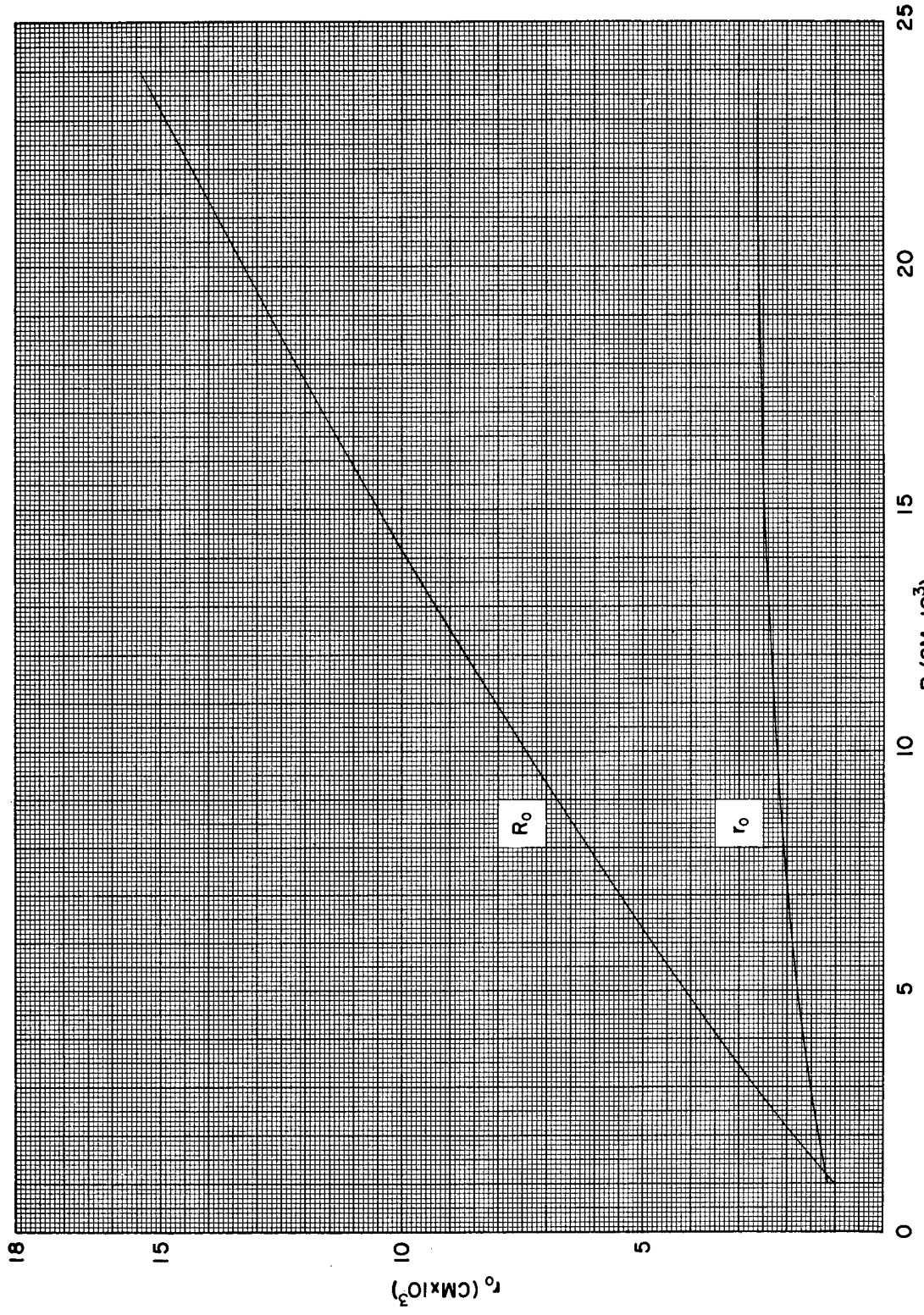

Fig. 3.9 Radius of internal radiation front (r_0) vs shock radius (R)

$$\frac{p_s}{p_i} = 2.205 \tag{3.66}$$

We can also write

$$r_0 = \left[1.030 \times 10^8 \; E^{0.942} \; p_i^{-0.244} - 6.015 \times 10^8\right]^{1/3} \tag{3.67}$$

Solution 3.64 was derived using the following relations.

(1) Mean free path for radiation

$$\lambda = \lambda_1 \left(\frac{T}{T_1}\right)^j \left(\frac{\rho_1}{\rho}\right)^m$$

j was taken as 1.5; $\frac{\rho_1}{\rho_0} = 0.1$

m was taken as 1.5; $T_1 = 5 \times 10^4$ °K

$\lambda_1 = 10$ cm

(2) Shock radius

$$R^{5/2} = \frac{5}{2}\sqrt{\frac{p_0(\gamma + 1)\, Qt}{2\rho_0}}$$

$\gamma = 1.25$

$Q = 4.156 \times 10^9 \; E_{tot}$

(3) Definition of W_0

$$W_0^{\;3} = z_0^{\;3} + \frac{M_0}{\frac{4\pi}{3}\rho_0} = z_0^{\;3} + 6.015 \times 10^8$$

(4) Equation of state

$$\frac{T}{T_1} = \frac{p}{p_1}\frac{\rho_1}{\rho}$$

(5) Specific heat

$$C_p = 9.52 \times 10^7 \text{ ergs/deg gram}$$

Figure 3.9 shows that as the shock front goes from 10 meters to 240 meters, the value of r_0 increases from 10 meters to about 26. There is therefore a considerable amount of air taken into the initial isothermal sphere as the shock develops. This calculation yields approximately correct results initially when the mean free path of the radiation is sufficiently small and given by the relation (1) above. From Fig. 3.2 we know that for temperature below about 50,000°K the Rosseland mean free path increases with decreasing temperature. Thus the calculation breaks down badly as the core temperature approaches this value. The direction of error in this calculation is clear: the internal front will move further than indicated here, since radiation transport is faster than assumed.

3.5.3 Radiative Cooling of the Hot Core

After the diffusion mechanism breaks down, the flux of radiation from the core into the region of the shock front starts increasing. In order to investigate this effect quantitatively, consistent starting conditions must be available. Our diffusion calculation of Section 3.5.2 took air temperature ahead of the internal radiation front as zero, and the IBM calculation neglected radiation altogether, so we are left without a consistent description of this period. However, a calculation of the radiation flux from the core into the 5000° temperature region using Eq. 3.17 and the IBM temperature and density contours shows how this growth occurs, and is given in Fig. 3.10. The first (rising) part of the dashed curve gives this calculation. This radiation is prevented from escaping through the shock front by means of the molecular absorbing materials formed in the air below 5000°K. The most important of these are O_2 and NO_2. It is clear that O_2 will be present in abundance in this temperature region but the NO_2 problem requires some consideration.

Formation of NO_2 in Shocked Air. Curtiss and Hirschfelder[13] have calculated the equilibrium concentrations of NO_2 in air for temperatures

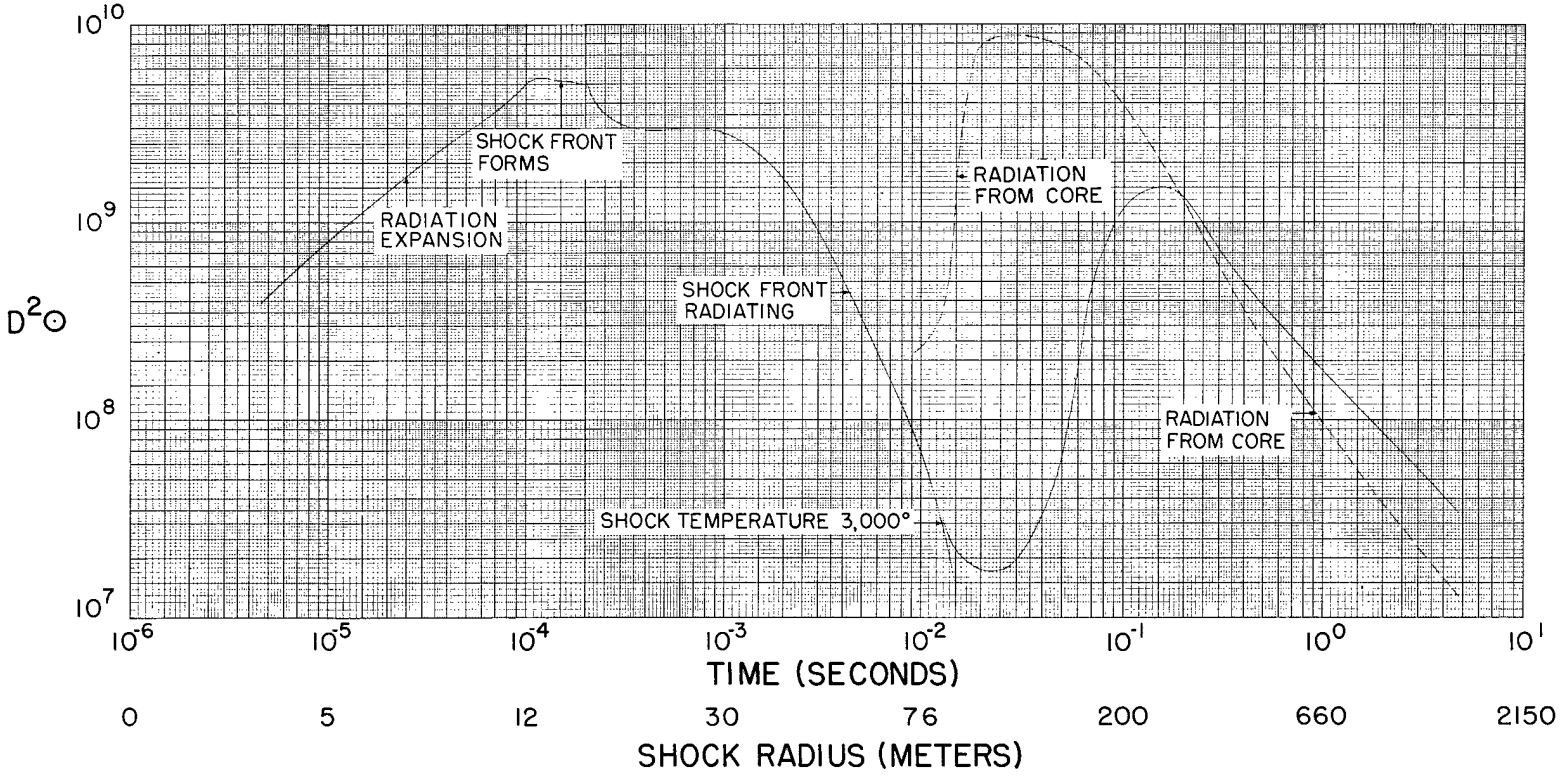

Fig. 3.10 Over-all time history of the blast wave

below 5000°K. Of course the air has no NO_2 at all before it enters the shock and so some time is required to form NO_2 after the air is heated by the shock. Formation of NO_2 in heated air under laboratory conditions has been studied by Daniels. Presumably the mechanism for formation is in two steps

(a) $N_2 + O_2 \rightarrow 2\ NO$

(b) $2\ NO + O_2 \rightarrow 2\ NO_2$

Reaction (b)[15] is extremely fast at all temperatures above 600°K and will always maintain equilibrium between NO, O_2 and NO_2. The rate of reaction (a) is strongly temperature dependent and so effectively one can say that it takes place above a certain temperature and does not occur below this temperature. We have selected 2000°K for this temperature from data furnished by Daniels.[16]

The NO_2 zone is therefore limited to the air which was initially within 100 meters, since the shock temperature is 2000°K at this distance.

Last Stage of the Cooling. At the time the core starts radiating most strongly, the shock front is most opaque and therefore the radiated energy

---

15. Hans J. Schumacker, Chemische Gasreactionen, T. Steinkopff, Dresden und Leipzig, 1938.

16. Farrington Daniels, private communication.

$$NO_2 + O_2 \underset{k_b}{\overset{k_j}{\rightleftharpoons}} 2\ NO \qquad k_j = 10^{8.5} \exp-(45{,}280/T)\ (\text{atm sec}^{-1})$$
$$k_b = 10^{9} \exp-(34{,}000/T)\ (\text{atm sec}^{-1})$$

Air at the shock front when the temperature is 2000°K has a pressure of about 10 atm O_2 and 40 atm N_2.

$$\frac{dp_{NO}}{dt} = 10^{8.5}\ e^{-22.640} \times 400 = 400 \times 10^{-1.33} = 18.7\ \text{atm/sec}$$

The rate of formation of NO is 0.019 atm/msec while the equilibrium partial pressure is 0.4 atm. The shock front moves about a meter per millisecond and so obviously the NO_2 equilibrium does not have time to be established. A similar calculation shows that at 2500°K the equilibrium is easily established within a millisecond. The indicated NO_2 "cutoff" is thus below 2500°K and we have arbitrarily taken 2000°K as the limit.

is essentially all absorbed behind the front. There are about two optical depths for high temperature radiation due to the NO_2 alone, and at this time O_2 in its lowest state is also very effective since the radiation has a temperature of about 40,000°K. We have not followed the decrease in opacity of the absorption layer as it expands, but by the time the shock front reaches 300 meters there is certainly negligible absorption of 20,000°K radiation by all outside layers. The ball of fire finally radiates as a hot mass of gas without self absorption. At the very last, only NO_2 can radiate visible light and so the ball of fire darkens as it drops to 2000°.

3.6 The Ball of Fire

The last two sections have described the effects of radiation in the formation and growth of the air blast. Except for the noted omissions,[17] this description is qualitatively complete for air blasts of this size. Other phenomena of interest have to do with the transmission of radiation energy ahead of the shock. Insofar as the description of the last two sections gives a complete model of the air blast, we can use it to determine the amount of energy transmitted through the shock front as a function of time. We also get a description of the quality (e.g., temperature) of the radiation, and the size and appearance of the ball of fire.

In the early phase, as long as the front is itself radiating strongly, there is a well-defined, spherical ball of fire. During this time the inner radiation front is, of course, not to be seen. When the shock front can no longer radiate, the hot core inside becomes more visible as the molecular absorbing layer becomes more tenuous. In the final stage, at the time of the second maximum and later, there is a hot core radiating, surrounded by a cooler fringe which is also radiating. At this time the ball has little absorption for its own radiation and is no longer a well-defined sphere with a sharp boundary.

The amount of radiant energy escaping per unit time into the air ahead of the shock front as a function of time is given in Fig. 3.10. This figure is largely schematic and has been obtained by methods which will be discussed below.

The unit ⊙ (used in Fig. 3.10) is 1.35×10^6 ergs/cm^2/sec, the flux of radiant energy incident into the earth's outer atmosphere from the sun. D is measured in meters.

---

17. Effects of gamma radiation, bomb materials, turbulence.

$$\text{unit } \odot = 1.35 \times 10^{6} \text{ ergs/cm}^2\text{/sec}$$

$$\text{unit } D^2\odot = 1.35 \times 10^{10} \text{ ergs/sec}$$

$$\text{unit } 4\pi D^2\odot = 1.70 \times 10^{11} \text{ ergs/sec}$$

In order to convert to tons of TNT per second the ordinates, $\odot$, must be divided by 2.46×10^5.

Dry air at 25°C transmits all light having longer wave length than 1860 A. The air in the vicinity of the bomb, however, has large quantities of ozone formed at the time of detonation by gamma radiation. This air absorbs essentially all light with wave length less than 3100 A. In this section, therefore, we have used a 3100 A cutoff so that the energies we give will indicate the amount transmitted through dry air to large distances. Corrections for moist air are easily made.

3.6.1 Radiation Expansion Period

During the radiation expansion period there is a large temperature gradient near the front. Just ahead of the front the temperature is normal (or essentially zero), while in the interior it is hundreds of thousands of degrees.

In order to calculate the flux of radiant energy through the front during this period, we assume that the situation described in Section 3.1.3 prevails. The temperature distribution for the air behind the front was given as

$$T = T_0 \left(1 - \frac{z}{z_0}\right)^{1/6} \tag{3.68}$$

where the coordinate axes are located at the shock front, and the radiation front extends out to $z = z_0$. This description, which assumes plane symmetry, is most satisfactory for the latter stages, i.e., for $r \approx 10$ meters. The radiation front just described was established with neglect of the fact that radiation in the region $h\nu_0 \geq h\nu \geq 6.6$ ev is transmitted in cold air. This neglect is justified since the temperatures in the isothermal sphere are so very large, $kT \sim 30$ to 60 ev; thus the fraction of energy in the radiation which can escape into the cold air is very small. Let us assume for this consideration that the front is correctly given by Eq. 3.68.

The flux calculated (with use of Eq. 3.17) for $z = z_0$ for the radiation escaping into the air is

$$\int_0^{\nu_0} (F_\nu)_z \, d\nu = \frac{1}{2} c \int_{-\infty}^{z_0} \rho\overline{K'}(z, z) \, U(z) \left\{ e^{-\beta} + \beta E_i(-\beta) \right\} dz \tag{3.69}$$

The temperature and hence $\overline{K'}$ and U are only functions of z. U is the energy density u_ν integrated over frequency from zero to ν_0. The quantity β is the "optical depth"

$$\beta(z) = \int_{z_0}^{z-z_0} \rho\overline{K'}(z', z) \, dz' \tag{3.70}$$

and $E_i(-\beta)$ is the exponential integral

$$-E_i(-\beta) = \int_\beta^\infty \frac{e^{-\beta'}}{\beta'} \, d\beta' \tag{3.71}$$

If the high temperature T_0 extended to the surface at $z = z_0$, the value of the flux would be given by

$$(F_z)_0 = \sigma T_0^{\,4} f_0 \tag{3.72}$$

where

$$f_0 = \frac{\int_0^{\nu_0} u_\nu(T_0) \, d\nu}{\int_0^\infty u_\nu(T_0) \, d\nu} \tag{3.73}$$

The lower temperatures closer to the front will to some extent shield the higher temperatures further back. We shall now attempt to calculate this effect by evaluating the flux as given by Eq. 3.69. Examination of the

opacity data for air in Section 3.3 (Fig. 3.1), shows that in normal density air it is a fairly good approximation to say that the mean free path for radiation is 1/2 cm for the entire range from 30,000°K to 300,000°K. It is not strictly logical to use Rosseland mean free paths for this purpose, but this calculation is rough. Taking

$$\beta(z) = 2z$$

and

$$\rho\overline{K}'(z, z) = 2$$

and using Eq. 3.68, the flux is found to be

$$F_z = \sigma T_0^4 f_0 \left[\frac{24}{13} (1/2)^{7/6} \frac{\Gamma(7/6)}{z_0^{1/6}}\right] \tag{3.74}$$

$\Gamma(7/6)$ is a complete gamma function. The factor in the bracket gives the effect of the shielding by lower temperatures. Calculating for some of the points in Table 3.4, we have results shown in Table 3.5

Table 3.5

EFFECT OF SHIELDING

Radiation Sphere Radius, meters	z_0, cm	Bracket of Eq. 3.74
5.07	226	0.31
8.41	98	0.36
10.15	13	0.50

Thus it seems that in the initial part of the air expansion, probably until after the shock is well formed, there is a partial shielding of the high temperatures. This shielding factor was used in obtaining the $D^2\odot$ curve for the radiation expansion period (Fig. 3.10).

The temperature as a function of radius for this period is given in Fig. 3.11.

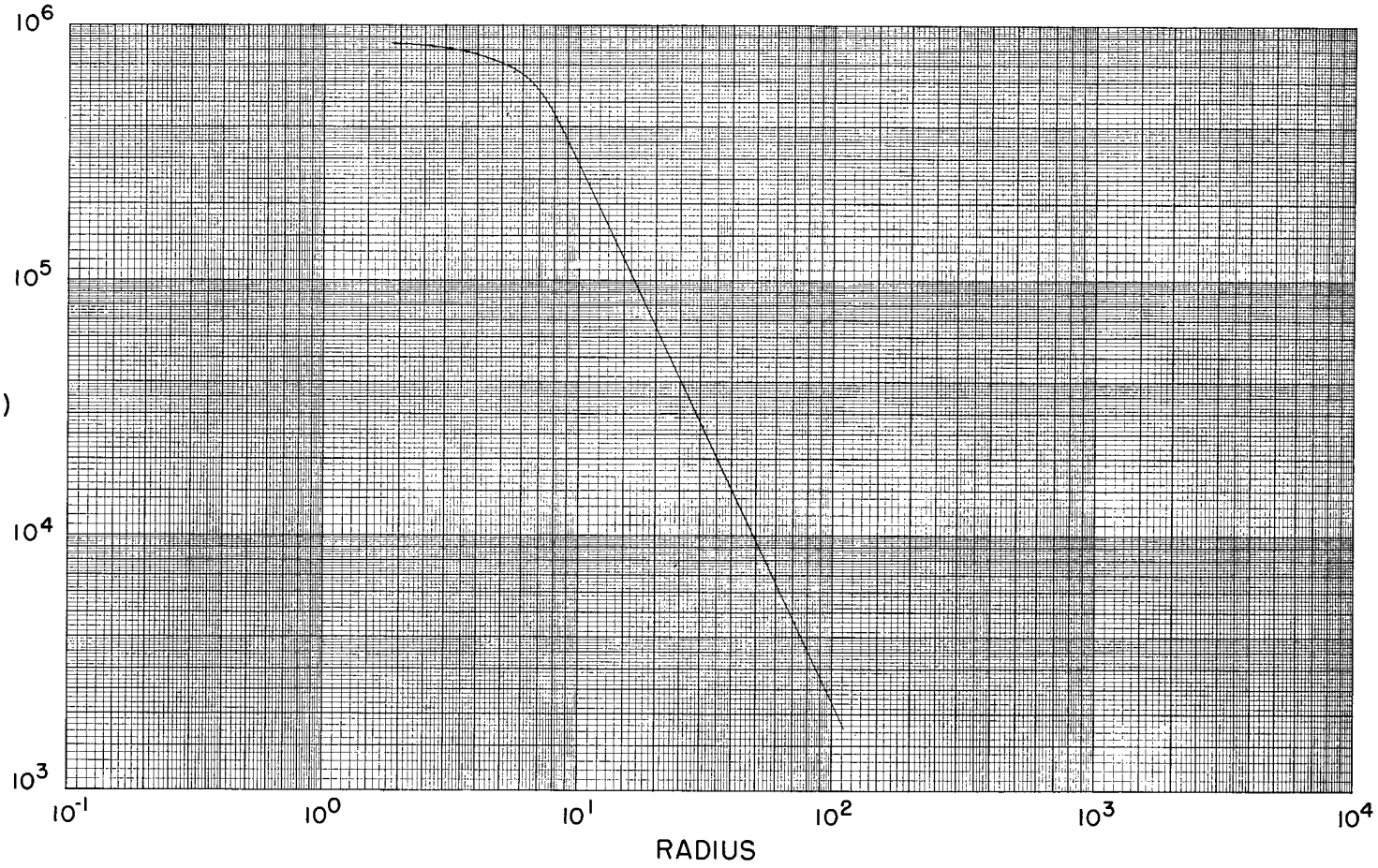

Fig. 3.11 Shock temperature vs shock radius

3.6.2 Radiating Shock Front

The shock front radiates as a black body until its temperature drops to about 2500 to 3000°K. It is able to radiate to such low temperatures by virtue of the NO_2 and other molecular species present. The temperatures at the front during the strong shock period are determined by hydrodynamical conditions and the equation of state of air. In Fig. 3.11 the shock temperature as a function of radius is given. During this period the temperature of the radiation drops from about 300,000 to 3000°K.

The rate of energy radiation per square centimeter of surface was taken to be $f\sigma T^4$, where f is the fraction of thermal radiation energy of temperature T with wave length longer than 3100 A. In Fig. 3.10, $D^2\odot$ gives this result.

The total amount of energy lost to the air blast, as determined by the integral of $D^2\odot$ over time up to the time the front stops radiating, is equivalent to about 30 tons of TNT, or about 0.3 per cent of the total energy. Thus, during the time in which the radiation affects the blast wave significantly, it only redistributes the energy behind the front, and there is only an insignificant loss of energy through the front.

3.6.3 Expanded Ball of Fire

The quantitative theory of the final stage has not been worked out as yet, but Fig. 3.10 has been extended through this period in a schematic way. The most difficult problem is the calculation of the energy and matter redistribution in the ball of fire following the separation of the ball of fire from the shock front (at 0.013 sec, shock temperature 3000°K). The rate of energy flow from the hot core into the lower temperature region has been calculated using the IBM density contours, opacity, and equation of state data. The hot core flux is shown in Fig. 3.10 as the dashed curve which rises steeply to a plateau. Beyond the plateau the dashed curve does not represent a calculation, but only a rough estimate of the behavior of the flux.

The steep rise occurs as the isothermal sphere temperature approaches 50,000°K, since at this temperature the opacity of air goes through a maximum. The air immediately ahead of the hot core is cooler and denser than the air of the core itself. When the opacity of air increases as the temperature falls, the air ahead of the core can absorb the core radiation and keep the flux low by radiating its own lower temperature radiation. When the opacity of air decreases as the temperature falls (i.e., below 50,000°K), the fringe of air between the hot core and low temperature region becomes transparent to the core radiation, and the flux rises to a maximum value.

During the next 0.1 to 0.2 sec the energy redistribution which has not been followed in detail occurs. At first all the core radiation is absorbed in the low temperature region. Later the entire ball becomes transparent to its own radiation. The last stage of the radiative cooling process (after 0.2 sec) was calculated with the use of a simple model: a core at 10,000°K and a fringe at 5000°K containing equal energies radiate without any self absorption.

The solid curve for $D^2\odot$ on integration gives approximately the correct total energy radiated, 35 per cent.

3.6.4 Ball of Fire Radius

The radius of the ball of fire as a function of time for very early times is given in Fig. 3.10. Until 0.013 sec, it is coincident with the shock radius. After the breakaway the ball of fire is essentially bounded by the air which had initially been heated to 2000°K or so by the shock. The maximum size is reached in about 0.2 sec.

3.7 Scaling Laws

The discussion of this chapter has dealt with air blasts of a definite size, namely, 10,000 ton TNT equivalent energy. It is of interest to examine the various radiation effects to see how they scale for blasts of different sizes.

3.7.1 Radiative Expansion Period

According to the discussion of Section 3.6.1 the radiative phase should end when the temperature drops to about 300,000°K. For explosions in which bomb materials can be neglected, the volume of air contained at this stage varies directly as yield, and thus the radius varies as the cube root of the yield, or

$$R_0 \sim E^{1/3} \tag{3.75}$$

where R_0 is the initial shock radius.

The energy loss due to radiation is negligible in this period and need not be considered.

3.7.2 Radiating Shock Front

It is easy to demonstrate that the energy radiated through the shock front during the time it radiates as a black body varies directly as the explosion energy. The rate at which the total surface loses energy in the frequencies transmitted by cold air can be given as (see Section 3.6; symbols are defined there)

$$4\pi D^2 \odot = 4\pi R^2 f \sigma T^4 \tag{3.76}$$

The total amount of energy lost is the integral of this quantity taken during the time the front radiates. With use of the identity

$$dt = \frac{dR}{\dot{R}}$$

we can write for the total radiated energy

$$\int_{R_0}^{R'} 4\pi D^2 \odot \, dt = 4\pi\sigma \int_{R_0}^{R'} f R^2 T^4 \frac{dR}{\dot{R}} \tag{3.77}$$

The scaling of these quantities has been discussed for shocks which have similarity.[18] We have the following relations for shocks which have similar conditions

$$\begin{aligned} f &\sim E^0 \\ T &\sim E^0 \\ \dot{R} &\sim E^0 \end{aligned} \tag{3.78}$$

since these are essentially intensive properties and determine which is meant by saying the condition of the shock is the same; and finally

$$R \sim E^{1/3} \tag{3.79}$$

---

18. See Chapter 2.

Thus the entire scaling of the energy loss depends upon

$$R^2 dR \sim E \tag{3.80}$$

and so the energy lost varies directly as E.

Since the percentage of energy lost was shown to be a negligible 0.3 per cent for the bomb with 10,000 ton yield, the energy lost in this period is not expected to be of importance for any bomb.

3.7.3 Strong Shock Period and the Total Radiation Yield

The motion of the inner radiation front, as given by Eq. 3.64, already has its scaling given explicitly. Since the power of E is 0.698 rather than unit, it is seen that the internal radiation front is relatively less effective in penetration of the shocked matter as the yield increases. As the yield increases, therefore, this particular radiation effect becomes a better approximation.

The other radiation effects of the strong blast period, and particularly the final stage, have not been treated quantitatively. Most of the radiation yield energy appears in this final stage and so the scaling of the total yield energy is uncertain. According to the discussion of the final stage given above, the ball of fire finally appears as a transparent mass of gas.

Such a mass of gas would radiate a certain fraction of its energy if there were no other mechanism of cooling involved. As the radius of the ball increases, any self absorption effects would decrease the rate of radiation of energy and favor competing processes, thus affecting the energy loss. Therefore, the fraction of energy radiated should decrease slightly as the yield increases, although the exact law is not to be obtained from this consideration.

Chapter 4

APPROXIMATION FOR SMALL $\gamma - 1$

by H. A. Bethe

4.1 General Procedure

The solution given in Chapter 2 is only valid for an exact point source explosion, for constant γ, for constant undisturbed density of the medium, and for very high shock pressures. It is very desirable to find a method which permits the treatment of somewhat more general shock wave problems and thereby comes closer to describing a real shock wave. The clue to such a method is found in the very peculiar nature of the point source solution of Taylor and von Neumann. It is characteristic for that solution that the density is extremely low in the inner regions and is high only in the immediate neighborhood of the shock front. Similarly, the pressure is almost exactly constant inside a radius of about 0.8 of the radius of the shock wave.

It is particularly the first of these facts that is relevant for constructing a more general method. The physical situation is that the material behind the shock moves outward with a high velocity. Therefore the material streams away from the center of the shock wave and creates a high vacuum near the center. The absence of any appreciable amount of material, together with the moderate size of the accelerations, immediately leads to the conclusion that the pressure must be very nearly constant in the region of low density. It is interesting to note that the pressure in that region is by no means zero, but is almost one-half of the pressure at the shock front.

The concentration of material near the shock front and the corresponding evacuation of the region near the center is most pronounced for values of the specific heat ratio γ close to 1. It is well known that the density at the shock increases by a factor

$$\frac{\rho_s}{\rho_0} = \frac{\gamma + 1}{\gamma - 1} \tag{4.1}$$

This becomes infinite as γ approaches unity. Therefore, for γ near 1 the assumption that all material is concentrated near the shock front becomes more and more valid. The density near the center can be shown to behave as $r^3/(\gamma - 1)$, where r is the radius.

The idea of the method proposed here is to make repeated use of the fact that the material is concentrated near the shock front. As a consequence of this fact, the velocity of nearly all the material will be the same as the velocity of the material directly behind the front. Moreover, if γ is near 1, the material velocity behind the front is very nearly equal to the shock velocity itself; the two quantities differ only by a factor $2/(\gamma + 1)$. The acceleration of almost all the material is then equal to the acceleration of the shock wave; knowing the acceleration one can calculate the pressure distribution in terms of the material coordinate, i.e., the amount of air inside a given radius. This calculation again is facilitated by the fact that nearly all the material is at the shock front and therefore has the same position in space (Eulerian coordinate).

The procedure followed is then simply this. We start from the assumption that all material is concentrated at the shock front. We obtain the pressure distribution. From the relation between pressure and density along an adiabatic, we can obtain the density of each material element if we know its pressure at the present time as well as when it was first hit by the shock. By integration of the density we can then find a more accurate value for the position of each mass element. This process could be repeated if required; it would then lead to a power series in powers of $\gamma - 1$.

The method leads directly to a relation between the shock acceleration, the shock pressure, and the internal pressure near the center of the shock wave. In order to obtain a differential equation for the position of the shock as a function of time, we have to use two additional facts. One is the Hugoniot relation between shock pressure and shock velocity. The other is energy conservation in some form: in some applications such as that to the point source solution itself, we may use the conservation of the total energy which requires that the shock pressure decrease inversely as the cube of the shock radius (similarity law). On the other hand, if there is a central isothermal sphere as described in Chapter 3, no similarity law holds, but we may consider the adiabatic expansion of the isothermal sphere and thus determine the decrease of the central pressure as a function of the radius of the isothermal sphere. If we wish to apply the method to the case of variable γ without isothermal sphere, we may again use the conservation of total

energy, but in this case the pressure will not be simply proportional to $1/Y^3$, where Y is the shock radius.

As has already been indicated, the applications of the method are very numerous. The case of not very high shock pressures can also be included; in this case the density behind the shock wave does not have the limiting value of Eq. 4.1 but depends itself on the shock pressure. This does not prevent the application of our method as long as the density increase at the shock is still very large so that most of the material is still near the shock front.

The only limitations of the method are its moderate accuracy and the possible complications of the numerical work. The accuracy seems satisfactory up to γ about 1.4. For the point source, a direct comparison with the exact solution is possible.

4.2 General Equations

We shall denote the initial position of an arbitrary mass element by r, and the position at time t by R. The position of the shock wave will be denoted by Y(t). The density at time t is denoted by ρ and the initial density by ρ_0. The pressure is p(r, t) and the pressure behind the shock is $p_s(Y)$.

The continuity equation takes the simple form

$$\rho R^2 \, dR = \rho_0 r^2 \, dr \tag{4.2}$$

From this we have

$$\frac{\partial R}{\partial r} = \frac{\rho_0}{\rho} \frac{r^2}{R^2} \tag{4.3}$$

The equation of motion becomes simply

$$\frac{d^2R}{dt^2} = -\frac{1}{\rho} \frac{\partial p}{\partial R} = -\frac{R^2}{\rho_0 r^2} \frac{\partial p}{\partial r} \tag{4.4}$$

The pressure for any given material element is connected with its density by the adiabatic law (conservation of energy). The particular adiabat to be taken is determined by the condition of the material element after it has been hit by the shock. If we assume constant γ the adiabatic relation gives

$$p(r,t) = p_s(r) \left[\frac{\rho(r,t)}{\rho_s}\right]^{\gamma} \tag{4.5}$$

We shall use this relation mostly to determine the density from the given pressure distribution. Using Eq. 4.1 for the density behind the shock ρ_s, and the continuity Eq. 4.2, we find

$$\frac{\partial R}{\partial r} = \frac{r^2}{R^2}\frac{\rho_0}{\rho} = \frac{\gamma - 1}{\gamma + 1}\frac{r^2}{R^2}\left[\frac{p_s(r)}{p(r,t)}\right]^{1/\gamma} \tag{4.6}$$

The three conservation laws, Eqs. 4.2, 4.4 and 4.6, must be supplemented by the Hugoniot equations at the shock front which are known to be, themselves, consequences of the same conservation laws. These relations give for the density at the shock front the result already quoted in Eq. 4.1, and for the relation between shock pressure and shock velocity $\dot{Y}$

$$\frac{p_s(Y)}{\rho_0} = \frac{2}{\gamma + 1}\dot{Y}^2 \tag{4.7}$$

and for the relation between the material velocity behind the shock, $\dot{R}$, and the shock velocity, $\dot{Y}$

$$\dot{R} = \frac{2\dot{Y}}{\gamma + 1} \tag{4.8}$$

The problem will now be to solve these eight equations for particular cases with the assumption that γ is close to 1. Then Eq. 4.4 reduces to

$$\frac{1}{r^2}\frac{\partial p}{\partial r} = -\rho_0 \frac{\ddot{Y}}{Y^2} \tag{4.9}$$

On the right hand side of this equation we have used the fact discussed in Section 4.1 that practically all the material is very near the shock front. Therefore the position R can be identified with the position of the shock Y, and the acceleration $\ddot{R}$ with the shock acceleration $\ddot{Y}$. Since the right hand side of Eq. 4.9 is independent of r, it integrates immediately to give

$$p(r,t) = p_s(Y) + \rho_0 \frac{\ddot{Y}}{3Y^2}(Y^3 - r^3) \tag{4.10}$$

If we use the Hugoniot relation, Eq. 4.7, and put $\gamma = 1$ in that relation we find further

$$\frac{p(r,t)}{\rho_0} = \dot{Y}^2 + \frac{\ddot{Y}}{3Y^2}(Y^3 - r^3) \tag{4.11}$$

This equation gives the pressure distribution at any time in terms of the position, velocity, and acceleration of the shock.

Of particular interest is the relation between the shock pressure and the pressure at the center of the shock wave. This relation is obtained by putting $r = 0$ in Eq. 4.10. Then we get

$$\frac{p(0,t)}{\rho_0} = \dot{Y}^2 + \frac{Y\ddot{Y}}{3} \tag{4.12}$$

The pressure near the center is in general smaller than the pressure at the shock because $\ddot{Y}$ is in general negative.

It can be seen that the derivation given here is even more general than was stated. In particular, it applies also to a medium which has, initially, nonuniform density. It is only necessary to replace $\rho_0 r^3$ by the mass enclosed in the sphere r (except for the factor $4\pi/3$).

From the pressure distribution Eq. 4.11 we can obtain the density or the position R using Eq. 4.6. The remaining problem is now to calculate this density distribution explicitly, and to determine the motion of the shock wave in particular cases.

4.3 The Point Source

The simplest application of the general theory developed in Section 4.2 is to a point source explosion. In this case, the theory of von Neumann and G. I. Taylor is available for comparison.

Equation 4.12 gives a relation between various quantities referring to the shock and the pressure at the center of the shock wave. To make any further progress we have to use the conservation of total energy in the shock wave. Since there is no characteristic length, time, or pressure involved in the problem, the blast wave from a point source explosion must

obey a similarity law as has been pointed out by Taylor and von Neumann. In other words, the pressure distribution will always have the same form; only the peak pressure and the scale of the spatial distribution will change as the shock wave moves out. Now the energy is mainly potential energy[1] if γ is close to 1; the potential energy per unit volume is $p/(\gamma - 1)$ and therefore the total potential energy will be proportional to $p_s\ Y^3/(\gamma - 1)$. Therefore p_s and $\dot{Y}^2$ (cf. Eq. 4.7) will be inversely proportional to Y^3. This gives immediately the equation

$$\dot{Y}^2 = AY^{-3} \tag{4.13}$$

where A is a constant related to the total energy. Integration gives

$$Y = \left(\frac{5}{2}\right)^{2/5} A^{1/5}\ t^{2/5} \tag{4.14}$$

and differentiation gives

$$Y\ddot{Y} = -\frac{3}{2}\dot{Y}^2 \tag{4.15}$$

Inserting this in Eq. 4.12 we find immediately

$$\frac{p(0,t)}{\rho_0} = \frac{1}{2}\dot{Y}^2 = \frac{1}{2}\frac{p_s}{\rho_0} \tag{4.16}$$

Therefore in the limit of γ close to 1, the internal pressure is just one-half of the shock pressure. This can be compared with the numerical result of von Neumann's theory in Chapter 2, Table 2.5, which gives the following values for the ratio of internal pressure to shock pressure:

Table 4.1

VARIATION OF RATIO OF INTERNAL PRESSURE TO SHOCK PRESSURE WITH GAMMA

γ =	1	1.1	1.2	1.4	1.67	2
$p(0)/p_s$ =	0.500	0.462	0.424	0.366	0.306	0.251

1. This assumption is not necessary for the validity of the following equations.

With the relation of internal and shock pressure known, we can now calculate the total potential energy content. We know that the potential energy per unit volume is $p/(\gamma - 1)$. We further know from Eq. 4.11 that the pressure is constant and equal to p(0) over the entire region which is nearly free of matter. Moreover, we know that all the matter is concentrated in a very thin shell near the shock front. Therefore, with the exception of a very small fraction of the volume occupied by the shock wave, the pressure is equal to the interior pressure. The total energy is then

$$E = \frac{4\pi}{3} \frac{Y^3\, p(0)}{\gamma - 1} = \frac{2\pi}{3} \frac{Y^3\, p_s}{\gamma - 1}$$

$$= \frac{2\pi}{3} \frac{\rho_0}{\gamma - 1} Y^3 \dot{Y}^2 = \frac{2\pi}{3} \frac{\rho_0\, A}{\gamma - 1} \quad \text{(cf. Eq. 4.13)} \qquad (4.17)$$

In the following listing, we give the exact numerical factor in the last expression in Eq. 4.17, according to calculations of Hirschfelder.

γ	=	1	1.1	1.2	1.4	1.67	2
$(\gamma - 1)E/\rho_0\, A$	=	2.094	2.152	2.148	2.144	2.05	1.95

It is seen that this factor is very close to $2\pi/3$, for all values of γ up to 1.4. This is due to a compensation of various errors. The internal pressure is actually less than one-half of the shock pressure, but this is compensated by the fact that the pressure near the shock front is higher than the internal pressure. Indeed, the ratio of the volume average of the pressure to the shock pressure is much closer to 1/2 than the corresponding ratio for the internal pressure (cf. Eqs. 4.31a, 4.31b). A further error which has been made in Eq. 4.17 is that the factor $2/(\gamma + 1)$ in Eq. 4.7 has been neglected. On the other hand, the kinetic energy has been neglected. This kinetic energy is very nearly equal to

$$E_{kin} = \frac{2\pi}{3} \rho_0 Y^3 \dot{Y}^2 = (\gamma - 1)E \qquad (4.18)$$

because all the material moves almost with the shock velocity $\dot{Y}$. It is seen that this kinetic energy is small compared with the potential energy by a factor $\gamma - 1$; this justifies our neglect of the kinetic energy along with a large number of other quantities of the relative order $\gamma - 1$. It is, of course, only an accident that there is almost exact compensation of all these

neglected terms up to values of γ as high as 5/3.

We can now use our result to obtain the density distribution of the matter behind the shock front. We need only apply Eqs. 4.6 and 4.11 to 4.16 and find

$$\frac{\rho_0}{\rho} = \frac{\gamma - 1}{\gamma + 1}\left[\frac{p_s(r)}{p(r, Y)}\right]^{1/\gamma} = \frac{\gamma - 1}{\gamma + 1}\left[\frac{2}{x(1 + x)}\right]^{1/\gamma} \tag{4.19}$$

with

$$x = \frac{r^3}{Y^3} \tag{4.19a}$$

Setting also

$$y = \frac{R^3}{Y^3} \tag{4.19b}$$

Eq. 4.6 becomes

$$\frac{dy}{dx} = \frac{\gamma - 1}{\gamma + 1}\left[\frac{2}{x(1 + x)}\right]^{1/\gamma} \tag{4.20}$$

To integrate this equation, it is convenient to distinguish two cases:

(1) If x is not too small, more precisely for

$$x \gg e^{-1/(\gamma-1)} \tag{4.20a}$$

we may consider the exponent in Eq. 4.20 as equal to 1 since $\gamma - 1$ is assumed small. Then, neglecting quantities of order $(\gamma - 1)^2$, integration of Eq. 4.20 gives

$$y = \frac{R^3}{Y^3} = 1 - (\gamma - 1)\log\frac{1 + x}{2x} = 1 - (\gamma - 1)\log\frac{Y^3 + r^3}{2r^3} \tag{4.21}$$

(2) If

$$x \ll 1 \tag{4.21a}$$

we may neglect x compared to 1. Then, neglecting quantities of relative order $\gamma - 1$, we get

$$\begin{aligned} dy &= (\gamma - 1)\, x^{-1/\gamma}\, dx \\ y &= x^{(\gamma-1)/\gamma} + A \end{aligned} \tag{4.22}$$

where A is a constant. The regions defined by Eqs. 4.20a and 4.21a overlap very considerably. Comparing Eqs. 4.21 and 4.22 we find that

$$A = 0 \tag{4.22a}$$

neglecting a small term of order $\gamma - 1$. This value of A will make Eq. 4.22 sensible for small values of x. Inserting Eqs. 4.19a and 4.19b, we get

$$R = Y^{1/\gamma}\, r^{1-(1/\gamma)} \tag{4.23}$$

or

$$\frac{R}{Y} = \left(\frac{r}{Y}\right)^{(\gamma-1)/\gamma} \tag{4.23a}$$

From the position of any point we can deduce the velocity by a simple differentiation with respect to time. In this process, the material coordinate r should be kept constant. Equation 4.23 gives for the material velocity (neglecting terms of order $\gamma - 1$)

$$\dot{R} = \frac{\dot{Y}}{\gamma}\left(\frac{r}{Y}\right)^{\frac{\gamma-1}{\gamma}} \approx \dot{Y}\frac{R}{Y} \tag{4.24}$$

Over most of the volume the material velocity is nearly linear in R which is borne out by the numerical integrations of the exact solution (see Chapter 2). Over most of the mass the material velocity is nearly equal to the velocity of the shock wave.

4.4 Comparison of the Point Source Results with the Exact Point Source Solution

The results obtained in the last section can be compared with the exact solution described in Chapter 2. The results of that chapter can very easily be applied to the special case when γ is very nearly 1.

In going to this limit one should keep the exponent of θ correct because this quantity goes from 0 to 1, and if it is close to 0 a factor $\theta^{\gamma-1}$ will matter. In all other factors the base of the power becomes $(\theta + 1)/2$ in the limit $\gamma = 1$, which goes over the range from 1/2 to 1 and therefore never becomes very small. Consequently $\gamma - 1$ may be neglected in the exponent of these other factors except if higher accuracy is desired.

Neglecting small quantities in this manner, Eq. 2.34'' reduces to

$$\frac{r}{Y} = Z = \theta^{\frac{\gamma}{2\gamma+1}} \approx \theta^{1/3} \tag{4.25}$$

Z and θ being the notations used in Chapter 2 (cf. Eq. 2.39').

Equation 4.25 may be rewritten

$$\theta = Z^3 = \left(\frac{r}{Y}\right)^3 \tag{4.25a}$$

Equation 2.35 becomes then

$$\frac{R}{Y} = F = \theta^{\frac{\gamma-1}{2\gamma+1}} = \left(\frac{r}{Y}\right)^{\frac{\gamma-1}{\gamma}} \tag{4.26}$$

This result for the Eulerian position is identical with that obtained from our approximate theory in Eq. 4.23a). A more accurate evaluation, keeping terms of relative order $\gamma - 1$ throughout, gives

$$F = \left(\frac{2\theta}{\theta + 1}\right)^{\frac{\gamma-1}{2\gamma+1}} \tag{4.26a}$$

For the pressure we find from Eq. 2.43' in the limit $\gamma = 1$ the result

$$p = p_s \frac{\theta + 1}{2} = \frac{1}{2} p_s \left[1 + \left(\frac{r}{Y} \right)^3 \right] \tag{4.27}$$

This again is identical with the result of our approximate theory given in Eqs. 4.11 and 4.15. Again, a more accurate evaluation, neglecting only terms of relative order $(\gamma - 1)^2$, gives

$$\frac{p}{p_s} = \frac{\theta + 1}{2} \left[1 + 2\delta \ln \frac{\theta + 1}{2} + \delta \left(\frac{1}{\theta + 1} - \frac{1}{2} \right) \right] \tag{4.28}$$

with the abbreviation

$$\delta = \gamma - 1 \tag{4.28a}$$

Of particular interest is the relation between the total energy and such quantities as the shock pressure. We shall therefore calculate this relation including terms of relative order $\gamma - 1$. First of all, we shall calculate the potential (heat) energy

$$E_{pot} = 4\pi \int_0^Y R^2 \, dR \, \frac{p}{\gamma - 1}$$

$$= \frac{4\pi}{3} \frac{Y^3 p_s}{\gamma - 1} \int_0^1 d(F^3) \frac{p}{p_s} \tag{4.29}$$

Using Eqs. 4.26a and 4.28a, we have

$$d(F^3) = \left[d \; \theta^\delta \left(\frac{\theta + 1}{2} \right)^{-\delta} \right]$$

$$= \left[d(\theta^\delta) - \delta \frac{d\theta}{\theta + 1} \right] \left(1 - \delta \ln \frac{\theta + 1}{2} \right) \tag{4.29a}$$

neglecting[2] terms of relative order δ^2. Inserting Eq. 4.29a and p from

2. It is permissible to set the factor θ^δ, which should appear in the second term in the square bracket, equal to one; the error in Eq. 4.29 is only of order of δ^2.

Eq. 4.28 into Eq. 4.29 we get

$$I = 2\int_0^1 d(F^3)\,\frac{p}{p_s} = \int_0^1 \left[d(\theta^\delta) - \delta\,\frac{d\theta}{\theta+1}\right](\theta+1)$$

$$\left[1 + \delta\left(\ln\frac{\theta+1}{2} + \frac{1}{\theta+1} - \frac{1}{2}\right)\right] \qquad (4.30)$$

up to the order δ. This integral can be evaluated very easily. We note that θ^δ changes from 0 to 1 at very small values of θ, so that in first approximation for this part of the integral, the integrand should be taken at $\theta = 0$. (This corresponds to the physical fact that most of the material is near the shock front; $F^3 = \theta^\delta$ becomes close to 1 already for relatively small values of θ or of the material coordinate $Z = \theta^{1/3}$.) Evaluation of Eq. 4.30 gives

$$I = 1 + \delta\left(\ln\frac{1}{2} + 1 - \frac{1}{2}\right) + \delta - \delta \qquad (4.30a)$$

or

$$E_{pot} = \frac{2\pi}{3}\,\frac{p_s\,Y^3}{\gamma-1}\left[1 + \delta\left(\frac{1}{2} - \ln 2\right)\right] \qquad (4.31)$$

This result, except for the last factor, is identical with the result of our approximate theory, Eq. 4.17. The last factor is seen to differ only very slightly from 1, the factor of δ being only -0.2. It is of some interest to define the average pressure (volume average); this is according to Eq. 4.31:

$$p_{A0} = \frac{1}{2}\,p_s\left[1 + \delta\left(\frac{1}{2} - \ln 2\right)\right] = \frac{1}{2}\,p_s\,[1 - 0.193\,\delta] \qquad (4.31a)$$

This may be compared with the central pressure (cf. Eq. 4.28)

$$p(0) = \frac{1}{2}\,p_s\left[1 + \delta\left(\frac{1}{2} - \ln 4\right)\right] = \frac{1}{2}\,p_s\,[1 - 0.886\,\delta] \qquad (4.31b)$$

The average pressure is, of course, higher than the central pressure; it differs from it only in the order δ as is to be expected; and it is much closer

to one-half the shock pressure than the central pressure is.

Now let us calculate the kinetic energy. According to Eq. 2.46, the ratio of kinetic to potential energy in any mass element is θ; therefore

$$E_{kin} = \frac{4\pi}{3} \frac{Y^3 p_s}{\gamma - 1} \int_0^1 d(F^3) \frac{p}{p_s} \theta$$

$$= \frac{2\pi}{3} \frac{Y^3 p_s}{\gamma - 1} \int_0^1 \delta d\theta \left(\frac{1}{\theta} - \frac{1}{\theta + 1} \right) (\theta + 1) \theta \qquad (4.32)$$

$$= \frac{2\pi}{3} Y^3 p_s$$

The simplifications in this integral, i.e., neglect of the last square bracket in Eq. 4.30 and replacement of $d(\theta^\delta)$ by $\delta d\theta/\theta$, are possible because of the factor θ in the integrand. This also makes the integral of order δ. The result, Eq. 4.32, agrees with that of the approximate theory, Eq. 4.18.

Adding Eqs. 4.31 and 4.32, we find for the total energy

$$E = \frac{2\pi}{3} \frac{p_s Y^3}{\gamma - 1} \left[1 + \delta \left(\frac{3}{2} - \ln 2 \right) \right] \qquad (4.33)$$

This gives the shock pressure as a function of the radius, including terms of relative order $\gamma - 1$, which will be useful for the calculation of the waste energy. We may also replace p_s by the shock velocity $\dot{Y}$ according to Eq. 4.7:

$$E = \frac{2\pi}{3} \frac{Y^3 \dot{Y}^2}{\gamma - 1} [1 + \delta(1 - \ln 2)] \qquad (4.33a)$$

Here again the correction factor in the bracket differs only slightly from 1, in agreement with the numerical results reported in Table 4.1.

A further quantity of interest is $\partial R/\partial r = dF/dz$ for which Eq. 2.37 gives the result (for small $\gamma - 1$):

$$\frac{\partial R}{\partial r} = F' = \frac{\gamma - 1}{\gamma + 1} \theta^{-1/3} \left(\frac{\theta + 1}{2} \right)^{-(\gamma - 1)} \qquad (4.34)$$

From this expression or directly from Eq. 2.41 we can find the density which turns out to be

$$\frac{\rho}{\rho_0} = \frac{\gamma + 1}{\gamma - 1}\,\theta^{\frac{3}{2\gamma+1}}\,\frac{\theta + 1}{2} = \frac{\gamma + 1}{\gamma - 1}\,z^{3/\gamma}\,\frac{1 + z^3}{2} \tag{4.35}$$

We can also express this density in terms of the Eulerian position, in which case we get from Eq. 4.26

$$\frac{\rho}{\rho_0} = \frac{\gamma + 1}{\gamma - 1}\left(\frac{R}{Y}\right)^{\frac{3}{\gamma-1}}\frac{1}{2}\,(1 + z^3) \tag{4.35a}$$

This equation shows that the density becomes extremely low for all points away from the shock front even if they are only moderately close to the center of the explosion. This is in agreement with our basic assumption that most of the material is concentrated near the shock front.

Finally combining Eqs. 2.42' and 2.40' we find, in the limit $\gamma = 1$,

$$\frac{u}{R} = \frac{2}{5t} \tag{4.36}$$

However, from the similarity solution we know that

$$Y = at^{2/5} \tag{4.36a}$$

where a is a constant, and therefore

$$\frac{u}{R} = \frac{\dot{Y}}{Y} \tag{4.36b}$$

This result is again identical with the result of our approximate theory given in Eq. 4.24.

We see, therefore, that our approximate solution is identical with the limit of the exact solution of the point source for $\gamma = 1$ if terms of the relative order $\gamma - 1$ are consistently neglected.

4.5 The Case of the Isothermal Sphere

We shall now consider the somewhat more complicated problem of the production of a shock wave by a sphere which is initially heated to a high uniform temperature and then exerts pressure on its surroundings. The relevance of this problem of the isothermal sphere has been discussed in Chapters 1 and 3 and is connected with the great influence of energy transport by radiation.

The problem now no longer permits the application of similarity arguments. For this reason we can no longer use the conservation of total energy to advantage. Instead of this we can now assume adiabatic expansion of the isothermal sphere. This is completely equivalent to an application of the energy conservation law because the adiabatic law itself is based on the assumption that there is no energy transport out of the isothermal sphere.

Let us assume that the material coordinate of the surface of the isothermal sphere is r_0. The initial position of this surface is then equal to r_0. At a later time when the isothermal sphere has expanded to R_0 its average density has decreased by a factor $(r_0/R_0)^3$. If we assume that the density and pressure in the isothermal sphere are uniform, the pressure will be equal to

$$p_0 = P\left(\frac{r_0}{R_0}\right)^{3\gamma} \tag{4.37}$$

where P is the initial pressure in the isothermal sphere which is related to the total energy by the equation

$$E = \frac{4\pi}{3}\frac{P\, r_0^{\,3}}{\gamma - 1} \tag{4.37a}$$

We shall now proceed in two steps. First of all we shall consider the case when the radius of the shock wave is not extremely great compared with the initial radius of the isothermal sphere, more precisely

$$\frac{Y}{r_0} \ll e^{\frac{1}{\gamma-1}} \tag{4.37b}$$

We shall show that with this assumption the solution with an isothermal

sphere approaches the point source solution as Y/r_0 increases. Afterwards, for large values of Y/r_0 where Eq. 4.37b is not valid, the approximations used in the first part of our calculation will break down; but we can then use the results of the last section to obtain R_0/Y for the surface of the isothermal sphere, and this will enable us to solve the problem for the case of large values of Y/r_0.

(1) Case I: Y/r_0 moderate

If Y/r_0 is not very great we can replace the exponent 3γ in Eq. 4.37 by 3. At the same time we can use our general assumption that practically all material is close to the shock front and that, therefore, R_0 is very nearly equal to Y. With this approximation we find from Eq. 4.12

$$\dot{Y}^2 + \frac{Y\ddot{Y}}{3} = \frac{P\, r_0^{\,3}}{\rho_0} Y^{-3} \tag{4.38}$$

This equation can be integrated without difficulty by setting

$$\dot{Y}^2 = \phi(Y) \tag{4.39}$$

and

$$\frac{P\, r_0^{\,3}}{\rho_0} = A = \frac{3(\gamma - 1)}{4\pi} \frac{E}{\rho_0} \tag{4.39a}$$

Then

$$\ddot{Y} = \frac{1}{2} \frac{d\phi}{dY} \tag{4.39b}$$

and Eq. 4.38 becomes

$$\phi + \frac{1}{6} Y \frac{d\phi}{dY} = A\, Y^{-3} \tag{4.40}$$

This can be integrated and gives

$$\phi\, Y^6 = 2A\, Y^3 + B \tag{4.41}$$

where B is a new constant.

Now the initial condition is, for $Y = r_0$,

$$\frac{p_s}{\rho_0} = \dot{Y}^2 = \frac{P}{\rho_0} \tag{4.42}$$

or with Eqs. 4.39 and 4.39a

$$\phi(r_0)\ r_0^{\,3} = A \tag{4.42a}$$

so that

$$B = -A\ r_0^{\,3} \tag{4.42b}$$

and finally

$$p_s = \rho_0\ \dot{Y}^2 = \rho_0\ A \left(\frac{2}{Y^3} - \frac{r_0^{\,3}}{Y^6} \right)$$

$$= \frac{3(\gamma - 1)}{2\pi} \frac{E}{Y^3} \left(1 - \frac{r_0^{\,3}}{2Y^3} \right) \tag{4.43}$$

Equation 4.43 shows that for large values of Y/r_0, the shock pressure p_s approaches the value given in Eq. 4.17, i.e., the value corresponding to the point source solution. This result appears rather important because it shows (1) that the point source solution is stable and is approached even under conditions which initially deviate strongly from those assumed in the point source solution, and (2) that the simple and well-known point source solution can be used at late times for our problem including the isothermal sphere.

(2) Case II: Y/r_0 large

We know from the discussion of Case I that our solution approaches the point source solution as soon as $Y/r_0 \gg 1$. We can then use Eq. 4.23 for the position R_0 of the surface of the isothermal sphere, and obtain, neglecting terms of second order in $\gamma - 1$,

$$p_0 = P \frac{r_0^{3\gamma}}{Y^3 r_0^{3\gamma-3}} = P\left(\frac{r_0}{Y}\right)^3 \tag{4.44}$$

This is the same expression which we used in Case I and which we then justified simply by neglecting γ in the exponent of Eq. 4.25. Therefore the further development is identical with that leading to Eq. 4.43.

We have thus shown that Eq. 4.43 is valid both for small and for large expansions of the isothermal sphere. It is possible to derive the density distribution, the position, and the velocity, as we did in the previous section for a point source case. However, the analytical expressions are fairly involved and there does not seem to be any particular application for them. The ratio of the shock pressure to the central pressure in the isothermal sphere is according to Eqs. 4.43 and 4.35

$$\frac{p_s}{p_0} = 2 - \frac{r_0^3}{Y^3} \tag{4.44a}$$

It changes from 1 in the very early stages to 2 in the late stages. At any reasonably late stage the energy in the blast is related to the velocity of the shock front in the same way as for the point source solution.

4.6 Variable Gamma

The theory developed here can be used to solve the problem of a shock wave in a medium with variable γ. The assumption is, of course, that $\gamma - 1$ still remains small throughout. We also assume that the shock pressure is high enough so that the Hugoniot relations hold in their limiting form.

We shall make the further simplifying assumption that γ is a function of the entropy only, so that it remains constant for any given mass element r as soon as that element has been traversed by the shock. This assumption is fairly well fulfilled by air, with the value of γ decreasing from 1.4 to about 1.2 with increasing entropy, and later on increasing again to 1.67. The more general problem in which γ is a function both of the entropy and the density can also be solved by the same method, but the algebra becomes so involved that it seems hardly worth while to use the present method instead of direct numerical integration.

The pressure distribution (Eq. 4.11) will still be valid. However, the relation between Y, $\dot{Y}$, and $\ddot{Y}$ will no longer be given by Eq. 4.15. We

introduce the pressure at the front and the pressure at the center of the shock wave separately by writing

$$p_s = \frac{3}{2\pi} \frac{E}{Y^3} \alpha$$

$$p(0) = \frac{3}{4\pi} \frac{E}{Y^3} \beta \tag{4.45}$$

where α and β are slowly variable with the shock radius Y. In the case of constant γ we have (cf. Eq. 4.17)

$$\alpha = \gamma - 1 \tag{4.46}$$

It is our aim to calculate α and β for a given variation of γ with the material coordinate r.

Using Eq. 4.11 we have

$$\frac{p(0)}{\rho_0} = \dot{Y}^2 + \frac{1}{3} Y \ddot{Y} = \phi + \frac{1}{6} Y \frac{d\phi}{dY} \tag{4.47}$$

where ϕ is an abbreviation for $\dot{Y}^2$. Inserting the expression Eq. 4.45 and remembering Eq. 4.7 we get the following relation between α and β:

$$\beta = \alpha + \frac{1}{3} \frac{d\alpha}{d \log Y} \tag{4.48}$$

where $\gamma + 1$ has been set equal to 2. It will be shown in the following that α changes very slowly with log Y; in fact $d\alpha/d \log Y$ is of the order $\gamma - 1$ relative to α itself. Therefore, in our theory in which $\gamma - 1$ is considered as small, we have

$$\beta = \alpha \tag{4.49}$$

Therefore, even with variable γ the ratio of the shock pressure to the internal pressure is equal to 2.

In order to find α for a given function $\gamma(r)$ we use the fact that both the geometrical and the material coordinate must be equal to Y at the shock front. We shall calculate the geometrical coordinate R as a function of r with the help of the density distribution. The required condition is then

$$R^3_{r=Y} = \int_0^Y d(r^3)\,\frac{\rho_0}{\rho} = Y^3 \tag{4.50}$$

The density of the material element r at the time when the shock wave is at Y is given by (cf. Eq. 4.6)

$$\frac{\rho}{\rho_0} = \frac{\gamma+1}{\gamma-1}\left[\frac{p_{r=Y}}{p_s(r)}\right]^{1/\gamma} = \frac{\gamma+1}{\gamma-1}\left[\frac{p_0(Y)\ (1 + r^3/Y^3)}{p_s(r)}\right]^{1/\gamma}$$

$$= \frac{2}{\gamma(r)-1}\,\frac{\alpha(Y)}{2\alpha(r)}\left(1 + \frac{r^3}{Y^3}\right)\left(\frac{r}{Y}\right)^{3/\gamma} \tag{4.51}$$

In this equation we have made use of the pressure distribution (4.11) and also of Eqs. 4.45 and 4.49. Furthermore, we have put γ in the exponent equal to 1 in all those terms where this makes an error of the order $\gamma - 1$. Combining Eq. 4.51 with 4.3 we find R^3 as a function of r as follows:

$$R^3 = \frac{1}{\alpha(Y)}\int_0^r d(r^3)\left(\frac{Y}{r}\right)^{3/\gamma}\ [\gamma(r)-1]\ \alpha(r)\left(1 + \frac{r^3}{Y^3}\right)^{-1} \tag{4.52}$$

No appreciable error is made by neglecting the last factor in this expression because it is different from 1 only over a region in R of the order $\gamma - 1$. In fact, only by neglecting this last factor do we get the correct result for constant γ, owing to other neglected terms in our theory. In any case, this last factor is no different for constant and variable γ and can, therefore, not be relevant for the theory of variable γ.

With this simplification we obtain

$$R^3 = \frac{1}{\alpha(Y)}\int_0^r \frac{d(r^3)}{r^{3/\gamma(r)}}\,Y^{3/\gamma(r)}\ [\gamma(r)-1]\ \alpha(r) \tag{4.53}$$

and in particular for r = Y we find, after dividing by Y^3,

$$\alpha(Y) = \int_0^Y \frac{d(r^3)}{r^{3/\gamma(r)}}\, Y^{-3} \left[1 - \frac{1}{\gamma(r)}\right] [\gamma(r) - 1]\ \alpha(r) \tag{4.54}$$

This is the desired equation determining $\alpha(Y)$. It is seen to be a linear integral equation.

Let us first consider the case of constant γ. In this case, Eq. 4.54 reduces to

$$\alpha(Y) = \int_0^Y \alpha(r)\, d\left(\frac{r}{Y}\right)^{3(\gamma-1)} \tag{4.55}$$

which is solved by α = constant, with the value of the constant arbitrary. From previous considerations, particularly Eq. 4.17, we know that in this case $\alpha = \gamma - 1$.

Let us now assume that γ is constant and equal to γ_1, for all values of r up to r_1; then $\alpha = \alpha_1 = \gamma_1 - 1$ in that region. Further, for $Y > r_1$ the integral of Eq. 4.54 reduces to

$$\alpha(Y) = \alpha_1 \left(\frac{r_1}{Y}\right)^{3(\gamma_1-1)} + \int_{r_1}^Y \frac{d\, r^3}{r^{3/\gamma(r)}}\, Y^{-3+3/\gamma(r)} [\gamma(r) - 1]\ \alpha(r) \tag{4.56}$$

In order to solve this equation we proceed in two steps, similar to the calculations in Section 4.5. In the first step we shall consider Y/r_1 as moderate so that the $\gamma - 1$ power of the quantity can be considered equal to 1. In this case we shall be able to obtain a general and rather simple differential equation for α which can be solved by quadratures. As a second step we shall then admit large values of Y/r_1; in this case we shall obtain a solution only in the special case of having a step-wise variation of γ.

(1) Case I: Y/r_1 moderate

In this case we may replace the exponent $3/\gamma$ in Eq. 4.56 by 3. Also we shall expand the first term on the right hand side of that equation in a Taylor series. Then Eq. 4.56 reduces to

$$\alpha(Y) = \alpha_1 - 3(\gamma_1 - 1)\alpha_1 \log \frac{Y}{r_1} + 3\int_{r_1}^{Y} d \log r\, [\gamma(r) - 1]\, \alpha(r) \tag{4.57}$$

To solve this integral equation we need only differentiate with respect to Y, or better with respect to

$$X = 3 \log \frac{Y}{r_1} \tag{4.58}$$

Then we obtain

$$\frac{d\alpha}{dX} = -\alpha_1(\gamma_1 - 1) + \alpha(X)\, [\gamma(X) - 1] \tag{4.59}$$

This equation can be integrated with the result

$$\alpha(X) = \exp\left\{\int_0^X [\gamma(X') - 1]\, dX'\right\}\alpha_1 \left\{1 - (\gamma_1 - 1)\int_0^X dX' \exp\int_{-0}^{X'} [\gamma(X'') - 1]\, dX''\right\} \tag{4.60}$$

The result (Eq. 4.60) as well as the differential Eq. 4.59 show that α does not have a discontinuity at a point at which γ has one, but only $d\alpha/dX$ has a discontinuity. This may be set even more in evidence by solving Eq. 4.59 for small values of X; i.e., for points just beyond the place at which γ begins to change. In this case we find

$$\alpha(X) = \alpha_1\left\{1 + \int_0^X dX'\, [\gamma(X') - \gamma_1]\right\} \tag{4.61}$$

A special case, which is of some interest because it is the simplest possible model of a substance with changing γ, is obtained by assuming that γ has the value γ_2 for all values of $r > r_1$. In this case Eq. 4.59 can be solved explicitly with the result

$$\alpha = \frac{\gamma_1 - 1}{\gamma_2 - 1}\left[(\gamma_2 - \gamma_1)\, e^{(\gamma_2 - 1)X} + \gamma_1 - 1\right] \tag{4.62}$$

For small values of X this reduces to

$$\alpha = (\alpha_1 - 1)\left[1 + (\gamma_2 - \gamma_1)\, X + \cdots\right] \tag{4.63}$$

Another result which follows from Eq. 4.59 is that $d\alpha/dX$ is of the order $\alpha(\gamma - 1)$. This result has been used above in obtaining the relation $\beta = \alpha$.

(2) Case II: Y/r_1 large

We shall consider this problem only in the particularly simple case when γ has the constant value γ_2 for all values of $r > r_1$. In this case Eq. 4.56 reduces to

$$\alpha(Y) = \alpha_1 \left(\frac{r_1}{Y}\right)^{3(\gamma_1 - 1)} + \int_{r_1}^{Y} d\left(\frac{r}{Y}\right)^{3(\gamma_2 - 1)} \alpha(r) \tag{4.64}$$

Similarly, as in Case I, we solve this equation by differentiating with respect to X. Then we obtain

$$\frac{d\alpha}{dX} = -(\gamma_1 - 1)\, \alpha_1 \left(\frac{r_1}{Y}\right)^{3(\gamma_1 - 1)} + (\gamma_2 - 1)\, \alpha(X) - (\gamma_2 - 1) \int_{r_1}^{Y} d\left(\frac{r}{Y}\right)^{3(\gamma_2 - 1)} \alpha(r) \tag{4.65}$$

The integral in this equation can be expressed by means of Eq. 4.64. Neglecting terms of higher order in $\gamma - 1$, we get then

$$\frac{d\alpha}{dX} = \alpha_1 (\gamma_2 - \gamma_1) \left(\frac{r_1}{Y}\right)^{3(\gamma_1 - 1)} \tag{4.66}$$

This equation is actually even simpler than the differential Eq. 4.59 which we obtained in the approximate theory of Case I. Using the boundary condition $\alpha = \gamma_1 - 1$ for $Y = r_1$, Eq. 4.66 integrates immediately to

$$\alpha = \gamma_2 - 1 - (\gamma_2 - \gamma_1)\left(\frac{r_1}{Y}\right)^{3(\gamma_1 - 1)} \tag{4.67}$$

For small values of X this reduces to

$$\alpha = (\gamma_1 - 1)\left[1 + 3(\gamma_2 - \gamma_1)\ln\frac{Y}{r_1}\right] \tag{4.68}$$

which is identical with the result of Eq. 4.63.

Equation 4.67 shows that the value of α goes gradually from the original value $\gamma_1 - 1$ to the value $\gamma_2 - 1$ which corresponds to the new value of γ. It is seen that this asymptotic value is reached only for extremely large values of Y/r_1. As long as Y/r_1 is moderate, the shock pressure is still influenced largely by the previous value of γ instead of by the present one. For air in particular we may take $\gamma_1 = 1.2$ and $\gamma_2 = 1.4$. The shock pressure in a substance with γ constant = 1.4 should be twice as great as that for γ constant, and equal to 1.2 for the same radius Y of the shock wave and the same energy E. Actually, when the shock pressure falls low enough so that γ increases to 1.4, the coefficient α does not immediately increase by a factor 2, but increases very slowly. Physically the reason for this is that the interior part of the shock volume still has the low value of γ and therefore has a high internal energy for a given pressure. Only when the hot gases which possess the low γ fill a small part of the volume included in the shock wave will the γ in the outer regions of the shock determine the shock pressure.

4.7 The Waste Energy

G. I. Taylor has introduced the concept of the waste energy, i.e., the energy which remains in the hot gases traversed by the shock wave after an adiabatic expansion to a pressure of 1 atm. The knowledge of this waste energy is useful because it permits one to calculate the energy which remains available to the shock wave at small overpressures.

The waste energy can be calculated very simply for the point source solution. Let us consider a material element which is traversed by the

shock at a shock pressure p_s. When this element has been expanded adiabatically to atmospheric pressure p_0, its density will be

$$\rho = \rho_0 \frac{\gamma + 1}{\gamma - 1}\left(\frac{p_0}{p_s}\right)^{1/\gamma} \tag{4.69}$$

Its temperature will be p_0/ρ and its energy content per unit mass

$$\epsilon = \frac{\gamma p_0}{\rho(\gamma - 1)} = \frac{\gamma}{\rho_0(\gamma + 1)} p_0^{(\gamma-1)/\gamma} p_s^{1/\gamma} \tag{4.70}$$

In calculating the energy content, we have used the specific heat at constant pressure; the reason for this is that our final state is obtained from normal air by heating it at constant pressure p_0 to the temperature p_0/ρ. Strictly speaking, in order to get the waste energy, we should subtract from Eq. 4.70 the expression $\gamma p_0/\rho_0(\gamma - 1)$, but we shall confine our discussion to the case when $p_s \gg p_0$.

The total energy wasted in the shock wave is then

$$W = 4\pi\rho_0 \int Y^2 \, dY \, \epsilon \tag{4.71}$$

We can now use the relation between shock pressure and radius, Eq. 4.33. We are using this fairly exact relation because it will turn out that we have to know the waste energy including terms of relative order $\gamma - 1$. We solve Eq. 4.33 for Y; inserting the result and Eq. 4.70 into Eq. 4.71 we obtain

$$W = C \, E(p_0)^{(\gamma-1)/\gamma} \int_{Kp_0}^{\infty} (p_s)^{1/\gamma} \frac{d\, p_s}{p_s^2} \tag{4.72}$$

where K is some undetermined multiplicative constant (cf. following discussion). Here

$$C = 2(\gamma - 1)\left[1 - (\gamma - 1)\left(\frac{3}{2} - \ln 2\right)\right]\frac{\gamma}{\gamma + 1}$$

$$\approx (\gamma - 1)\,[1 - (\gamma - 1)\,(1 - \ln 2)] \tag{4.72a}$$

neglecting terms of relative order $(\gamma - 1)^2$. Equation 4.72 gives the energy wasted up to the time when the shock pressure has fallen to the value Kp_0.

Equation 4.72 can be integrated immediately and gives

$$W = \frac{\gamma}{\gamma - 1} C E \left(\frac{p_0}{Kp_0}\right)^{(\gamma-1)/\gamma}$$

$$= [1 + (\gamma - 1) \ln 2] E K^{-(\gamma-1)/\gamma} \tag{4.73}$$

Subtracting this expression from the total energy E we obtain the energy which is still available:

$$E_{eff} = E\left[1 - \left(\frac{K}{2}\right)^{-(\gamma-1)/\gamma}\right] \tag{4.74}$$

It is clear that for small values of $\gamma - 1$ and moderate K this expression is proportional to $\gamma - 1$. This shows the necessity of knowing the relation between p_s and E up to terms of the order $\gamma - 1$, i.e., of using Eq. 4.33 rather than Eq. 4.17.

It is somewhat problematic what to use for K. Clearly the relation 4.33 will break down at too low values of p_s; namely, when the limiting form of the Hugoniot relations ceases to be valid. This requires

$$K \gg \frac{\gamma + 1}{\gamma - 1} \tag{4.75}$$

Setting

$$K = 2 \frac{n}{\gamma - 1} \tag{4.76}$$

then $n \gg 1$, and using the fact that $\gamma - 1$ is small, Eq. 4.74 reduces to

$$E_{eff} = E(\gamma - 1) \log \frac{n}{\gamma - 1} \tag{4.77}$$

Of course the available energy will be further reduced as the shock pressure is reduced closer to atmospheric pressure. In fact, Penney has shown that the dissipation of energy continues indefinitely as the shock wave expands (see Chapter 5, Section 5.7). It is therefore not possible to give any accurate

definition of the percentage of energy wasted but it would be necessary to specify the shock pressure for which this statement is made. In order to obtain the percentage wasted for shock pressures of the order of 1 atm, it would be necessary to follow the shock wave through the region of intermediate pressures which can adequately be done only by numerical methods (see Chapter 6).

However, it is clear from our Eq. 4.77 that the energy available for the shock wave is smaller, the smaller $\gamma - 1$. The fact that the air has a small value of γ at high temperatures leads to increased dissipation of energy at the shock and, therefore, to a relatively smaller blast wave at large distances. This is the main reason why the blast wave from a nuclear explosion is less strong at a given distance than that from a TNT explosion liberating the same total energy. In the latter case the temperatures reached are only moderate, and the energy wasted is, therefore, less than for the nuclear explosion.

The greater wastage of energy for smaller γ is also related to the result obtained in Section 4.6; namely, that the shock pressure after a sudden change of γ does not correspond to the new value of γ, but is rather close to the value for the original value of γ. This slow variation of the shock pressure is in turn important if one wants to calculate the waste energy for a gas with variable γ. In fact, if it were not for this gradual change, gases might occur in which the waste energy would be greater than the total energy available, which would be obvious nonsense. The change of α derived in Section 4.6 is just sufficiently gradual to keep the waste energy always below the total available energy.

Chapter 5

ASYMPTOTIC THEORY FOR SMALL BLAST PRESSURE

by H. A. Bethe and K. Fuchs

5.1 Introduction

It is very desirable to have a theory of shock waves which is valid for small overpressure. One purpose of such a theory is to provide a natural transition to the well-known acoustic theory, and to set in evidence the limitations of the latter. Another purpose is to give practical results for the pressure up to arbitrarily large distances and to make it possible to stop the numerical calculation with IBM machines (see Chapter 6) at some finite low pressure. This numerical calculation would become increasingly inaccurate and cumbersome with increasing radius of the shock wave; the use of asymptotic formulae therefore improves both the accuracy and the ease of the calculation.

The theory presented in this chapter represents the first terms of an expansion in powers of the ratio L/Y where Y is the radius of the shock wave and L its length, i.e., the distance from the first shock to a point at which the pressure has decreased to a small fraction of the peak pressure. We shall in general retain the first and second power of L/Y and neglect the third. One strong reason for stopping at just this point is that the entropy in the shock is proportional to p^3, where p is the overpressure at the shock front which in turn is proportional to 1/Y. Therefore, if we neglect terms of order $(L/Y)^3$, we can consider the entire process as adiabatic which involves a great simplification. At one point in our development, however (Section 5.7), we shall calculate the actual energy transformed into heat at the shock front and at this point we shall, of course, carry terms of order $(L/Y)^3$.

Ordinary acoustic theory does not represent the first term in an expansion of the type considered here. We shall find that the length of a

spherical shock wave increases gradually as the shock wave moves away from its center, whereas an acoustic wave retains its wavelength all the time. Similarly, the decay of the pressure at the shock front is somewhat faster than that of the pressure in an acoustic wave. However, acoustic theory is very useful to provide some guiding ideas for our theory, and we shall therefore start by a recapitulation of the acoustic theory of an outgoing spherical wave.

5.2 Acoustic Theory

In the ordinary hydrodynamic equations (see below, Eq. 5.12) all terms should be neglected which are of second or higher order in pressure p or material velocity u. Then the hydrodynamic equations become

$$\frac{\partial u}{\partial t} = - c \frac{\partial \sigma}{\partial r}$$

$$\frac{\partial \sigma}{\partial t} = - c \left(\frac{\partial u}{\partial r} + \frac{2u}{r} \right) \tag{5.1}$$

where σ is Riemann's quantity, (cf. Eq. 5.10) which for small pressures is given by

$$\sigma = p/\rho_c \tag{5.2}$$

Combining the two equations of 5.1, we get the wave equation

$$D^2\sigma \equiv \frac{\partial^2 \sigma}{\partial r^2} + \frac{2}{r} \frac{\partial \sigma}{\partial r} = c^2 \frac{\partial^2 \sigma}{\partial t^2} \tag{5.3}$$

which has the solution

$$\sigma = \frac{f'(\tau)}{r} \tag{5.4}$$

where[1]

$$\tau = t - \frac{r}{c} \tag{5.5}$$

1. We consider only outgoing spherical waves; for ingoing waves, σ would be a function of $t + r/c$.

and f' is an arbitrary function of τ which is determined by the source which produces the sound. Instead of f', we may also assume $f(\tau)$ as given; $f' = df/d\tau$. Inserting Eq. 5.4 into the first equation of 5.1 and integrating, we get

$$u = \frac{f'(\tau)}{r} + c\frac{f(\tau)}{r^2} \tag{5.6}$$

We see therefore that σ and the pressure p are propagated with sound velocity outwards, and at the same time decay as $1/r$. On the other hand, the material velocity u has one term which behaves in the same way and is actually equal to σ, and a second term which decreases as $1/r^2$. This second term is proportional to

$$f(\tau) = \int f'(\tau)\, dt \tag{5.7}$$

i.e., it depends on the pressure which has existed in the wave at earlier times. For this reason the second term of Eq. 5.6 is known as the after-flow term. It is interesting that this term contains a factor c; therefore, it will become very large in the limit of incompressible theory, which corresponds to infinite sound velocity. In this limit the material velocity becomes

$$u = c\frac{f(\tau)}{r^2} \tag{5.8}$$

At any given time, u is inversely proportional to r^2, meaning that the flow through any spherical surface is the same, as would be expected in incompressible theory.

For finite sound velocity the second term in Eq. 5.6 may or may not be important. If the sound signal is of finite duration $T = L/c$, the ratio of the second to the first term in Eq. 5.6 is of the order L/r. With increasing distance r from the source, therefore, the second term becomes unimportant in comparison with the first.

We shall find that a more accurate theory of pressure waves can be constructed in close analogy to the acoustic theory here outlined.

5.3 General Theory

The equations of motion in Eulerian coordinates are

$$\frac{\partial u}{\partial t} + u\frac{\partial u}{\partial r} = -\frac{1}{\rho}\frac{\partial p}{\partial r}$$

$$\frac{\partial \log \rho}{\partial t} + u\frac{\partial \log \rho}{\partial r} = -\frac{\partial u}{\partial r} - 2\frac{u}{r} \qquad (5.9)$$

The first of these is the equation of motion; the second is the continuity equation. The equation of energy conservation is replaced in our approximation by the condition that the motion is adiabatic (see Section 5.1).

It is convenient to introduce, instead of the pressure, the quantity

$$\sigma = \int c\frac{d\rho}{\rho} = \int \frac{dp}{\rho c} \qquad (5.10)$$

in which c is the sound velocity which itself depends on the density. In Eq. 5.10 we have used the definition

$$c^2 = dp/d\rho \qquad (5.11)$$

Inserting Eq. 5.10 into 5.9 we obtain

$$\frac{\partial u}{\partial t} + u\frac{\partial u}{\partial r} = -c\frac{\partial \sigma}{\partial r}$$

$$\frac{\partial \sigma}{\partial t} + u\frac{\partial \sigma}{\partial r} = -c\left(\frac{\partial u}{\partial r} + \frac{2u}{r}\right) \qquad (5.12)$$

In the acoustic limit the terms containing u as a factor can be neglected and Eq. 5.12 reduces to Eq. 5.1.

We know from the acoustic theory that σ and u behave approximately as 1/r at large distances. We therefore introduce the abbreviations

$$\Sigma = r\sigma \qquad (5.13)$$

$$U = ru$$

With this notation the equations of 5.12 become

$$\frac{\partial U}{\partial t} + c\frac{\partial \Sigma}{\partial r} + u\frac{\partial U}{\partial r} - c\frac{\Sigma}{r} - \frac{U^2}{r^2} = 0$$

$$\frac{\partial \Sigma}{\partial t} + c\frac{\partial U}{\partial r} + u\frac{\partial \Sigma}{\partial r} + c\frac{U}{r} - \frac{U\Sigma}{r^2} = 0 \tag{5.14}$$

We know further from acoustic theory that u becomes asymptotically equal to σ for large distances. We therefore further set

$$U = \Sigma + D \tag{5.15}$$

and we expect that D will become small compared with Σ for large r. Equations 5.14 now become

$$\frac{\partial \Sigma}{\partial t} + (c + u)\frac{\partial \Sigma}{\partial r} + c\left(\frac{\partial D}{\partial r} + \frac{U}{r}\right) - \frac{U\Sigma}{r^2} = 0$$

$$\frac{\partial D}{\partial t} - (c - u)\frac{\partial D}{\partial r} - c\,\frac{2\Sigma + D}{r} - U\frac{D}{r^2} = 0 \tag{5.16}$$

In the first approximation we may neglect the last three terms in the first equation of 5.16. We should expect that d/dr of any quantity is of the order of that quantity divided by L. Therefore the term U/r, which is approximately equal to Σ/r, is small compared to $d\Sigma/dr$, the ratio of the two terms being of the order L/r. The term D/r is small because D is expected to be small compared to Σ as will be proved below. The last term is, in turn, small compared to the second last term.

In the first approximation, therefore, the first equation of 5.16 reduces to

$$\frac{\partial \Sigma}{\partial t} + (c + u)\frac{\partial \Sigma}{\partial r} = 0 \tag{5.17}$$

This equation means that Σ propagates with the velocity $c - u$. This is the analogue of acoustic theory in which Σ propagates with velocity c_o. The replacement of the ordinary sound velocity c_o by the effective sound velocity $c - u$ is physically obvious and is analogous to the well-known Riemann method for treating plane problems.

The solution of Eq. 5.17 is

$$\Sigma = \Sigma(\tau) \tag{5.18}$$

with

$$\tau = t - \int \frac{dr}{c + u} \tag{5.19}$$

The integration in the expression of Eq. 5.19 is to be extended over a path along which Σ is constant. The integral therefore depends on Σ and the equation does not give an explicit solution of Eq. 5.17. The lower limit in the integral may be a function of Σ. If we choose the same lower limit r_0 for all Σ, then τ is the time when the value of Σ to which it belongs passes the point r_0. For the present we shall not specify the lower limit. The function $\Sigma(\tau)$ must be determined from the shape of the shock wave at some initial time. This will be discussed in Section 5.10.

5.4 Second Approximation

We shall now try to determine the function D from the second equation of 5.16 and also to get a better approximation for Σ. In this second equation we can certainly neglect the last term. The first two terms can be transformed by introducing instead of t the variable τ defined in Eq. 5.19. We have then

$$\left(\frac{\partial D}{\partial t}\right)_r = \left(\frac{\partial D}{\partial \tau}\right)_r$$

$$\left(\frac{\partial D}{\partial r}\right)_t = \left(\frac{\partial D}{\partial r}\right)_\tau - \left(\frac{\partial D}{\partial \tau}\right)_r \frac{1}{c + u} \tag{5.20}$$

and the second equation of 5.16 becomes

$$\frac{2c}{c + u}\left(\frac{\partial D}{\partial \tau}\right)_r = \frac{2c\Sigma}{r} + c\left[\frac{D}{r} + \left(\frac{\partial D}{\partial r}\right)_\tau\right] + u\left(\frac{D}{r} - \frac{\partial D}{\partial r}\right) \tag{5.21}$$

Neglecting all terms of smaller order of magnitude, the right hand side reduces to $2c\Sigma/r$ and the factor on the left to 2. Then Eq. 5.21 can be integrated and gives

$$D = \frac{c}{r} \int \Sigma \, d\tau \tag{5.22}$$

This result shows that D is actually of the order $\Sigma\, L/r$, and is therefore small compared to Σ according to our assumptions. This justifies the first approximation given in the last section, as well as the treatment given in this section. It is of interest, however, to write down the right hand side of Eq. 5.21 to the next approximation. For this purpose we note that according to Eq. 5.22

$$\left(\frac{\partial D}{\partial r}\right)_{\tau} = -\frac{D}{r} \tag{5.23}$$

Therefore Eq. 5.21 becomes

$$\left(\frac{\partial D}{\partial \tau}\right)_{r} = (c + u)\frac{\Sigma}{r} \tag{5.24}$$

in which only terms of order uD/r are neglected, but terms of order cD/r and $u\Sigma/r$ have been taken into account.

The form of Eq. 5.22 shows that D has the character of an after-flow term and therefore corresponds in all respects to the after-flow term in Section 5.2.

The integral in Eq. 5.22 must be extended from the shock front to the point at which D is to be calculated. To prove this, it must be shown that D behind the shock front is of smaller order than Eq. 5.22. This can easily be done by using the Hugoniot relations and the definition of σ. We have behind the shock front

$$u^2 = (p - p_0)(V_0 - V) \tag{5.25}$$

where the subscript 0 refers to the undisturbed material, and V is the specific volume. Further, we have generally

$$\sigma = \int_{\rho_0}^{\rho} \sqrt{\frac{dp}{d\rho}}\,\frac{d\rho}{\rho} = \int_{V}^{V_0} \sqrt{-\frac{dp}{dV}}\; dV \tag{5.26}$$

The value of D behind the shock front is by definition

$$D = r(u - \sigma) \tag{5.27}$$

To evaluate Eqs. 2.25 and 2.26 it is convenient to introduce the quantity

$$x = \frac{V_0 - V}{V_0} \tag{5.28}$$

and to express the pressure in terms of this quantity

$$p = p_0 - V_0 \frac{dp}{dV} x + \frac{V_0^2}{2} \frac{d^2p}{dV^2} x^2 - \frac{V_0^3}{6} \frac{d^3p}{dV^3} x^3 + \ldots \tag{5.29}$$

Using the definition of the sound velocity we have

$$-\frac{dp}{dV} = \frac{c_0^2}{V_0^2} \tag{5.30}$$

and we write

$$\frac{d^2p}{dV^2} = 2\alpha \frac{c_0^2}{V_0^3}$$

$$-\frac{d^3p}{dV^3} = 6\beta \frac{c_0^2}{V_0^4} \tag{5.31}$$

where α and β are dimensionless coefficients. If the adiabatic law is of the usual form

$$p = p_0 \left(\frac{V}{V_0} \right)^{-\alpha} \tag{5.32}$$

the values of α and β are

$$\alpha = \frac{(\gamma + 1)}{2}$$

$$\beta = \frac{(\gamma + 1)(\gamma + 2)}{6} \tag{5.33}$$

With these abbreviations Eq. 5.29 becomes

$$p - p_0 = \frac{c_0^2}{V_0}(x + \alpha x^2 + \beta x^3 + \ldots) \tag{5.34}$$

Inserting Eqs. 5.34 and 5.28 into the Hugoniot relation (Eq. 5.25) we obtain

$$u = c_0 x\left[1 + \frac{1}{2}\alpha x + \left(\frac{1}{2}\beta - \frac{1}{8}\alpha^2\right)x^2 + \ldots\right] \tag{5.35}$$

Further we find,

$$\sqrt{-\frac{dp}{dV}} = \frac{c_0}{V_0}\left[1 + \alpha x + \left(\frac{3\beta}{2} - \frac{\alpha^2}{2}\right)x^2 + \ldots\right] \tag{5.36}$$

or for the sound velocity

$$c = c_0\left[1 + (\alpha - 1)x + \left(\frac{3\beta}{2} - \frac{\alpha^2}{2} - \alpha\right)x^2 + \ldots\right] \tag{5.37}$$

Inserting Eq. 5.36 into the expression 5.26 we find

$$\sigma = c_0 x\left[1 + \left(\frac{\alpha}{2}\right)x + \left(\frac{\beta}{2} - \frac{\alpha^2}{6}\right)x^2 + \ldots\right] \tag{5.38}$$

and subtracting we get

$$u - \sigma = c_0\, \alpha^2 \frac{x^3}{24} \tag{5.39}$$

This relation holds generally behind the shock front. It is interesting that it depends on the quantity α, i.e., on d^2p/dV^2 which is also the quantity determining the entropy change at the shock front (see Section 5.5). For our present purpose the important point is that $u - \sigma$ is proportional to x^3 and therefore to σ^3, and therefore falls off as $1/Y^3$ where Y is the shock radius. The quantity D just behind the shock front will therefore fall off as $1/Y^2$ which makes it of smaller order of magnitude than the expression of Eq. 5.22.

We note in passing that, according to Eqs. 5.35 and 5.37, the velocity of wave propagation is in first approximation

$$c + u = c_0(1 + \alpha x) \tag{5.40}$$

We shall now insert our expression for D back into the first equation of 5.16. We have to calculate the quantity

$$\left(\frac{\partial D}{\partial r}\right)_t \tag{5.41}$$

Using Eqs. 5.20, 5.23, and 5.24 and the definition of τ, this becomes

$$\left(\frac{\partial D}{\partial r}\right)_t = -\frac{D}{r} - \frac{\Sigma}{r} = -\frac{U}{r} \tag{5.42}$$

As was explained above, only quantities of the order $(u/c)(D/r)$ are neglected in this expression.

Inserting Eq. 5.42 into the first equation of 5.16 we see that the terms U/r cancel. Therefore the first equation of 5.16 becomes, neglecting the very small term $D\Sigma/r^2$,

$$(c + u)\left(\frac{\partial \Sigma}{\partial r}\right)_\tau = \frac{\partial \Sigma}{\partial t} + (c + u)\left(\frac{\partial \Sigma}{\partial r}\right)_t = \frac{\Sigma^2}{r^2} \tag{5.43}$$

Neglecting u in c + u, this can be integrated to give

$$\frac{1}{\Sigma} = \frac{1}{\Sigma_0} + \frac{1}{cr} \tag{5.44}$$

In other words, along a line of constant τ, not Σ itself is a constant, but the somewhat more complicated quantity

$$\frac{\Sigma}{1 - \frac{\Sigma}{cr}} = \Sigma_0 \tag{5.44a}$$

Σ itself therefore increases as the wave propagates outwards.

5.5 The Motion of the Shock Front

Let us assume that the shock front moves from a radius Y to a radius Y + dY. The shock velocity can easily be shown to be in first approximation midway between the effective sound velocities ahead and behind the shock. The former sound velocity is c_0, the latter c + u, so that the shock velocity is

$$\dot{Y} = \frac{1}{2}(c_0 + c + u) \tag{5.45}$$

and the time needed for the shock to travel the distance dY is

$$dt = \frac{2dY}{c_0 + c + u} \tag{5.46}$$

The shock velocity is smaller than the velocity of sound waves behind the shock, c + u. Therefore these sound waves will catch up with the shock wave, and if the shock is followed by a rarefaction as it is in the case of a blast wave, then the rarefaction will gradually cut down the strength of the shock. In our notation, the value of τ at the shock will gradually change; if it has the value τ when the shock is at Y, it will have the value $\tau + d\tau$ when the shock has moved to Y + dY.

In order to calculate the variation of τ along the shock front, we have to complete the definition of τ which was left somewhat arbitrary. It is convenient to define the arbitrary constant of integration in Eq. 5.19 as follows.

$$\tau = t - \int_Y^r \frac{dr}{c + u} - \frac{Y}{c_0}$$

where Y is the shock radius at the time when the signal Σ reaches the shock front. Y, therefore, is a function of Σ and this is permissible since the constant of integration was allowed to depend on Σ. If we use the definition above, then $\tau + Y/c_0$ is the time when the signal Σ reaches the shock, or τ is the difference in the actual time and the time which would be required for a signal traveling from the origin with normal sound velocity c_0.

The time difference dt between the arrival of the signals τ and $\tau + d\tau$ at the shock front is therefore

$$dt = d\tau + \frac{dY}{c_0} \tag{5.47}$$

Comparison with Eq. 5.46 yields

$$\frac{d\tau}{dY} = \frac{2}{c_0 + c + u} - \frac{1}{c_0} = \frac{c_0 - c - u}{c_0(c + c + u)} \cong \frac{c_0 - c - u}{2c_0^2} \tag{5.48}$$

This equation describes the catching up of the rarefaction wave with the shock front.

From Eqs. 5.40 and 5.38 follows

$$c + u = c_0 + \alpha\sigma \tag{5.49}$$

Hence Eq. 5.48 becomes

$$\frac{d\tau}{dY} = \frac{-\alpha\sigma}{2c_0^2} = -\frac{\alpha\Sigma}{2c_0^2 Y} \tag{5.50}$$

where we have also used the definition of $\Sigma = \sigma Y$.

5.6 Results for Very Large Distances

Up till now we have not made any special assumptions about the function $\Sigma(\tau)$, i.e., about the shape of the shock wave. We can get further results if we assume that initially (at small distances from the origin) the shock wave was of short duration, and that most of the duration at shock radius Y is due to the excess of the shock velocity over the unperturbed sound velocity c_0. This assumption is quite well justified for blast waves at sufficiently large distance. If t_0 is the time at which a given value of Σ exists at a given small radius r_0, then we have for the arrival time of this value of Σ at the distance r (cf. Eq. 5.40)

$$t = t_0 + \int_{r_0}^{r} \frac{dr}{c + u} \approx t_0 + \int_{r_0}^{r} \frac{dr}{c_0 + \frac{\alpha\Sigma}{r}}$$

$$= \frac{r}{c_0} - \frac{r_0}{c_0} + t_0 - \frac{\Sigma\alpha}{c_0^2} \ln \frac{r}{r_0} \tag{5.51}$$

If we neglect small difference in the values of t_0 and r_0 for different values of Σ, it follows that for fixed r, Σ is a linear function of t and therefore the pressure assumes a linear shape also.

We apply Eq. 5.51 in particular at the shock front $r = Y$, $\Sigma = \Sigma_s$. Then t is the time of arrival of the signal Σ_s at the shock radius Y. However, this time was also equal to $\tau_s + Y/c_0$ where τ_s is the value of τ corresponding to Σ_s. Neglecting again r_0 and t_0 as small quantities, we find therefore

$$\tau_s = -\frac{\Sigma_s \alpha}{c_0^2} \ln \frac{Y}{r_0} \tag{5.52}$$

In the approximation in which r_0 and t_0 are neglected, $|\tau_s|$ is by definition the difference in the arrival time of the shock and of the signal $\Sigma = 0$, since the latter travels with sound velocity c_0; i.e., $|\tau_s|$ is identical with the duration of the positive pressure pulse. This is easily verified from Eq. 5.51.

In order to obtain τ_s as function of Σ_s only, we have to express the shock radius Y in terms of Σ_s. For this purpose we substitute Eq. 5.52 into 5.50. Then we get

$$\frac{d\Sigma_s}{dY} = -\frac{\Sigma_s}{2Y \ln (Y/r_0)} \tag{5.53}$$

which can immediately be integrated to give

$$\Sigma_s = \frac{A}{\sqrt{\ln (Y/r_0)}} \tag{5.54}$$

where A is a constant. In other words, the value of Σ at the shock front is not constant but decreases due to the catching up of the rarefaction. This decrease is very slow; it goes only as the inverse square root of the logarithm of the shock radius.

The derivation given above may give rise to the impression that r_0 may be chosen arbitrarily as long as it is small compared to all values Y for which the formula (Eq. 5.54) is applied. This is not so. In fact, it is easily shown that we are led to contradictions if we allow r_0 to vary over any appreciable range.

We shall see later that a detailed analysis will allow us to determine the correct value of r_0 which should be inserted in Eq. 5.54. For the present let it suffice to point out that a pressure pulse of the asymptotic shape requires two parameters to determine its initial conditions, namely the strength and duration of the pulse. We require, therefore, two constants in the asymptotic law and thus both the constant A and the constant r_0 are determined by the properties of the pulse.

Going back to Eq. 5.51, we find then that the duration of the pressure pulse will increase as the square root of log Y. The product of peak pressure, p_f, and duration, θ, or the so-called impulse of the wave, will therefore behave exactly as 1/Y, namely

$$p_f\theta = \frac{\text{const}}{Y} \tag{5.55}$$

We have thus seen that in our approximation a shock wave will spread out gradually, in contrast to the acoustic theory in which the wave retains its shape for all time. The spreading of a shock wave in three dimensions is very slow. It would be considerably faster in two, and still faster in one, dimension. On the other hand, for a space of more than three dimensions this effect will not occur.

Connected with the spreading of the wave there is a decrease of the front pressure which is faster than 1/Y. Again, in three dimensions this effect is small; in one dimension, elementary acoustic theory would give constant front pressure whereas the actual behavior is as $1/\sqrt{Y}$. The case of two dimensions is again intermediate, and for more than three dimensions, acoustic theory becomes the correct asymptotic limit.

Another interesting phenomenon which is connected with the variation of the sound velocity c + u is the fact that a second shock must be formed in the negative phase of a shock wave. The regions of negative pressure have a particularly small propagation velocity, c + u, which is smaller than normal sound velocity, c_0. Therefore the very end of the shock wave tends to catch up with the regions of negative pressure and a second shock will result. This will be discussed in more detail in Section 5.9.

Another interesting problem is the motion of the point $\Sigma = 0$, which marks the end of the positive pressure phase ($p > p_0$) and the beginning of the negative phase. In our approximation the propagation velocity of this point is just the normal sound velocity c_0. Actually, however, u is somewhat greater than σ by the amount D/r. Therefore the point $\Sigma = 0$ propagates with a velocity slightly greater than normal sound velocity. Since the very tail of the shock wave moves with velocity c_0, the end of the positive phase $\Sigma = 0$ moves with a velocity slightly greater than the end of the negative

phase. Consequently the positive phase will tend to become somewhat shorter and the negative phase somewhat longer than the elementary theory indicates. This corresponds to observations.

A very important remark about the shape of shock waves has been made by Penney. It is most easily deduced from the fact that the total mass of air behind the shock must be equal to the original mass of air within the radius Y. This means

$$\int_0^Y \rho r^2 \, dr = \rho_0 \frac{Y^3}{3} \tag{5.56}$$

There are two regions in which the density is appreciably different from the normal density ρ_0. One is the central region in which the gases have been left at high temperature by the shock and therefore have low density. If the shock wave is far out, these regions have returned to atmospheric pressure and therefore to a definite density. If X denotes a radius small compared to Y, but large compared to the region of the hot gases, we shall have

$$\int_0^X \rho r^2 \, dr = \rho_0 \frac{X^3}{3} - M \tag{5.57}$$

where M is a constant independent of X and of the time. Subtracting Eq. 5.57 from 5.56 we get

$$\int_X^Y (\rho - \rho_0) r^2 \, dr = M \tag{5.58}$$

The shock region itself may be assumed to be small in extension compared to Y. Therefore in this region we can replace r by Y. Furthermore, the deviation of the density from normal, $\rho - \rho_0$, is proportional to σ. Therefore we obtain from Eq. 5.58

$$Y^2 \int_{\text{shock}} \sigma \, dr = Y \int_{\text{shock}} \Sigma \, dr = M \tag{5.59}$$

From this follows that

$$\int \Sigma \, dr \sim 1/Y \tag{5.60}$$

However, we know that the value of Σ at the front is nearly constant. Therefore the integral in relation 5.60 must consist of two contributions which nearly cancel each other. The shock wave must consist of a phase of positive σ (overpressure) and a phase of negative σ (underpressure) such that the impulses of the two phases cancel each other in first approximation. This argument is also a proof of the existence of the negative phase; it was first given by Penney using the energy rather than the amount of material.

In particular, in the limit in which the pressure depends linearly on the time, the shape of the shock wave becomes symmetrical, with equal shocks at the beginning and at the end as illustrated in Fig. 5.1.

5.7 The Energy

The energy flux through a given surface consists of two parts, namely, (1) the work done by the material on one side, on the material on the other side, and (2) the energy transported with the material itself. Since we have proved at the end of the last section that the pressure pulse in a shock wave has a negative phase balancing the positive phase, the final displacement of any point is zero in first approximation

$$\int u dt = 0 \frac{1}{Y} \tag{5.61}$$

This means that the net transport of energy with the material is zero of higher order than the work term mentioned as part (1) above.

Therefore the energy flux in the shock wave through a sphere of radius Y is in sufficient approximation

$$W = 4\pi Y^2 \int p u dt \tag{5.62}$$

If we set $u = \sigma$, $p = \rho c \sigma$, and $\sigma = \Sigma/Y$, and if we further assume that the pressure distribution is as indicated in Fig. 5.1, the energy flux becomes

$$W = 4\pi\rho c \int \Sigma^2 \, dt = 4\pi\rho c \Sigma_f^2 \theta \int_{-1}^{1} x^2 dx \tag{5.63}$$

where θ is the duration of the positive phase which, according to Eq. 5.52,

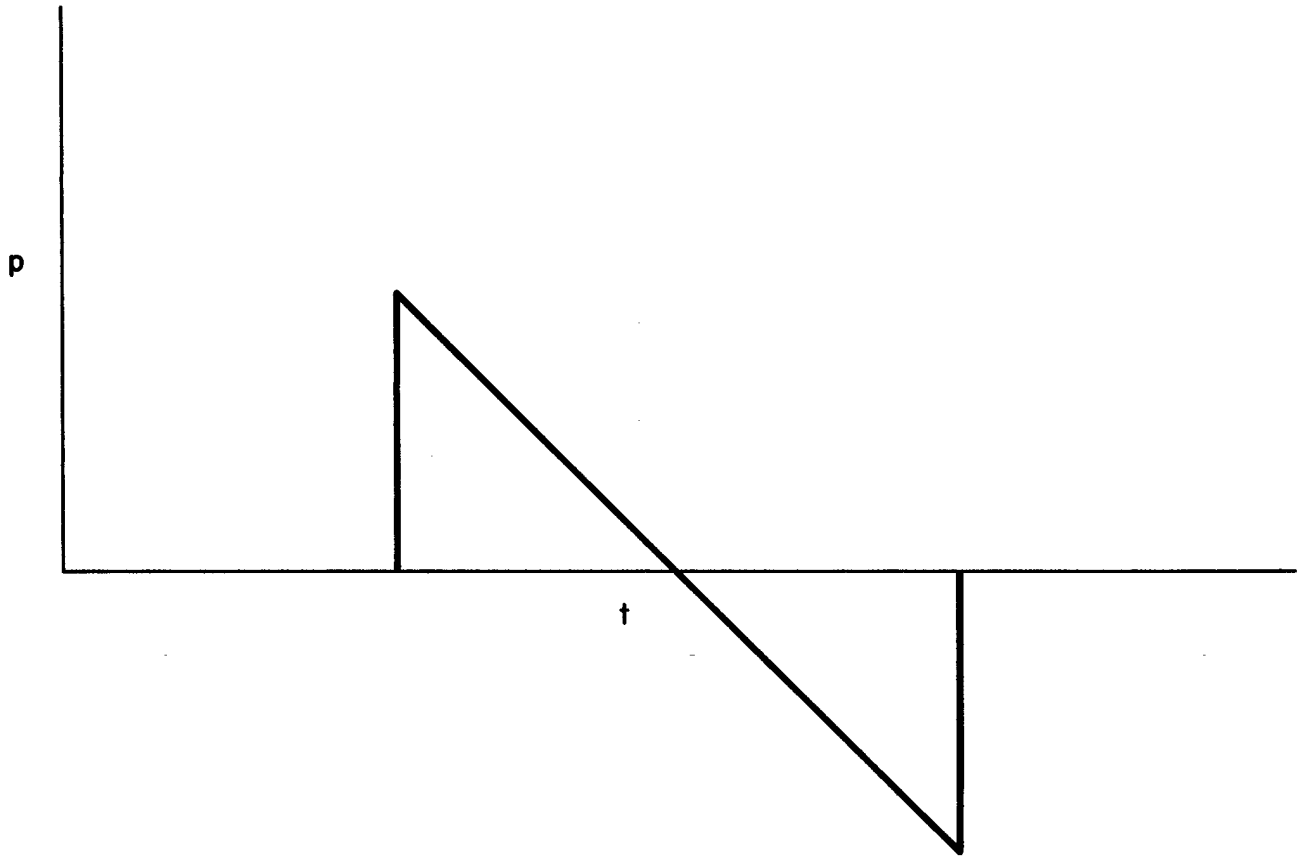

Fig. 5.1 Symmetrical equal shock waves

has the value

$$\theta = \frac{\alpha \Sigma_f}{c_0^2} \ln \frac{Y}{r_0} \tag{5.64}$$

so that

$$W = \frac{8\pi\alpha\rho}{3c_0} \Sigma_f^3 \ln \frac{Y}{r_0} \tag{5.65}$$

Using the relation of Eq. 5.54 for Σ this becomes

$$W = \frac{8\pi\alpha\rho}{3c_0} \frac{A^3}{\sqrt{\ln (Y/r_0)}} \tag{5.66}$$

Equation 5.66 shows that the total energy in the shock wave decreases slowly as the shock wave propagates. This fact was first pointed out by Penney and means that it is impossible to define in any general way the energy wasted in the shock wave, but that this waste will depend on the distance to which the shock wave has gone. It is interesting to determine the decay of the energy in the shock wave in a different way also. This is based on the fact that energy is irreversibly converted into heat at the shock front at all times. To determine this wasted energy or increase in entropy, we use the Hugoniot equation for the energy

$$E - E_0 = \frac{1}{2}(p + p_0)(V_0 - V) \tag{5.67}$$

where the quantities without subscript are behind, those with subscript 0 in front of, the shock wave. The energy can be expanded in a Taylor series in the change of volume and of entropy, as follows

$$E - E_0 = \frac{\partial E}{\partial V}(V - V_0) + \frac{1}{2}\frac{\partial^2 E}{\partial V^2}(V - V_0)^2$$

$$+ \frac{1}{6}\frac{\partial^3 E}{\partial V^3}(V - V_0)^3 + \ldots + \frac{\partial E}{\partial S}(S - S_0) + \ldots \tag{5.68}$$

If we remember that

$$\left(\frac{\partial E}{\partial V}\right)_S = -p_0$$

$$\left(\frac{\partial E}{\partial S}\right)_V = T_0 \tag{5.69}$$

and introduce the abbreviation of Eq. 5.28, Eq. 5.68 becomes

$$E - E_0 = p_0 V_0 x - \frac{1}{2}\frac{\partial p}{\partial V} V_0^2 x^2 + \frac{1}{6}\frac{\partial^2 p}{\partial V^2} V_0^3 x^3 + \ldots + T_0(S - S_0) + \ldots \tag{5.70}$$

Further, we have

$$p = p_0 - \frac{\partial p}{\partial V} V_0 x + \frac{1}{2}\frac{\partial^2 p}{\partial V^2} V_0^2 x^2 \tag{5.71}$$

Inserting Eqs. 5.70 and 5.71 into 5.67, we find

$$T_0(S - S_0) = \frac{1}{12}\frac{\partial^2 p}{\partial V^2} V_0^3 x^3 \tag{5.72}$$

This is the energy wasted per gram of material swept over by the shock. If we now use Eqs. 5.31 and 5.38 we obtain

$$\frac{dW}{dY} = -4\pi\rho Y^2 T_0(S - S_0) = -\frac{2\pi}{3}\alpha\rho c_0^2 x^3 Y^2$$

$$= -\frac{2\pi}{3}\frac{\rho\alpha}{c_0}\sigma^3 Y^2 \tag{5.73}$$

In our shock wave at very large distances, there are two shocks of equal strength and therefore the energy loss Eq. 5.73 occurs twice. Thus we find for the decrease of energy in the shock wave itself

$$\frac{dW}{dY} = -\frac{4\pi}{3}\frac{\rho\alpha}{c_0}\frac{\Sigma_f^3}{Y} \tag{5.74}$$

Comparing this with the expression for the energy itself, Eq. 5.66, we find

$$\frac{dW}{dY} = -\frac{W}{2Y\ \ln\ (Y/r_0)} \tag{5.75}$$

which integrates immediately to

$$W = \frac{\text{const.}}{\sqrt{\ln\ (Y/r_0)}} \tag{5.76}$$

This result is exactly the same as deduced above by explicit evaluation of W, Eq. 5.66. We therefore have found the decay of the energy by two entirely independent methods. Both methods are only applicable if the shape of the pressure pulse remains unchanged.

5.8 The Propagation of the Shock at Intermediate Distances

The asymptotic form of the pressure pulse behind the shock is usually reached only at very large distances when the shock pressure has become extremely small. There is an intermediate region, in which the shock pressure is quite small, but the pressure distribution behind the shock is not yet linear. We shall now consider this intermediate region, i.e., we make all the assumptions which led to the first approximation considered in the preceding section, but we allow, within certain limitations, an arbitrary shape of the pulse.

Since we are interested in applying the theory to the IBM calculations, we shall slightly change the procedure used in the preceding sections. Instead of introducing as initial condition the shape of the pulse at a fixed point as function of time, we introduce the pulse at a fixed time t_0 as function of the radius y. Hence, we write the solution of Eq. 5.17 in the form

$$\Sigma = \Sigma(y) \tag{5.77}$$

$$y = r - \int_{t_0}^{t} (c + u)dt \tag{5.78}$$

Then Σ as function of y is given by the initial pressure distribution at time t_0. Using Eq. 5.49 we find

$$y = r - c_0(t - t_0) - \int_{t_0}^{t} \alpha\sigma \, dt \tag{5.79}$$

The remaining integral is a small term and therefore we may replace dt by $d\tau/c_0$. Also $\sigma = \Sigma/r$ and Σ is constant for the purpose of integration. Thus

$$y = r - c_0(t - t_0) - \alpha\frac{\Sigma}{c_0} \ln\frac{r}{y} \tag{5.80}$$

Alternatively we might have replaced r in the integral by $y + c_0(t - t_0)$ and found

$$y = r - c_0(t - t_0) - \frac{\alpha\Sigma}{c_0} \ln\frac{y + c_0(t - t_0)}{y} \tag{5.81}$$

Since Σ/c_0 must be small compared to y, the two equations differ only by terms of the order $(\Sigma/yc_0)^2$.

We introduce the abbreviation

$$g(\Sigma) = \frac{c_0 y}{\alpha} - \Sigma \ln y - k \tag{5.82}$$

which is a constant. For convenience we define k in such a way that

$$g(0) = 0 \tag{5.82a}$$

Then Eq. 5.80 takes the form

$$r = c_0(t - t_0) + \frac{\alpha}{c_0} [g(\Sigma) + \Sigma \ln r + k] \tag{5.83}$$

In particular, if Σ_s is the value of Σ at the shock front R

$$R = c_0(t - t_0) + \frac{\alpha}{c_0}\left[g(\Sigma_s) + \Sigma_s \ln R + k\right] \tag{5.84}$$

Differentiation yields

$$\frac{dR}{dt}\left[1 - \frac{\alpha\Sigma}{c_0 R}\right] = c_0 + \frac{d\Sigma_s}{dt}\frac{\alpha}{c_0}\left[\frac{dg}{d\Sigma_s} + \ln R\right] \tag{5.85}$$

The shock velocity is also equal to the average value of c + u in front and behind the shock, i.e.,

$$\frac{dR}{dt} = \frac{1}{2}\left[c_0 + c + u\right] = c_0\left[1 + \frac{\alpha\Sigma_s}{2c_0 R}\right] \tag{5.86}$$

Here we have made use of Eq. 5.49. Comparing the two equations for dR/dt and observing that Σ/c_0R is a small quantity, one finds

$$\frac{\Sigma_s}{2R} + \frac{1}{c_0}\frac{d\Sigma_s}{dt}\left[\frac{dg}{d\Sigma_s} + \ln R\right] = 0 \tag{5.87}$$

or

$$\frac{\Sigma_s}{2R}\frac{dR}{d\Sigma_s} + \frac{dg}{d\Sigma_s} + \ln R = 0 \tag{5.88}$$

This is an inhomogeneous linear equation in ln R and can therefore be solved with the result

$$\ln R = \frac{2}{\Sigma_s^2}\int_{\Sigma_s}^{\Sigma_0} \Sigma\frac{dg}{d\Sigma}\,d\Sigma + \frac{\Sigma_0^2}{\Sigma_s^2}\ln R_0 \tag{5.89}$$

Here Σ_0 is the value of Σ_s at time $t = t_0$, when $R = R_0$.

Partial integration yields

$$\ln R = 2\left[\frac{g_0}{\Sigma_0} - \frac{g_s}{\Sigma_s} - \frac{1}{\Sigma_s^2}\int_{\Sigma_s}^{\Sigma_0} g(\Sigma)\, d\Sigma\right] + \frac{\Sigma_0^2}{\Sigma_s^2}\ln R_0 \tag{5.90}$$

This form of the equation is more convenient if g is given as function of Σ in numerical form, since it avoids numerical differentiation.

Either of the two equations gives the shock radius R as function of $\Sigma = R\sigma$. Now from Eq. 5.10

$$\Delta p = \rho_0 c_0 \sigma \tag{5.91}$$

and, since

$$c_0^2 = \gamma \frac{p_0}{\rho_0} \tag{5.92}$$

it follows that

$$\frac{\Delta p}{p_0} = \gamma \frac{\sigma}{c_0} = \gamma \frac{\Sigma}{R c_0} \tag{5.93}$$

Thus we obtain the shock pressure Δp_s as function of the shock radius.

Since $g(\Sigma)$ and Σ are finite, the right hand side of Eq. 5.90 is finite except for $\Sigma_s = 0$. Hence Σ_s tends to zero as R tends to infinity.

Let us write Eq. 5.89 in the form

$$\ln R = \frac{2}{\Sigma_s^2}\int_0^{\Sigma_0} \Sigma \frac{dg}{d\Sigma}\, d\Sigma + \frac{\Sigma_0^2}{\Sigma_s^2}\ln R_0$$

$$-\left(\frac{dg}{d\Sigma}\right)_{\Sigma=0} \frac{1}{\Sigma_s^2}\int_0^{\Sigma_s} \Sigma\left[\frac{dg}{d\Sigma} - \left(\frac{dg}{d\Sigma}\right)_{\Sigma=0}\right] d\Sigma \tag{5.89a}$$

Then the last term tends to zero if Σ_s tends to zero and we have asymptotically

$$\Sigma_s = \frac{A}{\sqrt{\ln (R/R^*)}} \tag{5.94}$$

where

$$A^2 = 2 \int_0^{\Sigma_0} \Sigma \frac{dg}{d\Sigma} d\Sigma + \Sigma_0^2 \ln R_0$$

$$\ln R^* = -\left(\frac{dg}{d\Sigma}\right)_{\Sigma=0} \tag{5.95}$$

This is essentially the equation derived previously for very large distances. However, we have obtained here the constant A in terms of the initial conditions and furthermore we have now a definite radius R* in terms of which the radius R should be measured. The contradictions which arose previously are therefore avoided.

It will be observed that the asymptotic law (Eq. 5.94) is obtained only if Σ is sufficiently small; if we plot Σ against y, it will have some shape of the form shown in Fig. 5.2, approximating roughly the initial pressure

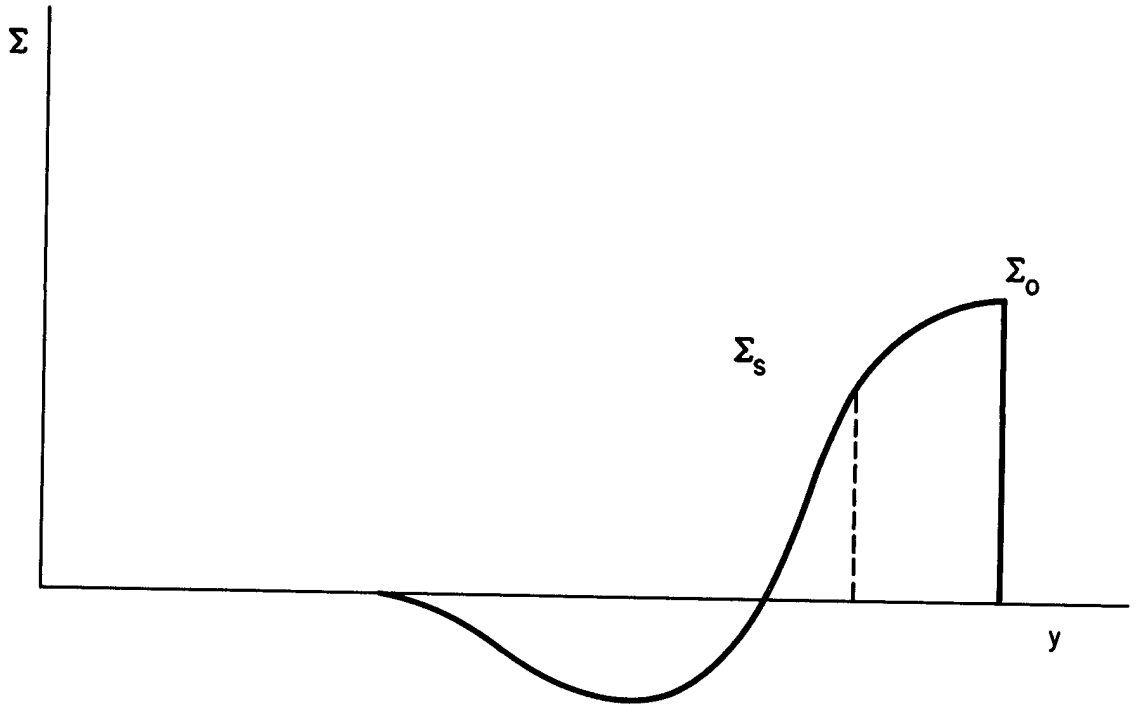

Fig. 5.2 Initial pressure pulse

pulse. As time goes on various Σ values catch up with the shock front and the range of values which initially extended to Σ_0 contracts and extends only to Σ_s. The asymptotic law holds only if Σ_s has become small compared to Σ_0, or more precisely if Σ_s is so small that Σ may be considered a linear function of y between $\Sigma = 0$ and $\Sigma = \Sigma_s$. The smaller Σ the longer it takes for this Σ to catch up with the shock front, and therefore it may take an appreciable time before the asymptotic law is established, unless the initial pulse is already close to a linear function.

The pressure distribution behind the shock in space is most easily obtained from Eq. 5.81

$$r = y + c_0(t - t_0) + \frac{\alpha\Sigma}{c_0} \ln \frac{y + c_0(t - t_0)}{y} \tag{5.96}$$

Asymptotically Σ tends to zero. (We have proved this only for the positive phase, but previous considerations have shown that asymptotically the positive and negative phase become symmetric. We shall consider the negative phase in some detail below.) At the same time y tends to a fixed value y_0. Hence Σ and, therefore, also the pressure become linear in r. The length of the positive phase is obtained from Eq. 5.96 by subtracting r for $\Sigma = 0$ from R for $\Sigma = \Sigma_s$; i.e.,

$$L_+ = y_s - y_0 + \frac{\alpha\Sigma_s}{c_0} \ln \frac{y_s + c_0(t - t_0)}{y_s} \tag{5.97}$$

Asymptotically we have $y_s \to y_0$ and

$$y_0 + c_0(t - t_0) = R - L_+ \cong R \tag{5.98}$$

Inserting this expression into the ln of Eq. 5.97 and using Eq. 5.94 one finds

$$L_+ \to \frac{\alpha A}{c_0} \frac{\ln (R/y_0)}{\sqrt{\ln (R/R^*)}} \tag{5.99}$$

If we wish to obtain the pressure as function of time at a fixed point, it is more convenient to use Eq. 5.80 instead of Eq. 5.81

$$c_0(t - t_0) = r - y - \frac{\alpha\Sigma}{c_0} \ln\frac{r}{y}$$

Following the same arguments as above one finds that the pulse is asymptotically linear. The duration of the positive pulse is given by

$$T_+ = \frac{1}{c_0}\left(y_s - y_0 + \frac{\alpha\Sigma_s}{c_0} \ln\frac{R}{Y_s} \right) \tag{5.100}$$

or asymptotically

$$T_+ \to \frac{\alpha A}{c_0^2} \frac{\ln (R/y_0)}{\sqrt{\ln (R/R^*)}} = \frac{1}{c_0} L_+ \tag{5.101}$$

as it should be. Alternatively we may use Eq. 5.83 to determine the length of the pulse; with Eq. 5.82a we find

$$L_+ = \frac{\alpha}{c_0} [g(\Sigma_s) + \Sigma_s \ln R] \tag{5.99a}$$

and for the duration

$$T_+ = \frac{\alpha}{c_0^2} [g(\Sigma_s) + \Sigma_s \ln R] \tag{5.100a}$$

The shape of the pulse is obtained from Eq. 5.83. If Δt is the time interval between the arrival of the shock and the arrival of the signal Σ at the point r, one finds

$$\Delta t = \frac{\alpha}{c_0^2} [g(\Sigma_s) - g(\Sigma) + (\Sigma_s - \Sigma) \ln r] \tag{5.102}$$

5.9 The Negative Phase. Development of the Back Shock

We assume that the initial conditions are as indicated in Fig. 5.2, so that the negative phase gradually returns to normal pressure. The value $\Sigma = 0$ travels with normal sound velocity, whereas all other Σ values in the negative phase travel more slowly. In fact, throughout the whole region in which $d\Sigma/dy$ is negative, the Σ values have a tendency of catching up with each other. At some stage a Σ value in this region will overtake another and then a shock starts.

As long as r increases with increasing y, the Σ values are in the correct initial order. If r as function of y has an extremum, some Σ values have already overtaken others. A shock starts at the boundary between the two cases, when r as function of y has a point where both the first and second derivatives vanish.

From Eq. 5.83 follows for fixed t

$$\frac{dr}{dy}\left(1 - \frac{\alpha\Sigma}{c_0 r}\right) = \frac{\alpha}{c_0}\left(\frac{dg}{dy} + \frac{d\Sigma}{dy}\ln r\right) \tag{5.103}$$

The condition that $dr/dy = 0$ gives

$$\frac{dg}{dy} + \frac{d\Sigma}{dy}\ln r = 0 \tag{5.104}$$

Now from Eq. 5.82

$$\frac{dg}{dy} = \frac{c_0}{\alpha}\left(1 - \frac{\alpha\Sigma}{c_0 y}\right) - \frac{d\Sigma}{dy}\ln y \tag{5.105}$$

and (since $\alpha\Sigma/c_0 y$ is small), dg/dy and $d\Sigma/dy$ cannot vanish simultaneously. Hence they must both be finite in Eq. 5.104 and we may write

$$\frac{dg}{d\Sigma} + \ln r = 0 \tag{5.106}$$

If we differentiate Eq. 5.103 once more and put $dr/dy = d^2r/dy^2 = 0$, we find

$$\frac{d}{dy}\frac{dg}{d\Sigma} = 0 \tag{5.107}$$

or

$$\frac{d^2g}{d\Sigma^2} = 0$$

If we neglect small terms of the order $\Sigma/c_0 y$ and L/y, this condition can easily be reduced to

$$\frac{d^2\Sigma}{dy^2} = 0 \tag{5.107a}$$

and similarly Eq. 5.106 yields with Eq. 5.105

$$\ln \frac{r}{y} = \frac{(c_0/\alpha)}{(d\Sigma/dy)} \tag{5.106a}$$

Equation 5.107 determines the value $\Sigma = \Sigma_1$, at which the back shock starts. Substitution into Eq. 5.106 gives the radius $r = r_1$ and finally Eq. 5.83 gives the time $t = t_1$.

The back shock starts somewhere inside the negative phase and for some time at least the pressure in the rear and in front of the back shock differs from normal. If Σ_f and Σ_r are the corresponding Σ values, we have for the shock velocity in analogy to Eq. 5.86

$$\frac{dY}{dt} = c_0\left(1 + \alpha \frac{\Sigma_f + \Sigma_r}{2c_0 Y}\right) \tag{5.108}$$

where Y is the position of the back shock. In addition we have two equations similar to Eq. 5.84,

$$\begin{aligned} \frac{c_0}{\alpha}[Y - c_0(t - t_0)] &= g(\Sigma_f) + \Sigma g \ln Y + k \\ &= g(\Sigma_r) + \Sigma_r \ln Y + k \end{aligned} \tag{5.109}$$

Following the procedure used for the first shock, we find equations similar to 5.88.

$$\frac{\Sigma_f - \Sigma_r}{2Y}\frac{dY}{d\Sigma_f} + \frac{dg}{d\Sigma_f} + \ln Y = 0$$

$$\frac{\Sigma_r - \Sigma_f}{2Y}\frac{dY}{d\Sigma_r} + \frac{dg}{d\Sigma_r} + \ln Y = 0 \tag{5.110}$$

Combining the two equations we find

$$\frac{d\Sigma_r}{d\Sigma_f} + \frac{\ln Y + \frac{dg}{d\Sigma_f}}{\ln Y + \frac{dg}{d\Sigma_r}} = 0 \tag{5.111}$$

Eliminating Y by means of Eq. 5.109 one finds

$$\frac{d\Sigma_r}{d\Sigma_f} + \frac{g(\Sigma_r) - g(\Sigma_f) + (\Sigma_f - \Sigma_r)\frac{dg}{d\Sigma_f}}{g(\Sigma_r) - g(\Sigma_f) + (\Sigma_f - \Sigma_r)\frac{dg}{d\Sigma_r}} = 0 \tag{5.112}$$

This equation requires in general numerical integration.

Since both Σ_r and Σ_f are negative, the shock travels with a velocity below the velocity of sound. Hence the value $\Sigma = 0$ will eventually catch up with the back shock, and then the back shock leaves the material behind at normal pressure. Then the equations for the propagation of the back shock take a form similar to those for the first shock

$$\frac{\Sigma_f}{2Y}\frac{dY}{d\Sigma_f} + \frac{dg}{d\Sigma_f} + \ln Y = 0 \tag{5.113}$$

$$\Sigma_r = 0$$

with the solution

$$\ln Y = \frac{2}{\Sigma_f^2}\int_{\Sigma_f}^{\Sigma_2} \Sigma \frac{dg}{d\Sigma}\, d\Sigma + \frac{\Sigma_2^2}{\Sigma_f^2}\ln Y_2 \tag{5.114}$$

Here Σ_2 and Y_2 are the values of Σ_f and Y at the time when Σ_r reaches 0.

Just as for the first shock it follows that Σ_f approaches zero for large Y and one has asymptotically

$$\Sigma_f = \frac{-B}{\sqrt{\ln Y/Y^*}} \tag{5.115}$$

$$B^2 = 2\int_0^{\Sigma_2} \Sigma \frac{dg}{d\Sigma}\, d\Sigma + \Sigma_2^2 \ln Y_2 \tag{5.116}$$

$$\ln Y^* = \left(\frac{dg}{d\Sigma}\right)_{\Sigma=0} = \ln R^* \tag{5.117}$$

We have seen previously that asymptotically the strength of the back shock must be the same as that of the first shock. Hence A should be equal to B, i.e.,

$$2\int_{\Sigma_2}^{\Sigma_0} \Sigma \frac{dg}{d\Sigma}\, d\Sigma + \Sigma_0^2 \ln R_0 - \Sigma_2^2 \ln Y_2 = 0 \tag{5.118}$$

Using the expression of Eq. 5.82 for g we find by means of partial integration

$$2\int^{\Sigma} \Sigma \frac{dg}{d\Sigma}\, d\Sigma = -\Sigma^2 \ln Y + \int \frac{c_0}{\alpha} \Sigma \left\{2 - \frac{\alpha\Sigma}{c_0 y}\right\} dy \tag{5.119}$$

The last term in the integral is small and we require therefore

$$\int_{\Sigma_2}^{\Sigma_0} \Sigma\, dy = \frac{\alpha}{2c_0} \Sigma_2^2 \ln\frac{Y_2}{y_2} \tag{5.120}$$

Here y_2 is the value of y corresponding to Σ_2 and we have made use of the fact that $y = R_0$ for $\Sigma = \Sigma_0$. If we choose our initial conditions at the time when Σ just vanishes behind the back shock, then $y_2 = Y_2$, and the integral of Σ taken over the whole pulse vanishes. The same is true if we choose the initial conditions at any later time.

For later application we shall finally write down the equations which result if the initial pulse has linear shape. We assume

$$\Sigma = \Sigma_0 \frac{y + L_0 - R_0}{L_0} \text{ , for } t = t_0,\ R_0 - 2L_0 < y < R_0 \qquad (5.121)$$

where R_0 is the shock radius and L_0 the length of the positive pulse at time $t = t_0$. Σ_0 is the value of Σ at the shock front, which is related to the shock pressure by Eq. 5.93

$$\Sigma_0 = \frac{R_0 c_0}{\alpha} \frac{\Delta p_s}{p_0} \qquad (5.122)$$

Differentiating the function $g(\Sigma)$ defined by Eq. 5.82, one finds with the help of Eq. 5.121

$$\frac{dg}{d\Sigma} = \frac{c_0}{\alpha} \frac{L_0}{\Sigma_0} - \left(1 - \frac{\alpha\Sigma}{c_0 y}\right) - \ln y \qquad (5.123)$$

Neglecting the second term in the bracket, which is small, and observing that y is for practical purposes constant and equal to R_0, we find that $dg/d\Sigma$ is constant

$$\frac{dg}{d\Sigma} = \frac{c_0}{\alpha} \frac{L_0}{\Sigma_0} - \ln R_0 = - \ln R^* \qquad (5.124)$$

Here we have used the definition of Eq. 5.95 for R*.

For the constant A^2 defined also by Eq. 5.95 we find

$$A^2 = \Sigma_0^2 \left(\frac{dg}{d\Sigma} + \ln R_0\right) = \frac{c_0}{\alpha} L_0 \Sigma_0 = \Sigma_0^2 \ln (R_0/R^*) \qquad (5.125)$$

The pulse is characterized by the two constants, R* and A^2; A^2 is essentially the product of the duration $\theta = L_0/c_0$ and the shock pressure Δp_s, multiplied by the radius R. More precisely

$$A^2 = \frac{c_0^3}{\alpha\gamma} \theta \frac{\Delta p_s}{p_0} R \qquad (5.125a)$$

The radius R* is similarly given by

$$R^* = R \exp\left\{\frac{-\gamma}{\alpha}\left[\frac{c_0\theta}{R(\Delta p_s/p_0)}\right]\right\} \qquad (5.124a)$$

Here the subscript 0 for R has been dropped, since these quantities are constants and apply therefore at any time.

5.10 The Case of Two Pressure Pulses Catching Up with Each Other

If the explosion takes place at some considerable height and the pressure pulse is measured by airborne instruments, the problem arises as to whether or not the reflected shock from the ground catches up with the first shock, and what happens if it does.

We assume for simplicity that both pressure pulses have reached the asymptotic form. As long as the front of the second pulse has not reached the rear of the first pulse, the two pulses behave independently and the calculations of the preceding sections apply. The mid-point of either pulse travels with sound velocity c_0 and they keep, therefore, at a constant distant (apart from geometrical factors arising from the fact that the reflected shock has a center different from that of the first shock; these are neglected in the following considerations). However, the length of each pulse increases indefinitely and therefore the reflected shock will some time catch up with the rear of the first pulse. We then have three shocks as shown in Fig. 5.3

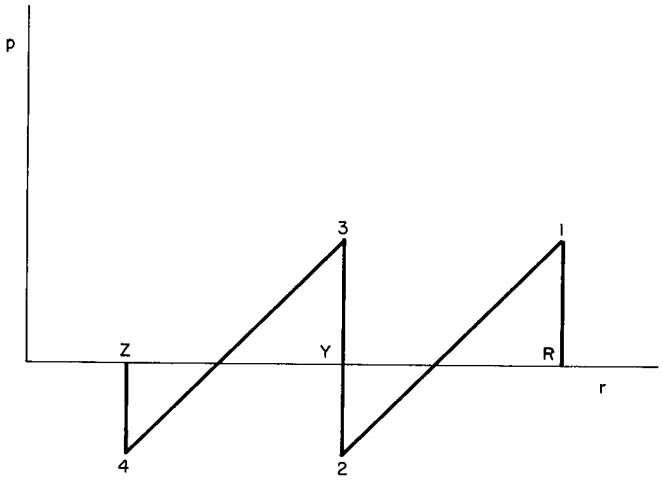

Fig. 5.3 Three shocks where the reflected shock will sometime catch up with the rear of the first pulse

The equation for the first shock, of course, remains unaltered, i.e.,

$$\Sigma_1 = \Sigma_{1\,0}\sqrt{\frac{\ln R_0/R^*}{\ln R/R^*}} \tag{5.126}$$

where the suffix 1 refers to the first shock, and the suffix 0 to some specified time, e.g., to the time when the second shock just catches up with the first pulse. R^* is given by Eq. 5.124a. Observing that the length of the positive pulse at time t_0 is equal to $1/2(R_0 - Y_0)$, we find

$$\ln R^* = \ln R_0 - \frac{1}{2}\frac{c_0}{\alpha}\frac{R_0 - Y_0}{\Sigma_{1\,0}} \tag{5.127}$$

Similarly we have for the back shock of the second pulse

$$\Sigma_4 = -\Sigma_{3\,0}\sqrt{\frac{\ln Z_0/Z^*}{\ln Z/Z^*}} \tag{5.128}$$

$$\ln Z^* = \ln Z_0 - \frac{1}{2}\frac{c_0}{\alpha}\frac{Y_0 - Z_0}{\Sigma_{3\,0}} \tag{5.129}$$

For the central shock we have to use the equations devised for the case when both the air in front and in the rear of the shock deviate from normal. These occurred previously in the treatment of the back shock and are given by Eq. 5.110.

$$\frac{\Sigma_2 - \Sigma_3}{2Y}\frac{dY}{d\Sigma_2} + \frac{dg}{d\Sigma_2} + \ln Y = 0 \tag{5.130}$$

$$\frac{\Sigma_3 - \Sigma_2}{2Y}\frac{dY}{d\Sigma_3} + \frac{dg}{d\Sigma_3} + \ln Y = 0$$

In the first of these equations $dg/d\Sigma_2$ is to be taken from the g function of the first pulse; i.e., it is equal to $-\ln R^*$ (see Eq. 5.124). Similarly, in the second equation $dg/d\Sigma_3 = -\ln Z^*$. Thus

$$\frac{\Sigma_2 - \Sigma_3}{2Y}\frac{dY}{d\Sigma_2} + \ln Y - \ln R^* = 0$$

$$\frac{\Sigma_3 - \Sigma_2}{2Y}\frac{dY}{d\Sigma_3} + \ln Y - \ln Z^* = 0 \qquad (5.131)$$

These equations may be combined to give

$$\frac{2Y}{\Sigma_3 - \Sigma_2}\frac{d(\Sigma_3 - \Sigma_2)}{dY} + \frac{1}{\ln Y/R^*} + \frac{1}{\ln Y/Z^*} = 0 \qquad (5.132)$$

Integration yields

$$\Sigma_3 - \Sigma_2 = (\Sigma_{3\,0} - \Sigma_{2\,0})\sqrt{\frac{\ln (Y_0/R^*)\ln(Y_0/Z^*)}{\ln (Y/R^*)\ln (Y/Z^*)}} \qquad (5.133)$$

If we substitute this expression into one of the equations of 5.130 and integrate, we obtain Σ_2 and Σ_3 separately. The result is

$$\Sigma_2 = -A\,\frac{\sqrt{\ln (Y/Z^*)} - \sqrt{\ln (Y/R^*)}}{\sqrt{\ln (Y/R^*)}} + B$$

$$\Sigma_3 = A\,\frac{\sqrt{\ln (Y/Z^*)} - \sqrt{\ln (Y/R^*)}}{\sqrt{\ln (Y/Z^*)}} + B \qquad (5.134)$$

where

$$A = (\Sigma_{3\,0} - \Sigma_{2\,0})\,\frac{\sqrt{\ln (Y_0/Z^*)\ln (Y_0/R^*)}}{\ln (R^*/Z^*}$$

$$B = \frac{\Sigma_{2\,0}\sqrt{\ln (Y_0/R^*)} + \Sigma_{3\,0}\sqrt{\ln (Y_0/Z^*)}}{\sqrt{\ln (Y_0/R^*)} + \sqrt{\ln (Y_0/Z^*)}} \qquad (5.135)$$

If $\ln (Y/R^*) >> \ln (R^*/Z^*)$, the equations can be simplified.

$$\Sigma_2 = -\frac{1}{2} (\Sigma_{3\,0} - \Sigma_{2\,0}) \frac{\sqrt{\ln (Y_0/R^*) \ln (Y_0/Z^*)}}{\ln (Y/R^*)} + B$$

$$\Sigma_3 = \frac{1}{2} (\Sigma_{3\,0} - \Sigma_{1\,0}) \frac{\sqrt{\ln (Y_0/R^*) \ln (Y_0/Z^*)}}{\ln (Y/Z^*)} + B \qquad (5.136)$$

The shock strength of the central shock is related to $\Sigma_3 - \Sigma_2$. According to Eq. 5.133 it drops much faster than either the rear shock or the front shock. However, the pressure level at which this shock occurs tends, according to Eq. 5.136, to a finite Σ value. This implies that the central shock must either catch the first shock (if $B > 0$) or the rear shock must catch the central shock (if $B < 0$).

Let us consider first the exceptional case $B = 0$. Since $\Sigma_{2\,0} = -\Sigma_{1\,0}$, $B = 0$ implies that

$$\Sigma_{1\,0} \sqrt{\ln (Y_0/R^*)} = \Sigma_{3\,0} \sqrt{\ln (Y_0/Z^*)} \qquad (5.137)$$

Neglecting the small difference between Y_0 and R_0, these quantities are identical with the quantity A defined by Eq. 5.125 which in turn is related to the "impulse" of the pulse $\theta \Delta p_s$ multiplied with the shock radius (see Eq. 5.125a). We conclude that $B = 0$ if the impulse of the two pulses is the same at the same radius. It will be noticed that R^* and Z^* may nevertheless differ. Thus, one pulse may have long duration and low shock pressure; the other short duration and comparatively large shock pressure.

If $B = 0$, then both Σ_2 and Σ_3 tend to 0 more rapidly than either Σ_1 or Σ_4. Thus the positive phase of the second pulse and the negative phase of the first pulse are eventually eliminated, and there remains the positive phase of the first pulse, which combines with the negative phase of the second pulse. All this, of course, takes some time, until $\ln (Y/R^*) >> \ln (Y_0/R)$. If R^* and Z^* differ from each other the pressure gradients in the positive and negative phase will also differ; only the product of shock pressure and duration will be the same. If the two pulses were completely identical, the remaining pulse would be indistinguishable from either, so that the reflected shock would simply disappear.

If B is positive, we require that the impulse in the second pulse be greater than the impulse in the first, and in this case the central shock catches up with the first shock. Eventually the first pulse disappears and only the second pulse remains. Similarly, if B is negative, the second pulse will eventually disappear and only the first pulse remain.

Asymptotically the energy in the blast wave is therefore not equal to the sum of the energy in the two pulses, but equal to the energy in either the first or the second pulse, whichever is the greater. The remainder of the energy has been dissipated at the central shock. This increased energy dissipation is due to the fact that the shock front of the second pulse must go through the negative phase of the first pulse. E.g., the energy dissipation just before the second pulse catches up with the first is proportional to $4(\Delta p_s)^3$, assuming for simplicity equal shock strengths in both pulses. The factor 4 arises from the four shocks. Just after the second pulse has caught up with the first, there are two shocks of strength Δp_s and one of strength $2\Delta p_s$, and the energy dissipation is proportional to

$$2(\Delta p_s)^3 + (2\Delta p_s)^3 = 10(\Delta p_s)^3$$

and has, therefore, increased by a factor 2.5.

If $B > 0$, the radius at which the central shock catches up with the first shock is given by the condition $\Sigma_2 = \Sigma_1$. After some manipulation one finds as a consequence that $\Sigma_3 + \Sigma_4 = 0$, i.e., the front shock, which is now Σ_3, has the same value it would have had if there had been no first pulse. Also one finds for the radius R the condition

$$\sqrt{\ln (R/R^*)} = \sqrt{\ln (R_0/R^*)}$$

$$\frac{\Sigma_{1\,0}^2 \ln (R_0/R^*) + 2\Sigma_{1\,0}\,\Sigma_{3\,0} \ln (Z_0/Z^*) + \Sigma_{3\,0}^2 \ln (Z_0/Z^*)}{\Sigma_{3\,0}^2 \ln (Z/Z^*) - \Sigma_{1\,0}^2 \ln (R/R^*)} \qquad (5.138)$$

5.11 The Continuation of the IBM Run

The methods developed in the preceding sections have been used to continue the IBM results of Chapter 6. The IBM machines give us the pressure Δp as function of the radius at a fixed time. From these data we obtain immediately the function $\Sigma(y)$ and we can deduce the function $g(\Sigma)$ defined by Eq. 5.82. This function should, of course, be independent of the time. It is shown in Fig. 5.4. The circles refer to the last IBM cycle when the shock radius is 314.7 (we use here the IBM unit for the radius which is 19.97 meters). The triangles refer to an early cycle, when the shock radius is only 200.2.

For the numerical evaluation it was convenient to introduce, instead of Σ, the quantity

$$s = \frac{\gamma\Sigma}{c_0} = \frac{R\Delta p}{p_0} \tag{5.139}$$

and instead of g

$$g(s) = -\frac{\alpha g(\Sigma)}{c_0} \tag{5.140}$$

Then the positive phase can be represented in the form

$$g = 2.2s + 0.075s^2 \tag{5.141}$$

Substitution into Eq. 5.89 yields

$$\ln R = \frac{170.4}{s_F^2} + \frac{\gamma}{\alpha}[2.2 + 0.05s_F] \; ; \quad \frac{\Delta p_s}{p_0} = \frac{s_F}{R} \tag{5.142}$$

where s_F is the value of s at the shock front. Here we have used the boundary condition that at $R = 314.7$, $\Delta p_s = 0.0251 p_0$.

As s_F becomes small, we have approximately

$$\frac{\Delta p_s}{p_0} = \frac{\sqrt{170.4}}{\sqrt{R \ln (R/R^*)}}$$

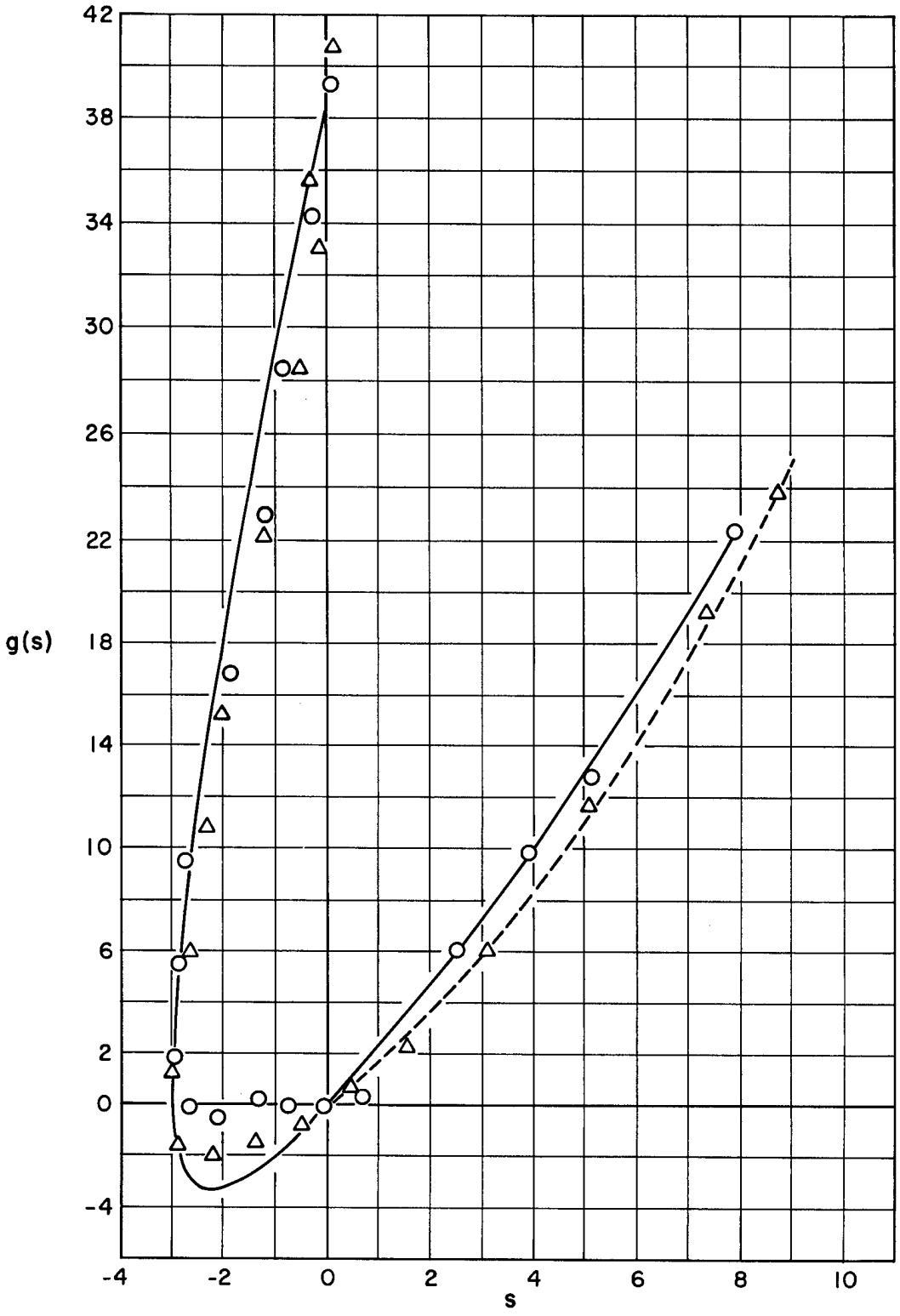

Fig. 5.4 Plot of g(s) vs s

$$\ln R^* = \frac{2.2\gamma}{\alpha}$$

$$R^2 = 13.03 \qquad \text{(R in IBM units)} \tag{5.143}$$

Introducing the meter as unit, one finds

$$\frac{\Delta p_s}{p_0} = \frac{260.7}{R\sqrt{\ln (R/260.1)}} \qquad \text{(R in meters)} \tag{5.144}$$

The data from the earlier cycle are better represented by the formula

$$g = 1.6s + 0.13s^2 \tag{5.141a}$$

which leads to

$$\ln R = \frac{194.6}{s_F^2} + \frac{\gamma}{\alpha}(1.6 + 0.0867 s_F) \tag{5.142a}$$

and asymptotically,

$$\frac{\Delta p_s}{p_0} = \frac{278.6}{R\sqrt{\ln (R/129.1)}} \qquad \text{(R in meters)} \tag{5.144a}$$

which differs by about 6 per cent from the previous formula. This is the error to be expected, since at the smaller radius the overpressure is 4.4 per cent. The data from the larger radius should be more reliable and have been used for all calculations.

For the negative phase, we get a good approximation by the formula

$$g = (11 + 0.38s)\{\sqrt{3} \pm \sqrt{3 + s}\} + 5.38s \qquad (s < 0) \tag{5.145}$$

The constants in this representation have been chosen in such a way that we get not only a good representation of the numerical data, but that also the slope of the function g is continuous at s = 0 and that the integral of the pressure taken over the pulse vanishes. In actual fact, the data from the

last IBM cycle are somewhat erratic in the neighborhood of s = 0. This must be due to an error in the IBM run, since the data from the earlier cycle are quite smooth. For this reason no attention has been paid to this erratic behavior and the condition that dg/ds be continuous at s = 0 has been used instead, in order to get a reasonable function g.

We have seen before (see Eq. 5.107) that the back shock will start at a value of s for which

$$\frac{d^2 g}{ds^2} = 0 \tag{5.146}$$

If we use the presentation of Eq. 5.145 we find that this condition cannot be satisfied for any negative s. However, this is due to the analytic representation; if we go back to the numerical data, we find that the curvature changes sign. The exact value of s where the change occurs is not easily determined; however, the minimum slope can be determined fairly accurately and is 8.2. The slope determines the radius at which the back shock starts (see Eq. 5.106).

$$\ln r = \frac{\gamma}{\alpha}\left(\frac{dg}{ds}\right)_{\text{minimum}} = \frac{1.4}{1.2}\ 8.2 \tag{5.147}$$

$$r = 1.4 \times 10^4 \text{ IBM units}$$

$$= 2.8 \times 10^5 \text{ meters}$$

We shall not be interested in such large distances.

For the duration of the positive pulse we find from Eq. 5.100a

$$\theta = \frac{1}{c_0}\left[\frac{\alpha}{\gamma} s_F \ln R - g(s_F)\right] \tag{5.148}$$

or with Eqs. 5.142 and 5.141

$$\theta = \frac{1}{c_0}\left[\frac{\alpha}{\gamma}\frac{170.4}{s_F} - 0.025\, s_F^2\right] \tag{5.148a}$$

The shape of the pulse at a fixed distance as function of time is similarly given by the formula (see Eq. 5.102)

$$T = \theta - \frac{1}{c_0}\left[\frac{\alpha}{\gamma}\, s\, \ln R - g(s)\right] \tag{5.149}$$

$$\frac{\Delta p}{p_0} = \frac{s}{R}$$

where s varies from its value s_F at the shock front to -3 at the pressure minimum and back to zero. In order to obtain the time in seconds, we should use for c_0 the "IBM value" $c_0 = 17.38$.

The peak pressure vs shock radius curve is shown in Fig. 5.5, using IBM units. For comparison, some points obtained if we stop the IBM run at an earlier instant are also shown.

The duration vs peak pressure is shown in Fig. 6.14 of Chapter 6.

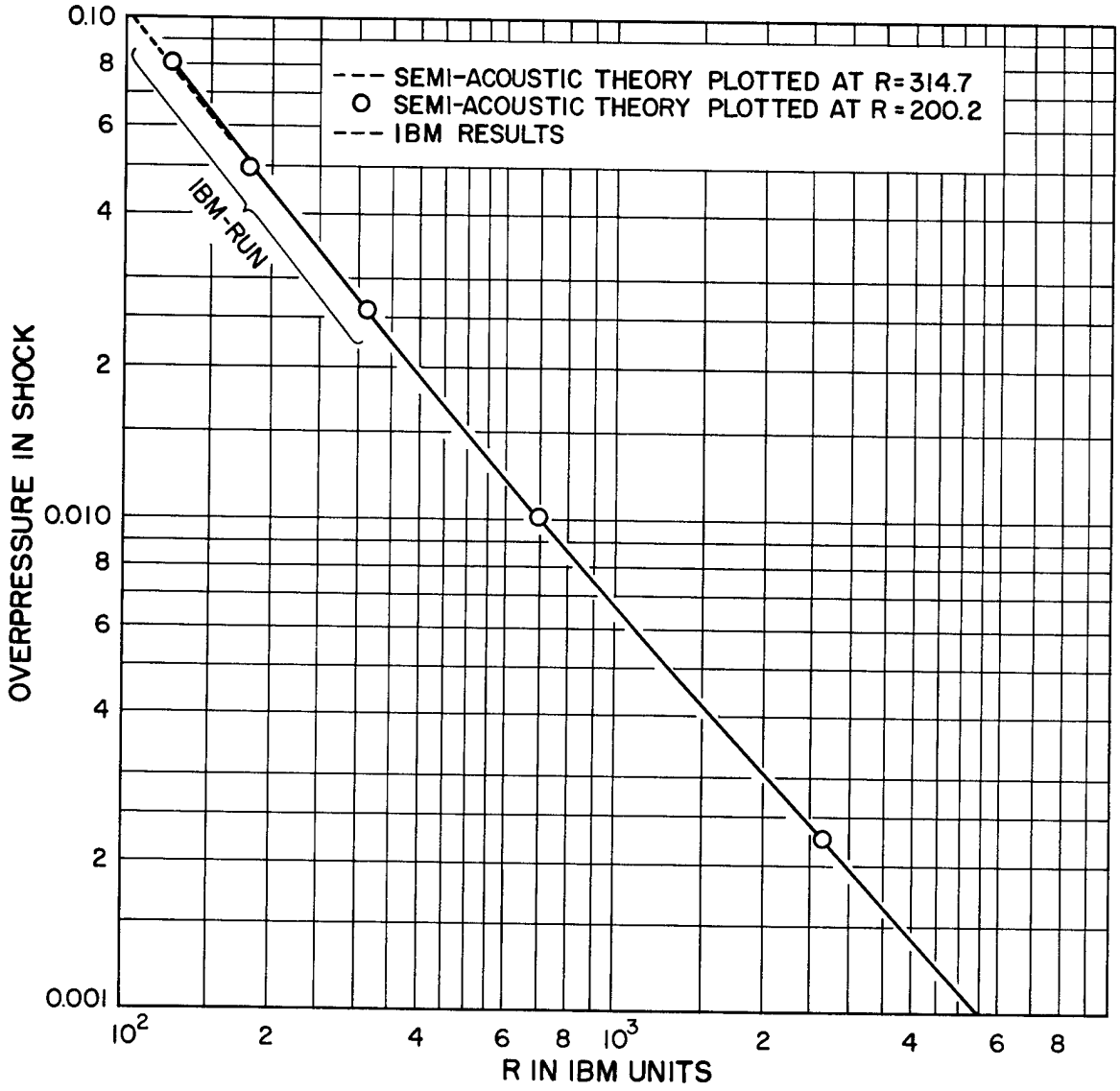

Fig. 5.5 Overpressure vs shock radius

Chapter 6

THE IBM SOLUTION OF THE BLAST WAVE PROBLEM

by K. Fuchs

6.1 Introduction

The discussion in the preceding chapters shows that the problem of the propagation of the blast wave from a nuclear explosion is quite complicated. Even if we disregard any transport of radiation, appreciable complications arise in view of the large variations in temperature and entropy. We may roughly divide the range of shock temperatures into two regions. First, the region from about one million degrees to about three thousand degrees absolute; here dissociation of molecules and ionization of the atoms takes place; consequently $\gamma - 1$ is fairly small but varies with temperature. Second, below 3000°; here γ is less variable and approaches eventually the value 1.4 in normal conditions.

The temperature varies also, of course, along an adiabatic. However, the total variation between the shock pressure and 1 atm is not excessive – about a factor 2 at shock temperature of 3000°K and slightly more than a factor 10 for a shock temperature of 1,000,000°. The effect of decreasing temperature along the adiabatic on the degree of ionization or dissociation is partly balanced by the decrease in density. For this reason the variation of γ along an adiabatic is not as pronounced as one might expect from the change in temperature. Therefore qualitative statements made about the conditions at the shock front hold to a large degree also for the subsequent expansion behind the shock.

A temperature of 3000°K is reached in the shock when the shock pressure is about 80 atm. (For an energy release of 10,000 tons of TNT the shock radius is then 80 meters.) We are, however, more interested in the pressure region from about 1 atm down (corresponding to shock radii of 500 meters or more). It was felt that the exact energy distribution at this

early stage could not have an appreciable effect on the pressure distribution in the later stages as long as the energy distribution is at least roughly correct. It was decided to start an IBM calculation at this point and to calculate the initial conditions for this instant by means of the approximations developed in the preceding chapters. The approximations made include (for details see Section 6.2):

(1) An approximate treatment of the isothermal sphere. In actual fact the isothermal sphere at this late stage has no significant influence on the propagation of the shock. However, in the first instance we are interested in the isothermal sphere as such; in the second instance the isothermal sphere greatly facilitates numerical computations, since it reduces the total range of temperatures and entropies which exist at any given moment, and eliminates the singularity at the centre.

(2) γ was assumed to be constant and an average value 1.25 was assumed. This is probably the least satisfactory of the assumptions made, but in view of the fact that we did not require a very accurate estimate of the initial conditions, and that a calculation with variable γ is hardly feasible without a great amount of computation, this assumption seemed justified.

(3) $\gamma - 1$ was assumed small. This assumption is not essential, but the error introduced thereby is small and it has the advantage that the isothermal sphere can be included as an integral part of the calculation.

For the IBM run it is of great advantage if the variation of the pressure along an adiabatic is a simple function of the density, though the variation from one adiabatic to another may be given in numerical form. In this case the adiabatic of each mass point is given by one or two constants and we require only a table of these constants as functions of one variable.

It would be difficult to find a simple presentation of the equation of state covering the whole region of adiabatics between the shock pressure curve and normal pressure. However, with the limitation to shock pressure below 80 atm the demand of a simple representation becomes feasible. In particular this is true for the adiabatics which start at shock pressures below 80 atm, since then no ionization or dissociation occurs. We require also, of course, the adiabatics of the inner mass points, which were shocked by stronger shocks. However we require only the tail end of these adiabatics. Furthermore, the highest entropies are eliminated by the equalization of entropy inside the isothermal sphere. The equation of state which has been used is discussed in Chapter 7. The requirement of a simple equation of state is the principal reason for starting the IBM run at such a comparatively late stage.

Although radiation transport has been taken into account insofar as it is responsible for the formation of the isothermal sphere, no allowance has

been made for the radiation transport from the isothermal sphere into the region in which NO_2 is formed. As explained in Chapter 3, this transport of energy becomes important when the shock radius has reached about 100 meters and it should affect the propagation of the shock shortly thereafter. The opacity data required for the purpose of calculating this transport are not sufficiently well known.[1] In neglecting the radiation transport altogether we are pessimistic, since it is of advantage to have the energy close to the shock front. Then the shock pressure decreases less rapidly than it would otherwise. The increased shock pressure would naturally lead to a greater degree of dissipation of energy by the shock, so that at larger distances the shock pressure might drop again more rapidly, and at sufficiently large distances the effect of the radiation transport on the shock pressure would be reversed. At present we are not in a position to make any definite statement about this possibility.

The IBM run was intended for an energy release of 10,000 tons of TNT. Owing to some unfortunate circumstances related in Section 6.3, no definite energy can be attributed to the run throughout its whole history. At sufficiently large distances the energy should be assumed to be 13,000 tons. Other energies can, of course, be obtained by the usual scaling laws.

6.2 The Initial Conditions of the IBM Run

The initial conditions of the IBM run were prepared by Hirschfelder and Magee. The principal data are summarized below without going into the details of the calculation. All data are for an energy release of 10,000 tons of TNT.

6.2.1 The Isothermal Sphere[2]

The Lagrangian coordinate of the radiation front is given in terms of the shock radius by Eq. 3.64 of Chapter 3. It can be rewritten in the form

$$r_0 = \left[11.85\ Y^{0.7326} - 601.5\right]^{1/3}\ 100\ \text{cm} \qquad (6.1)$$

Here both r_0 and Y are given in centimeters. It was convenient to choose

1. Chapter 3 contains a discussion of opacity data which postdates this statement.
2. Chapter 3 values are revised figures. Notations in equations used here are in the main those of Bethe in Chapter 4.

a simple value of Y/r_0 and the value 4 was chosen, which corresponds to a shock pressure very near to 80 atm. Then

$$r_0 = 1997 \text{ cm}, \quad Y = 7987 \text{ cm}, \quad Y/r_0 = 4 \tag{6.2}$$

The actual radius R_0 of the isothermal sphere is obtained from the conservation of mass. Since we assume constant density ρ and constant pressure in the isothermal sphere one has

$$\rho_0 r_0^3 = \rho R_0^3 \tag{6.3}$$

The value r_0 varies very slowly after the shock radius has reached about 10 meters, and the effect of the isothermal sphere on the shock is negligible a short while thereafter. Beyond a shock radius of 80 meters r_0 varies very slowly indeed.

It is a good assumption to assume that r_0 is constant. The actual radius R_0 then varies in accordance with Eq. 6.3 only because the air in the isothermal sphere expands. The initial value of R_0 is 60 meters.

The initial condition of the isothermal sphere is given by the following quantities:

Temperature	= 49,000°K
Pressure	= 37.0 atm
Density	= 0.0392 × normal density
Entropy $\Delta s/R$	= 85

Internal energy and enthalpy $E/R = 1.487 \times 10^6$, $H/R = 1.782 \times 10^6$

$R_0 = 60.23$ meters

$r_0 = 19.97$ meters

These data were obtained from a calculation indicated below.

6.2.2 Initial Pressure and Density Distribution

It has been shown by Bethe in Chapter 4, Section 5, that the isothermal sphere can be treated on the assumption of small $\gamma - 1$. The small $\gamma - 1$ approximation has been checked for a point source solution (see Chapter 4, Sections 3 and 4) and it was found satisfactory in the region in which we are interested. Since the solution which we require is in any case very close to the point source solution except in the neighborhood of the isothermal

sphere, the error of the small $(\gamma - 1)$ approximation is small.

We shall not go into the details of the calculation. The analysis is rather involved, but the lines along which it proceeds are sufficiently indicated in Bethe's Section 4.5. The resulting equations had previously been evaluated for two values of γ in order to see how sensitive they were to a change in γ. The values chosen were $\gamma = 1.2$ and $\gamma = 1.3$. The values for $\gamma = 1.25$ were then obtained by interpolation. In this way we find the initial pressure and density distribution as well as the velocities and the Eulerian coordinates of all mass points.

Some adjustments had to be made on the intial conditions. A minor adjustment arose from the fact that the small $\gamma - 1$ treatment of the isothermal sphere does not agree exactly with the treatment of Hirschfelder and Magee. The error, which may be due to either method, may be seen from the values of R_0/Y; the small $\gamma = 1$ treatment gives $R_0/Y = 0.850$ compared to 0.761 by means of the other method. The latter value was assumed to be more reliable.

Furthermore, at the start of the IBM calculation the value of γ at the shock front is larger than 1.25; instead of a compression ratio in the shock $\rho_s/\rho_0 = 9$, as would be expected for $\gamma = 1.25$, the value obtained from the correct Hugoniot curve for a pressure of 77.25 atm is $\rho_s/\rho_0 = 7.24$. The density contour was, therefore, adjusted to give the correct compression ratio at the shock, and the correct radius of the isothermal sphere. This required also an adjustment in the Eulerian coordinates R, since it is essential that the initial conditions satisfy the equation of continuity:

$$\frac{\rho_0}{\rho} = \frac{R^2}{r^2}\,\frac{dR}{dr} \tag{6.4}$$

where r is the Lagrangian coordinate.

The initial velocities were then calculated directly from the equation

$$u = \frac{\dot{Y}}{(\gamma + 1)^{1/3}}\,\frac{1 + \left(\frac{r}{Y}\right)^{3(\gamma-1)/\gamma}}{\left[1 + \gamma\left(\frac{r}{Y}\right)^{3(\gamma-1)/\gamma}\right]^{2/3}} \tag{6.5}$$

which follows from the small $\gamma - 1$ approximation. Here the correct shock velocity $\dot{Y}$ for the given shock pressure was used.

6.3 The Total Energy

The methods used to establish suitable initial conditions are in parts somewhat arbitrary. For this reason it is not surprising that the total energy corresponding to these conditions turned out to deviate appreciably from the assumed value of 10,000 tons of TNT. Unfortunately, the energy was recalculated from the initial conditions only after the IBM run had been completed. It was then found that the total energy was 13,500 tons TNT.

Since the initial shock pressure of 77.25 atm at the initial shock radius of 79.9 meters corresponds to an energy release of 10,000 tons, we have no remedy for the discrepancy. All that can be said is that the shock pressure vs distance curve corresponds to 10,000 tons up to 80 meter shock radius and to 13,500 tons for large radii. For intermediate radii it should slowly change between these values.

Actually the discrepancy is slightly less. A check of the total energy at a shock radius of 2000 meters gave only 13,100 tons. The "loss" of 400 tons is entirely due to errors of the IBM run and is of the order of magnitude to be expected from this source.

For most purposes the total energy in the IBM run should be assumed to be about 13,000 tons, except at small shock radii, where 10,000 tons is more appropriate.

6.4 The IBM Run

The hydrodynamical equations are

$$\rho_0 \frac{\partial^2 R}{\partial t^2} + \frac{R^2}{r^2} \frac{\partial p}{\partial r} = 0 \tag{6.6}$$

$$\frac{\rho_0}{\rho} = \frac{R^2}{r^2} \frac{dR}{dr} \tag{6.7}$$

In addition we have the equation of the adiabatics which were put in the form

$$\frac{p}{p_0} = g\left(\frac{\rho}{\rho_0}\right)^{1.5} + \eta \frac{\rho}{\rho_0} \tag{6.8}$$

where g and η are numerically known functions of the entropy.

The boundary conditions are that the velocity $\partial R/\partial t$ vanish at the center and that at the shock radius the Hugoniot conditions be satisfied. The latter determine also the entropy of any mass point as it passes through the shock front. The entropy is assumed to remain constant, so that essentially g and η are given functions of the Lagrange variable r.

The method employed first in solving the system of partial differential equations by means of the IBM machines was suitable as long as the shock pressure differed appreciably from 1 atm, but it became erratic as the overpressure became small. The method was therefore changed, so as to calculate changes in density and pressure rather than their absolute values. This change of procedure quickly suppressed the erratic behavior of the pressure.

The run was continued until the shock radius had reached a value of 6.270 meters. At that instant the overpressure in the shock was 0.0251 atm. The positive pulse was 290 meters long and the negative pulse 760 meters. Since the further propagation of the shock is influenced at these low overpressures only by the positive pulse, the approximations on which the semi-acoustic theory of Chapter 5 are based are well satisfied. They are (1) that the overpressure be small compared to 1 atm, and (2) that the length of the pressure pulse be small compared to the shock radius. Even the application of the semi-acoustic theory to the negative phase is not bad. Hence, the IBM run was discontinued and the semi-acoustic theory was used for the purpose of continuation.

6.5 Results

The shock pressure as a function of the distance of the shock front from the center of the explosion is shown in Fig. 6.1.

In this graph all data have been collected from the previous chapters, as well as from calculations which do not appear in this volume. From a shock radius of 10 to 80 meters the similarity solution has been used. The dotted lines show upper and lower limits for the effect of the bomb material on the propagation of the shock, as calculated for the Trinity test (sealed down to 10,000 tons of TNT). In this region the curve corresponds to an energy release of 10,000 tons.

For shock radii from 80 to 6300 meters, the shock pressures are obtained from the IBM run. Here the total energy is between 10,000 and 13,000 tons, the upper value being correct at sufficiently large distances. The time of arrival of the shock is indicated at various points. T = 0 is the start of the IBM run which was 0.012 sec after the explosion.

Beyond a radius of 6300 meters up to 67,000 meters, the semi-acoustic theory of Chapter 5 has been used.

A number of curves showing the pressure at a fixed distance as function of time are shown in Figs. 6.2 to 6.4. Graphs of the pressure vs distance at a fixed time are shown in Figs. 6.5 to 6.13.

The duration of the positive phase of the pulse as function of the shock pressure is given in Fig. 6.14.

Finally, there are shown in Fig. 6.15 the positive impulse I+ and the fraction of the total energy which is left in the blast as functions of the shock pressure divided by the normal pressure. The latter is independent of the energy release. The positive impulse has been scaled to an energy release of 40,000 tons in free air (or 20,000 tons on the ground) for the purpose of comparison with observations at Trinity.

6.6 Comparison with TNT Explosion. Efficiency of Nuclear Explosion

One purpose of the IBM run was to find the efficiency of a nuclear explosion compared to an explosion from an equivalent charge of TNT. In the nuclear explosion a greater amount of energy is used for the purpose of heating the air near the center of the explosion to high temperatures. A large fraction of this energy is useless for the propagation of the shock.

Since no comparable IBM run exists for a TNT explosion, we compared the results for the nuclear explosion with experimental data. For this purpose, the experimental curve prepared by Hirschfelder, Littler and Sheard[4] was used. It is based on experimental data for charges fired on the ground, and for shock pressures in the range from 15 to 2 pounds per square inch. The charges varied from 67 to 550 pounds. The curve is given by the expression

$$\Delta p = \frac{38.5}{x} + \frac{85}{x^2} + \frac{5760}{x^3} \tag{6.9}$$

$$x = Y/w^{1/3} \tag{6.10}$$

Here Y is the shock radius in feet; w the weight of the charge in pounds; and Δp the overpressure in psi.

---

4. Hirschfelder, Littler and Sheard, Estimated Blast Pressures from TNT charges of 2 to 10,000 tons, Los Alamos Scientific Laboratory Report LA-316, June 25, 1945 (classified).

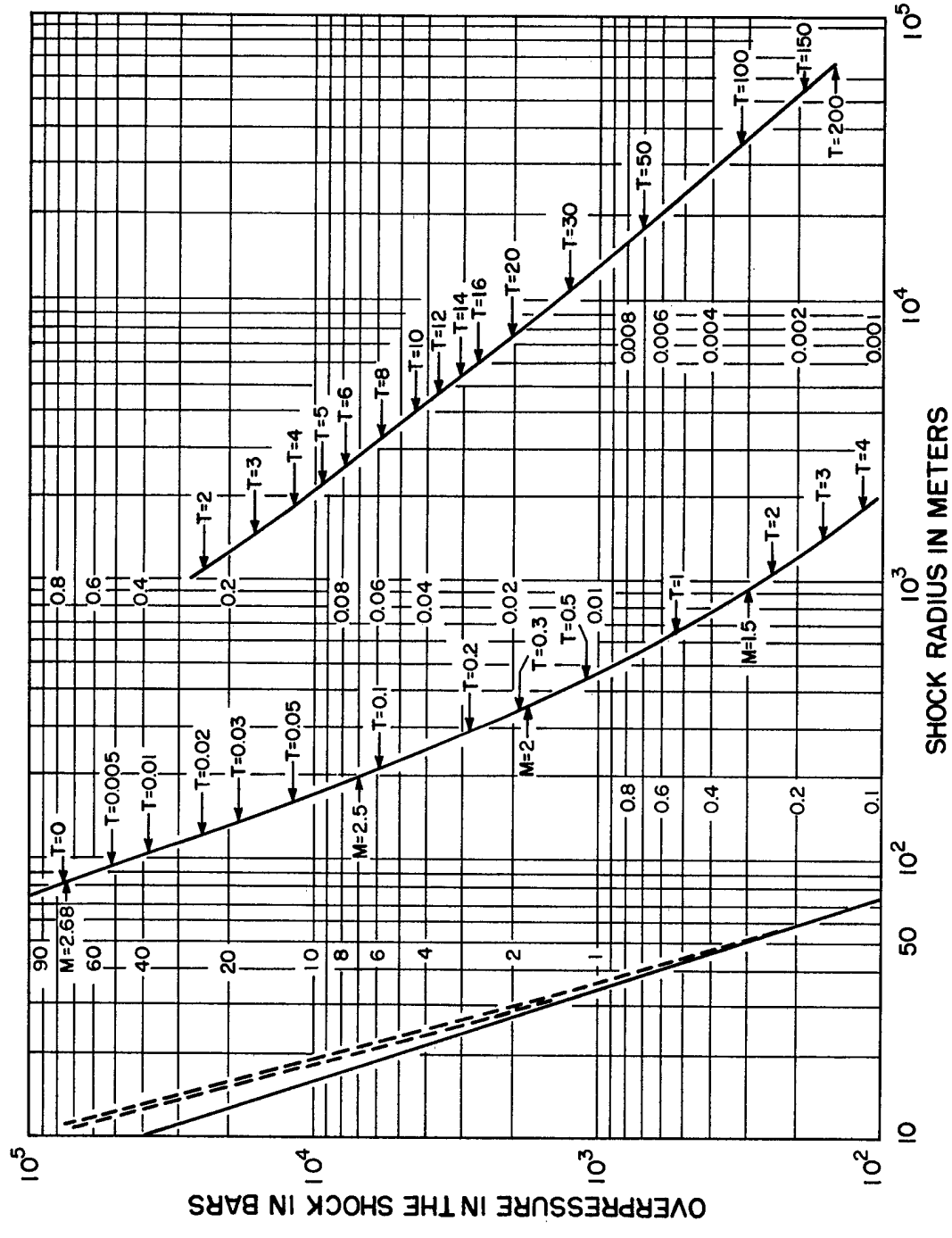

Fig. 6.1 Shock pressure vs distance for nuclear explosion. Time is given in seconds; T = 0 is start of IBM run, 0.012 sec after explosion.

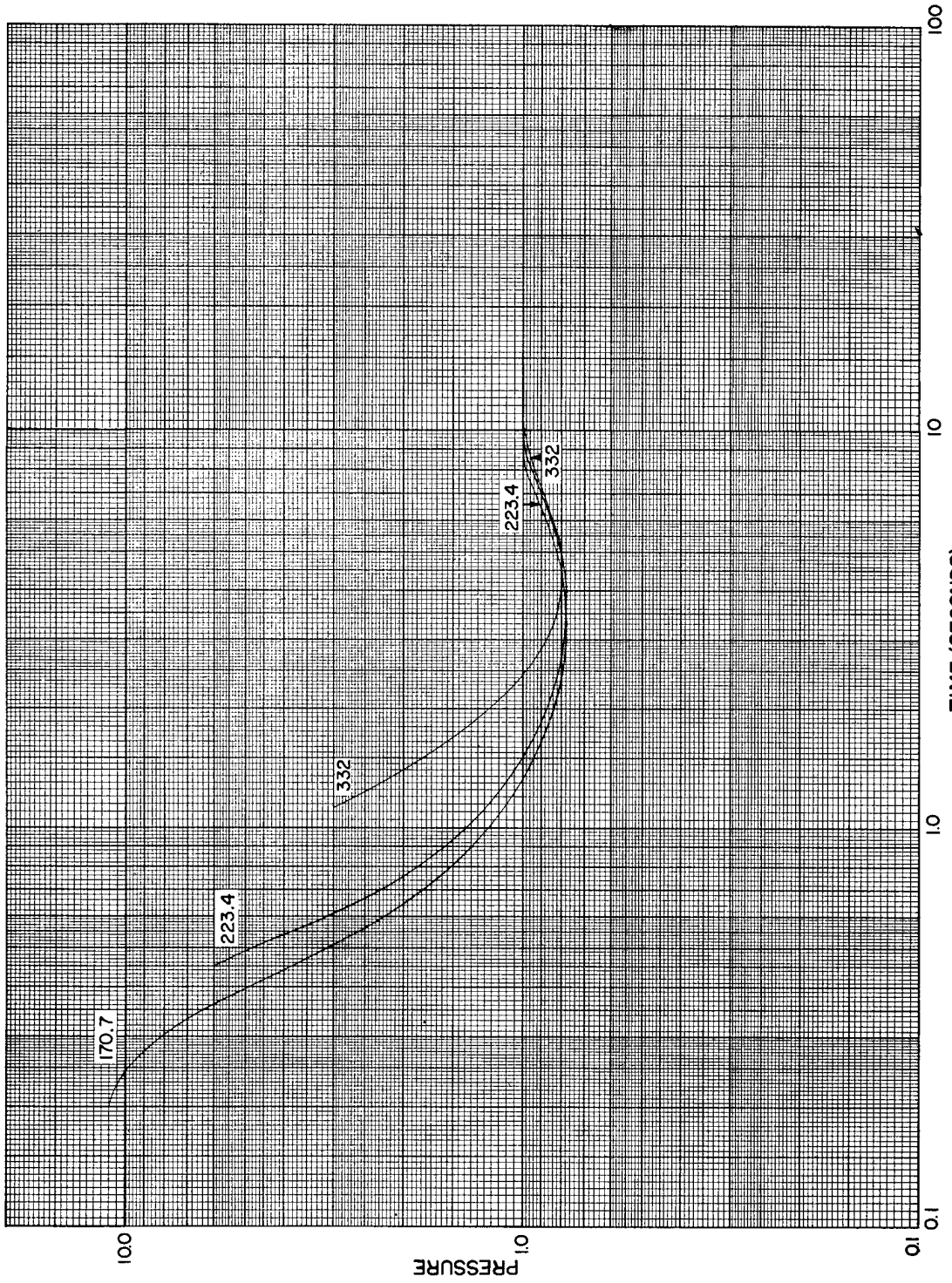

Fig. 6.2 Pressure vs time for radius of 170.7 meters, 223.4 meters, and 332 meters

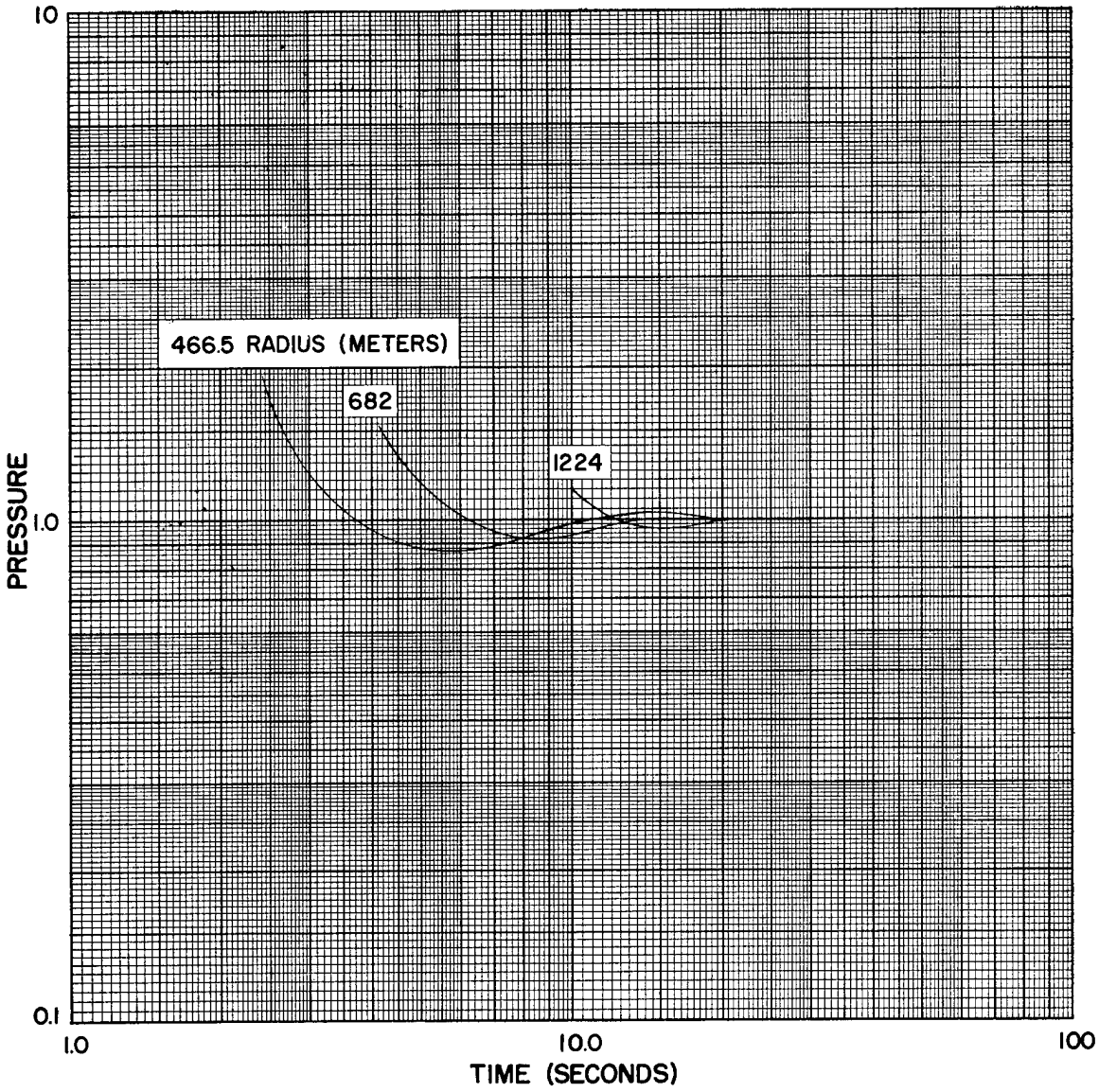

Fig. 6.3 Pressure vs time for radius of 466.5 meters, 682 meters, and 1224 meters.

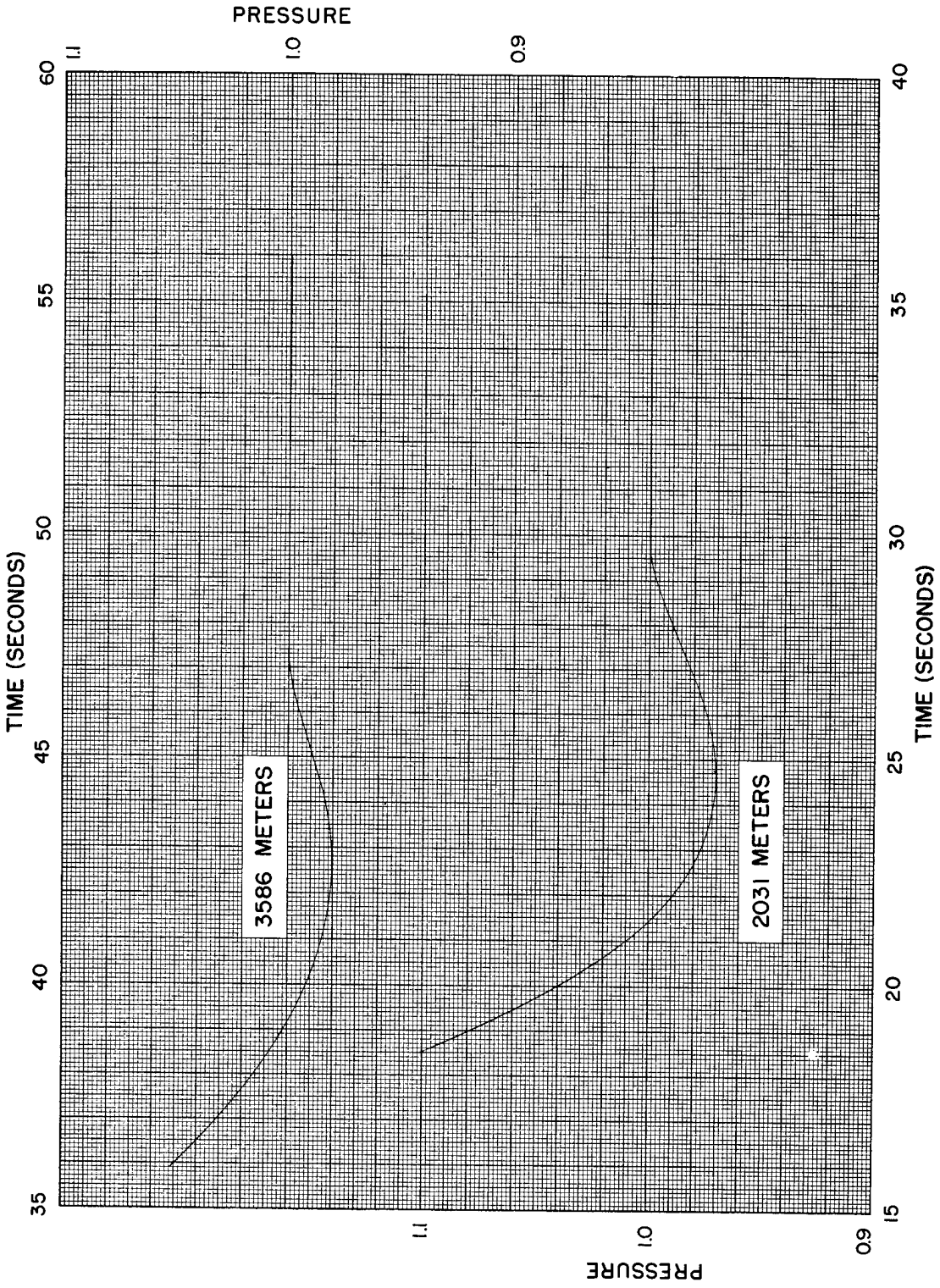

Fig. 6.4 Pressure vs time for radius of 2031 meters and 3586 meters

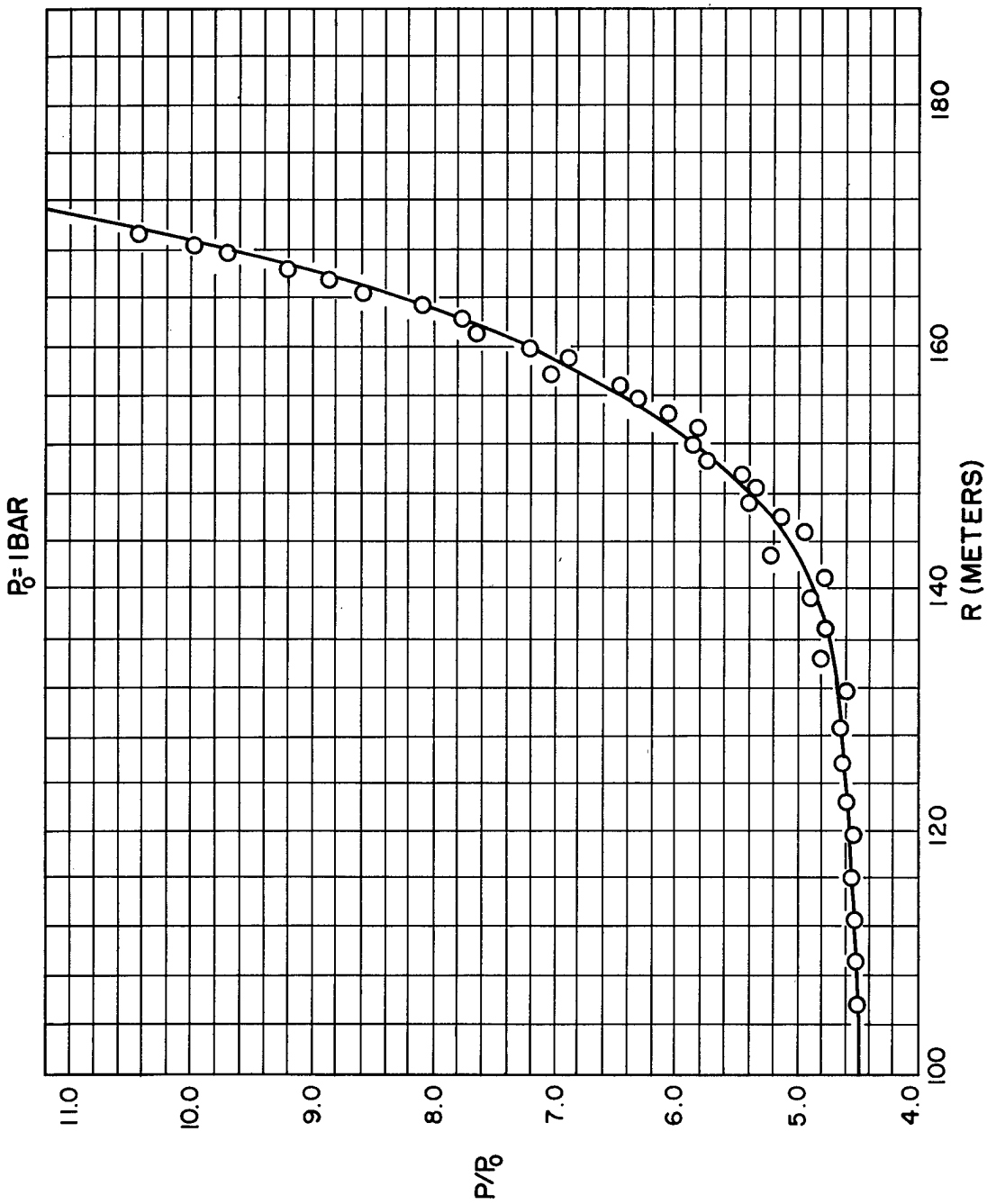

Fig. 6.5 Pressure vs distance at a fixed time

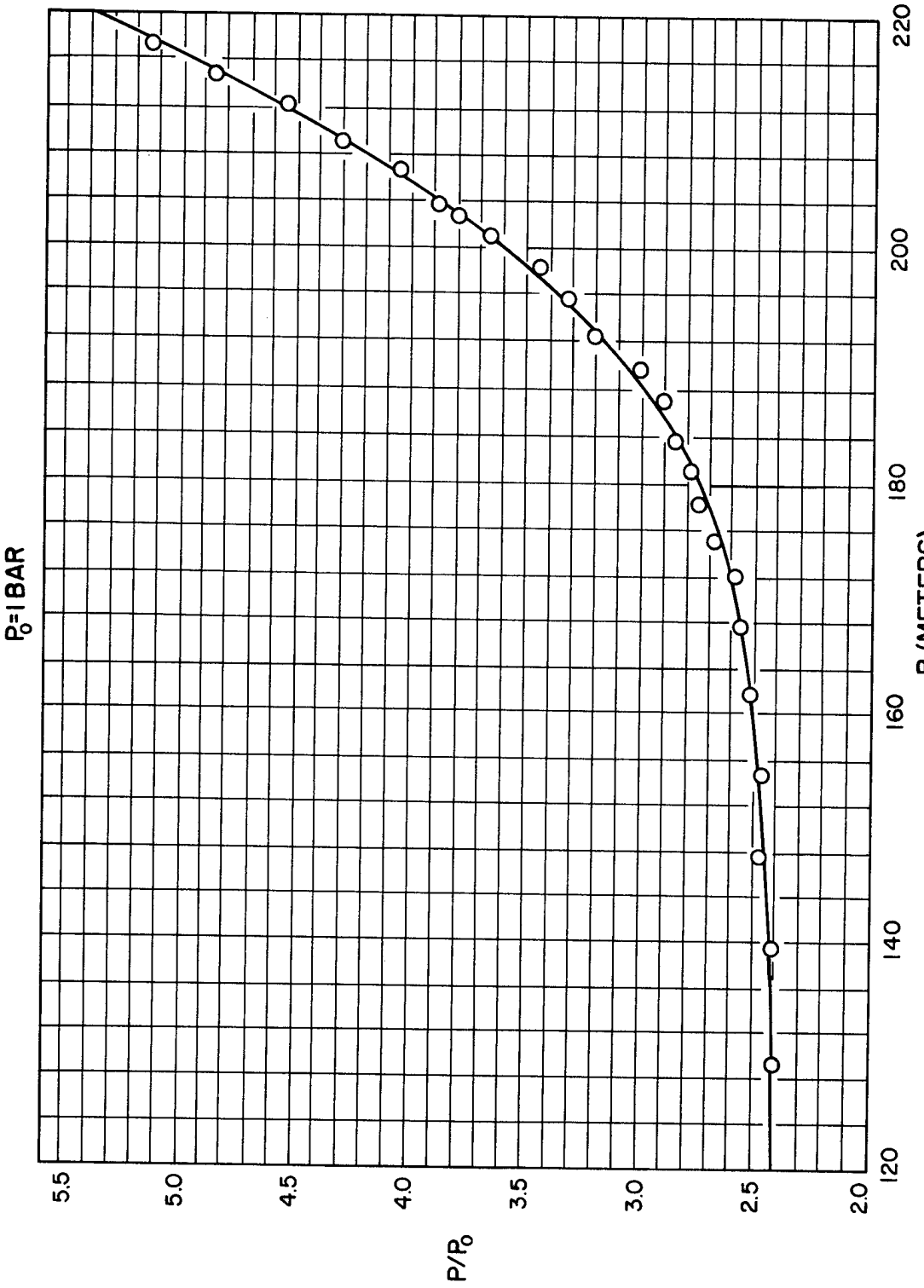

Fig. 6.6 Pressure vs distance at a fixed time

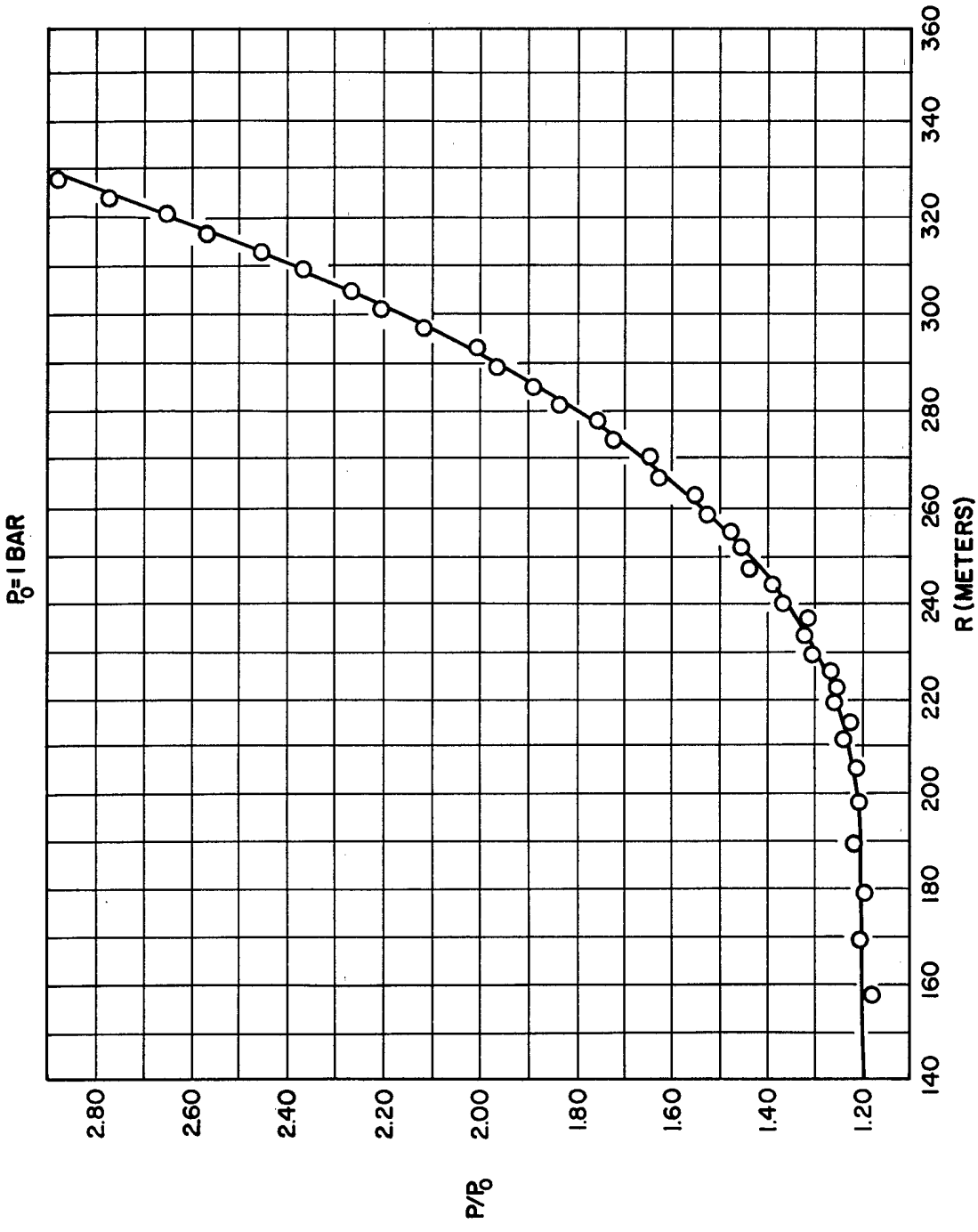

Fig. 6.7 Pressure vs distance at a fixed time

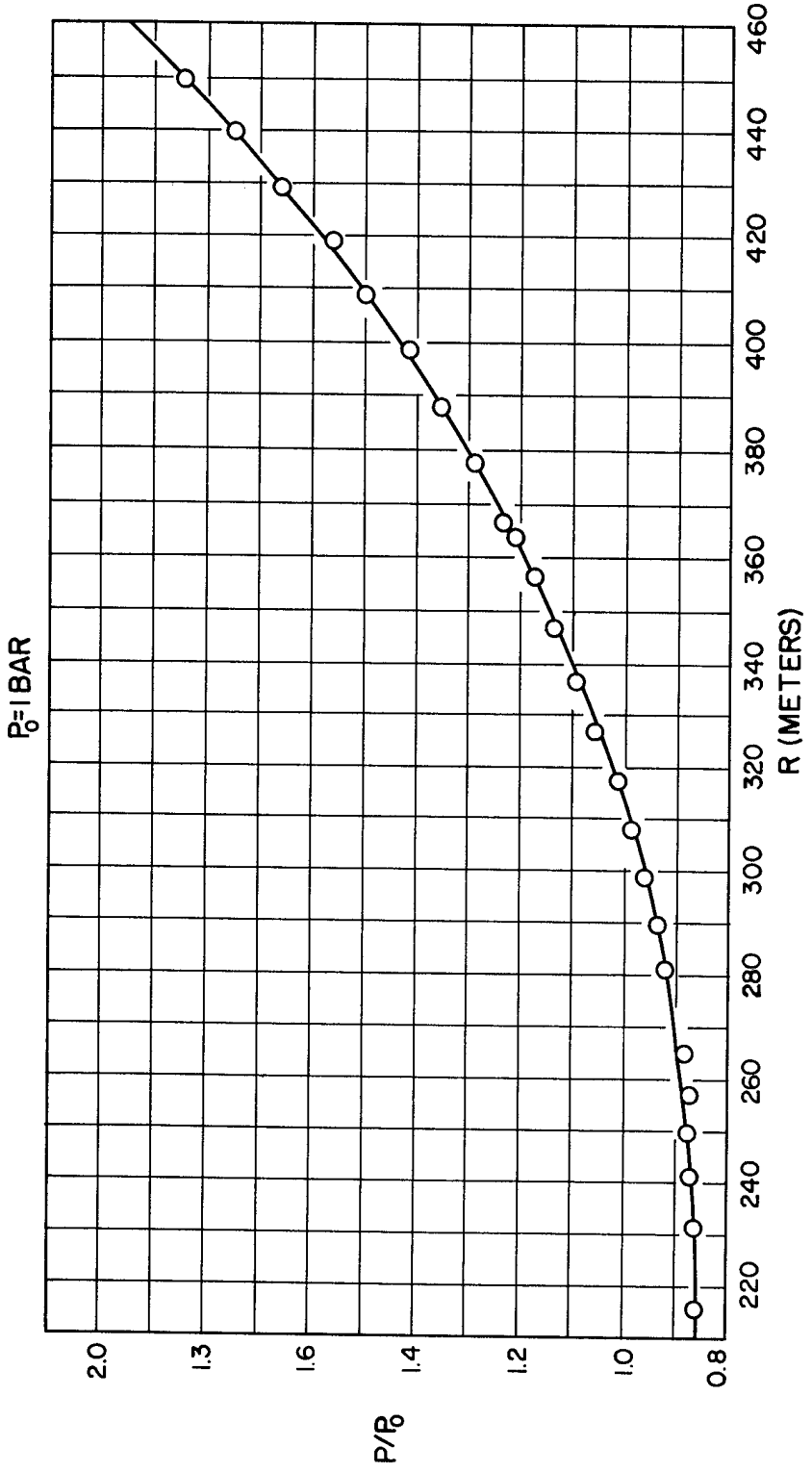

Fig. 6.8 Pressure vs distance at a fixed time

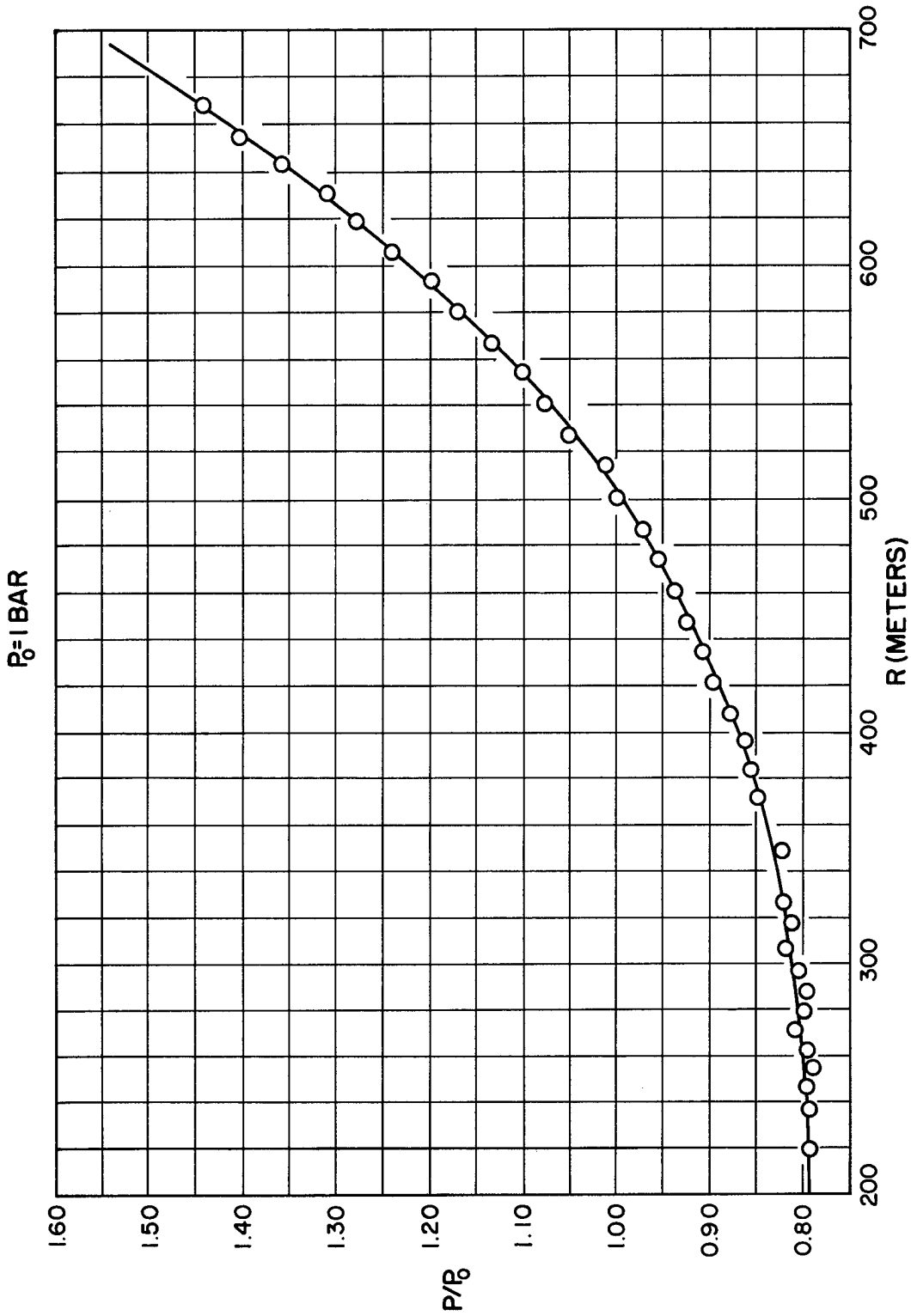

Fig. 6.9 Pressure vs distance at a fixed time

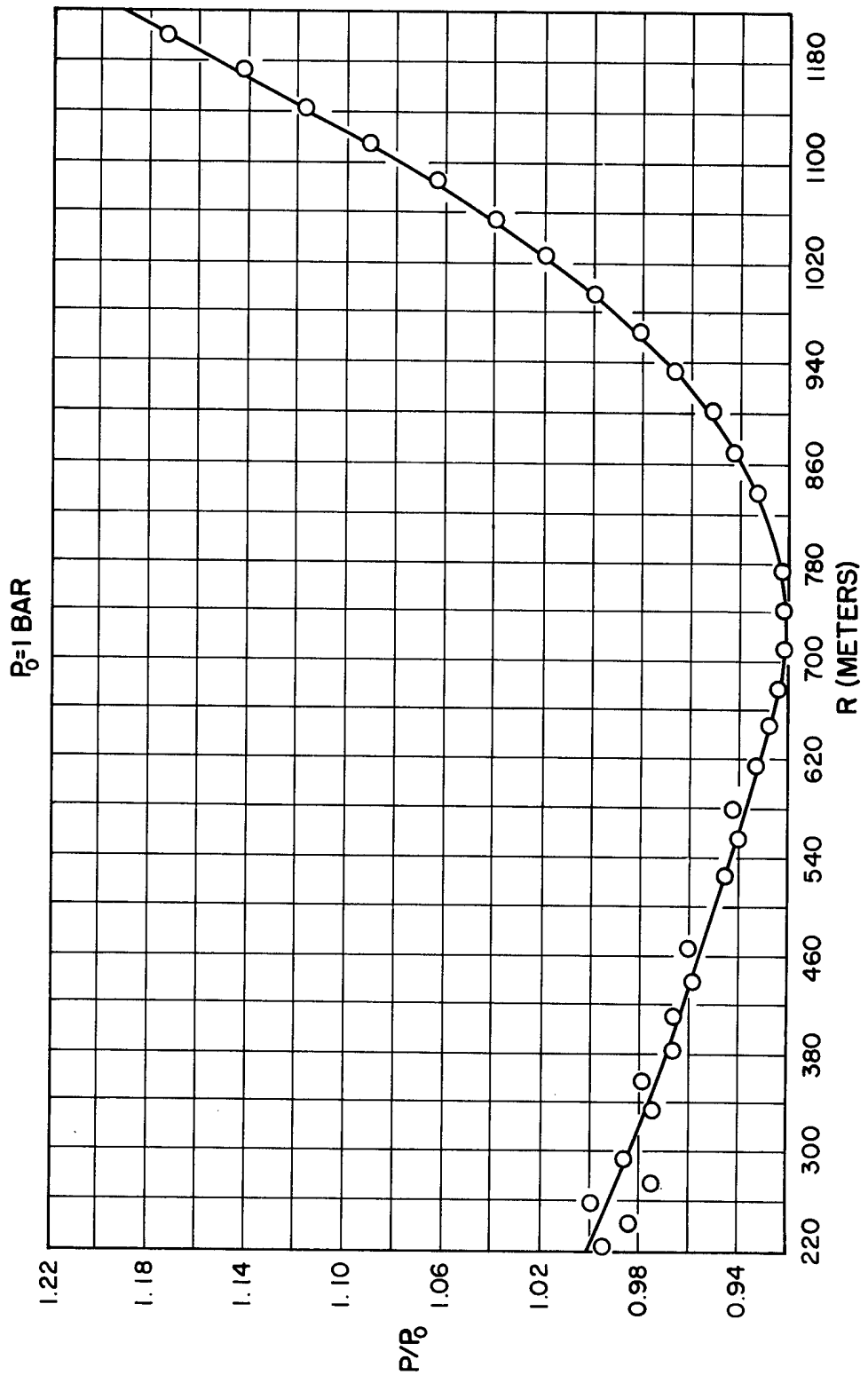

Fig. 6.10 Pressure vs distance at a fixed time

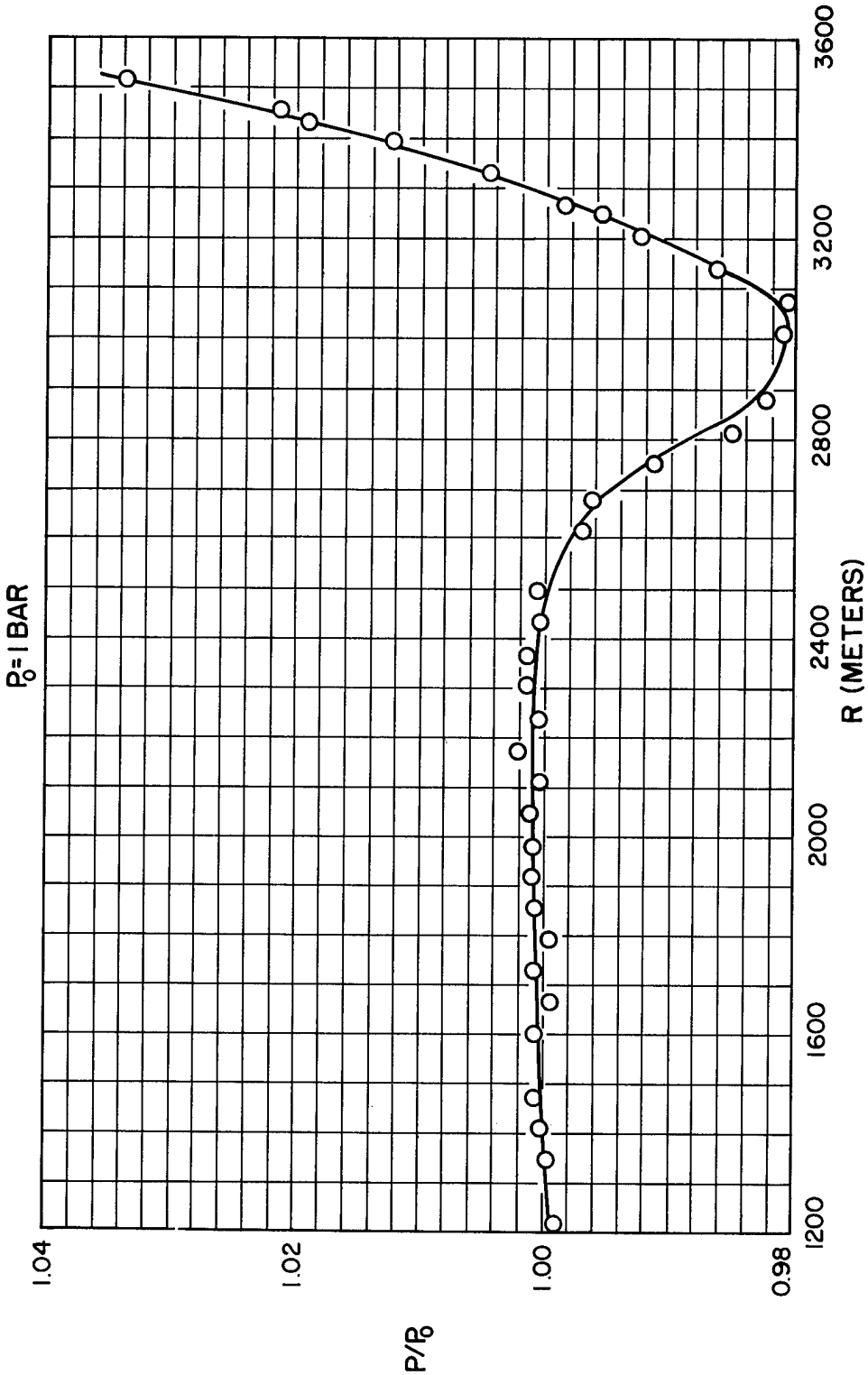

Fig. 6.11 Pressure vs distance at a fixed time

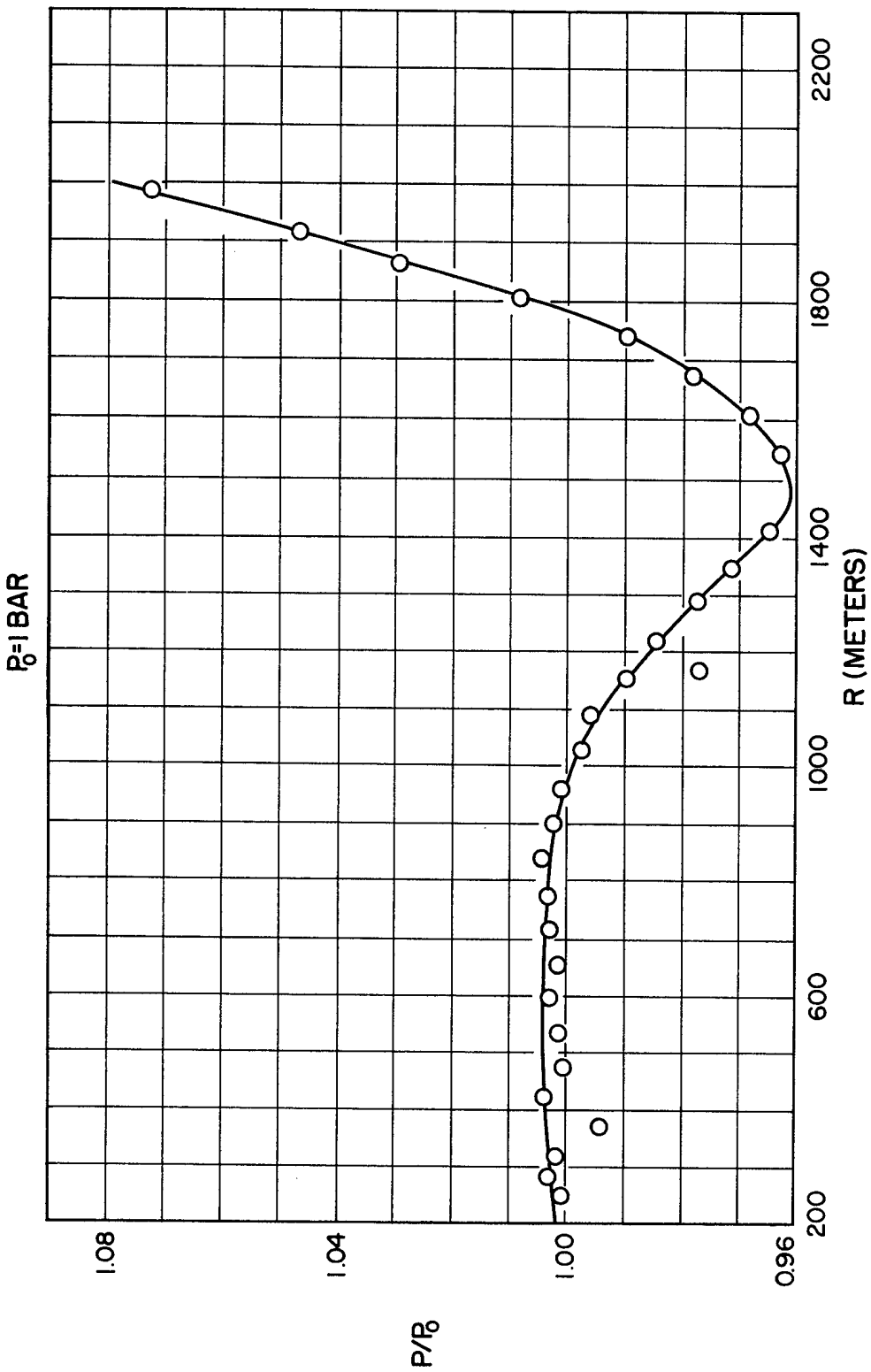

Fig. 6.12 Pressure vs distance at a fixed time

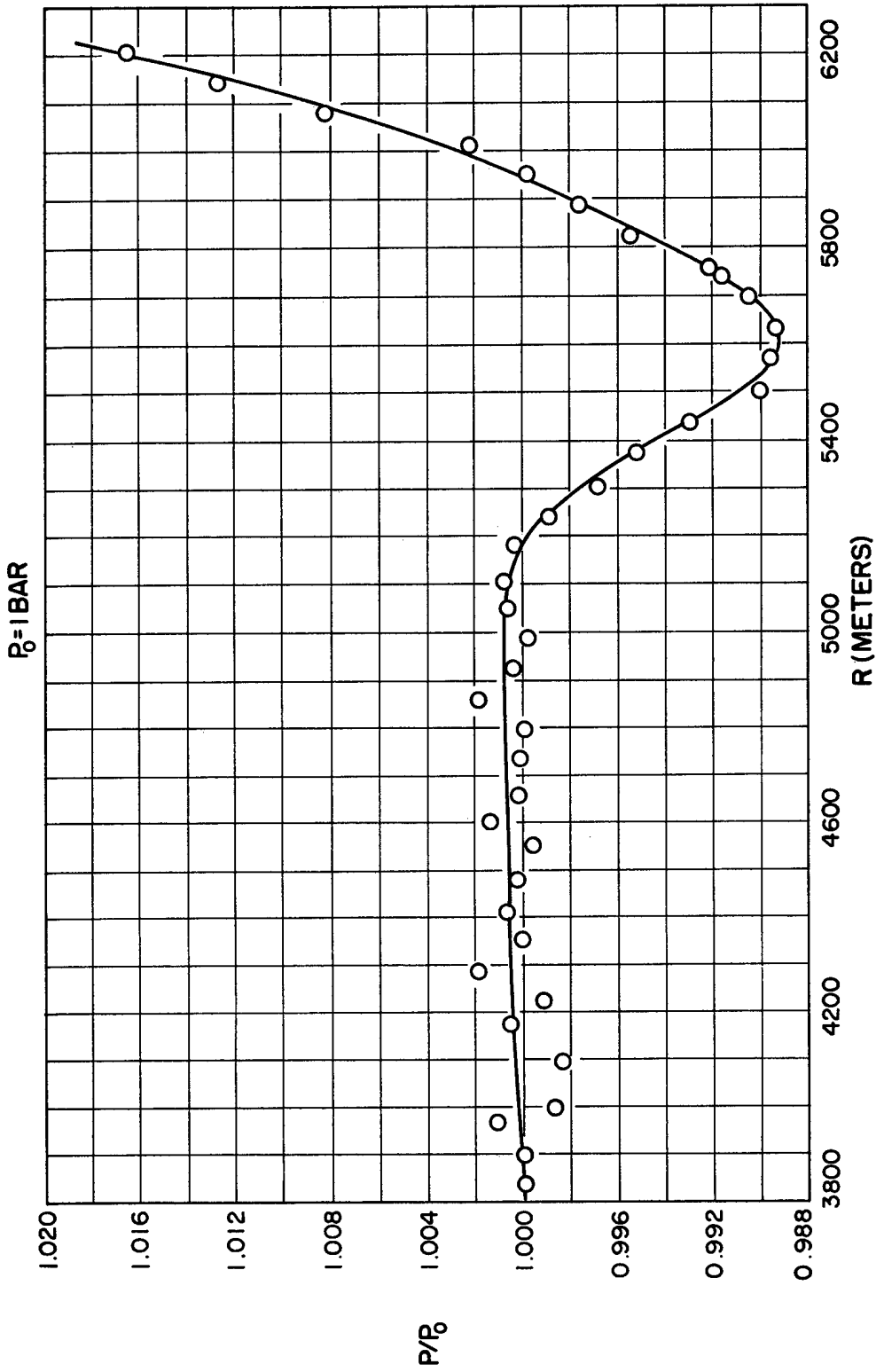

Fig. 6.13 Pressure vs distance at a fixed time

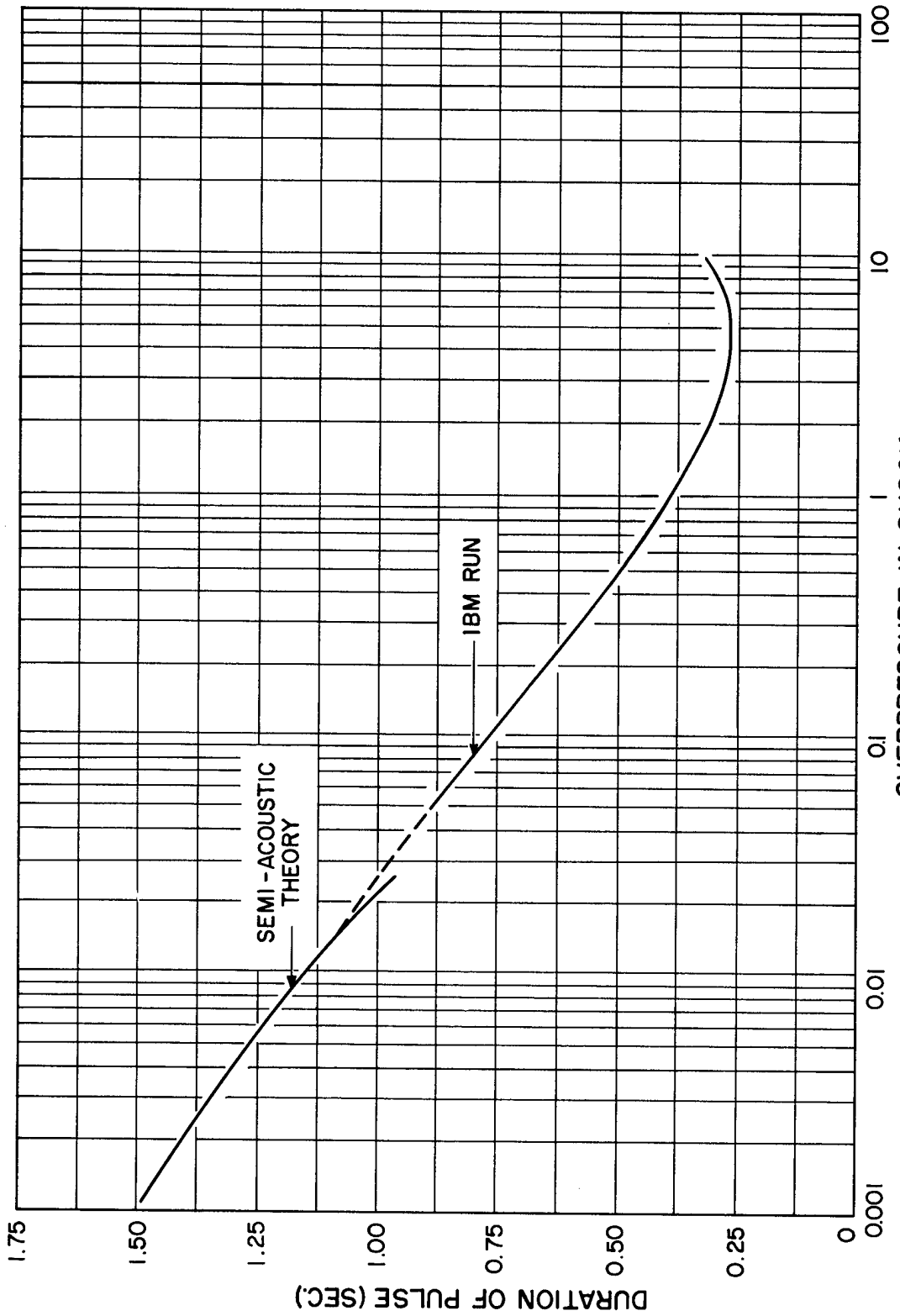

Fig. 6.14 Deviation of the positive phase of a pulse at a fixed distance

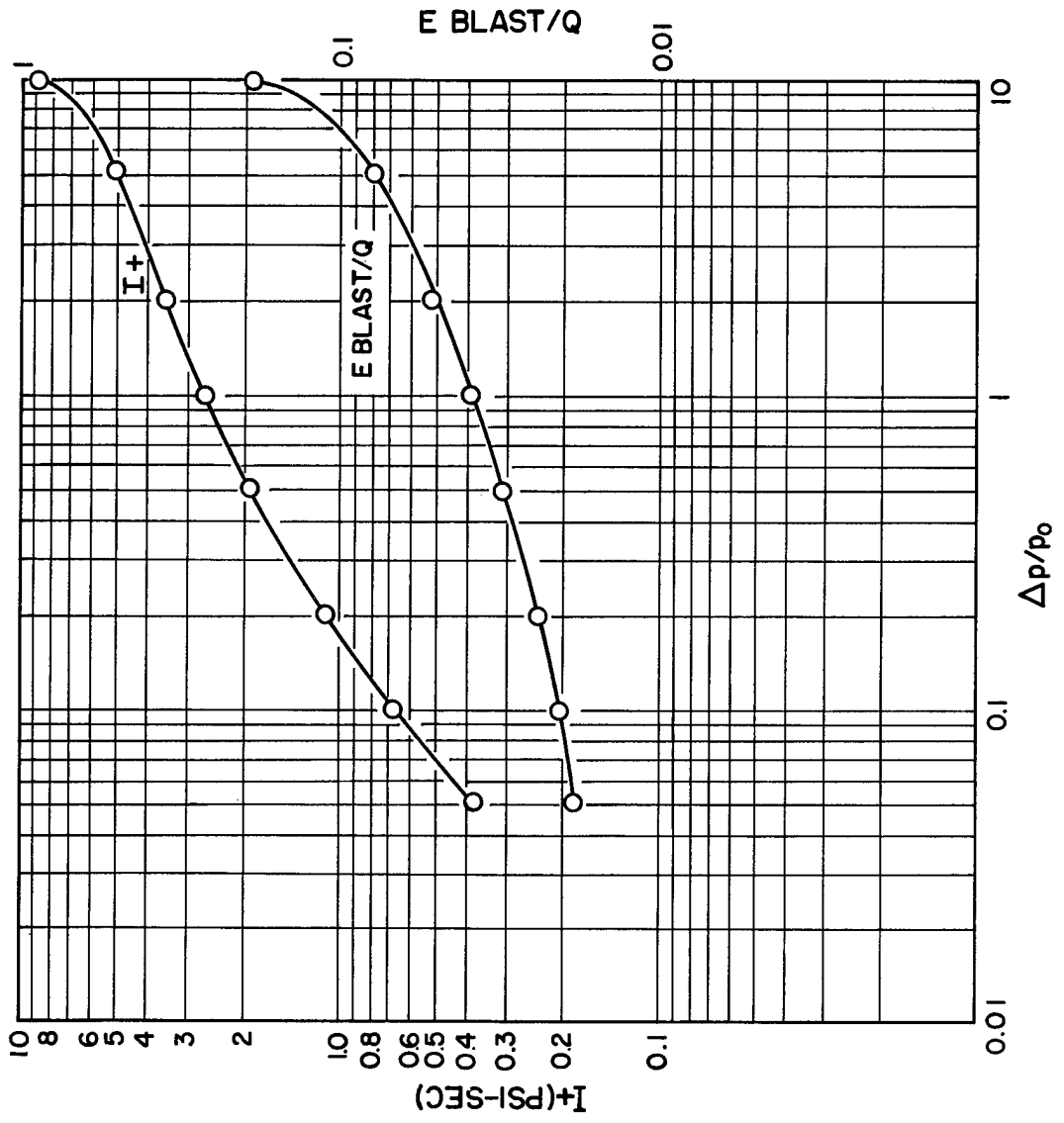

Fig. 6.15 The positive impulse and the energy in the blast. IBM run scaled to 40,000 tons in free air. (Q is the total energy.)

For lower pressure Hirschfelder, Sheard and Littler used the asymptotic formula

$$\Delta p = \frac{35.0}{x\sqrt{\log_{10} x - 0.928}} \tag{6.11}$$

The constants were obtained by fitting to the low pressure end of the curve (Eq. 6.9). The analytical form of the equation follows from the semi-acoustic theory presented in Chapter 5, provided the pressure pulse has reached its asymptotic linear shape.

From these formulae we calculated the weight of the TNT charge required to give the same shock pressure at the same distance as the nuclear explosion. Dividing this charge by the weight of 13,000 tons assumed for the IBM run, and multiplying by a factor 2 to take care of the fact that the TNT data apply to an explosion on the ground so that practically all energy is in a half sphere, we obtain the efficiency of the nuclear bomb compared to an equivalent charge of TNT.

The efficiency defined in this way depends on the shock pressure chosen for comparison, and it is not surprising that it should vary with the shock pressure; however, it is surprising that the efficiency should increase with decreasing shock pressure as shown in Fig. 6.16 over the range in which experimental data for TNT exist. However, the individual experimental points scatter appreciably, especially for high shock pressures and, therefore, this variation of efficiency with shock pressure is not necessarily correct. The most reliable data are those at the lower end of the experimental range, which would indicate an efficiency of about 0.6.

The curve has been extended on either side to higher and lower shock pressures. The extension to higher shock pressures by means of Eq. 6.9 is quite arbitrary and has been performed only since experimental data for the Trinity test have usually been compared with this formula. The extension to lower pressures depends on the assumption that the asymptotic formula is valid in this range, which is not necessarily correct. Again, the main reason for performing the extension is the fact that experimental data have been analyzed by means of this curve.

A similar comparison has been made by using the experimental curve of A. H. Taub,[5] for half-pound TNT charges in free air. These differ quite appreciably from the curve of Hirschfelder, Littler and Sheard,

5. A. H. Taub, Air and Earth Shock, Interim Report No. 1, NDRC-A-4076, September 5, 1944.

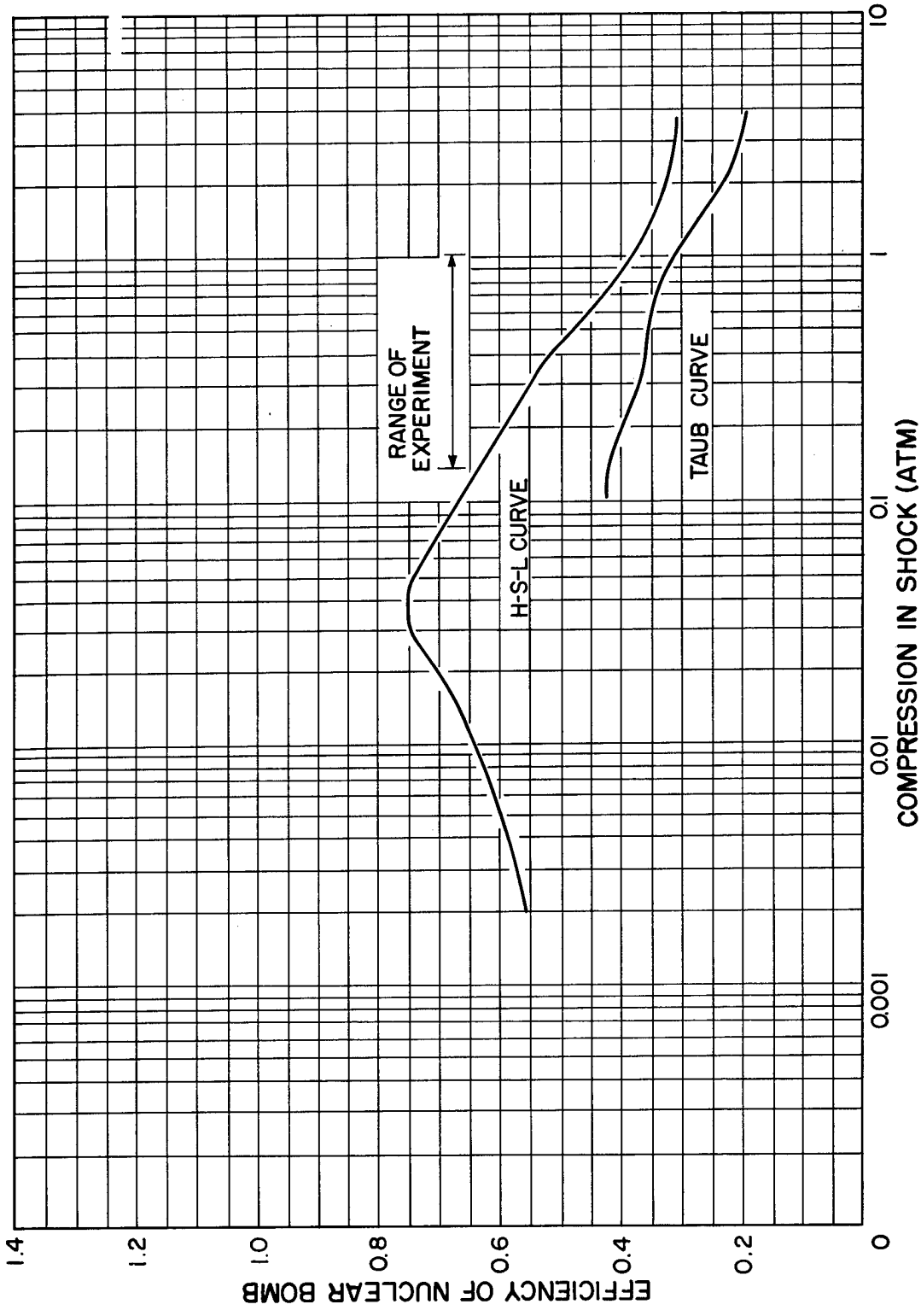

Fig. 6.16 Efficiency of nuclear bomb as compared to an equivalent charge of TNT

as may be seen from Fig. 6.16. This discrepancy shows the difficulty of assigning any definite value to the efficiency of the nuclear bomb for the purpose of producing blast and makes it desirable to have a comparable IBM run for TNT.

It should be noted that two factors, which might be important, have been disregarded in the IBM calculations. One of these is the radiation transport of energy from the ball of fire into the NO_2 layer, discussed in Chapter 3. This has the effect of equalizing the temperatures in the interior of the shock sphere and it will make the nuclear explosion more similar to a TNT explosion. Consequently, the efficiency of the nuclear bomb is improved. The other effect is the radiation which escapes to large distances. The arguments presented in Chapter 3 show that this radiation occurs at a time and place where it cannot affect the shock pressure in the region of practical interest, i.e., down to about 1 psi. However, it could reduce the efficiency at very low shock pressures.

6.7 Scaling Laws

The IBM run was made assuming a normal density of air, $\rho_0 = 1.163 \times 10^{-3}$ gm/cc; and a normal pressure, $p_0 = 1$ bar (10^6 dyn/cm^2). The sound velocity of normal air is then $c_0 = 347$ cm/sec. The total energy was $Q = 13{,}000$ tons.

For the change to a different energy release we have exact scaling laws, we keep all pressures and velocities fixed, but change all radii and times in the ratio of the cube root of the energy release.

For the change to different normal densities or pressures, no exact scaling laws exist. However, within the accuracy of the primary data which enter the IBM run, we can use the following scaling laws, which relate the primed quantities for arbitrary normal conditions to the IBM quantities:

$$\frac{p'}{p'_0} = \frac{p}{p_0} \qquad R' = \lambda R$$

$$\frac{u'}{c'_0} = \frac{u}{c_0} \qquad t' = \frac{c_0}{c'_0}\lambda t$$

$$\frac{\rho'}{\rho'_0} = \frac{\rho}{\rho_0} \qquad Q' = \frac{p'_0}{p_0}\lambda^3 Q \qquad (6.12)$$

i.e., we scale all pressures, velocities, and densities in the ratio of their normal values. The linear dimensions are scaled by an arbitrary factor λ, the times by the same factor λ and the inverse ratio of the normal sound velocities, and, finally, the energy release is scaled by λ^3 and the ratio of the normal pressures. The scaling laws for pressure, velocity and density are, of course, not independent of each other, since $\rho_0' c_0^2 = \rho_0 c_0^2 = p_0' = p_0$.

These scaling laws are based on the assumption that the equation of state of air can be written in the form

$$\frac{p}{p_0} = \text{function of } \left(\frac{\rho}{\rho_0}\right) \text{ and } \left(\frac{E\rho_0}{p_0}\right)$$

which is true for a γ law, but only approximately correct for the true equation of state of air. (E is the interval energy per unit mass.)

Chapter 7

THE EQUATION OF STATE OF AIR

by Klaus Fuchs and Rudolph E. Peierls

7.1 Equation of State of Air Between 2×10^4 and 2×10^6 Degrees

We shall briefly describe calculations on the equation of state of air in the region in which all molecules have been completely dissociated into atoms and in which the atoms are being stripped of their electrons until, in the neighborhood of two million degrees, there are only nuclei and free electrons left. These calculations were done by Fuchs, Kynch and Peierls at Birmingham.

7.1.1 Outline of Method

The most troublesome part of this work is the calculation at each temperature and density of the fraction of atoms in any given state of ionization. It is well known that even for low density, when the interaction forces between different atoms or ions are negligible, the degree of ionization depends on the density, since it represents the equilibrium between ionization and recombination. The probability of ionization per atom is independent of the density, whereas that of recombination per ion is proportional to the density of free electrons, which itself is proportional to the average degree of ionization. For the asymptotic case of extremely low density the problem is discussed in Section 7.3. At densities above ordinary atmospheric density, however, the asymptotic approximation is not very satisfactory since the effect on the energy of each ion of the free electrons in its neighborhood is not negligible. Conversely, the effect of the ions on the motion of the free electrons also has to be taken into account. In order to do this, and in order to treat the statistical mechanics of such an

assembly satisfactorily, it is evidently necessary to have a criterion which determines when an electron is to be regarded as free.

This is important since it is impracticable to consider the many-body problem to which a rigorous solution of the problem would lead, and instead, each electron has to be considered as moving in a given field of force, due to the average charge distribution of all other electrons. If we consider an ion of a given degree of ionization, the number of bound electrons is fixed by definition, whereas the number of free electrons within the space belonging to the ion depends on the average degree of ionization of all atoms; its correlation with the degree of ionization of the ion in question will be neglected.

It is therefore clear that the results of the calculation will be slightly different, according to whether a certain electron is regarded as free or as bound. This is an essential limitation of the kind of method used here but it is likely that, with a reasonable choice of the criterion, the errors will be small.

It is, however, essential that this criterion be made consistent, i.e., that each possible state of an electron be counted either as bound or as free, and that no states be omitted or counted twice; otherwise, the errors may be more serious.

If we ascribe to each atom a "cell," i.e., a sphere equal to the average gas volume per atom, it would at first sight appear to be most natural to choose a radius (e.g., the cell radius) and to regard an electron as free if its energy is sufficient to reach this radius. Care is necessary, however, since the energy of one particle is unambiguously defined only if we imagine it moving in a given potential field, and the meaning of its energy depends on the field. Since, as suggested above, free and bound electrons are assumed to move in slightly different fields, this may not lead to a consistent definition.

This difficulty can be avoided in the following way: Consider an electron which is bound to an ion of core charge, ze, where by core we shall always mean the ion minus its last electron. Then the condition that the electron cannot reach a distance b from the center of the ion is

$$\frac{m}{2}v^2 - \frac{ze^2}{r} < -\frac{ze^2}{b} \tag{7.1}$$

provided that in the region between r and b the field can be regarded as a pure Coulomb field.

In the case of a free electron, the opposite condition holds, i.e., we should replace the "smaller" sign in Eq. 7.1 by a "greater" sign. However,

Eq. 7.1 applies to the last electron in an ion of core charge ze, i.e., of total charge $(z-1)e$. If the electron has become free, the remaining ion has a total charge ze and is, therefore, according to our convention, considered as an ion of core charge $(z+1)e$. If we write all equations with reference to an ion of core charge z, we have to write the condition for a free electron as

$$\frac{m}{2}v^2 - \frac{(z-1)e^2}{r} > -\frac{(z-1)e^2}{b} \tag{7.2}$$

The inequalities, Eqs. 7.1 and 7.2, limit the states of bound and free electrons, respectively. Since these conditions are formulated in phase space, they can be applied in a simple way only if, for the relevant states, quantization can be neglected. This means that the highest bound state should be one with a quantum number large compared to unity, which is correct for all densities to be considered.

It is now necessary to choose the quantity b. This choice must be a compromise between the following requirements: b should be larger than the ionic core, since we have assumed that for some distance inside b the field is that of a point charge. On the other hand, it should be smaller than the cell radius a, since otherwise Eqs. 7.1 and 7.2 and all subsequent work ought to make allowance for the charge of the free electrons contained within a radius b. This requires that the volume of a sphere of radius b be a small fraction of the cell volume.

The results may be expected to be quite insensitive to the exact choice of b, since the consistency of Eq. 7.1 with Eq. 7.2 ensures that no electron is omitted and the difference in the treatment of free and bound electrons lies mainly in interactions and correlations which are not large effects. No doubt the best compromise would be different for different densities, but since this would very appreciably complicate the calculations, it was assumed

$$b = \frac{a}{\sqrt{2}} \tag{7.3}$$

where a is the cell radius, i.e., $4\pi a^3/3$ is the gas volume per atom.

We can now state the remaining assumptions and approximations: The energy levels of bound electrons are taken from spectroscopic data where available, and otherwise from hydrogen-like term formulae. This implies that the disturbance of these states due to the presence of free electrons is negligible. The interaction energy between the ion and the free electrons is replaced by that between a point charge and the free electrons.

In considering any free electron in any one cell, it is assumed that the density of free electrons within that cell equals the average density of free electrons. Hence, this neglects density fluctuations, the increase of the density inside the ion, and the fact that the presence of one free electron will reduce the probability of the presence of others. Similarly, we neglect fluctuations in the cell volume and the quantum effects in the motion of free electrons.

It is difficult to obtain an estimate of the errors caused by these approximations. They are likely to be quite small at very high temperatures, where fluctuations in the degree of ionization are small and where interaction forces between electrons are unimportant as against the strong forces due to the almost bare nuclei. They are also small at fairly low temperatures, where the number of free electrons is small and their effect unimportant. The errors might be worse at temperatures at which the degree of ionization varies rapidly with temperature and density.

We shall also neglect the presence of rare gases and other impurities in the air, treating it as a mixture of 21 per cent oxygen and 79 per cent nitrogen.

With these assumptions the mathematical problem is defined, and in the following sections we shall discuss details of procedure. We shall first discuss the partition functions of the individual ions and those of the free electrons, and thus show how to obtain the degree of ionization and other thermodynamic functions.

7.1.2 The Partition Function of the Ions

The partition function of an ion is the sum

$$F = \sum we^{-(E/kT)} \tag{7.4}$$

over all the "bound" energy levels of the ion; w is the weight of the energy level E. We shall measure E in this definition of F from the state of lowest energy of the ion, so that m − E is the work obtained by bringing the last electron from a large distance to the level of energy E, where m is the ionization potential. E does not include any interaction between the ion and the free electrons.

The levels have been measured experimentally in many cases and can be arranged in series

$$E = \frac{z^2 Ry}{(n - \delta)^2} + \text{const} \qquad n = 2, 3, 4, \ldots \tag{7.5}$$

where Ry is the Rydberg number, n the total quantum number, and δ the quantum defect of the series. For a singly excited ion δ has different values in the s, p, d states of the excited electron and also depends on the spin coupling between the electrons. We neglect its dependence on spin except for the very lowest states where $n < 3$ for all electrons. Then for a given series of levels of the first excited electron δ is almost independent of the state of the remaining electrons (unless two electrons are highly excited to similar levels which usually requires a large amount of energy.)

For the most highly excited atoms, for example O VII and O VIII, which have in their lowest state only K-electrons, the partition function is simply evaluated. For other atoms it is convenient to divide the levels into two groups. In the first group (i) are all levels with all the electrons in either the K or L shell ($n < 3$). Their energies are available from spectroscopic data. To the partition function F_z of an atom ionized $(z - 1)$ times, these contribute a sum similar to Eq. 7.4. In the second group (j) one or more electrons is excited to another shell $n \geq 3$. The experimental evidence available shows that for both singly-excited and doubly-excited levels the interaction energy of the excited electrons with the core or with one another is small compared with kT, so that the atom may be regarded as an atom ionized z times, to which an additional electron is added in a state $n \geq 3$.

By this procedure we include some levels which have been counted before, where two electrons are ionized so that the atoms have positive energy, but we have also counted these doubly-excited levels twice since we arbitrarily distinguish the two excited electrons, namely that electron in an excited state of the ion and the electron added to it. Since, however, the contribution of these doubly-excited states to the partition function is in any case small, the resulting error is unimportant.

The total partition function is

$$F_z = \left(\sum_i e^{-E/kT} \right) + \left(F_{z+1} \, e^{-m_z/kT} \right) \left(\sum_j w e^{(m_z - E)/kT} \right)$$

$$F_z = \sum_i w e^{-E/kT} + F_{z+1} \sum_j w e^{-E/kT} \tag{7.6}$$

The exponential $e^{-m_z/kT}$ enters with F_{z+1} since F_{z+1} is referred to the lowest state of the ion z, whereas F_z is referred to the lowest state of the ion $(z - 1)$.

The use of F_z for an atom ionized $(z-1)$ times is consistent with spectroscopic custom, which labels O V an oxygen atom ionized 4 times.

We can now define the weights w.

The sums have to be limited so as to include only bound electrons, i.e., according to our convention, electrons satisfying the inequality, Eq. 7.1. Since the energy levels (Eq. 7.5) arise from an energy expression which is identical with the left-hand side of Eq. 7.1 at large distance, this condition simply becomes

$$-\frac{z^2 Ry}{(n-\delta)^2} < -\frac{ze^2}{b} \tag{7.7}$$

If this limit falls somewhere between two levels, we must clearly include in our sum a fraction of the weight of the next level. If, in particular, we define a number n* as the value of $(n-\delta)$ for which Eq. 7.7 becomes an equality, and n* lies between $(n_1 - \delta + 1/2)$ and $(n_1 - \delta + 3/2)$, we must include the level of quantum number n_1 fully, and a fraction $n^* - (n_1 - \delta + 1/2)$ of the next one.

In the case of the higher ions for which the formula (Eq. 7.5) adequately represents all levels, it is convenient to introduce the dimensionless variable

$$l = \frac{z^2 Ry}{kT} \tag{7.8}$$

so that the sums are of the form

$$\sum_n e^{l[\text{const} + 1/(n-\delta)^2]} \tag{7.9}$$

Sums of this form were evaluated for simple values of l between 4 and 60 and the results for any z and T obtained by interpolation.

The data on energy levels, ionization potentials, and weights which were used for the computation of partition functions are summarized in Tables 7.1 and 7.2.

The values of the ionization potentials in Table 7.1 are those used in the actual numerical computation; however, the values in parentheses are preferable. The last two ionization potentials are not known experimentally and the formula $13.53\ Z^2$ was used for the ionization potential in electron volts, with Z the atomic number of the nucleus. This is exact for the last ionization

potential, but not for the one-but-last. Feynman has pointed out in the mean time that a reliable formula for the last-but-one ionization potential can be obtained by using a variational principle; the formula is

$$13.53\left(Z^2 - \frac{5}{4}Z + \frac{50}{256}\right)$$

The error in this formula decreases from 7 per cent for helium to 4 per cent for carbon. The ionization potentials obtained from this formula are given in parentheses in Table 7.1.

In Table 7.2 a distinction is made in accordance with the procedure explained above between the "lowest levels" of group (i) and the "series levels" of group (j); the latter are those in which one or more electrons are excited into a state $n \geq 3$. The weights given in the table do not include the weight of the configuration of the inner electrons, since this weight is already included in the partition function F_{z+1} of the previous ion.

7.1.3 The Partition Function of Free Electrons

The free electrons are, according to Section 7.1.1, assumed independent but they move in a field due to the ions and to the average free-electron charge distribution. The partition function is a sum of terms, each referring to a "cell," and depending on the degree of ionization of the ion in that cell, and also on the density of free electrons, i.e., the total degree of ionization. It may be written

$$G = \sum_z \left(p^O_{z+1} + p^N_{z+1}\right) g(z, \bar{z}) \tag{7.10}$$

Here p^O_{z+1}, p^N_{z+1} are, respectively, the fractions of all cells filled by oxygen or nitrogen atoms ionized z times. $g(z, \bar{z})$ is the partition function for free electrons in a cell containing an ion of net charge ze, the density of free electrons being $\bar{z}$ per cell.

Each free electron therefore has a potential energy

$$V = \frac{ze^2}{r} - \frac{\bar{z}e^2 r^2}{2a^3} + \frac{3\bar{z}e^2}{2a} \tag{7.11}$$

where, in accord with our assumptions, the possibility of penetrating into the core of the ion has been neglected. The last two terms in Eq. 7.11 are due

Table 7.1

IONIZATION ENERGIES

Potentials are given in units of $10^3 \times R$ ergs; R = Boltzmann's constant.

Oxygen

Ion	Ionization Potential
O VIII	10, 103
O VII	7, 750 (8, 580)
O VI	1, 607
O V	1, 321
O IV	898
O III	636.4
O II	407
O I	157.8

Nitrogen

Ion	Ionization Potential
N VII	7, 750
N VI	5, 700 (6, 410)
N V	1, 138
N IV	910
N III	550
N II	343.4
N I	168.7

Table 7.2

ENERGY LEVELS OF NITROGEN AND OXYGEN IONS

Energy is in units $10^3 \times$ R ergs. (n) denotes any set of one-electron quantum numbers for an ion not previously mentioned in the table.

Ion	Lowest Levels				Series		
	Configuration	State	Energy	Full Weight	Configuration	Energy	Full Weight
N VII	1s	^2S	7750	2	(n)	$7750/n^2$	$2n^2$
N VI	$1s^2$	^1S	5700	1	(1s)(n)	$5700/n^2$	$2n^2$
N V	$1s^2 2s$	^2S	$3940/1.86^2$	2	$1s^2$(ns) n≤5	$3940/(n - 0.14)^2$	2
	$1s^2 2p$	^2P	1066	6	$1s^2$(n)	$3940/n^2$	$2n^2 - 2$ or $2n^2$
N IV	$1s^2 2s^2$	^1S	910	1	2s(ns) n≤6	$2520/(n - 0.3)^2$	2
	$1s^2 2s2p$	^1P	710	3	2s(np) n≤6	$2520/(n - 0.14)^2$	6
		^3P	802	9			
	$2p^2$	$^1S\,^3P\,^1D$	620	15	2s(n)	$2520/n^2$	$(2n^2 - 8)$ or $2n^2$
N III	$1s^2 2s^2 2p$	^2P	550	6	$2s^2$(ns) n≤6	$1420/(n - 0.5)^2$	2
	$2s2p^2$	^2D	406	10	$2s^2$(np) n≤6	$1420/(n - 0.25)^2$	6
		$^2S\,^2P\,^4P$	355	20	$2s^2$(n)	$1420/n^2$	$(2n^2 - 8)$ or $2n^2$
	$2p^3$	$^2P\,^2D\,^4S$	250	20			
N II	$1s^2 2s^2 2p^2$	^3P	343.4	9	$2s^2 2p$(ns) n≤6	$631/(n - 0.8)^2$	2
		^1S	296.4	1	(np) n≤6	$631/(n - 0.5)^2$	6
		^1D	321.2	5	$2s^2 2p$(n)	$631/n^2$	$2(n^2 - 4)$ or $2n^2$
	$2s2p^3$	^3D	210.6	15			
		$^1P\,^1D\,^3S\,^3P$	186	20			
		^5S	83				
				20			
	$2p^4$		83				
N I	$1s^2 2s^2 2p^3$	^4S	168.7	4	$2s^2 2p^2$(3s)	49.6	2
		^2P	127.2	6	(3p)	32.0	6
		^2D	141.1	10	(3d)	17.8	10
	$2s2p^4$		42.0	12	(4s)	20.0	2
	$2p^5$	negative energy			(4p)	15.0	6
					(4df, 5spd)	11.0	32

Table 7.2 (Continued)

Ion	Lowest Levels				Series		
	Configuration	State	Energy	Full Weight	Configuration	Energy	Full Weight
O VIII	(n)		$10,103/n^2$	$2n^2$			
O VII	$1s^2$	^1S	7,750	1	(1s)(n)	$7750/n^2$	$2n^2$
O VI	$(1s)^2(2s)$	^2S	1,607	2	$(1s)^2$(ns) n≤5	$5690/(n-0.1)^2$	2
	$(1s)^2(2p)$	^2P	1,423	6	$(1s)^2$(n)	$5690/n^2$	$2(n^2-1)$ or $2n^2$
O V	$1s^2 2s^2$	^1S	1,321	1	(2s)(ns) n≤6	$3940/(n-0.3)^2$	2
	$1s^2 2s2p$	^3P	1,202	9	(2s)(np) n≤6	$3940/(n-0.14)^2$	6
		^1P	1,091	3	(2s)(n)	$3940/n^2$	$(2n^2-8)$ or $2n^2$
	$2p^2$		971	15			
O IV	$1s^2 2s^2 2p$	^2P	898	6	$2s^2$(ns) n≤6	$2520/(n-0.5)^2$	2
	$2s2p^2$	^2D	720	10	(np) n≤6	$2520/(n-0.25)^2$	6
		$^2S\,^2P\,^4P$	630	20	$2s^2$(n)	$2520/n^2$	$(2n^2-8)$ or $2n^2$
	$2p^3$	$^2P\,^2D\,^4S$	441	20			
O III	$1s^2 2s^2 2p^2$	^3P	636.4	9	2p(ns) n≤6	$1420/(n-0.8)^2$	2
		^1S	575	1	(np) n≤6	$1420/(n-0.5)^2$	6
		^1D	608	5	2p(n)	$1420/n^2$	$(2n^2-8)$ or $2n^2$
	$2s2p^3$	^3D	465	15			
		$^1P\,^1D\,^3S\,^3P$	432	20			
		^5S	310	20			
	$2p^4$						
O II	$1s^2 2s^2 2p^3$	^4S	407	4	$(2p)^2$(3s)	139	2
		^2D	369	10	(3p)	109.2	6
		^2P	349	6	(3d)	73.3	10
	$2s2p^4$	^4P	235	12	(4s)	63.2	2
		^2D	169	10	(4p)	51.7	6
		^2P	102	6	(4d, f)	40.7	24
					(5spdfg)	30.7	50
					(6sp)	22.7	72
O I	$1s^2 2s^2 2p^4$	^3P	157.8	9			
		^1D	135.1				
		^1S	109.1				
	$2s2p^5$		–13				

to the interaction of free electrons with each other. It would therefore be wrong to compute the total energy by adding the energies of all free electrons obtained from Eq. 7.11, since in this way each interaction would be counted twice. Since, however, with our assumptions the average interaction energy is independent of the states of the free electrons, the error can be remedied by subtracting from the total energy the expression $6\bar{z}e^2/10a$ for the self-energy (per electron) of a constant-density sphere of total charge $\bar{z}e$. Since this term is a constant it may be included in the expression for the potential energy per electron which therefore becomes, in effect,

$$V = -\frac{ze^2}{r} - \frac{\bar{z}e^2 r^2}{2a^3} + \frac{9}{10}\,\frac{\bar{z}e^2}{a} \tag{7.12}$$

Our cell partition function becomes now

$$g(z,\bar{z}) = \frac{2}{h^3}\int_0^a 4\pi r^2 dr \int_{p_1}^{\infty} \exp -\left(\frac{p^2}{2mkT} + \frac{V}{kT}\right) 4\pi p^2 dp \tag{7.13}$$

where h is Planck's constant and where

$$p_1 = \begin{cases} 0 & \text{if } r > b \\ \left[2\,mze^2\left(\frac{1}{r} - \frac{1}{b}\right)\right]^{1/2} & \text{if } r < b \end{cases} \tag{7.14}$$

according to condition 7.2, i.e.,

$$E' = \frac{p^2}{2m} - \frac{ze^2}{r} > -\frac{ze^2}{b}$$

If we consider first the part of the integral in which $r < b$, the second term in V of Eq. 7.12 is negligible as compared to the first, since it again represents the part of the charge density that has penetrated inside the ion.

This part of the integral can be written as

$$g_1 = \frac{16\pi^2(2m)^{3/2}}{h^3} \int_{\frac{-ze^2}{b}}^{\infty} dE' \exp -\left(\frac{9}{10}\,\frac{\bar{z}e^2}{akT}\right) \int_0^b \exp -\left(\frac{E'}{kT}\right)\left(\frac{ze^2}{r} + E'\right)^{1/2} r^2 dr \qquad (7.15)$$

Introducing the variables

$$\alpha = \frac{ze^2}{bkT}, \quad x^2 = \frac{r}{b}, \quad t^2 = \left|\frac{bE'}{ze^2}\right| \qquad (7.16)$$

we have, using Eq. 7.3,

$$g_1 = 64\pi^2\left(\frac{2mk}{h^2}\right)^{\frac{3}{2}} T^{\frac{3}{2}}\, b^3\, \alpha^{\frac{3}{2}} \exp -\left(\frac{9}{10}\,\frac{\alpha}{\sqrt{2}}\,\frac{\bar{z}}{z}\right)(I + J) \qquad (7.17)$$

where

$$\left.\begin{aligned} I &= \int_0^\infty tdt \int_0^1 \exp -(\alpha t^2)\ (1 + x^2t^2)^{1/2}\ x^4\, dx \\ J &= \int_0^1 tdt \int_0^1 \exp(\alpha t^2)\ (1 - x^2t^2)^{1/2}\ x^4\, dx \end{aligned}\right\} \qquad (7.18)$$

For range $r > b$ we use the substitution

$$\xi = \frac{ze^2}{rkT} = \xi_1\,\frac{a}{r}\ , \text{ where } \xi_1 = \frac{ze^2}{akT} = \frac{\alpha}{\sqrt{2}} \qquad (7.19)$$

$$g_2 = 64\pi^2 \left(\frac{2mk}{h^2}\right)^{\frac{3}{2}} T^{\frac{3}{2}} b^3 \frac{\sqrt{\pi}}{8} \alpha^3 K \exp -\left(\frac{9}{10} \frac{\alpha}{\sqrt{2}} \frac{\bar{z}}{z}\right) \tag{7.20}$$

where

$$K = \int_{\xi_1}^{\xi_1\sqrt{2}} \exp\left[\xi + (\bar{z}\xi_1^3/2z\xi^2)\right] \xi^{-4} \, d\xi \tag{7.21}$$

The partition function $g(z, \bar{z})$ is then obtained as the sum of g_1 and g_2. The integrals I and J are functions of the parameter α only. Values of $\alpha^{3/2}I$ and of $\alpha^{3/2}J$ are given in Table 7.3. K depends on the parameters α and $\bar{z}/z$.

Table 7.3

THE INTEGRALS $I(\alpha)$ AND $J(\alpha)$

α	$\alpha^{3/2} I(\alpha)$	α	$\alpha^{3/2} J(\alpha)$
0.0	0.07385	0.00	0.00784
0.25	0.09350	0.25	0.0110
0.49	0.10546	0.50	0.0352
1.0	0.12832	1.00	0.1284
1.44	0.14486	2.00	0.642
1.96	0.16217	3.0	2.245
2.56	0.18002	4.0	7.016
3.24	0.19817	5.0	20.919
4.00	0.21672		

For all practical purposes we can use an expansion of the integral K, which is obtained by expanding the second term in the exponential in powers of $[(\xi_1/\xi)^2 - (3/4)]$. Then

$$K = e^{3/8\ \xi_1\ \bar{z}/z} \sum_{\nu} (-1)^{\nu} \left(\frac{3}{8}\ \frac{\bar{z}}{z}\ \xi_1\right)^{\nu} L_{\nu} \qquad (7.22)$$

$$L_{\nu} = \sum_{n=0}^{\nu} \frac{1}{n!(\nu - n)!} \left(-\frac{4}{3}\ \xi_1^2\right)^n K_n$$

$$K_n = \int_{\xi_1}^{\xi_1\sqrt{2}} e^{\xi}\ \xi^{-2(n+2)}\ d\xi \qquad (7.23)$$

The integrals K_n are tabulated in the British Association Tables. The L_{ν} were calculated as functions of α and are tabulated in Table 7.4. If α is

Table 7.4

THE INTEGRALS L_{ν}

α	L_0	L_1	L_2	L_3
1.0	1.3890	–0.004	0.0258	0.0000
1.25	0.8747	+0.0006	0.0163	
1.50	0.6227	0.0029	0.0115	
1.75	0.4829	0.0041	0.0090	0.0001
2.00	0.3984	0.0051	0.0075	0.0001
2.5	0.3098	0.0065	0.0059	0.0001
3.0	0.2728	0.0079	0.0052	0.0001
3.5	0.2619	0.0097	0.0050	0.0001
4.0	0.2678	0.0121	0.0053	0.0002
5.0	0.3214	0.0197		

small the following expansions can be used

$$\alpha^{3/2}I = 0.07385 + 0.1108\alpha - \frac{1}{9}\alpha^{3/2} + 0.1108\alpha^2 \pm \frac{2}{15}\alpha^{5/2} + \ldots$$

$$\alpha^{3/2}J = 0.00784 + 0.03516\alpha + \ldots$$

$$\alpha^3 L_0 = 0.6095 + \frac{1}{2}\alpha + 0.2071\alpha^2 + 0.0578\alpha^3 + \ldots$$

$$\alpha^3 L_1 = -0.0114 + 0.0040\alpha^2 + \ldots$$

$$\alpha^3 L_2 = 0.01115 + 0.0093\alpha + \ldots$$

$$\alpha^3 L_3 = -0.0001273 + \ldots \qquad (7.24)$$

7.1.4 Degree of Ionization

The partition function of our system, omitting the motion of the ions, is

$$p_i = \left\{ \pi_z \left[\frac{\left(f_z^O\right)^{Np_z^O}}{\left(Np_z^O\right)!} \frac{\left(f_z^N\right)^{Np_z^N}}{\left(Np_z^N\right)!} \right] \right\} \frac{N!}{(N\bar{z})!} (NG)^{N\bar{z}} \qquad (7.25)$$

Here N is the total number of ions, G is the partition function of free electrons, as defined in Eq. 7.10, and the p_z^O, p_z^N are the fractions of cells occupied by oxygen and nitrogen atoms ionized z − 1 times. f_z^O and f_z^N are the partition functions of the ions referred to the energy level of the neutral atom, and are therefore related to the partition functions defined in Section 7.1.2 by

$$f_z^O = F_z^O \exp\left(-\frac{1}{kT} \sum_{z=1}^{z-1} m_z^O \right) \qquad (7.26)$$

where the m's are the successive ionization energies.

The free energy is, again omitting the motion of the ions,

$$F_i = -kT \ln P_i$$

$$= -RT\left\{\sum_z\left[p_z^O \ln f_z^O + p_z^N \ln f_z^N - p_z^O \ln p_z^O - p_z^N \ln p_z^N \right] + \bar{z} \ln G - \bar{z} \ln \bar{z} + \bar{z}\right\} \qquad (7.27)$$

The occupation numbers p_z^O and p_z^N and $\bar{z}$ have to be determined from the condition that the free energy should be a minimum with respect to the variation of these parameters, subject to the conditions

$$\sum_z p_z^O = k^O = \text{mole fraction of } O_2 = 0.21,$$

$$\sum_z p_z^N = k^N = \text{mole fraction of } N_2 = 0.79$$

$$\sum_z (z-1)(p_z^O + p_z^N) = \bar{z} \qquad (7.28)$$

The requirement that F be a minimum, subject to these conditions, leads to the equations

$$p_z^O = C^O f_z^O \left(\frac{G}{\bar{z}}\right)^z \exp \frac{\bar{z}[g(z-1,\bar{z}) + Hz]}{G}$$

$$p_z^N = C^N f_z^N \left(\frac{G}{\bar{z}}\right)^z \exp \frac{z[g(z-1,\bar{z}) + Hz]}{G} \qquad (7.29)$$

where C^O and C^N are normalizing factors which do not depend on z, and H is an abbreviation for

$$H = \frac{\partial G}{\partial \bar{z}} \qquad (7.30)$$

In practice the most convenient procedure for dealing with this set of equations is to guess values for G, H and $\bar{z}$. Then the p_z can be obtained from Eq. 7.29 together with the normalizing conditions of Eq. 7.28. From these we can determine new values of $\bar{z}$ from Eq. 7.28 and of G and H from Eqs. 7.21 and 7.30. The three quantities have to be adjusted until they

reproduce themselves. This procedure is not as cumbersome as it might appear since all quantities vary continuously with temperature, so that after the problem has been solved in a few cases, a reasonably good first guess can be made by extrapolation. The calculation is best started either at very high or at very low temperatures, where each atom is found only in two states of ionization, and where the equations can be solved analytically.

Table 7.5 gives the results of this operation, listing the occupation numbers and the average degree of ionization as function of the temperature for five different densities which are listed at the head of the table. The particular sequence was chosen from a consideration of economy: if two densities are in the ratio $2^{3/2}$, the value of a for one equals that of b for the other; hence in some of the integrals the upper limit in one case equals the lower limit in the other, and this leads to a slight saving.

The same results are shown in Fig. 7.1. The temporary slowing down of ionization near 4×10^5 degrees is due to the fact that at that point the ionization of the L-shell is practically complete, whereas that of the K-shell has hardly started yet.

7.1.5 The Free Energy, Thermal Energy, Entropy, and Pressure

Substitution of Eq. 7.29 into Eq. 7.27 yields

$$F_i = RT\left(k^O \ln C^O + k^N \ln C^N + \ln \frac{G}{\bar{z}} + \bar{z}(\bar{z}+1)\frac{H}{G} \right) \tag{7.31}$$

which is most convenient for the purpose of numerical calculation.

The pressure can be obtained by differentiation

$$p_i V = \frac{\partial F_i}{\partial \ln V} \tag{7.32}$$

The thermal energy is given by

$$E_i = -RT \frac{\partial}{\partial \ln T}\left(\frac{F_i}{RT}\right) \tag{7.33}$$

and the entropy is given by

$$S_i = \frac{E_i - F_i}{T} \tag{7.34}$$

Table 7.5

THE DEGREES OF IONIZATION AND NUMBER OF FREE ELECTRONS

	ρ/ρ_0 =	0.367	1.831	3.66	5.44	7.33
$T = 2.526 \times 10^6$	p_8^O	0.002	0.004	0.006	0.008	0.010
	p_9^O	0.208	0.206	0.204	0.202	0.200
	$\bar{z}$	7.208	7.206	7.204	7.202	7.200
$T = 1.263 \times 10^6$	p_7^O	0.0003	0.004	0.007	0.012	0.016
	p_8^O	0.024	0.074_5	0.102	0.117	0.130
	p_9^O	0.185_5	0.131_5	0.101	0.081	0.064
	p_8^N	0.767	0.712	0.660	0.618	0.582
	p_7^N	0.023	0.076	0.126	0.166	0.200
	p_6^N	0.00008	0.001	0.003_5	0.006	0.008
	$\bar{z}$	7.164	7.048_5	6.959	6.89	6.832
$T = 9.6875 \times 10^5$	p_6^O	0.00008	0.001	0.003	0.004	0.006
	p_7^O	0.008	0.035	0.057	0.072	0.084
	p_8^O	0.131	0.155	0.141	0.128	0.116
	p_9^O	0.071	0.019	0.009	0.006	0.004
	p_5^N	0.0_55	0.0002	0.000_5	0.001	0.015
	p_6^N	0.001_5	0.015	0.033_5	0.052	0.065_5
	p_7^N	0.120	0.336	0.443	0.493	0.513

Table 7.5 (Continued)

	ρ/ρ_0 =	0.367	1.831	3.66	5.44	7.33
	p_8^N	0.668	0.438_5	0.312	0.244	0.196
	$\bar{z}$	6.94	6.615	6.436	6.326	6.217
$T = 7.125 \times 10^5$	p_9^O	0.001	0.0008	0.00002	0.00001	0.000007
	p_8^O	0.102	0.036	0.021	0.015	0.011
	p_7^O	0.104	0.163	0.172	0.173	0.172
	p_6^O	0.003	0.011	0.017	0.021	0.025
	p_5^O				0.001	0.002
	p_8^N	0.151	0.033	0.015	0.009	0.006
	p_7^N	0.589	0.576	0.491	0.431	0.381
	p_6^N	0.050	0.175	0.269	0.328	0.374
	p_5^N	0.001	0.006	0.014	0.022	0.029
	$\bar{z}$	6.201	5.870	5.722	5.629	5.558
$T = 4.925 \times 10^5$	p_8^O	0.001	0.0002	0.0001	0.00007	0.00005
	p_7^O	0.198_5	0.183	0.173	0.159	0.151
	p_6^O	0.010	0.025	0.034	0.046	0.052
	p_5^O	0.0003	0.002	0.003	0.006	0.008
	p_8^N	0.0003	0.00002	0.0_55		
	p_7^N	0.203	0.053	0.031	0.019	0.014_5

Table 7.5 (Continued)

	ρ/ρ_0 =	0.367	1.831	3.66	5.44	7.33
	p_6^N	0.568	0.678	0.672	0.660	0.645
	p_5^N	0.018	0.057	0.082	0.102	0.120
	p_4^N		0.002_5	0.005	0.008	0.011
	$\bar{z}$	5.386	5.172	5.109	5.054	5.017
$T = 3.283 \times 10^5$	p_7^O	0.181	0.135	0.105	0.087_5	0.074
	p_6^O	0.028	0.066_5	0.086_5	0.096	0.101_5
	p_5^O	0.001	0.008	0.016	0.023	0.029_5
	p_4^O	0.00005	0.001	0.002	0.003	0.005
	p_7^N	0.0005	0.0001	0.00005	0.00003	0.00002
	p_6^N	0.732	0.647	0.578_5	0.536	0.493
	p_5^N	0.055	0.131	0.185	0.215	0.246
	p_4^N	0.002	0.012	0.025	0.035	0.047
	p_3^N	0.00004	0.001	0.002	0.003	0.004
	$\bar{z}$	5.121	4.967	4.845	4.764	4.682
$T = 2.4625 \times 10^5$	p_7^O	0.126	0.048	0.027	0.018	0.013
	p_6^O	0.073	0.110	0.097	0.087	0.077
	p_5^O	0.010_5	0.045	0.070	0.082	0.090
	p_4^O	0.001	0.007	0.016	0.023	0.029
	p_3^O	0.0_58	0.0002	0.0003	0.001	0.001

Table 7.5 (Continued)

	ρ/ρ_0 =	0.367	1.831	3.66	5.44	7.33
	p_6^N	0.673	0.495	0.389	0.327	0.279
	p_5^N	0.110	0.250	0.315	0.346	0.362
	p_4^N	0.007	0.042	0.078	0.105	0.132
	p_3^N	0.0003	0.003	0.008	0.013	0.017
	p_2^N					0.0004
	$\bar{z}$	4.989	4.645	4.428	4.296	4.185
$T = 1.8 \times 10^5$	p_7^O	0.018	0.002	0.001	0.0004	0.0003
	p_6^O	0.106	0.046	0.027	0.019	0.015
	p_5^O	0.076	0.115_5	0.113	0.105	0.098
	p_4^O	0.010	0.044	0.065	0.078	0.088
	p_3^O	0.0001	0.002	0.004	0.007	0.009
	p_6^N	0.462	0.196	0.112	0.078	0.060
	p_5^N	0.285	0.405	0.385	0.356	0.326
	p_4^N	0.040	0.167	0.249	0.293_5	0.325
	p_3^N	0.002	0.022	0.044	0.061	0.078
	p_2^N	0.00001	0.0002	0.000_5	0.001	0.001
	$\bar{z}$	4.548	3.987	3.729	3.589	3.483
$T = 1.4 \times 10^5$	p_7^O	0.0003	0.00002			
	p_6^O	0.025	0.005	0.002	0.001	0.001

Table 7.5 (Continued)

	ρ/ρ_0 =	0.367	1.831	3.66	5.44	7.33
	p_5^O	0.132	0.086	0.060	0.046	0.038
	p_4^O	0.050	0.104	0.118	0.119	0.117
	p_3^O	0.002	0.014	0.027_5	0.038	0.047
	p_2^O	0.0001	0.001	0.003	0.005	0.007
	p_6^N	0.142	0.027	0.011_5	0.007	0.005
	p_5^N	0.453	0.296	0.205	0.160_5	0.132
	p_4^N	0.179	0.378	0.423_5	0.439	0.435
	p_3^N	0.016	0.087	0.141_5	0.178	0.210
	p_2^N	0.0001	0.002	0.004	0.006	0.009
	$\bar{z}$	3.903	3.339	3.109	2.985	2.891
$T = 10.14 \times 10^4$	p_5^O	0.034	0.007	0.003	0.002	0.001
	p_4^O	0.134	0.090	0.065	0.051	0.042
	p_3^O	0.039	0.097	0.116	0.123	0.125
	p_2^O	0.002	0.016	0.025	0.033	0.040
	p_1^O	0.00005	0.000	0.001	0.001	0.001
	p_6^N	0.002	0.0002			
	p_5^N	0.149	0.036	0.018	0.012	0.009
	p_4^N	0.518	0.432	0.337	0.302	0.265
	p_3^N	0.119	0.302	0.393_5	0.419	0.442

Table 7.5 (Continued)

	ρ/ρ_0 =	0.367	1.831	3.66	5.44	7.33
	p_2^N	0.002	0.019	0.040	0.055	0.072
	p_1^N		0.000_5	0.002	0.002	0.003
	$\bar{z}$	3.02	2.572	2.372	2.287	2.208
$T = 7.1 \times 10^4$	p_4^O	0.029	0.007	0.004	0.003	0.002
	p_3^O	0.153	0.133	0.112	0.101	0.092
	p_2^O	0.027	0.067_5	0.090	0.100_5	0.110
	p_1^O	0.000_5	0.002_5	0.004	0.006	0.006
	p_5^N	0.002	0.00002	0.0001		
	p_4^N	0.257	0.085	0.049	0.035	0.027
	p_3^N	0.487	0.533	0.480	0.438	0.403
	p_2^N	0.043	0.164	0.246	0.297	0.336_5
	p_1^N	0.001	0.008	0.015	0.020	0.023_5
	$\bar{z}$	2.218	1.841	1.678	1.588	1.523
$T = 5 \times 10^4$	p_3^O	0.092_5	0.040	0.026	0.020_5	0.017
	p_2^O	0.113	0.158	0.165	0.166_5	0.167_5
	p_1^O	0.004	0.012	0.019	0.023	0.026
	p_4^N	0.007	0.001	0.000_5		
	p_3^N	0.435	0.209	0.141	0.112	0.092_5
	p_2^N	0.336	0.536_5	0.580_5	0.593	0.602

Table 7.5 (Continued)

	ρ/ρ_0 =	0.367	1.831	3.66	5.44	7.33
	p_1^N	0.012	0.043_5	0.068	0.085	0.095
	$\bar{z}$	1.527	1.195	1.081	1.026	0.989
$T = 3 \times 10^4$	p_3^O	0.001	0.0002	0.0001	0.0001	0.0_47
	p_2^O	0.177	0.134	0.112	0.101_5	0.091_5
	p_1^O	0.032_5	0.076	0.098	0.108	0.118
$T = 3 \times 10^4$	p_3^N	0.008	0.002	0.001	0.001	0.001
	p_2^N	0.679	0.542	0.465	0.428	0.391_5
	p_1^N	0.102	0.246	0.323	0.361	0.397_5
	$\bar{z}$	0.874	0.681	0.580	0.532	0.485
$T = 2 \times 10^4$	p_2^O	0.067	0.033	0.024	0.022	0.018
	p_1^O	0.143	0.177	0.186	0.188	0.192
	p_2^N	0.334	0.179_5	0.135	0.120_5	0.101
	p_1^N	0.456	0.610_5	0.655	0.669_5	0.689
	$\bar{z}$	0.401	0.213	0.159	0.142	0.119

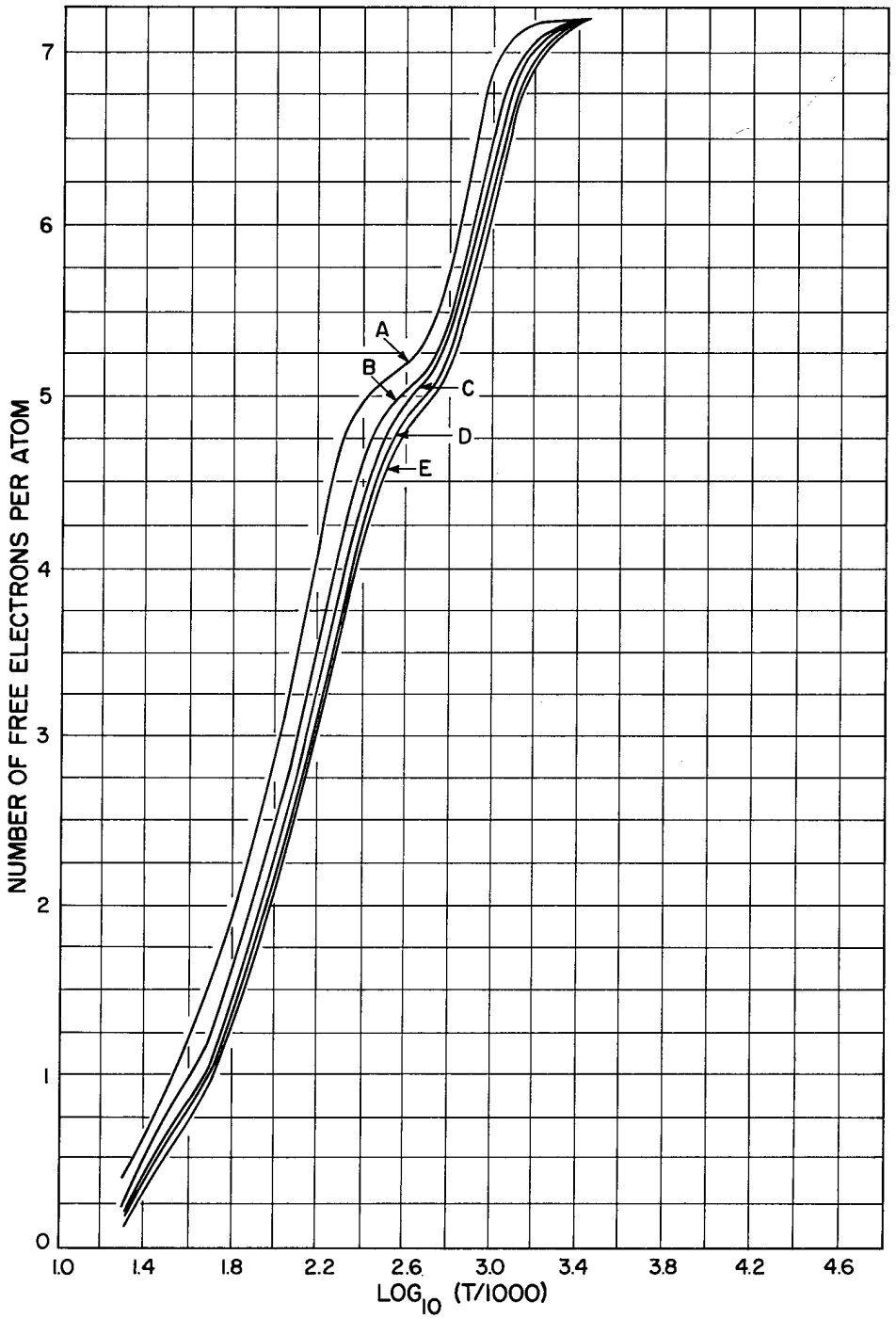

Fig. 7.1 Degree of Ionization: (A) $\rho/\rho_0 = 0.367$; (B) $\rho/\rho_0 = 1.831$; (C) $\rho/\rho_0 = 3.66$; (D) $\rho/\rho_0 = 5.44$; (E) $\rho/\rho_0 = 7.33$

Here all quantities refer to one gram atom.

The pressure has been obtained by graphical differentiation. However, in order to obtain the energy, graphical differentiation was not accurate enough.

In differentiating the free energy (Eq. 7.27) with respect to T, the p and $\bar{z}$ may be assumed to be constant, since the free energy is a minimum for a variation of these parameters. Hence Eq. 7.33 yields

$$\frac{E_i}{RT} = \sum_z \left(p_z^O \frac{\partial \ln f_z^O}{\partial \ln T} + p_z^N \frac{\partial \ln f_z^N}{\partial \ln T} + \bar{z} \frac{\partial \ln G}{\partial \ln T} \right) \tag{7.35}$$

Now from Eq. 7.10

$$G = \sum_z (p_z^O + p_z^N)\, g(z - 1, \bar{z}), \tag{7.36}$$

and from Eqs. 7.17 and 7.20 g is equal to $T^{3/2}$ multiplied by a function depending only on $(z - 1)/T$ and $\bar{z}/T$. Hence

$$\frac{\partial g(z - 1, \bar{z})}{\partial \ln T} = \frac{3}{2} g - \bar{z} \frac{\partial g}{\partial z} - (z - 1) \frac{\partial g}{\partial z}$$

$$\frac{\partial \ln G}{\partial \ln T} = \frac{3}{2} - \bar{z} \frac{H}{G} - \frac{1}{G} \sum_z (p_z^O + p_z^N)\,(z - 1) \frac{\partial\, g(z - 1, \bar{z})}{\partial z} \tag{7.37}$$

The terms containing $\partial g/\partial z$ were in general small, and since g had been obtained for various values of z, $\partial g/\partial z$ could easily be obtained by numerical differentiation.

Further from Eq. 7.26, observing that F_z is given as a function of the parameter l_z (defined by Eq. 7.8),

$$\frac{\partial \ln f_z}{\partial \ln T} = K_z - l_z \frac{\partial \ln F_z}{\partial l_z} \tag{7.38}$$

The differential can be obtained by graphical differentiation. Hence

$$\frac{E_i}{RT} = \frac{3}{2}\bar{z} - \bar{z}^2\frac{H}{G} - \frac{\bar{z}}{G}\cdot\sum_z\left(p_z^O + p_z^N\right)(z-1)\ \frac{\partial g(z-1,\ \bar{z})}{\partial z}$$

$$+\sum_z p_z^O\left(K_z^O - l_z\frac{\partial \ln F_z^O}{\partial l_z}\right) + \sum_z p_z^N\left(K_z^N - l_z\frac{\partial \ln F_z^N}{\partial l_z}\right)$$

To the internal thermodynamic functions those due to the motion of the ions have to be added. One has

$$\frac{pV}{RT} = \frac{p_i V}{RT} + 1$$

$$\frac{E}{RT} = \frac{E_i}{RT} + \frac{3}{2} + \frac{40,030}{T}$$

$$\frac{S}{R} = \frac{S_i}{R} + \frac{3}{2}\ln T + \ln V + \text{const} \qquad (7.39)$$

Here the last term in E in the middle equation of 7.39 arises from the dissociation energy of the molecules.

At the highest temperatures (above 2.5×10^6), when the ionization is complete but the ionization energy is still comparable with the thermal energy, one finds

$$\frac{pV}{RT} = 8.21$$

$$\frac{E}{RT} = \frac{3}{2}\,8.21 - \frac{1.792 \times 10^7}{T} \qquad T > 2.5 \times 10^6$$

$$\frac{S}{R} = 8.21\left(\frac{3}{2}\ln T + \ln V\right) + \text{const} \qquad (7.40)$$

pV/RT, E/RT, and S/R are given in Table 7.6. The entropy S/R is not normalized.

The curves of constant entropy (adiabatics) are easily obtained by graphical methods. The result is given in Table 7.7, containing the values of p for the five different densities and for various values of the entropy.

Table 7.6

PRESSURE, ENERGY, AND ENTROPY

ρ/ρ_0 / T	Pressure, pV/RT					Energy, E/RT					Entropy, S/R				
	0.367	1.831	3.66	5.44	7.33	0.367	1.831	3.66	5.44	7.33	0.367	1.831	3.66	5.44	7.33
2.526×10^6	8.2	8.1	8.1	8.1	8.1	19.4	19.39	19.38	19.37	19.36	117.16	104.03	98.41	95.17	92.74
1.263×10^6	8.1	7.9	7.8	7.8	7.8	25.96	24.92	24.17		22.93	108.60	94.66	88.46		81.80
9.6875×10^5	7.9	7.6	7.3	7.0	6.8	27.77	24.64	22.93	21.92	20.99	103.24	87.74	80.86	77.00	74.03
7.125×10^5	7.2	6.8	6.6	6.4	6.4	24.40	20.82	19.44	18.51	17.83	91.68	76.93	70.89	67.41	64.78
4.925×10^5	6.6	6.2	5.9	5.8	5.8	18.97	16.62	16.02	15.71	15.38	78.21	65.85	61.08	58.46	56.39
3.283×10^5	6.3	5.8	5.6	5.5	5.4	19.44	18.58	18.03	17.54	17.25	71.82	60.43	55.94	53.24	51.35
2.4625×10^5	6.0	5.4	5.2	5.1	5.0	22.18	20.12	19.01	18.24	17.62	67.96	56.80	52.01	49.19	47.07
1.8×10^5	5.1	4.8	4.5	4.4	4.4	23.91	20.06	18.30	17.26	16.80	62.45	50.41	45.42	42.64	40.87
1.4×10^5	4.6	4.2	4.0	3.8	3.7	22.56	18.33	16.64	15.49	15.04	55.24	43.83	39.35	36.87	35.10
10.143×10^4	3.8	3.5	3.2	3.2	3.1	18.92	15.75	14.13	13.45	12.83	44.85	35.82	31.94	29.95	28.43
7.1×10^4	2.9	2.7	2.5	2.5	2.5	15.50	12.50	11.25	10.58	10.17	35.10	27.55	24.47	22.82	21.68
5×10^4	2.4	2.1	2.0	2.0	2.0	12.25	9.65	8.80	8.41	8.13	27.13	20.87	18.59	17.38	16.55
3×10^4	1.9	1.6	1.5	1.5	1.5	9.48	8.11	7.40	7.00	6.68	19.16	14.96	13.15	12.13	11.38
2×10^4	1.3	1.2	1.1	1.1	1.1	8.01	6.25	5.75	5.59	5.37	13.98	10.16	8.85	8.24	7.68

Table 7.7

THE ADIABATICS
(pressure in 10^3 atm)

S/R \ ρ/ρ_0	0.367	1.831	3.66	5.44	7.33
15	0.078	0.62	1.58	2.8	4.0
20	0.17	1.2	3.0	5.3	7.9
25	0.27	1.9	4.9	8.2	12.3
30	0.38	3.0	7.2	12.5	18
35	0.53	4.3	10.4	17.7	26
40	0.75	6.0	15.1	26	38
45	1.00	8.1	20.4	36	54
50	1.29	10.9	28.5	51	81
53	1.5	12.9	36	68	106
55	1.6	14.9	43	80	130
58	1.9	18.9	58	103	168
60	2.1	24	68	121	188
62	2.3	28.5	80	134	207
65	2.9	37	93	158	236
67	3.5	42	102	172	256
70	4.7	47	117	195	286
75	7.3	58	142	238	355
80	9.0	70	174	299	471
90	12.6	104	278	516	833

7.1.6 The Hugoniot Curve

The Hugoniot conditions, which are to be satisfied for a shock-wave, are:

$$u = U(1 - \rho_0/\rho)$$

$$p - p_0 = \rho_0 u U$$

$$\epsilon - \epsilon_0 = \frac{1}{2}(p + p_0)\left(\frac{1}{\rho_0} - \frac{1}{\rho}\right) \tag{7.41}$$

Here U is the shock velocity, u the material velocity behind the shock, and ϵ the internal energy per unit mass; p, p_0 and ρ, ρ_0 are pressure and density behind the shock and in front of the shock, respectively. ϵ is related to the energy E used in the preceding sections by the relation

$$E = \epsilon \rho V \tag{7.42}$$

In the region in which we are interested ϵ_0 and p_0 will be negligible compared to ϵ and p. Combining the third equation of 7.41 with 7.42 we find

$$\frac{2E}{pV} = \frac{\rho}{\rho_0} - 1 \tag{7.43}$$

This equation determines the Hugoniot curve. In particular for high temperatures above 2.5×10^6 it follows from Eq. 7.41 that

$$\frac{\rho}{\rho_0} = 4 + \frac{4.367}{T} 10^6$$

$$pV = 8.21\ RT \tag{7.44}$$

The Hugoniot curve is tabulated in Table 7.8, assuming for ρ_0 the density of air at 1 atm and a temperature of 285°K. It is also shown in Fig. 2. The curve has two maximum values of ρ/ρ_0 corresponding to the ionization of the K-shell and L-shell. The increase in ρ/ρ_0 at the lowest pressures is due to the dissociation energy. It has an effect similar to that arising from the ionization energy at the highest temperatures, which is clearly evident from Eq. 7.44.

Table 7.8

THE SHOCK WAVE CURVE

ρ/ρ_0	p/p_0	T
4.22	4.86×10^6	2×10^7
4.44	2.56×10^6	10×10^6
4.54_5	2.09×10^6	8×10^6
4.73	$1.63_5 \times 10^6$	6×10^6
4.87	$1.40_3 \times 10^6$	5×10^6
4.97	$1.28_8 \times 10^6$	4.5×10^6
5.09	$1.17_3 \times 10^6$	4×10^6
5.25	$1.05_8 \times 10^6$	3.5×10^6
5.46	9.44×10^5	3×10^6
5.8	8.3×10^5	2.526×10^6
6.8	4.7×10^5	1.263×10^6
7.2	3.4×10^5	9.6875×10^5
6.7	2.1×10^5	7.125×10^5
6.4	$1.2_8 \times 10^5$	4.925×10^5
7.4	9.2×10^4	3.283×10^5
8.0	6.9×10^4	2.4625×10^5
8.5	4.7×10^4	1.8×10^5
9.1	3.2×10^4	1.4×10^4
9.2	2.0×10^4	10.143×10^4
9.0	1.12×10^4	7.1×10^4
9.0	6.3×10^3	5×10^4
9.5	3.0×10^3	3×10^4
10.2	1.6×10^3	2×10^4

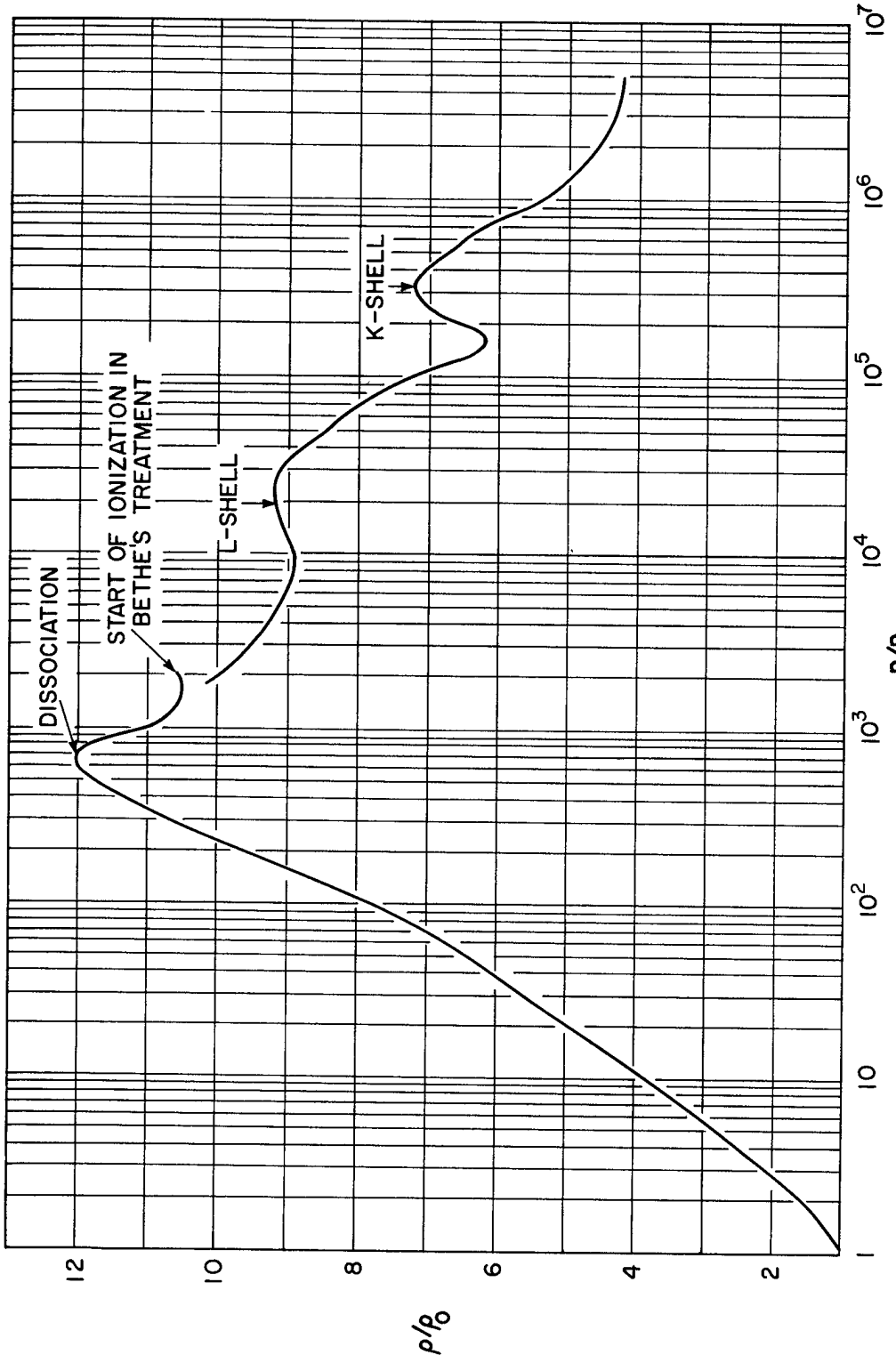

Fig. 7.2 Hugoniot curve; density vs pressure

The part of the curve in Fig. 7.2 below 10^3 atm will be discussed in the next section.

Fig. 7.3 shows the temperature as a function of the shock pressure.

7.2 The Equation of State of Air Below 25,000°K

Air shocks with a shock pressure up to about 1 kilobar and temperatures of the order of 10,000° are produced by ordinary high explosives. For this reason the equation of state of air up to temperatures of this order has been calculated by Bethe from 5000° to 25,000°,[1] and by Bethe and Teller from 300° to 5000°.[2] The Hugoniot curve and the adiabatics have been calculated by Brinkley, Kirkwood and Richardson.[3]

7.2.1 The Range from 12,000 to 25,000°K

The highest temperatures included in the report of Bethe are in the range in which dissociation of the nitrogen and oxygen molecules is completed and the ionization of the atoms is beginning to be important. Conditions in this region are therefore directly comparable with those treated in Section 7.1, and the temperatures in Section 7.1 were chosen in such a way that there is some overlapping with Bethe's calculations.

Bethe's treatment differs from that outlined in Section 7.1. He uses simpler approximations which make the computation less formidable, but this advantage is necessarily gained at the expense of some loss in accuracy.

An electron is assumed to be free if it has positive energy. The energy of a free electron is assumed to be kinetic and its potential energy is neglected. This leads to an underestimate of the pressure of the free electrons.

A bound electron is one of negative energy; only those electrons are counted whose classical orbit has a radius less than half the mean distance between atoms. States of bound electrons with larger orbits are neglected.

---

1. H. A. Bethe, The Specific Heat of Air up to 25,000°C, OSRD-369 (NDRC B-171), February 9, 1942.
2. Hans A. Bethe and Edward Teller, Deviations from Thermal Equilibrium in Shock Waves, Report AM-562, no date.
3. S. R. Brinkley, John Kirkwood, and J. M. Richardson, Tables of the Properties of Air Along the Hugoniot Curve and the Adiabatics Terminating in the Hugoniot Curve, Report OSRD-3550 (NDRC B-3550), April 27, 1944.

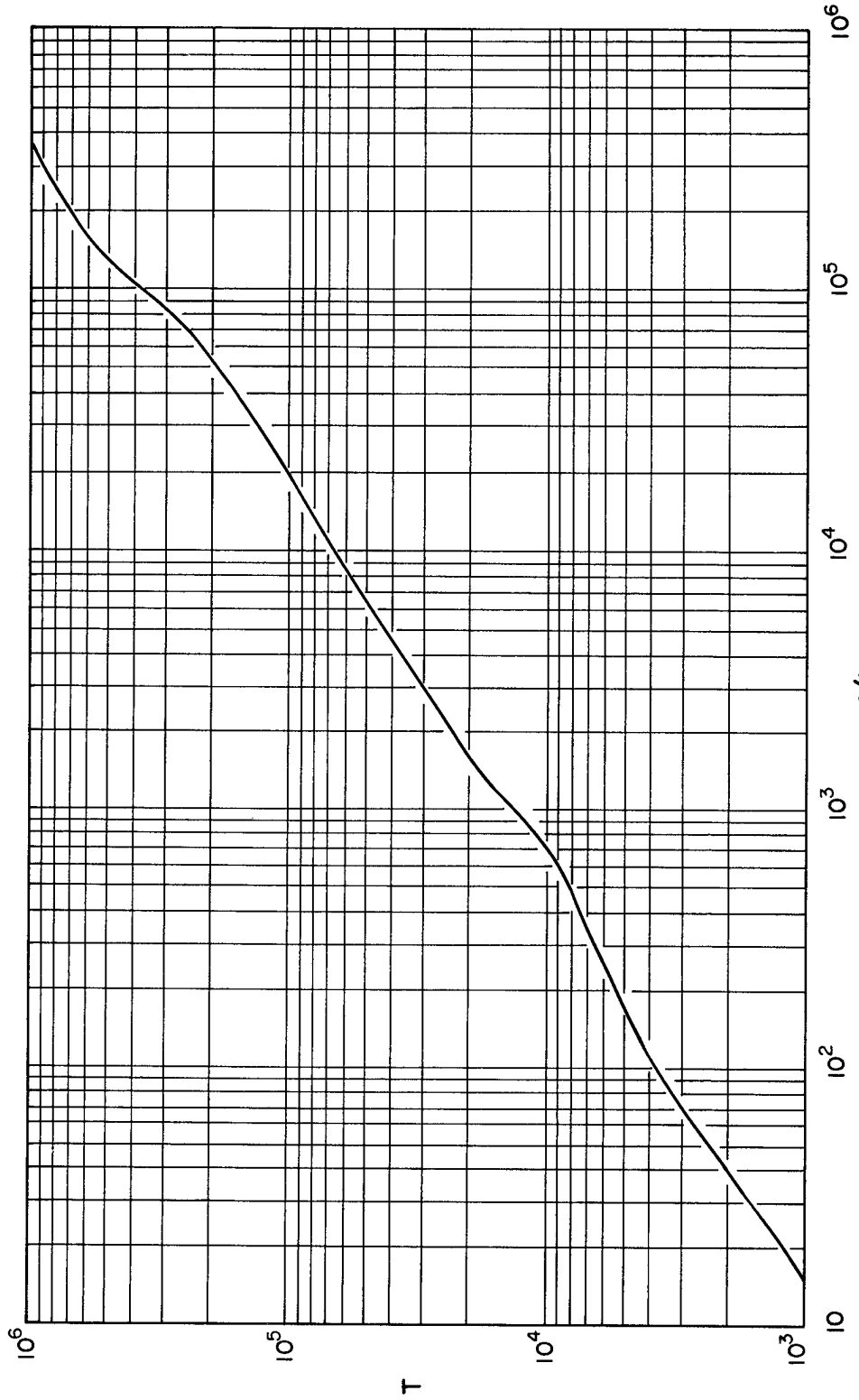

Fig. 7.3 Hugoniot curve; temperature as a function of shock pressure

Nevertheless, the partition function of the bound electrons is probably overestimated, since the highest permitted states of neighboring atoms overlap appreciably.

The (negative) pressure of the bound electrons has been neglected. This is probably a fairly small contribution and therefore the total pressure will be underestimated.

This conclusion is borne out by the Hugoniot curve shown in Fig. 7.2. The effect of the ionization of the L-shell starts at a shock pressure slightly above 1 kilobar, whereas in the calculations of Section 7.1 it started somewhat below 10 kilobars.

This discrepancy is rather disappointing, since it shows that the results are sensitive to the assumptions made. Although the calculations of Section 7.1 should be expected to be more accurate, it is difficult to assign any definite magnitude of error to either calculation.

7.2.2 The Range from 300 to 12,000°K

Below 12,000° ionization of the atoms is unimportant. The following effects have to be considered.

(1) The kinetic energy of translation $3p/2\rho$.

(2) The energy of molecular rotation, which is zero, RT or 3RT/2, depending on the molecular structure.

(3) The energy of vibration, depending on the frequencies of the normal modes which are obtained from band spectra. It becomes important at about 600°K.

(4) The energy of electronic excitation of the molecules, which can be obtained from the spectra but is usually not very important compared to either vibrations or dissociation.

(5) The dissociation of the molecules, which becomes important at about 3000°K.

(6) The electronic excitation of the atoms, which of course is important only if dissociation occurs.

In addition Bethe, and Bethe and Teller included terms arising from the anharmonicity of the vibrations, from the interaction between oscillation and rotation, and second order rotation effect; all these are important only at high temperatures, provided there are still undissociated molecules.

The Hugoniot curve obtained from these calculations is included in Fig. 7.2. The shock velocity and temperature are shown in Fig. 7.3.

7.3 The Equation of State of Air at Low Pressures

7.3.1 Introduction

The equation of state calculated in Section 7.1 for high temperatures has been extended only to a lowest density of 0.367. However, we require the equation of state at much lower densities, at least in this high temperature range, since the air which has been shocked by very strong shocks expands considerably when it returns to normal pressure.

In the region of low density considerable simplification can be introduced; this is not quite justified at a density of 0.367 but the intermediate region may be covered by interpolation.

The low density approximation presented in the following was proposed by Christy and developed by Hirschfelder and Magee. It is essentially based on the fact that at low densities the various particles (electrons, ions, molecules) are on the average so far apart from each other that their partition functions become independent of the density and concentrations of the various constituent particles. In that case the equations for chemical equilibrium are much simpler. Furthermore, the assembly behaves like a perfect gas as far as composition and pressure are concerned.

If the density is very low, a further simplification can be introduced. Then the volume at the disposal of the free electrons has such a large statistical weight that eventually it outweighs the Boltzmann factor and ionization will occur before there is any chance of exciting the higher electronic states. Then the partition function of the ions is simply given by the statistical weight of the ground state, and the assembly is a perfect gas for all purposes.

Similarly, dissociation of the molecules will eventually occur before the vibrations can be excited. However, for this purpose the density has to be very low indeed. In the region in which we shall be interested this simplification is not valid.

It will be more convenient in the following calculation to refer all quantities to a mole rather than to a gram atom.

7.3.2 The Composition of Air

In the conditions of a perfect gas the equilibrium of a composite system AB with its two components A and B is determined by the following equation

$$\frac{N_A N_B}{N_{AB}} = \left(\frac{2\pi mRT}{h^2} \right)^{3/2} V e^{-Q/RT} \frac{F(A)\, F(B)}{F(AB)} \tag{7.45}$$

Here the F's are the partition functions (assumed to be independent of the density and concentration). Q is the energy of dissociation of the system AB into the components A and B, R is Boltzmann's constant (1.379×10^{-16}), and h is Planck's constant (6.620×10^{-27}). m is the reduced mass

$$m = \frac{m_A m_B}{m_A + m_B} \tag{7.46}$$

and N_A, N_B, N_{AB} are the respective number of particles in volume V.

We choose for V the mole volume and define the occupation numbers such that $N_A = N_{p_A}$ etc., where N is Avogadro's number (6.027×10^{23}); for example, p_z^O will be the number of $(z - 1)$ times ionized oxygen ions for each molecule (oxygen and nitrogen) which was originally present. These are therefore twice the occupation numbers of Section 7.1.

Then Eq. 7.45 is conveniently written in the form

$$\frac{p_A p_B}{p_{AB}} = K_{AB} \frac{V}{V_0} = K_{AB} \frac{\rho_0}{\rho} \tag{7.47}$$

$$K_{AB} = \Lambda M^{3/2} T^{3/2} e^{-Q/RT} \frac{F(A)F(B)}{F(AB)} \tag{7.48}$$

$$\Lambda = \frac{V_0}{N} \left(\frac{2\pi R}{Nh^2} \right)^{3/2} \tag{7.49}$$

Here we have introduced the atomic weights $M = Nm$, and V_0 is a standard volume, which we shall choose as the mole volume of a perfect gas at a pressure of 1 atm and a temperature of 300°K. Then N/V_0 is the number of molecules per cubic centimeter in standard condition

$$\frac{N}{V_0} = 2.44_5 \times 10^{19}$$

and

$$\Lambda = 7.68 \text{ cgs units} \tag{7.50}$$

ρ_0 is then the normal density of air.

For the equilibrium between ions and electrons, Eq. 7.47 yields

$$\frac{\bar{z}\, p^{O}_{z+1}}{p^{O}_{z}} = K^{O}_{z} \frac{\rho_0}{\rho} \; ; \quad \frac{\bar{z}\, p^{N}_{z+1}}{p^{N}_{z}} = K^{N}_{z} \frac{\rho_0}{\rho} \tag{7.51}$$

where $\bar{z}$ is the average number of free electrons per molecule and

$$K^{O}_{z} = 1.973 \times 10^{-4}\, T^{3/2} \exp\left(\frac{-I^{O}_{z}}{RT}\right) \frac{F^{O}_{z+1}}{F^{O}_{z}}$$

$$K^{N}_{z} = 1.973 \times 10^{-4}\, T^{3/2} \exp\left(\frac{-I^{N}_{z}}{RT}\right) \frac{F^{N}_{z+1}}{F^{N}_{z}} \tag{7.52}$$

Here the reduced mass has been replaced in sufficient approximation by the atomic weight of the electron (1/1823) and the statistical weight of the electron is taken as 2. I_z is the z-th ionization potential and the F_z are the partition functions of the ions.

The formula (Eq. 7.51) could also have been obtained from Eq. 7.29 by going to the limit of large volumes (i.e., $a \to \infty$, $\alpha \to 0$). In this limit the partition function of the electrons as defined in Section 7.1 becomes independent of z and $\bar{z}$.

$$\lim_{\alpha \to 0} g(z, \bar{z}) = \lim_{\alpha \to 0} g(\bar{z}) = 2\left(2\pi\, mk \frac{T}{h^2}\right)^{3/2} 4\pi \frac{a^3}{3}$$

where a was the radius of the average volume per atom. It is now easily verified that the expressions, Eq. 7.29, reduce essentially to Eq. 7.45.

The condition of applicability of Eq. 7.51 can therefore be stated in the form that the quantity α used in Section 7.1 (see Eq. 7.16) should be sufficiently small for those ions which are present in appreciable numbers. This condition may be written in the form

$$\frac{\bar{z}e^2}{aRT} \ll 1, \text{ or} \left(\frac{p}{\rho_0}\right)^{1/3} \ll \frac{RT}{\bar{z}e^2}\left(\frac{3}{4\pi} \frac{V_0}{N}\right)^{1/3} = 1.63 \times 10^{-4}\, T/\bar{z} \tag{7.53}$$

It should be noticed that $\bar{z}$ increases less rapidly than T. Hence the approximation extends to much higher densities if the temperature is high. This is due to the fact that with increasing temperature the kinetic energy of the free electrons increases and the potential energy, which was neglected, becomes relatively less important.

Unfortunately the primary calculations of the partition functions of the ions F_z^O, F_z^N reported in Section 7.1 were not available at the time, and it was therefore decided to use the further simplification of neglecting electronic excitation and replacing the partition functions of the ions by the weights of the ground states. This simplification further reduces the range of densities in which Eq. 7.51 applies. The weights and ionization potentials have been tabled in Section 7.1.

The equilibrium between atoms and molecules is determined by

$$\frac{(p_1^O)^2}{p_{O_2}} = K_{O_2} \frac{\rho_0}{\rho}; \quad K_{O_2} = 7.68 \times 8^{3/2} T^{3/2} e^{-59,390/T} \frac{\left(F_1^O\right)^2}{F_{O_2}}$$

$$\frac{(p_1^N)^2}{p_{N_2}} = K_{N_2} \frac{\rho_0}{\rho}; \quad K_{N_2} = 7.68 \times 7^{3/2} T^{3/2} e^{-85,560/T} \frac{\left(F_1^N\right)^2}{F_{N_2}} \qquad (7.54)$$

For the partition functions in Eq. 7.54 the values of Bethe have been used. It should be noted that, in the approximation used, the partition functions of the ions and electrons become volume dependent only because of "pressure ionization," i.e., the omission of highly excited states by the "cut-off" requirement. For ions this usually means that the partition functions do not differ very much from the statistical weight of the ground state, since the excitation energy of the first excited state is usually of the same order as that of other excited states. For the molecules on the other hand there is an appreciable range of temperatures in which the partition function is temperature dependent because of the excitation of vibrations and rotations, but independent of the volume. Hence the validity of the formulae (Eq. 7.54) would be much more restricted if we used the statistical weight of the ground state. In fact because of rotations of the molecules, it could be used only at extremely low temperatures.

The partition functions of Bethe are given in Table 7.9.

Table 7.9

PARTITION FUNCTIONS OF MOLECULES AND ATOMS

Temperature, °K	F_{N_2}	F_1^N	F_{O_2}	F_1^O
5,000	1,841	4.042	11,478	9.053
5,500	2,176	4.069	13,994	9.081
6,000	2,539	4.106	16,817	9.114
6,500	2,934	4.153	20,015	9.153
7,000	3,362	4.210	23,534	9.196
7,500	3,818	4.276	27,380	9.244
8,000	4,314	4.351	31,770	9.295
9,000	5,383	4.525	41,750	9.406
10,000	6,550	4.728	54,780	9.524

The occupation numbers satisfy the conservation law

$$\frac{1}{2}\sum_z p_z^O + p_{O_2} = 0.21$$

$$\frac{1}{2}\sum_z p_z^N + p_{N_2} = 0.79$$

$$\bar{z} = \sum_z (z-1)(p_z^O + p_z^N) \qquad (7.55)$$

These equations together with 7.51 and 7.54 constitute a complete set of equations for the determination of the occupation numbers. They are solved by introducing the quantity

$$W = \frac{\rho_0}{\rho_{\bar{z}}} \qquad (7.56)$$

From Eq. 7.51 follows

$$p_2^O = K_1^O W p_1^O ; \quad p_2^N = K_1^N W p_1^N$$

$$p_3^O = K_2^O K_1^O W^2 p_1^O ; \quad p_3^N = K_2^N K_1^N W^2 p_1^N \tag{7.57}$$

and so on; and from Eq. 7.54

$$p_{O_2} = (p_1^O)^2 \frac{\rho}{\rho_0} K_{O_2} ; \quad p_{N_2} = (p_1^N)^2 \frac{\rho}{\rho_0} K_{N_2} \tag{7.58}$$

Substitution into Eq. 7.55 yields

$$A_1 p_1^O + \frac{\rho}{\rho_0 K_{O_2}} (p_1^O)^2 = 0.21$$

$$A_2 p_1^N + \frac{\rho}{\rho_0 K_{N_2}} (p_1^N)^2 = 0.79$$

$$A_3 p_1^O + A_4 p_1^N = \frac{\rho_0}{\rho W} \tag{7.59}$$

where the A's depend only on W and are given by the following:

$$A_1 = \frac{1}{2}\left\{1 + K_1^O W + K_1^O K_2^O W^2 + \ldots + K_1^O K_2^O K_3^O K_4^O K_5^O K_6^O K_7^O K_8^O W^8\right\}$$

$$A_2 = \frac{1}{2}\left\{1 + K_1^N W + K_1^N K_2^N W^2 + \ldots + K_1^N K_2^N K_3^N K_4^N K_5^N K_6^N K_7^N W^7\right\}$$

$$A_3 = K_1^O W + 2K_1^O K_2^O W^2 + \ldots + 8K_1^O K_2^O \ldots K_8^O W^8$$

$$A_4 = K_1^N W + 2K_1^N K_2^N W^2 + \ldots + 7K_1^N K_2^N \ldots K_7^N W^7 \tag{7.60}$$

We consider the equations of 7.59 as three simultaneous equations for the quantities p_1^O, p_1^N and ρ/ρ_0 for given value of W. The first two combined yield

$$0.79\left[A_1\left(\frac{\rho p_1^O}{\rho_0}\right)+\frac{1}{K_{O_2}}\left(\frac{\rho p_1^O}{\rho_0}\right)^2\right]$$

$$=0.21\left[A_2\left(\frac{\rho p_1^N}{\rho_0}\right)+\frac{1}{K_{N_2}}\left(\frac{\rho p_1^N}{\rho_0}\right)^2\right] \qquad (7.61)$$

Eliminating $\rho p_1^N/\rho_0$ in terms of $\rho p_1^O/\rho_0$ by means of the third equation of 7.59, one finds the quadratic equation for $\rho p_1^O/\rho_0$

$$\left(\frac{\rho p_1^O}{\rho_0}\right)^2\left(\frac{1}{K_{O_2}}-\frac{0.21\,A_3^2}{0.79\,A_4^2}\frac{1}{K_{N_2}}\right)+\left(\frac{\rho p_1^N}{\rho_0}\right)\left(A_1+\frac{0.21}{0.79}\frac{A_2A_3}{A_4}\right.$$

$$\left.+\frac{0.21}{0.79}\frac{A_3}{A_4^2}W\frac{2}{K_{N_2}}\right)=\frac{0.21}{0.79}\left(\frac{1}{K_{N_2}W^2A_4^2}+\frac{A_2}{WA_4}\right) \qquad (7.62)$$

The remaining quantities are determined by

$$\frac{\rho p_1^N}{\rho_0}=\frac{1}{A_4}\left[\frac{1}{W}-A_3\left(\frac{\rho p_1^O}{\rho_0}\right)\right] \qquad (7.63)$$

$$\frac{\rho}{\rho_0}=\frac{1}{0.21}\left[A_1\left(\frac{\rho p_1^O}{\rho_0}\right)+\frac{1}{K_{O_2}}\left(\frac{\rho p_1^O}{\rho_0}\right)^2\right] \qquad (7.64)$$

If there are no undissociated molecules present the quadratic terms drop out. Then

$$p_1^O=\frac{0.21}{A_1}\;;\quad p_1^N=\frac{0.79}{A_2} \qquad (7.65)$$

$$\frac{\rho_0}{\rho} = W\left(0.21\,\frac{A_3}{A_1} + 0.79\,\frac{A_4}{A_2}\right) \tag{7.66}$$

7.3.3 The Thermodynamical Quantities

Until now we have included the undissociated molecules into the calculation. The main purpose of this was to be able to decide whether the molecules could be neglected in the region in which we are interested. We shall see that this is the case. The reason for this is that the very low densities will be obtained only at fairly high temperatures (of the order of 10,000° or more).

For this reason we shall in the following neglect the molecules. There is in principle no difficulty in including the molecules, but the equations are no longer those for a perfect gas, since the partition function of the molecules is temperature dependent.

For a perfect gas the pressure depends only on the number of particles in a given volume and the temperature. If V is the mole volume, then[4]

$$\frac{pV}{RT} = \text{number of particles per molecule} = \alpha + 1 \tag{7.67}$$

where, with the help of Eq. 7.55,

$$\alpha = \bar{z} + 1 \tag{7.68}$$

In normal conditions air behaves again like a perfect gas and $\alpha = 0$; then

$$p_0 V_0 = RT_0 \tag{7.69}$$

and therefore

$$\frac{p}{p_0} = (\alpha + 1)\frac{T}{T_0}\,\frac{\rho}{\rho_0} \tag{7.70}$$

---

4. Since the partition function of the molecules may be assumed to be volume independent, this equation holds also if molecules are included; then $\alpha = \bar{z} + 1 - p_2^O - p_2^N$. The perfect gas equations break down, however, if we consider the energy and entropy.

The specific heat of the electrons and ions is 3R/2. In the energy we must in addition include the energy of dissociation and ionization. Then

$$\frac{E}{RT} = \frac{3}{2}(\bar{z} + 2) + \sum_z \left(\frac{p_z^O J_2^O + p_2^N J_z^N}{T} \right) \tag{7.71}$$

where $$J_1^O = 59,390 \; ; \quad J_{z+1}^O = J_z^O + \frac{I_z^O}{R}$$

$$J_1^N = 85,560 \; ; \quad J_{z+1}^N = J_z^N + \frac{I_z^N}{R} \tag{7.72}$$

The enthalpy, which is of interest for some calculations, is given by

$$H = E + pV \tag{7.73}$$

Finally we require the entropy. If there are n particles of type i with partition function f_i and mass m_i in a volume V, the entropy is

$$S = R \sum_i n_i \left\{ \frac{5}{2} + \frac{3}{2} \ln\left(\frac{2\pi m_i RT}{h^2} \right) + \ln\left(\frac{V}{n_i} \right) + \ln f_i + \frac{d \ln f_i}{d \ln T} \right\} \tag{7.74}$$

If f_i is of the form $f_i = g_i e^{-E_i/RT}$ then the last two terms give just ln g. For the electrons we have $f_{el} = g_{el} = 2$; and $n_{el} = N\bar{z}$. Hence,

$$\frac{S_{el}}{R} = \bar{z} \left\{ \frac{3}{2} \ln \frac{T}{T_0} + \ln \frac{\rho_0}{\rho} - \ln \bar{z} + A \right\} \tag{7.75}$$

$$A = \frac{5}{2} + \frac{3}{2} \ln\left(\frac{2\pi m_{el} RT_0}{h^2} \right) + \ln\left(\frac{V_0}{N} \right) + \ln 2 = 2.556 \tag{7.76}$$

for $T_0 = 300°$, $p_0 = 1$ atm. Similarly for the ions: $n_i = Np_z$. Observing that $\Sigma(p_z^O + p_z^N) = 2$, one finds

$$\frac{S_i}{R} = \sum_z \left[p_z^O \ln \left(\frac{g_z^O}{p_z^O} \right) + p_z^N \ln \left(\frac{g_z^N}{p_z^N} \right) \right] + 3 \ln \frac{T}{T_0} + 2 \ln \left(\frac{\rho_0}{\rho} \right) + B' \qquad (7.77)$$

$$B' = 5 + 2 \ln \left(\frac{V_0}{N} \right) + 3 \ln \left(\frac{2\pi m_p RT_0}{h^2} \right) + 3 (0.21 \ln 16 + 0.79 \ln 14) + 2 \ln \left(\frac{V_0}{N} \right) \qquad (7.78)$$

Here m_p is the proton mass.

For air at normal conditions we can again apply the perfect gas equations, since the rotations are fully excited and the vibrations are not excited. Then

$$f_i = g_{el} \frac{RT}{hB} \frac{1}{2} \qquad (7.79)$$

where g_{el} is the statistical weight of the electronic ground state (3 for O_2 and 1 for N_2) and B is the rotational constant (2.87 cm^{-1} for N_2 and 2.08 cm^{-1} for O_2). Then

$$\frac{S_0}{R} = \frac{7}{2} + \frac{3}{2} \ln \left(\frac{2\pi m_p RT_0}{h^2} \right) + \ln \frac{V_0}{N} + 0.21 \left[\frac{\ln f_{O_2}}{0.21} + \frac{3}{2} \ln 32 \right] + 0.79 \left[\frac{\ln f_{N_2}}{0.79} + \frac{3}{2} \ln 28 \right] \qquad (7.80)$$

Thus

$$S - \frac{S_0}{R} = \left(\frac{3}{2} \ln \frac{T}{T_0} + \ln \frac{\rho_0}{\rho} \right) (\bar{z} + 2) - \bar{z} \ln \bar{z} + \bar{z} A + \sum_z \left[p_z^O \ln \frac{g_z^O}{p_z^O} + p_z^N \ln \frac{g_z^N}{p_z^N} \right] + B \qquad (7.81)$$

$$B = B' - \frac{S_0}{R} = 10.68 \tag{7.82}$$

This entropy can be related to that used in Section 7.1, by observing that at very high temperatures, when ionization is complete,

$$\frac{S - S_0}{R} \rightarrow 16.42\left(\frac{3}{2} \ln \frac{T}{T_0} + \ln \frac{\rho_0}{\rho}\right) + 6.833 \tag{7.83}$$

Comparison with the data of Section 7.1 gives

$$\frac{S - S_0}{R} = 2\,\frac{S_1}{R} + 11.59 \tag{7.84}$$

where S_1 is the entropy of Section 7.1 and the factor 2 arises, because here we use 1 mole as standard amount.

Unfortunately, some errors were made in the calculation of the entropy. The formula used in numerical calculations contained an additional term $(\bar{z} + 2) \ln (\bar{z} + 2)$ and the values of the constants A and B were 1.750 and 24.638. These errors have not yet been corrected in all results for the entropy, and adiabatics given in the following tables are subject to correction at very low densities.

The data obtained are given in Table 7.10.

It will be noted that at the lowest temperature of 7000°, the number of N_2 molecules is no longer negligible, except for very low densities. At this temperature the approximation used breaks down.

Table 7.10

LOW-DENSITY EQUATION-OF-STATE DATA

T = 7,000°K

ρ/ρ_0	α	$1/2\,\bar{z}$	n=H/RT	E/RT	p	$\Delta s/R$	$1/2\,p_1^O$	$1/2\,p_2^O$	$1/2\,p_{O_2}$	$1/2\,p_3^O$	$1/2\,p_4^O$	$1/2\,p_5^O$	$1/2\,p_1^N$	$1/2\,p_2^N$	$1/2\,p_{N_2}$	$1/2\,p_3^N$	$1/2\,p_4^N$	$1/2\,p_5^N$
1.981×10^{-2}	9.7913×10^{-1}	4.5887×10^{-4}	16.183	14.204	9.149×10^{-1}	30.94	2.099×10^{-1}	9.522×10^{-5}	2.307×10^{-5}				7.679×10^{-1}	3.637×10^{-4}	1.087×10^{-2}			
2.398×10^{-2}	9.7852×10^{-1}	4.1695×10^{-4}	16.176	14.197	1.107	30.56	2.099×10^{-1}	8.657×10^{-5}	2.794×10^{-5}				7.674×10^{-1}	3.304×10^{-4}	1.113×10^{-2}			
2.995×10^{-2}	9.6737×10^{-1}	3.7099×10^{-4}	16.032	14.065	1.375	29.97	2.099×10^{-1}	7.791×10^{-5}	3.490×10^{-5}				7.564×10^{-1}	2.931×10^{-4}	1.665×10^{-2}			
3.816×10^{-2}	9.6082×10^{-1}	3.2756×10^{-4}	15.948	13.987	1.746	29.40	2.098×10^{-1}	6.925×10^{-5}	4.446×10^{-5}				7.500×10^{-1}	2.583×10^{-4}	1.988×10^{-2}			
1.035×10^{-1}	9.1800×10^{-1}	1.9325×10^{-4}	15.380	13.471	4.630	26.86	2.097×10^{-1}	4.325×10^{-5}	1.204×10^{-4}				6.968×10^{-1}	1.500×10^{-4}	4.152×10^{-2}			
3.295×10^{-1}	7.9222×10^{-1}	1.0115×10^{-4}	13.798	12.006	13.781	23.05	2.092×10^{-1}	2.589×10^{-5}	3.817×10^{-4}				5.827×10^{-1}	7.526×10^{-5}	1.036×10^{-1}			
5.111×10^{-1}	7.3606×10^{-1}	7.8257×10^{-5}	13.084	11.348	20.705	21.52	2.088×10^{-1}	2.153×10^{-5}	5.896×10^{-4}				5.270×10^{-1}	5.672×10^{-5}	1.315×10^{-1}			
8.913×10^{-1}	6.6225×10^{-1}	5.6101×10^{-5}	12.126	10.464	34.568	19.57	2.079×10^{-1}	1.716×10^{-5}	1.020×10^{-3}				4.523×10^{-1}	3.895×10^{-5}	1.688×10^{-1}			

T = 10,000°K

1.502×10^{-2}	1.0472	2.3782×10^{-2}	14.917	12.870	1.025	33.94	2.064×10^{-1}	3.556×10^{-3}					7.694×10^{-1}	2.023×10^{-2}	1.904×10^{-4}			
2.924×10^{-2}	1.0334	1.7099×10^{-2}	14.656	12.623	1.982	32.32	2.075×10^{-1}	2.553×10^{-3}	3.322×10^{-7}				7.747×10^{-1}	1.455×10^{-2}	3.832×10^{-4}			
5.180×10^{-2}	1.0243	1.2871×10^{-2}	14.488	12.464	3.495	30.99	2.081×10^{-1}	1.920×10^{-3}	5.916×10^{-6}				7.776×10^{-1}	1.095×10^{-2}	7.258×10^{-4}			
8.077×10^{-2}	1.0185	1.0317×10^{-2}	14.384	12.365	5.667	30.06	2.084×10^{-1}	1.539×10^{-3}	8.958×10^{-6}				7.791×10^{-1}	8.778×10^{-3}	1.048×10^{-3}			
1.162×10^{-1}	1.0141	8.6046×10^{-2}	14.309	12.295	7.803	29.18	2.087×10^{-1}	1.284×10^{-3}	1.346×10^{-5}				7.796×10^{-1}	7.320×10^{-4}	1.519×10^{-3}			
2.734×10^{-1}	1.0110	5.6268×10^{-3}	14.173	12.153	18.263	27.31	2.091×10^{-1}	8.363×10^{-3}	3.487×10^{-5}				7.851×10^{-1}	4.791×10^{-4}	2.529×10^{-3}			

T = 15,000°K

6.543×10^{-3}	2.0361	5.1804×10^{-1}	24.473	21.437	9.768×10^{-1}	52.31	1.231×10^{-1}	8.686×10^{-2}		1.663×10^{-8}			3.588×10^{-1}	4.312×10^{-1}		1.736×10^{-6}		
1.195×10^{-2}	1.8371	4.168×10^{-1}	21.763	18.926	1.694	47.68	1.428×10^{-1}	6.717×10^{-2}		8.573×10^{-9}			4.386×10^{-1}	3.514×10^{-1}		9.431×10^{-7}		
1.898×10^{-2}	1.7025	3.512×10^{-1}	19.928	17.226	2.565	44.51	1.552×10^{-1}	5.476×10^{-2}		5.241×10^{-9}			4.935×10^{-1}	2.965×10^{-1}		5.968×10^{-7}		
3.761×10^{-2}	1.5318	2.660×10^{-1}	17.600	15.068	4.760	40.32	1.700×10^{-1}	3.998×10^{-2}		2.551×10^{-9}			5.641×10^{-1}	2.259×10^{-1}		3.032×10^{-7}		
6.231×10^{-2}	1.4280	2.140×10^{-1}	16.183	13.754	7.564	37.62	1.785×10^{-1}	3.148×10^{-2}		1.507×10^{-9}			6.075×10^{-1}	1.825×10^{-1}		1.837×10^{-7}		
1.300×10^{-1}	1.3078	1.539×10^{-1}	14.541	12.234	14.996	34.21	1.879×10^{-1}	2.209×10^{-2}	2.153×10^{-6}	7.049×10^{-10}			6.581×10^{-1}	1.318×10^{-1}	5.706×10^{-5}	8.843×10^{-8}		
4.789×10^{-1}	1.1670	8.352×10^{-2}	12.618	10.450	51.880	29.33	1.983×10^{-1}	1.166×10^{-2}	9.523×10^{-6}	1.860×10^{-10}			7.176×10^{-1}	7.186×10^{-2}	2.529×10^{-4}	2.411×10^{-8}		

T = 20,000°K

4.224×10^{-3}	2.8940	9.470×10^{-1}	29.5539	25.659	1.097	65.10	1.744×10^{-2}	1.925×10^{-1}		4.173×10^{-5}			3.674×10^{-2}	7.521×10^{-1}		1.185×10^{-3}		
7.296×10^{-3}	2.8275	9.137×10^{-1}	28.8255	24.998	1.862	62.20	2.755×10^{-2}	1.824×10^{-1}		2.372×10^{-5}			5.943×10^{-2}	7.299×10^{-1}		6.898×10^{-4}		
1.142×10^{-2}	2.7515	8.758×10^{-1}	28.0015	24.250	2.856	59.61	3.878×10^{-2}	1.712×10^{-1}		1.484×10^{-6}			8.593×10^{-2}	7.036×10^{-1}		4.434×10^{-4}		
2.565×10^{-2}	2.5594	7.797×10^{-1}	25.9234	22.364	6.087	54.49	6.547×10^{-2}	1.445×10^{-1}		6.264×10^{-6}			1.551×10^{-1}	6.348×10^{-1}		2.000×10^{-4}		
6.240×10^{-2}	2.2820	6.410×10^{-1}	22.9220	19.640	13.655	48.12	9.982×10^{-2}	1.102×10^{-1}		2.388×10^{-6}			2.592×10^{-1}	5.307×10^{-1}		8.359×10^{-5}		
2.381×10^{-1}	1.8400	4.200×10^{-1}	19.5430	16.703	45.080	38.91	1.457×10^{-1}	6.432×10^{-2}		5.576×10^{-7}			4.344×10^{-1}	3.557×10^{-1}		2.241×10^{-5}		

T = 25,000°K

3.157×10^{-3}	3.118	1.0559	28.481	24.369	1.082	70.15	2.032×10^{-3}	2.036×10^{-1}		4.335×10^{-3}			5.563×10^{-3}	7.252×10^{-1}		5.918×10^{-2}	3.061×10^{-7}	
4.847×10^{-3}	3.0633	1.0316	27.742	23.679	1.641	67.62	3.054×10^{-3}	2.041×10^{-1}		2.896×10^{-3}			8.527×10^{-3}	7.412×10^{-1}		4.032×10^{-2}	1.390×10^{-7}	
1.001×10^{-2}	2.9971	9.9853×10^{-1}	26.828	22.831	3.336	63.73	6.062×10^{-3}	2.025×10^{-1}		1.437×10^{-3}			1.731×10^{-2}	7.523×10^{-1}		2.046×10^{-2}	3.528×10^{-8}	
2.073×10^{-2}	2.9294	9.6471×10^{-1}	26.048	22.119	6.789	60.09	1.182×10^{-2}	1.975×10^{-1}		7.007×10^{-4}			3.431×10^{-2}	7.456×10^{-1}		1.014×10^{-2}	8.740×10^{-9}	
4.364×10^{-2}	2.8333	9.1663×10^{-1}	25.087	21.254	13.940	56.03	2.242×10^{-2}	1.873×10^{-1}		3.322×10^{-4}			6.617×10^{-2}	7.189×10^{-1}		4.889×10^{-3}	2.107×10^{-9}	
1.241×10^{-1}	2.6121	8.0605×10^{-1}	23.014	19.402	37.344	49.81	4.835×10^{-2}	1.615×10^{-1}		1.146×10^{-4}			1.475×10^{-1}	6.408×10^{-1}		1.743×10^{-3}	3.005×10^{-10}	
2.970×10^{-1}	2.3468	6.7341×10^{-1}	20.569	17.222	82.833	44.02	7.863×10^{-2}	1.313×10^{-1}		4.660×10^{-5}			2.487×10^{-1}	5.405×10^{-1}		7.351×10^{-4}	6.337×10^{-11}	

T = 30,000°K

2.270×10^{-3}	3.9354	1.4577	37.093	32.158	1.121	85.17	4.366×10^{-4}	1.474×10^{-1}		6.216×10^{-2}	3.763×10^{-6}		3.225×10^{-4}	3.835×10^{-1}		4.061×10^{-1}	1.081×10^{-4}	
3.650×10^{-3}	3.7428	1.3714	34.345	29.602	1.730	79.97	7.257×10^{-4}	1.633×10^{-1}		4.593×10^{-2}	1.851×10^{-6}		5.838×10^{-4}	4.627×10^{-1}		3.266×10^{-1}	5.795×10^{-5}	
8.140×10^{-3}	3.4566	1.2283	30.293	25.836	3.628	71.99	1.624×10^{-3}	1.828×10^{-1}		2.570×10^{-2}	5.197×10^{-7}		1.471×10^{-3}	5.828×10^{-1}		2.057×10^{-1}	1.825×10^{-5}	
1.778×10^{-3}	3.2496	1.1248	27.399	23.149	7.556	65.55	3.430×10^{-3}	1.930×10^{-1}		7.358×10^{-3}	7.372×10^{-8}		3.374×10^{-3}	6.686×10^{-1}		1.180×10^{-1}	5.230×10^{-6}	
3.296×10^{-2}	3.1362	1.0681	25.833	21.697	13.633	61.35	6.131×10^{-3}	1.960×10^{-1}		7.830×10^{-3}	6.131×10^{-9}		6.326×10^{-3}	7.122×10^{-1}		7.143×10^{-2}	1.771×10^{-6}	
1.004×10^{-1}	2.9868	9.934×10^{-1}	24.037	20.050	40.012	54.91	1.687×10^{-2}	1.904×10^{-1}		2.683×10^{-3}	5.433×10^{-9}		1.874×10^{-2}	7.449×10^{-1}		2.637×10^{-2}	1.874×10^{-7}	

T = 40,000°K

1.243×10^{-3}	5.0210	2.0105	43.839	37.818	9.983×10^{-1}	105.87	2.971×10^{-6}	7.670×10^{-3}		1.974×10^{-1}	4.913×10^{-3}	4.372×10^{-8}	2.561×10^{-6}	2.549×10^{-2}		7.258×10^{-1}	3.876×10^{-2}	3.068×10^{-7}
2.556×10^{-3}	4.9121	1.9560	42.371	36.459	2.015	99.97	1.160×10^{-5}	1.496×10^{-2}		1.926×10^{-1}	2.397×10^{-3}	1.066×10^{-8}	1.017×10^{-5}	5.058×10^{-2}		7.202×10^{-1}	1.923×10^{-2}	7.610×10^{-8}
5.303×10^{-3}	4.7717	1.8856	40.652	34.880	4.081	93.81	4.352×10^{-5}	2.808×10^{-2}		1.807×10^{-1}	1.125×10^{-3}	2.502×10^{-9}	3.866×10^{-5}	9.617×10^{-2}		6.847×10^{-1}	9.140×10^{-3}	1.809×10^{-8}
1.122×10^{-2}	4.5641	1.7820	38.223	32.659	8.326	86.88	1.538×10^{-4}	4.964×10^{-2}		1.597×10^{-1}	4.969×10^{-4}	5.526×10^{-10}	1.385×10^{-4}	1.723×10^{-1}		6.134×10^{-1}	4.095×10^{-3}	4.052×10^{-9}
2.445×10^{-2}	4.2726	1.6363	34.874	29.601	17.186	78.96	4.973×10^{-4}	8.023×10^{-2}		1.291×10^{-1}	2.008×10^{-4}	1.117×10^{-10}	4.557×10^{-4}	2.834×10^{-1}		5.044×10^{-1}	1.684×10^{-3}	8.329×10^{-10}
7.111×10^{-2}	3.8123	1.4062	29.633	24.821	45.631	67.83	1.961×10^{-3}	1.266×10^{-1}		8.143×10^{-2}	5.065×10^{-5}	1.127×10^{-11}	1.850×10^{-3}	4.601×10^{-1}		3.276×10^{-1}	4.373×10^{-4}	8.654×10^{-11}
1.604×10^{-1}	3.4940	1.2469	26.052	21.558	95.107	60.14	4.811×10^{-3}	1.552×10^{-1}		4.995×10^{-2}	1.554×10^{-6}	1.728×10^{-13}	4.655×10^{-3}	5.791×10^{-1}		2.061×10^{-1}	1.376×10^{-5}	1.361×10^{-12}
4.578×10^{-1}	3.1841	1.0921	22.691	18.507	255.43	51.94	1.349×10^{-2}	1.741×10^{-1}		2.241×10^{-2}	2.788×10^{-7}	1.204×10^{-13}	1.366×10^{-2}	6.796×10^{-1}		9.675×10^{-2}	2.583×10^{-5}	1.023×10^{-12}
9.936×10^{-1}	3.0129	1.0064	21.100	16.997	531.63	46.95	2.669×10^{-2}	1.722×10^{-1}		1.108×10^{-2}	6.896×10^{-7}	1.534×10^{-14}	2.857×10^{-2}	7.108×10^{-1}		5.060×10^{-2}	6.756×10^{-6}	1.337×10^{-13}

Table 7.10 (Continued)

T = 50,000°K

ρ/ρ_0	α	$1/2\,\bar{z}$	n=H/RT	E/RT	p	$\Delta e/R$	$1/2\,p_1^O$	$1/2\,p_2^O$	$1/2\,p_3^O$	$1/2\,p_4^O$	$1/2\,p_5^O$	$1/2\,p_6^O$	$1/2\,p_7^O$	$1/2\,p_1^N$	$1/2\,p_2^N$	$1/2\,p_3^N$	$1/2\,p_4^N$	$1/2\,p_5^N$	$1/2\,p_6^N$	$1/2\,p_7^N$
8.683×10^{-4}	6.1187	2.5594	49.0228	41.904	1.030	126.66	3.903×10^{-8}	3.486×10^{-4}	1.080×10^{-1}	1.016×10^{-1}	1.266×10^{-4}			2.822×10^{-8}	1.026×10^{-3}	3.387×10^{-1}	4.450×10^{-1}	5.247×10^{-3}		
2.128×10^{-3}	5.6993	2.3496	44.2390	37.540	2.376	114.09	2.696×10^{-7}	1.074×10^{-3}	1.473×10^{-1}	6.159×10^{-2}	3.412×10^{-5}			2.091×10^{-7}	3.380×10^{-3}	4.956×10^{-1}	2.895×10^{-1}	1.517×10^{-3}		
4.538×10^{-3}	5.4073	2.2037	40.8971	34.490	4.846	104.73	1.257×10^{-6}	2.494×10^{-3}	1.716×10^{-1}	3.588×10^{-2}	9.940×10^{-6}			1.020×10^{-6}	8.247×10^{-3}	6.048×10^{-1}	1.766×10^{-2}	4.626×10^{-4}		
7.107×10^{-3}	5.1883	2.0942	38.4691	32.281	9.850	99.77	5.425×10^{-6}	5.384×10^{-3}	1.852×10^{-1}	1.936×10^{-2}	2.682×10^{-6}			4.544×10^{-6}	1.836×10^{-2}	6.732×10^{-1}	9.829×10^{-2}	1.288×10^{-4}		
1.920×10^{-2}	5.0236	2.0118	36.7417	30.781	1.996×10	89.87	2.215×10^{-5}	1.099×10^{-2}	1.891×10^{-1}	9.883×10^{-3}	6.845×10^{-7}			1.892×10^{-5}	3.822×10^{-2}	7.006×10^{-1}	5.114×10^{-2}	3.350×10^{-5}		
5.251×10^{-2}	4.8090	1.9045	34.7683	28.960	5.084×10^{2}	81.09	1.317×10^{-4}	2.615×10^{-2}	1.800×10^{-1}	3.762×10^{-3}	1.042×10^{-7}			1.144×10^{-4}	9.241×10^{-2}	6.777×10^{-1}	1.979×10^{-2}	5.185×10^{-6}		
1.114×10^{-1}	4.5895	1.7948	32.9478	27.358	1.038×10^{2}	73.88	4.716×10^{-4}	4.681×10^{-2}	1.610×10^{-1}	1.683×10^{-3}	2.332×10^{-8}			4.140×10^{-4}	1.673×10^{-1}	6.133×10^{-1}	8.955×10^{-3}	1.173×10^{-6}		
1.427×10^{-1}	4.5021	1.7511	32.2438	26.741	1.309×10^{2}	71.38	6.982×10^{-4}	5.544×10^{-2}	1.526×10^{-1}	1.276×10^{-3}	1.414×10^{-8}			6.155×10^{-4}	1.990×10^{-1}	5.836×10^{-1}	6.817×10^{-3}	7.144×10^{-7}		
1.975×10^{-1}	4.3759	1.6880	31.2408	25.865	1.769×10^{2}	68.02	1.140×10^{-3}	6.787×10^{-2}	1.401×10^{-1}	8.788×10^{-4}	7.304×10^{-9}			1.011×10^{-3}	2.451×10^{-1}	5.392×10^{-1}	4.723×10^{-3}	3.712×10^{-7}		

T = 71,000°K

4.442×10^{-4}	8.5038	3.7519	78.2438	68.740	9.991×10^{-1}	175.34	3.631×10^{-12}	1.861×10^{-7}	1.444×10^{-3}	1.320×10^{-1}	7.527×10^{-2}	1.332×10^{-3}	1.049×10^{-7}	1.296×10^{-12}	2.885×10^{-7}	1.634×10^{-3}	1.157×10^{-1}	6.684×10^{-1}	4.331×10^{-3}	
9.202×10^{-4}	8.2450	3.6225	74.3200	65.075	2.013	164.18	3.529×10^{-11}	9.044×10^{-7}	3.510×10^{-3}	1.604×10^{-1}	4.573×10^{-2}	4.046×10^{-4}	1.594×10^{-8}	1.803×10^{-11}	2.007×10^{-6}	5.684×10^{-3}	2.012×10^{-1}	5.813×10^{-1}	1.883×10^{-3}	
1.416×10^{-3}	8.0604	3.5302	71.5634	62.503	3.037	157.20	1.274×10^{-10}	2.177×10^{-6}	5.633×10^{-3}	1.716×10^{-1}	3.262×10^{-2}	1.924×10^{-4}	5.051×10^{-9}	8.039×10^{-11}	5.965×10^{-5}	1.126×10^{-2}	2.658×10^{-1}	5.119×10^{-1}	1.106×10^{-3}	
2.989×10^{-3}	7.6896	3.3448	66.1486	57.459	6.148	144.60	1.075×10^{-9}	9.181×10^{-6}	1.188×10^{-2}	1.809×10^{-1}	1.720×10^{-3}	5.070×10^{-5}	6.657×10^{-10}	9.330×10^{-10}	3.462×10^{-4}	3.268×10^{-2}	3.856×10^{-1}	3.713×10^{-1}	4.010×10^{-4}	
6.381×10^{-3}	7.2684	3.1342	60.2824	52.014	12.487	131.70	8.467×10^{-9}	3.616×10^{-5}	2.339×10^{-2}	1.781×10^{-1}	8.465×10^{-3}	1.248×10^{-4}	8.193×10^{-11}	9.260×10^{-9}	1.718×10^{-4}	8.107×10^{-2}	4.783×10^{-1}	2.303×10^{-1}	1.244×10^{-4}	
1.374×10^{-2}	6.8206	2.9103	54.4876	46.667	25.439	117.93	6.205×10^{-8}	1.325×10^{-4}	4.285×10^{-2}	1.631×10^{-1}	3.877×10^{-3}	2.858×10^{-6}	9.382×10^{-12}	7.737×10^{-8}	7.177×10^{-4}	1.694×10^{-1}	4.996×10^{-1}	1.203×10^{-1}	1.248×10^{-5}	
3.837×10^{-2}	6.2126	2.6063	47.3266	40.114	65.494	103.42	7.467×10^{-7}	6.378×10^{-4}	8.252×10^{-2}	1.275×10^{-1}	1.195×10^{-3}	3.522×10^{-7}	4.624×10^{-13}	9.789×10^{-7}	3.632×10^{-3}	3.429×10^{-1}	4.046×10^{-1}	3.896×10^{-2}	3.248×10^{-6}	
8.368×10^{-2}	5.8804	2.3902	41.6904	34.810	134.27	92.68	4.269×10^{-6}	1.823×10^{-3}	1.180×10^{-1}	8.980×10^{-2}	4.268×10^{-4}	6.293×10^{-9}	4.131×10^{-14}	5.503×10^{-6}	1.021×10^{-2}	4.818×10^{-1}	2.842×10^{-1}	1.369×10^{-3}	4.207×10^{-7}	
2.316×10^{-1}	5.5180	2.1590	37.9800	31.462	346.28	80.65	3.535×10^{-5}	6.039×10^{-3}	1.562×10^{-1}	4.759×10^{-2}	9.049×10^{-5}	5.337×10^{-9}	1.401×10^{-15}	4.359×10^{-5}	3.235×10^{-2}	6.107×10^{-1}	1.441×10^{-1}	2.776×10^{-3}	7.391×10^{-8}	
																			5.995×10^{-8}	

T = 101,400°K

2.518×10^{-4}	10.9274	4.9637	92.6380	80.710	1.015	227.08	4.004×10^{-18}	9.096×10^{-13}	9.488×10^{-8}	2.732×10^{-4}	1.572×10^{-2}	1.674×10^{-1}	2.657×10^{-2}		7.752×10^{-13}	4.251×10^{-8}	7.570×10^{-5}	4.647×10^{-2}	7.435×10^{-1}	
5.862×10^{-4}	10.7484	4.8742	89.9279	78.180	2.328	214.16	2.424×10^{-16}	2.409×10^{-11}	1.038×10^{-6}	1.385×10^{-3}	3.487×10^{-2}	1.624×10^{-1}	1.128×10^{-2}		1.967×10^{-11}	4.717×10^{-7}	3.675×10^{-4}	9.870×10^{-2}	6.909×10^{-1}	
8.293×10^{-4}	10.6468	4.8234	88.4906	76.844	3.265	207.96	1.233×10^{-15}	8.753×10^{-10}	2.693×10^{-5}	2.567×10^{-3}	4.617×10^{-2}	1.536×10^{-1}	7.621×10^{-3}		7.192×10^{-11}	1.232×10^{-6}	6.858×10^{-4}	1.316×10^{-1}	6.578×10^{-1}	
1.411×10^{-2}	10.4488	4.7244	85.6726	74.224	5.461	198.36	1.374×10^{-14}	5.853×10^{-10}	1.081×10^{-5}	6.181×10^{-3}	6.669×10^{-2}	1.332×10^{-1}	3.963×10^{-3}		4.988×10^{-10}	5.128×10^{-6}	1.712×10^{-3}	1.971×10^{-1}	5.912×10^{-1}	
2.548×10^{-2}	8.8502	3.9251	62.4165	52.566	8.482×10^{2}	146.34	8.556×10^{-10}	2.430×10^{-6}	2.991×10^{-3}	1.140×10^{-1}	8.203×10^{-2}	1.092×10^{-2}	2.166×10^{-5}		5.050×10^{-6}	3.462×10^{-2}	7.705×10^{-2}	5.912×10^{-1}	1.182×10^{-1}	
6.834×10^{-2}	8.3163	3.6582	57.7425	48.426	2.152×10^{2}	125.65	1.799×10^{-8}	2.043×10^{-5}	6.598×10^{-3}	1.534×10^{-1}	4.414×10^{-2}	2.351×10^{-3}	1.865×10^{-6}		7.309×10^{-5}	2.004×10^{-2}	1.784×10^{-1}	5.476×10^{-1}	4.381×10^{-2}	
9.371×10^{-2}	8.1144	3.5572	55.6525	46.438	2.887×10^{2}	119.96	4.447×10^{-7}	3.789×10^{-5}	1.399×10^{-2}	1.601×10^{-1}	3.458×10^{-2}	1.379×10^{-3}	8.210×10^{-7}		1.602×10^{-4}	3.295×10^{-2}	2.200×10^{-1}	5.065×10^{-1}	3.038×10^{-2}	
1.469×10^{-1}	7.8066	3.4033	52.2169	43.410	4.373×10^{2}	114.01	1.539×10^{-6}	8.744×10^{-4}	2.152×10^{-2}	1.641×10^{-1}	2.361×10^{-2}	6.287×10^{-4}	2.495×10^{-7}		4.586×10^{-4}	6.287×10^{-2}	2.799×10^{-1}	4.296×10^{-1}	1.718×10^{-2}	
3.238×10^{-1}	7.1764	3.0882	45.7550	37.579	8.949×10^{2}	97.57	1.178×10^{-6}	3.346×10^{-4}	4.118×10^{-2}	1.570×10^{-1}	1.130×10^{-2}	1.504×10^{-4}	2.983×10^{-8}		2.313×10^{-3}	1.585×10^{-1}	3.529×10^{-1}	2.708×10^{-1}	5.416×10^{-3}	

T = 140,000°K

9.501×10^{-3}	11.0246	5.0123	76.6523	64.628	53.311	186.16		3.049×10^{-11}	3.870×10^{-7}	2.834×10^{-4}	7.986×10^{-3}	1.315×10^{-1}	7.021×10^{-2}		7.917×10^{-11}	4.576×10^{-7}	1.581×10^{-4}	4.906×10^{-2}	7.408×10^{-1}	
1.843×10^{-2}	10.8649	4.9324	74.7440	62.879	102.05	176.00		4.608×10^{-10}	3.064×10^{-6}	1.175×10^{-3}	1.735×10^{-2}	1.496×10^{-1}	4.184×10^{-2}		9.949×10^{-10}	3.078×10^{-6}	5.452×10^{-4}	8.861×10^{-2}	7.008×10^{-1}	
4.172×10^{-2}	10.5872	4.7936	71.5920	60.005	225.61	162.78		1.067×10^{-8}	3.223×10^{-5}	5.619×10^{-3}	3.771×10^{-2}	1.478×10^{-1}	1.879×10^{-2}		2.049×10^{-8}	2.882×10^{-4}	2.320×10^{-2}	1.714×10^{-1}	6.162×10^{-1}	
1.101×10^{-1}	10.0825	4.5412	66.1036	55.021	569.43	140.81		3.067×10^{-7}	3.708×10^{-4}	2.586×10^{-2}	6.940×10^{-2}	1.089×10^{-1}	5.534×10^{-3}		5.967×10^{-7}	3.357×10^{-3}	1.081×10^{-2}	3.195×10^{-1}	4.594×10^{-1}	
2.333×10^{-1}	9.5731	4.2865	60.7488	50.176	1151.07	131.08		2.889×10^{-6}	1.746×10^{-3}	6.087×10^{-2}	8.169×10^{-2}	6.407×10^{-2}	1.629×10^{-3}		6.592×10^{-6}	1.854×10^{-3}	2.985×10^{-2}	4.411×10^{-1}	3.171×10^{-1}	
3.110×10^{-1}	9.4975	4.2487	59.4109	48.913	1523.33	127.06		6.520×10^{-6}	2.982×10^{-3}	7.870×10^{-2}	7.994×10^{-2}	4.745×10^{-2}	9.131×10^{-4}		1.659×10^{-5}	3.532×10^{-3}	4.304×10^{-2}	4.814×10^{-1}	2.620×10^{-1}	

T = 180,000°K

1.288×10^{-2}	11.3513	5.1756	66.7891	54.438	95.457	183.79			7.243×10^{-10}	1.516×10^{-6}	1.850×10^{-4}	2.582×10^{-2}	1.840×10^{-1}			7.060×10^{-9}	5.952×10^{-6}	8.149×10^{-3}	7.818×10^{-1}	
1.988×10^{-2}	11.3211	5.1606	66.4668	54.146	143.253	178.15			3.450×10^{-9}	4.815×10^{-6}	3.916×10^{-4}	3.645×10^{-2}	1.731×10^{-1}			2.403×10^{-8}	1.351×10^{-5}	1.232×10^{-2}	7.886×10^{-1}	
3.905×10^{-2}	11.2428	5.1214	65.6355	53.393	286.862	168.80			4.681×10^{-8}	3.226×10^{-5}	1.328×10^{-3}	6.182×10^{-2}	1.468×10^{-1}			1.868×10^{-7}	5.248×10^{-5}	2.395×10^{-2}	7.660×10^{-1}	
9.930×10^{-2}	11.0704	5.0352	63.8590	51.788	719.161	155.36			1.238×10^{-6}	3.455×10^{-4}	5.621×10^{-3}	1.046×10^{-1}	9.940×10^{-2}			2.790×10^{-6}	3.136×10^{-4}	5.726×10^{-2}	7.324×10^{-1}	
2.026×10^{-1}	11.6716	4.8358	61.6165	50.022	1443.120	144.51			1.246×10^{-5}	1.738×10^{-3}	1.414×10^{-2}	1.316×10^{-1}	6.251×10^{-2}			2.079×10^{-5}	1.168×10^{-3}	1.067×10^{-1}	6.822×10^{-1}	
2.723×10^{-1}	10.5943	4.7971	60.8636	49.269	1926.720	140.20			3.093×10^{-5}	3.238×10^{-3}	1.975×10^{-2}	1.378×10^{-1}	4.812×10^{-2}			4.710×10^{-5}	1.985×10^{-3}	1.360×10^{-1}	6.520×10^{-1}	
3.099×10^{-1}	10.3104	4.6552	59.9842	48.673	2177.480	137.68			4.492×10^{-5}	4.166×10^{-3}	2.252×10^{-2}	1.393×10^{-1}	4.397×10^{-2}			6.618×10^{-5}	2.472×10^{-3}	1.500×10^{-1}	6.375×10^{-1}	
3.452×10^{-1}	10.2700	4.6350	59.5648	48.294	2417.190	135.97			6.158×10^{-5}	5.148×10^{-3}	2.509×10^{-2}	1.399×10^{-1}	3.981×10^{-2}			8.844×10^{-5}	2.978×10^{-3}	1.629×10^{-1}	6.241×10^{-1}	

T = 246,250°K

1.280×10^{-2}	11.4148	5.2074	57.8678	45.453	130.46	188.47				1.376×10^{-9}	1.028×10^{-6}	1.655×10^{-3}	2.084×10^{-1}			3.570×10^{-11}	1.096×10^{-7}	9.362×10^{-4}	7.890×10^{-1}	2.403×10^{-5}
3.845×10^{-2}	11.4046	5.2023	57.7816	45.377	391.45	174.72				3.657×10^{-8}	9.106×10^{-6}	4.886×10^{-3}	2.051×10^{-1}			9.617×10^{-10}	9.838×10^{-7}	2.802×10^{-3}	7.872×10^{-1}	7.990×10^{-6}
1.933×10^{-1}	11.3468	5.1734	57.3028	44.953	1959.00	154.14				4.178×10^{-6}	2.081×10^{-4}	2.233×10^{-2}	1.875×10^{-1}			1.185×10^{-7}	2.425×10^{-5}	1.381×10^{-2}	7.762×10^{-1}	1.576×10^{-6}
2.583×10^{-1}	11.3242	5.1621	57.1172	44.786	2612.90	150.34				9.557×10^{-6}	3.570×10^{-4}	2.873×10^{-2}	1.809×10^{-1}			2.793×10^{-7}	4.286×10^{-5}	1.831×10^{-2}	7.716×10^{-1}	1.175×10^{-6}
3.558×10^{-1}	11.2920	5.1460	56.8530	44.544	3589.90	146.07				2.351×10^{-5}	6.395×10^{-4}	3.718×10^{-2}	1.789×10^{-1}			7.171×10^{-7}	8.013×10^{-5}	2.493×10^{-2}	7.650×10^{-1}	8.482×10^{-7}

7.4 Collected Results

Using the various sources as described in the preceding sections, a number of tables were made by Hirschfelder and Magee which present the data in a form convenient for use. These are reproduced in Tables 7.11 through 7.17.

Table 7.11 gives the pressure for various temperatures and densities. Table 7.12 gives various quantities along the Hugoniot curve. The quantity γ in that table is defined by

$$E = \frac{pV}{\gamma - 1} \quad \text{or} \quad \gamma - 1 = \frac{\alpha + 1}{E/RT} \tag{7.85}$$

It should not be confused with the adiabatic γ defined as $(d \ln p/d \ln \rho)_S$. Table 7.13 gives various properties after expansion to 1 atm. Tables 7.14 and 7.16 give properties along the adiabatics. Table 7.15 gives various properties as function of temperature and entropy. Table 7.17 gives values of $d[\ln (p_S/p_0)] / d[\Delta(S/R)]$.

7.5 Approximate Form of Adiabatics for IBM Run of Nuclear Explosion

For the purpose of numerical integration of the hydrodynamic equations for the blast wave, it is unfortunate that there are regions of rapid change in the various thermodynamical quantities. These regions have probably not a very marked effect on the propagation of the shock at large distances and it appears therefore justified to smooth the primary data. For the procedure used on the IBM machines we require furthermore that the equation of the adiabatics be given in semi-analytical form, so that only tables of one variable need be given.

Hirshfelder and Magee assumed the equation of the adiabatics in the form

$$\frac{p}{p_0} = g(S)\left(\frac{\rho}{\rho_0}\right)^{1.5} + h(S)\frac{\rho}{\rho_0} \tag{7.86}$$

or the equivalent form

$$\frac{p}{p_0} = b(S)(X + X^{1.5}) \tag{7.87}$$

(Text continues on page 289)

Table 7.11

PRESSURE VS TEMPERATURE FOR VARIOUS COMPRESSIONS
(pressure is in atmospheres)

T \ ρ/ρ_0	20	11	10	8	5
1,000,000		46,081		46,798	
900,000		40,140		40,739	
800,000		34,277		34,793	
750,000		31,840		32,273	
700,000		29,088		29,470	
650,000		26,519		26,854	
600,000		24,013		24,303	
550,000		21,545		21,790	
500,000		19,186		19,391	
450,000		16,950		17,117	
400,000		14,938		15,071	
350,000		12,804		12,904	
300,000		10,811		10,897	
250,000		8,559.4		8,640.1	
200,000		5,909.7		6,033.3	
180,000		5,039.8		5,159.3	5,346.3
160,000		4,270.7		4,365.1	
140,000		3,476.2		3,564.8	3,640.9
120,000		2,674.9		2,754.2	
100,000		1,932.4		1,999.0	
90,000		1,573.0		1,632.2	
80,000		1,263.8		1,310.6	
70,000		1,037.8		1,074.7	
60,000		821.95		849.29	
50,000		621.91		641.14	663.80
45,000		524.58		540.22	
40,000		433.00		445.58	
35,000		345.37		355.26	
30,000		269.71		277.43	281.65
25,000	189.99	195.17	198.62	201.13	209.49

Table 7.11 (Continued)

T \ ρ/ρ_0	20	11	10	8	5
24,000			186.75		
22,000			158.53		
20,000	140.47	141.44	141.70	142.54	147.22
18,000			125.37		
16,000			108.65		
15,000	90.86	100.08	101.07	101.53	102.21
12,000	75.30		77.40		78.74
10,000	57.01	59.75	60.19	61.06	62.65
9,000					
8,000	37.65		40.14		42.82
7,000	29.60	32.86	32.34	32.61	32.91
6,500	26.22		27.36		28.66
6,000	23.18		23.92		24.87
5,500	20.36		20.94		21.61
5,000			18.23		18.68
4,500			15.83		16.13
4,000			13.70		13.83
3,500			11.78		11.84
3,000			10.01		10.04
2,500			8.34		8.34
2,000			6.67		6.67
1,500			5.00		5.00
1,000			3.33		3.33

T \ ρ/ρ_0	4	2	1	0.8
1,000,000	48,358	49,918	51,478	
900,000	42,038	43,339	44,639	
800,000	35,914	37,037	38,159	
750,000	33,217	34,241	35,104	
700,000	30,302	31,135	31,967	
650,000	27,582	28,310	29,037	
600,000	24,935	25,565	26,198	
550,000	22,325	22,859	23,393	
500,000	19,838	20,286	20,733	20,877
450,000	17,481	17,844	18,208	18,325

Table 7.11 (Continued)

T \ ρ/ρ_0	4	2	1	0.8
400,000	15,362	15,653	15,943	16,037
350,000	13,120	13,336	13,553	13,622
300,000	11,084	11,272	11,459	11,519
250,000	8,815.7	9,032.1	9,166.9	9,223.5
200,000	6,302.2	6,571.2	6,840.1	6,926.7
180,000	5,419.3	5,679.5	5,939.6	6,023.4
160,000	4,570.5	4,776.0	4,981.6	5,047.7
140,000	3,757.9	3,950.9	4,144.0	4,206.1
120,000	2,926.8	3,099.6	3,272.2	3,327.8
100,000	2,143.9	2,288.8	2,433.7	2,480.4
90,000	1,758.2	1,884.3	2,010.4	2,051.0
80,000	1,412.3	1,514.1	1,615.9	1,648.6
70,000	1,155.0	1,235.4	1,405.6	1,341.6
60,000	908.96	968.54	1,028.1	1,047.3
50,000	682.98	724.84	766.69	780.17
45,000	574.13	608.09	642.04	652.97
40,000	473.07	500.54	527.99	536.84
35,000	376.84	398.40	419.97	426.91
30,000	294.31	311.17	328.03	333.46
25,000	214.06	227.02	239.96	244.12
24,000			226.93	
22,000			194.66	
20,000	148.20	156.29	163.39	165.45
18,000			137.77	
16,000			115.13	
15,000	102.48	103.53	105.23	106.35
12,000		79.81	80.31	
10,000	64.36	64.76	65.95	66.32
9,000		56.26	57.80	
8,000		46.36	48.68	
7,000	33.36	35.64	37.93	39.06
6,500		30.71	32.53	
6,000		26.31	27.62	
5,500		22.62	23.49	
5,000		19.40	20.01	
4,500		16.57	17.03	

Table 7.11 (Continued)

T \ ρ/ρ_0	4	2	1	0.8
4,000		14.07	14.33	
3,500		11.93	12.02	
3,000		10.06	10.08	
2,500		8.34	8.34	
2,000		6.67	6.67	
1,500		5.00	5.00	
1,000		3.33	3.33	

T \ ρ/ρ_0	0.6	0.4	0.2	0.1
500,000	21,078	21,325	21,772	22,220
450,000	18,476	18,689	19,052	19,416
400,000	16,157	16,327	16,618	16,908
350,000	13,712	13,838	14,055	14,272
300,000	11,597	11,708	11,895	12,082
250,000	9,296.3	9,398.8	9,574.9	9,750.2
200,000	7,038.3	7,195.1	7,464.7	7,733.4
180,000	6,131.3	6,283.8	6,543.5	6,804.2
160,000	5,133.0	5,253.0	5,458.8	5,663.7
140,000	4,286.2	4,399.2	4,592.4	4,785.7
120,000	3,399.5	3,500.5	3,673.0	3,854.6
100,000	2,540.5	2,625.1	2,769.8	2,914.5
90,000	2,103.4	2,176.7	2,302.5	2,429.2
80,000	1,690.9	1,750.7	1,852.3	1,953.8
70,000	1,374.9	1,421.8	1,502.7	1,582.6
60,000	1,072.1	1,107.2	1,166.5	1,225.8
50,000	797.54	822.05	863.66	905.90
45,000	667.06	686.89	720.86	754.92
40,000	548.23	564.30	591.71	619.21
35,000	435.86	448.46	470.03	491.60
30,000	340.45	350.32	367.13	384.02
25,000	249.50	257.03	269.97	283.01
24,000				267.10
22,000				230.79

Table 7.11 (Continued)

T \ ρ/ρ_0	0.6	0.4	0.2	0.1
20,000	166.76	171.19	178.99	182.89
18,000				150.18
16,000				121.60
15,000	107.42	108.79	109.54	110.09
12,000				83.22
10,000	66.70	66.78	66.91	67.23
9,000				65.34
8,000				57.25
7,000	39.92	41.24	42.73	44.76
6,500				37.75
6,000				31.28
5,500				26.06
5,000				21.84
4,500				18.24
4,000				14.95
3,500				12.31
3,000				10.16
2,500				8.34
2,000				6.67

T \ ρ/ρ_0	0.05	0.02	0.01	0.005
300,000	12,269	12,517	12,704	
250,000	9,925.4	10,158	10,333	
200,000	8,002.2	8,357.8	8,627.7	
180,000	7,063.9	7,407.9	7,668.0	
160,000	5,869.5	6,141.1	6,346.6	6,608.3
140,000	4,978.0	5,233.4	5,466.9	5,619.7
120,000	4,018.2	4,336.4	4,419.2	4,591.5
100,000	3,059.2	3,251.2	3,396.1	3,409.4
90,000	2,555.0	2,721.5	2,847.6	2,973.8
80,000	2,056.3	2,190.4	2,292.2	2,394.2
70,000	1,663.5	1,769.5	1,849.8	1,930.4

Table 7.11 (Continued)

T \ ρ/ρ_0	0.05	0.02	0.01	0.005
60,000	1,286.1	1,364.4	1,424.0	1,483.8
50,000	947.25	1,002.9	1,044.8	1,086.5
45,000	789.07	833.65	867.65	901.41
40,000	647.07	682.93	710.43	737.93
35,000	513.17	541.66	563.22	584.79
30,000	400.83	423.11	440.01	456.55
25,000	295.68	313.02	325.96	338.82
24,000			307.27	
22,000			266.92	
20,000	191.00	203.02	212.46	218.34
18,000			162.58	
16,000			128.07	
15,000	111.02	112.45	114.95	
12,000			86.10	
10,000	67.40	68.04	76.57	
9,000			72.89	
8,000			65.79	
7,000	45.38		51.49	
6,500			37.75	
6,000			34.96	
5,500			28.58	
5,000			23.55	
4,500			19.41	
4,000			15.55	
3,500			12.51	
3,000			10.23	
2,500			8.34	
2,000			6.67	

T \ ρ/ρ_0	0.002	0.001	0.0001	0.00001
140,000	5,748.9	6,068.1		
120,000	4,819.8	4,992.3	5,566.6	
100,000	3,732.4	3,877.1	4,358.8	

Table 7.11 (Continued)

T \ ρ/ρ_0	0.002	0.001	0.0001	0.00001
90,000	3,140.1	3,266.8	3,685.6	
80,000	2,528.1	2,630.5	2,968.5	
70,000	2,036.5	2,116.5	2,383.4	
60,000	1,562.0	1,622.2	1,819.9	
50,000	1,142.3	1,183.6	1,322.9	
45,000	946.35	980.50	1,092.8	
40,000	774.15	801.65	892.87	
35,000	612.92	634.49	706.48	
30,000	479.02	496.09	551.99	
25,000	355.89	369.37	422.85	
24,000		347.44	387.62	427.79
22,000		303.05	339.17	375.30
20,000		221.89	241.39	260.90
18,000		174.98	187.38	199.78
16,000		134.54	141.01	147.48
15,000		119.80	124.65	129.50
12,000		89.06	91.94	94.90
10,000		82.05	87.53	93.02
9,000		80.43	86.10	91.94
8,000		74.32	82.86	91.40
7,000		58.33	65.07	71.90
6,500		41.43	45.12	48.80
6,000		38.64	42.33	46.01
5,500		31.19	33.70	36.22
5,000		25.34	27.14	28.94
4,500		20.64	21.84	23.10
4,000		16.18	16.81	17.44
3,500		12.75	13.00	13.24
3,000		10.30	10.37	10.44
2,500		8.34	8.34	8.34
2,000		6.67	6.67	6.67

Table 7.12

PROPERTIES OF AIR ALONG THE HUGONIOT CURVE

$\Delta S/R$	T	p_s/p_0	ρ_s/ρ_0	E/R	H/R	α	$\gamma - 1$
11.89	7,000	347	11.02	4.8433×10^4	5.7690×10^4	0.3495	0.19504
17.68	10,000	727	12.03	1.0080×10^5	1.1893×10^5	0.8130	0.17986
22.07	15,000	1,100	10.7	1.4654×10^5	1.7757×10^5	1.0561	0.21046
25.20	20,000	1,600	10.2	2.0768×10^5	2.5283×10^5	1.2574	0.21739
28.39	25,000	2,250	9.8	2.6288×10^5	3.2834×10^5	1.6173	0.24891
31.21	30,000	3,000	9.5	3.8250×10^5	4.7250×10^5	2.0000	0.23529
36.68	40,000	4,500	9.2	5.7156×10^5	7.1096×10^5	2.4851	0.24390
41.71	50,000	6,300	9.0	7.9800×10^5	9.9750×10^5	2.9900	0.25000
51.56	71,000	11,200	9.0	1.4187×10^6	1.7733×10^6	3.9953	0.24999
64.31	101,430	20,000	9.2	2.5410×10^6	3.1607×10^6	5.1101	0.24390
77.40	140,000	32,000	9.1	4.0589×10^6	5.0611×10^6	6.1586	0.24692
89.73	180,000	47,000	8.5	5.9095×10^6	7.4854×10^6	7.7549	0.26667
102.64	246,250	69,000	8.0	8.6034×10^6	1.1062×10^7	8.9822	0.28571
112.32	328,300	92,000	7.4	1.1338×10^7	1.4882×10^7	9.7027	0.30990
124.33	492,500	128,000	6.4	1.5390×10^7	2.1091×10^7	10.5736	0.37037
140.87	712,500	210,000	6.7	2.5459×10^7	3.4391×10^7	11.5373	0.35087
158.12	968,750	340,000	7.2	4.1721×10^7	5.5179×10^7	12.8925	0.32258

Table 7.13

THERMODYNAMIC PROPERTIES OF AIR AT A PRESSURE OF 1 BAR

$\Delta S/R$	T	ρ/ρ_0	E/R	H/R	α	$\gamma - 1$
11.37	3,400	8.252×10^{-2}	1.5408×10^{4}	1.9034×10^{4}	0.0692	0.23594
12.20	3,600	7.576×10^{-2}	1.7993×10^{4}	2.1953×10^{4}	0.1000	0.22009
13.05	3,800	6.967×10^{-2}	2.0736×10^{4}	2.5042×10^{4}	0.1331	0.20765
13.87	4,000	6.432×10^{-2}	2.3548×10^{4}	2.8212×10^{4}	0.1661	0.19808
14.68	4,200	5.958×10^{-2}	2.6457×10^{4}	3.1492×10^{4}	0.1988	0.19031
15.52	4,400	5.532×10^{-2}	2.9609×10^{4}	3.5033×10^{4}	0.2326	0.18317
16.42	4,600	5.134×10^{-2}	3.2194×10^{4}	3.9063×10^{4}	0.2704	0.18152
17.42	4,800	4.755×10^{-2}	3.7414×10^{4}	4.3723×10^{4}	0.3144	0.16863
18.58	5,000	4.393×10^{-2}	4.2291×10^{4}	4.9120×10^{4}	0.3659	0.16149
30.72	7,000	2.223×10^{-2}	9.9388×10^{4}	1.1345×10^{5}	1.0236	0.14252
34.10	10,000	1.457×10^{-2}	1.2890×10^{5}	1.4952×10^{5}	1.0502	0.15905
52.16	15,000	6.719×10^{-3}	3.2024×10^{5}	3.6581×10^{5}	1.9770	0.13944
65.60	20,000	3.837×10^{-3}	5.1539×10^{5}	5.9398×10^{5}	2.8996	0.15133
70.73	25,000	2.907×10^{-3}	6.1429×10^{5}	7.1568×10^{5}	3.1274	0.16847
86.73	30,000	2.008×10^{-3}	9.7532×10^{5}	1.1374×10^{6}	3.9801	0.15318
105.86	40,000	1.246×10^{-3}	1.5127×10^{6}	1.7535×10^{6}	5.0208	0.15921
127.097	50,000	8.415×10^{-4}	2.1022×10^{6}	2.4589×10^{6}	6.1323	0.16964
175.33	71,000	4.446×10^{-4}	4.8803×10^{6}	5.5551×10^{6}	8.5036	0.13826

Table 7.14

PROPERTIES OF AIR ALONG THE ADIABATICS TERMINATING IN THE HUGONIOT CURVE

$\Delta S/R$	ρ/ρ_0	p/p_0	T	E/R	H/R	α
20	0.0414	1.000	5,234	4.897×10^4	5.665×10^4	0.4428
	0.8074	31.51	7,000	7.461×10^4	8.636×10^4	0.6726
	1.858	86.77	8,000	8.677×10^4	1.008×10^5	0.7512
	3.841	208.9	9,000	9.673×10^4	1.130×10^5	0.8127
	6.6489	409.3	10,000	1.048×10^5	1.232×10^5	0.8469
	11.47	900.	12,024	1.240×10^5	1.476×10^5	0.9577
21	0.0396	1.000	5,399	5.364×10^4	7.075×10^4	0.4970
	0.6125	24.40	7,000	7.779×10^4	8.942×10^4	0.7074
	1.3916	66.49	8,000	9.021×10^4	1.045×10^5	0.7917
	2.699	149.9	9,000	1.001×10^5	1.167×10^5	0.8515
	4.576	288.03	10,000	1.083×10^5	1.272×10^5	0.8883
	8.527	664.3	12,000	1.237×10^5	1.470×10^5	0.9448
	11.07	993.	13,392	1.354×10^5	1.631×10^5	1.0095
22	0.0378	1.00	5,563	5.838×10^4	7.443×10^4	0.5512
	0.4542	18.53	7,000	8.088×10^4	9.316×10^4	0.7484
	1.785	101.0	9,000	1.031×10^5	1.200×10^5	0.8864
	3.104	198.5	10,000	1.110×10^5	1.302×10^5	0.9188
	5.103	401.6	12,000	1.259×10^5	1.495×10^5	0.9677
	10.72	1094.	14,920	1.458×10^5	1.764×10^5	1.0522
23	0.0360	1.00	5,727	6.308×10^4	7.890×10^4	0.6054
	0.3355	14.01	7,000	8.389×10^4	9.642×10^4	0.7897
	1.230	70.65	9,000	1.055×10^5	1.227×10^5	0.9147
	1.817	117.9	10,000	1.135×10^5	1.331×10^5	0.9470
	3.723	294.8	12,000	1.272×10^5	1.510×10^5	0.9798

Table 7.14 (Continued)

$\Delta S/R$	ρ/ρ_0	p/p_0	T	E/R	H/R	α
23	7.935	801.2	15,000	1.488×10^5	1.791×10^5	1.0193
	10.55	1248.6	16,486	1.643×10^5	1.998×10^5	1.1159
24	0.0342	1.00	5,893	6.778×10^4	8.338×10^4	0.6595
	0.2732	11.50	7,000	8.660×10^4	9.930×10^4	0.8040
	1.083	70.98	10,000	1.153×10^5	1.349×10^5	0.9665
	2.253	179.6	12,000	1.287×10^5	1.526×10^5	0.9929
	4.914	500.0	15,000	1.513×10^5	1.818×10^5	1.0350
	10.39	1408.3	18,083	1.838×10^5	2.239×10^5	1.1802
25	0.0325	1.000	6,058	7.336×10^4	8.785×10^4	0.7137
	0.2138	9.097	7,000	8.929×10^4	1.022×10^5	0.8235
	0.7984	53.43	10,000	1.169×10^5	1.370×10^5	1.0008
	1.4513	116.23	12,000	1.291×10^5	1.531×10^5	1.0022
	2.4864	257.4	15,000	1.395×10^5	1.706×10^5	1.0705
	10.23	1568.1	19,680	2.034×10^5	2.480×10^5	1.2445
26	0.0307	1.000	6,222	7.718×10^4	9.233×10^4	0.7679
	0.1545	6.695	7,000	9.198×10^4	1.052×10^5	0.8571
	0.5711	38.21	10,000	1.189×10^5	1.391×10^5	1.0098
	2.060	209.2	15,000	1.409×10^5	1.722×10^5	1.0717
	5.761	844.9	20,000	2.121×10^5	2.561×10^5	1.2000
	10.10	1763.0	21,253	2.215×10^5	2.718×10^5	1.3477
27	0.0288	1.000	6,387	8.189×10^4	9.680×10^4	0.8221
	0.0999	4.471	7,000	9.450×10^4	1.080×10^5	0.9183
	0.3240	21.65	10,000	1.211×10^5	1.412×10^5	1.0108
	1.157	121.3	15,000	1.435×10^5	1.752×10^5	1.0973

Table 7.14 (Continued)

$\Delta S/R$	ρ/ρ_0	p/p_0	T	E/R	H/R	α
27	3.749	555.4	20,000	2.305×10^5	2.745×10^5	1.2220
	9.974	1966.8	22,821	2.388×10^5	2.954×10^5	1.4605
28	0.0271	1.000	6,552	8.660×10^4	1.013×10^5	0.8762
	0.0741	3.335	7,000	9.592×10^4	1.095×10^5	0.9270
	0.2154	14.40	10,000	1.221×10^5	1.422×10^5	1.0121
	0.7862	83.65	15,000	1.511×10^5	1.832×10^5	1.1280
	2.994	449.2	20,000	2.377×10^5	2.849×10^5	1.2504
	9.849	2170.5	24,389	2.561×10^5	3.191×10^5	1.5733
29	0.0253	1.000	6,717	9.130×10^4	1.059×10^5	0.9304
	0.0484	2.200	7,000	9.734×10^4	1.110×10^5	0.9460
	0.1313	8.810	10,000	1.228×10^5	1.430×10^5	1.0138
	0.5551	59.76	15,000	1.554×10^5	1.878×10^5	1.1531
	2.550	390.8	20,000	2.424×10^5	2.901×10^5	1.2986
	3.794	803.3	25,000	2.693×10^5	3.443×10^5	1.5407
	9.736	2412.2	26,081	2.888×10^5	3.595×10^5	1.7008
30	0.0235	1.000	6,881	9.600×10^4	1.101×10^5	0.8810
	0.0296	1.361	7,000	9.850×10^4	1.123×10^5	0.9672
	0.0832	5.813	10,000	1.236×10^5	1.438×10^5	1.0182
	0.4310	46.80	15,000	1.604×10^5	1.932×10^5	1.2680
	1.8519	298.92	20,000	2.498×10^5	2.983×10^5	1.4211
	3.2337	697.49	25,000	2.840×10^5	3.498×10^5	1.5883
	9.629	2678.2	27,854	3.317×10^5	4.106×10^5	1.8358
35	0.01384	1.000	10,249	1.384×10^5	1.603×10^5	1.096
	0.1143	12.56	15,000	1.888×10^5	2.238×10^5	1.197

Table 7.14 (Continued)

$\Delta S/R$	ρ/ρ_0	p/p_0	T	E/R	H/R	α
35	0.5694	94.29	20,000	4.070×10^5	3.612×10^5	1.484
	2.186	478.3	25,000	3.363×10^5	4.084×10^5	1.625
	4.541	1362.4	30,000	4.321×10^5	5.253×10^5	2.000
	9.292	4039.3	36,929	5.135×10^5	6.377×10^5	2.336
40	0.01166	1.000	11,633	1.914×10^5	2.202×10^5	1.353
	0.04054	5.093	15,000	2.237×10^5	2.613×10^5	1.513
	0.2173	41.36	20,000	3.410×10^5	3.989×10^5	1.856
	1.139	281.3	25,000	3.885×10^5	4.671×10^5	1.964
	1.621	536.1	30,000	4.909×10^5	5.947×10^5	2.307
	9.068	5688.	46,600	7.210×10^5	9.001×10^5	2.818
45	0.009491	1.000	13,018	2.444×10^5	2.801×10^5	1.610
	0.01789	2.430	15,000	2.623×10^5	3.032×10^5	1.716
	0.1219	24.30	20,000	3.729×10^5	4.355×10^5	1.991
	0.2677	75.13	25,000	4.398×10^5	5.245×10^5	2.368
	0.7535	270.0	30,000	5.316×10^5	6.420×10^5	2.583
	5.023	3333.1	50,000	8.502×10^5	1.054×10^6	2.982
	9.000	7936.7	57,014	1.005×10^6	1.256×10^6	3.326
50	0.007318	1.000	14,402	2.974×10^5	3.399×10^5	1.866
	0.009239	1.335	15,000	3.028×10^5	3.468×10^5	1.889
	0.05064	11.42	20,000	4.089×10^5	4.720×10^5	2.383
	0.1216	36.63	25,000	4.865×10^5	5.769×10^5	2.614
	0.2896	110.98	30,000	5.782×10^5	6.895×10^5	2.832
	0.6661	362.81	40,000	7.168×10^5	8.815×10^5	3.085
	2.393	1637.5	50,000	9.389×10^5	1.155×10^6	3.106

Table 7.14 (Continued)

$\Delta S/R$	ρ/ρ_0	p/p_0	T	E/R	H/R	α
50	9.000	10424.	67,674	1.320×10^6	1.650×10^6	3.836
55	0.006112	1.000	16,057	3.616×10^5	4.140×10^5	2.172
	0.02423	5.765	20,000	4.510×10^5	5.226×10^5	2.568
	0.05696	17.82	25,000	5.237×10^5	6.186×10^5	2.754
	0.09942	39.64	30,000	6.022×10^5	7.219×10^5	2.988
	0.34612	195.6	40,000	7.861×10^5	9.581×10^5	3.238
	0.6998	559.5	50,000	1.104×10^6	1.345×10^6	3.797
	5.730	6780.7	71,000	1.495×10^6	1.860×10^6	4.146
	9.054	13574.	79,210	1.722×10^6	2.148×10^6	4.296
60	0.005043	1.000	17,917	4.341×10^5	4.989×10^5	2.515
	0.01080	2.706	20,000	4.873×10^5	5.625×10^5	2.759
	0.02124	6.948	25,000	5.525×10^5	6.507×10^5	2.925
	0.04709	19.16	30,000	6.405×10^5	7.637×10^5	3.069
	0.1647	98.44	40,000	8.605×10^5	1.040×10^6	3.489
	0.5143	386.99	50,000	1.172×10^6	1.419×10^6	3.950
	3.259	3863.5	71,000	1.636×10^6	2.022×10^6	4.427
	9.132	17025.	91,143	2.112×10^6	2.692×10^6	4.733
65	0.003975	1.0000	19,777	5.067×10^5	5.838×10^5	2.858
	0.004316	1.1198	20,000	5.128×10^5	5.906×10^5	2.891
	0.008044	2.691	25,000	5.773×10^5	6.778×10^5	3.014
	0.01977	8.352	30,000	6.888×10^5	8.158×10^5	3.225
	0.1040	64.207	40,000	9.448×10^5	1.133×10^6	3.695
	0.3123	238.8	50,000	1.242×10^6	1.499×10^6	4.141
	1.784	2145.9	71,000	1.785×10^6	2.189×10^6	4.695

Table 7.14 (Continued)

ΔS/R	ρ/ρ_0	p/p_0	T	E/R	H/R	α
	1.195	20633.	103,463	2.621×10^6	3.261×10^6	5.165
70	0.003030	1.000	24,349	5.999×10^5	6.998×10^5	3.098
	0.003243	1.111	25,000	6.082×10^5	7.039×10^5	3.109
	0.01030	4.516	30,000	7.488×10^5	8.805×10^5	3.385
	0.06202	40.08	40,000	1.030×10^6	1.226×10^6	3.902
	0.1385	149.8	50,000	1.319×10^6	1.592×10^6	4.450
	0.9689	1236.4	71,000	1.962×10^6	2.383×10^6	4.926
	5.266	11721.	101,430	2.741×10^6	3.409×10^6	5.255
	9.157	25216.	118,196	3.201×10^6	3.987×10^6	5.566
75	0.002667	1.000	26,334	7.093×10^5	8.282×10^5	3.355
	0.006446	2.912	30,000	8.177×10^5	9.546×10^5	3.517
	0.04105	27.31	40,000	1.116×10^6	1.320×10^6	4.108
	0.1023	95.58	50,000	1.380×10^6	1.612×10^6	4.624
	0.4579	648.7	71,000	2.104×10^6	3.541×10^6	5.162
	3.707	8412.1	101,430	2.939×10^6	3.632×10^6	5.376
	9.118	29800.	132,928	3.781×10^6	4.713×10^6	5.966
80	0.002386	1.000	27,897	8.227×10^5	9.600×10^5	3.621
	0.003642	1.725	30,000	8.885×10^5	1.031×10^6	3.741
	0.02271	16.02	40,000	1.200×10^6	1.413×10^6	4.311
	0.06142	58.84	50,000	1.436×10^6	1.725×10^6	4.776
	0.3505	484.6	71,000	2.205×10^6	2.663×10^6	5.446
	2.149	5103.5	101,430	3.137×10^6	3.854×10^6	5.672
	7.282	26457.	140,000	4.214×10^6	5.305×10^6	6.396
	8.974	35163.	148,435	4.449×10^6	5.572×10^6	6.495

Table 7.14 (Continued)

$\Delta S/R$	ρ/ρ_0	p/p_0	T	E/R	H/R	α
85	0.002105	1.000	29,459	9.361×10^5	1.092×10^6	3.888
	0.002320	1.142	30,000	9.614×10^5	1.109×10^6	3.919
	0.01441	10.43	40,000	1.277×10^6	1.497×10^6	4.495
	0.03767	37.09	50,000	1.487×10^6	1.782×10^6	4.905
	0.2236	334.8	71,000	2.247×10^6	2.711×10^6	5.538
	1.640	3942.4	101,430	3.319×10^6	3.474×10^6	5.757
	4.884	18297.	140,000	4.438×10^6	5.565×10^6	6.627
	8.730	41246.	164,655	5.200×10^6	6.556×10^6	7.142
90	0.001878	1.000	31,709	1.067×10^6	1.243×10^6	4.158
	0.008558	6.415	40,000	1.346×10^6	1.573×10^6	4.657
	0.01904	19.83	50,000	1.537×10^6	1.838×10^6	5.026
	0.1621	246.7	71,000	2.345×10^6	2.820×10^6	5.688
	1.130	2781.3	101,430	3.502×10^6	4.270×10^6	5.917
	3.335	12861.	140,000	4.743×10^6	5.904×10^6	7.289
	8.489	47460.	181,385	5.966×10^6	7.560×10^6	7.781
95	0.001678	1.000	34,323	1.208×10^6	1.404×10^6	4.430
	0.004772	3.682	40,000	1.407×10^6	1.639×10^6	4.799
	0.01293	14.72	50,000	1.576×10^6	1.882×10^6	5.109
	0.07389	119.4	71,000	2.553×10^6	3.046×10^6	5.967
	0.7440	1878.	101,430	3.680×10^6	4.474×10^6	6.466
	2.315	9166.	140,000	5.007×10^6	6.199×10^6	7.512
	5.437	29792.	180,000	6.214×10^6	7.866×10^6	8.179
	8.296	55981.	207,044	7.009×10^6	8.945×10^6	8.256
100	0.001479	1.000	36,937	1.348×10^6	1.565×10^6	4.702

Table 7.14 (Continued)

$\Delta S/R$	ρ/ρ_0	p/p_0	T	E/R	H/R	α
100	0.002549	2.009	40,000	1.459×10^6	1.695×10^6	4.913
	0.006988	9.618	50,000	1.619×10^6	1.929×10^6	5.198
	0.05280	87.39	71,000	2.728×10^6	3.232×10^6	6.107
	0.3581	974.7	101,430	3.860×10^6	4.678×10^6	7.050
	1.651	6727.4	140,000	5.293×10^6	6.527×10^6	7.808
	3.836	21679.	180,000	6.551×10^6	8.248×10^6	8.430
	8.102	64501.	232,702	8.053×10^6	1.033×10^7	8.731
105	0.001280	1.000	39,550	1.489×10^6	1.726×10^6	4.974
	0.001384	1.109	40,000	1.505×10^6	1.745×10^6	5.006
	0.004455	4.762	50,000	1.729×10^6	2.050×10^6	5.416
	0.03569	61.13	71,000	2.899×10^6	3.416×10^6	6.279
	0.2828	783.0	101,430	4.053×10^6	4.898×10^6	7.190
	1.308	5420.1	140,000	5.599×10^6	6.883×10^6	8.169
	2.845	16395.	180,000	6.871×10^6	8.614×10^6	8.688
	6.817	58299.	246,250	8.761×10^6	1.133×10^7	8.897
	7.854	74607.	266,254	9.270×10^6	1.199×10^7	9.180
110	0.001167	1.000	41,949	1.628×10^6	1.891×10^6	5.238
	0.002922	3.198	50,000	1.809×10^6	2.137×10^6	5.568
	0.02720	47.33	71,000	3.059×10^6	3.591×10^6	6.488
	0.2074	591.2	101,430	4.247×10^6	5.118×10^6	7.596
	0.9654	4112.7	140,000	5.906×10^6	7.240×10^6	8.529
	1.928	11479.	180,000	7.188×10^6	8.978×10^6	8.947
	4.837	42325.	246,250	9.112×10^6	1.204×10^7	9.127
	7.544	86488.	308,635	1.068×10^7	1.397×10^7	9.598

Table 7.14 (Continued)

$\Delta S/R$	ρ/ρ_0	p/p_0	T	E/R	H/R	α
115	0.001072	1.000	44, 304	1.766×10^6	2.057×10^6	5.499
	0.002000	2.242	50, 000	1.893×10^6	2.229×10^6	5.729
	0.01872	33.53	71, 000	3.219×10^6	3.766×10^6	6.698
	0.1505	439.7	101, 430	4.478×10^6	5.381×10^6	7.906
	0.7598	3328.3	140, 000	6.089×10^6	7.454×10^6	8.746
	1.291	8051.8	180, 000	7.417×10^6	9.343×10^6	9.704
	3.385	30458.	246, 250	9.445×10^6	1.213×10^7	9.891
	6.030	75880.	328, 300	1.146×10^7	1.523×10^7	9.924
	7.177	100030.	364, 941	1.224×10^7	1.627×10^7	9.967
120	0.000977	1.000	46, 658	1.905×10^6	2.223×10^6	5.761
	0.001380	1.586	50, 000	1.979×10^6	2.324×10^6	5.895
	0.01264	23.492	71, 000	3.370×10^6	3.931×10^6	6.888
	0.09353	288.17	101, 430	4.710×10^6	5.645×10^6	8.215
	0.4109	2085.2	140, 000	6.483×10^6	7.906×10^6	9.166
	0.8252	5483.	180, 000	7.685×10^6	9.706×10^6	9.803
	2.204	21970.	246, 250	9.769×10^6	1.249×10^7	10.029
	4.184	53543.	328, 300	1.174×10^7	1.557×10^7	10.111
	6.761	115020.	433, 301	1.393×10^7	1.885×10^7	10.292
125	0.000881	1.000	49, 013	2.044×10^6	2.389×10^6	6.023
	0.000968	1.139	50, 000	2.066×10^6	2.419×10^6	6.073
	0.009964	18.79	71, 000	3.508×10^6	4.080×10^6	7.051
	0.07240	225.6	101, 430	4.894×10^6	5.839×10^6	8.325
	0.2732	1698.3	140, 000	6.734×10^6	8.190×10^6	9.394
	0.6440	4322.9	180, 000	8.058×10^6	1.006×10^7	9.628
	1.684	15688.	246, 250	1.001×10^7	1.281×10^7	9.782

Table 7.14 (Continued)

$\Delta S/R$	ρ/ρ_0	p/p_0	T	E/R	H/R	α
125	2.966	38580.	328, 300	1.198×10^7	1.584×10^7	10.294
	6.184	123960.	492, 500	1.534×10^7	2.130×10^7	10.600
	6.412	131320.	501, 412	1.580×10^7	2.163×10^7	10.613
130	0.000818	1.000	52, 264	2.269×10^6	2.645×10^6	6.275
	0.007290	14.086	71, 000	3.646×10^6	4.229×10^6	7.213
	0.05127	163.07	101, 430	5.077×10^6	6.033×10^6	8.434
	0.2552	1256.3	140, 000	6.975×10^6	8.261×10^6	9.547
	0.4628	3162.7	180, 000	8.430×10^6	1.042×10^7	9.820
	1.249	11900.	246, 250	1.031×10^7	1.316×10^7	10.025
	1.947	25911.	328, 300	1.218×10^7	1.609×10^7	10.552
	4.295	86914.	492, 500	1.567×10^7	2.167×10^7	10.809
	6.503	156110.	567, 917	1.884×10^7	2.565×10^7	10.904
135	0.000776	1.000	53, 441	2.557×10^6	2.966×10^6	6.521
	0.005514	1.087	71, 000	3.792×10^6	4.387×10^6	7.376
	0.04338	139.13	101, 430	5.154×10^6	6.124×10^6	8.561
	0.1837	916.77	140, 000	7.298×10^6	8.807×10^6	9.778
	0.3608	2435.8	180, 000	8.632×10^6	1.064×10^7	10.143
	0.8144	8112.7	246, 250	1.061×10^7	1.351×10^7	10.529
	1.5463	20744.	328, 300	1.231×10^7	1.625×10^7	10.646
	3.0599	63018.	492, 500	1.597×10^7	2.201×10^7	10.918
	6.594	180900.	634, 423	2.189×10^7	2.967×10^7	11.195

Table 7.15

THERMODYNAMIC PROPERTIES OF AIR

T	ΔS/R	ρ/ρ_0	p/p_0	E/R	H/R
7,000	11	1.911×10	5.759×10^2	4.570×10^4	5.263×10^4
	12	1.413×10	4.860×10^2	4.613×10^4	5.528×10^4
	13	8.243	2.598×10^2	5.145×10^4	5.988×10^4
	14	5.406	1.765×10^2	5.677×10^4	6.374×10^4
	15	4.031	1.344×10^2	5.745×10^4	6.759×10^4
	16	2.899	9.925×10	6.099×10^4	7.144×10^4
	17	1.908	6.821×10	6.455×10^4	7.531×10^4
	18	1.457	5.319×10	6.817×10^4	7.924×10^4
	19	1.007	3.816×10	7.180×10^4	8.317×10^4
	20	8.074×10^{-1}	3.151×10	7.461×10^4	8.636×10^4
	21	6.125×10^{-1}	2.440×10	7.779×10^4	8.942×10^4
	22	4.542×10^{-1}	1.853×10	8.088×10^4	9.316×10^4
	23	3.355×10^{-1}	1.401×10	8.389×10^4	9.642×10^4
	24	2.732×10^{-1}	1.150×10	8.660×10^4	9.930×10^4
	25	2.138×10^{-1}	9.097	8.929×10^4	1.022×10^5
	26	1.545×10^{-1}	6.695	9.198×10^4	1.051×10^5
	27	9.989×10^{-2}	4.471	9.450×10^4	1.079×10^5
	28	7.417×10^{-2}	3.335	9.592×10^4	1.095×10^5
	29	4.845×10^{-2}	2.200	9.734×10^4	1.110×10^5
	30	2.965×10^{-2}	1.361	9.850×10^4	1.123×10^5
10,000	17	1.773×10	1.024×10^3	9.485×10^4	1.122×10^5
	18	1.275×10	7.565×10^2	9.924×10^4	1.170×10^5
	19	8.965	5.442×10^2	1.024×10^5	1.206×10^5

Table 7.15 (Continued)

T	ΔS/R	ρ/ρ_0	p/p_0	E/R	H/R
10,000	20	6.649	4.093×10^{2}	1.048×10^{5}	1.232×10^{5}
	21	4.576	2.880×10^{2}	1.083×10^{5}	1.272×10^{5}
	22	3.104	1.985×10^{2}	1.110×10^{5}	1.302×10^{5}
	23	1.817	1.179×10^{2}	1.135×10^{5}	1.330×10^{5}
	24	1.083	7.098×10	1.153×10^{5}	1.350×10^{5}
	25	7.984×10^{-1}	5.343×10	1.169×10^{5}	1.370×10^{5}
	26	5.711×10^{-1}	3.821×10	1.189×10^{5}	1.391×10^{5}
	27	3.240×10^{-1}	2.165×10	1.211×10^{5}	1.413×10^{5}
	28	2.154×10^{-1}	1.440×10	1.221×10^{5}	1.422×10^{5}
	29	1.313×10^{-1}	8.809	1.228×10^{5}	1.430×10^{5}
	30	8.319×10^{-2}	5.813	1.236×10^{5}	1.438×10^{5}
	31	5.163×10^{-2}	3.484	1.247×10^{5}	1.449×10^{5}
	32	3.467×10^{-2}	2.346	1.258×10^{5}	1.461×10^{5}
	33	2.327×10^{-2}	1.580	1.273×10^{5}	1.477×10^{5}
	34	1.468×10^{-2}	1.002	1.288×10^{5}	1.493×10^{5}
15,000	21	1.127	1.139×10^{3}	1.308×10^{5}	1.613×10^{5}
	22	1.032	1.042×10^{3}	1.308×10^{5}	1.614×10^{5}
	23	5.025	5.137×10^{2}	1.347×10^{5}	1.654×10^{5}
	24	4.522	4.618×10^{2}	1.358×10^{5}	1.666×10^{5}
	25	2.486	2.574×10^{2}	1.395×10^{5}	1.706×10^{5}
	26	2.020	2.092×10^{2}	1.409×10^{5}	1.722×10^{5}
	27	1.157	1.213×10^{2}	1.435×10^{5}	1.752×10^{5}
	28	7.862×10^{-1}	8.365×10	1.511×10^{5}	1.832×10^{5}
	29	5.551×10^{-1}	5.976×10	1.553×10^{5}	1.878×10^{5}

Table 7.15 (Continued)

T	ΔS/R	ρ/ρ_0	p/p_0	E/R	H/R
15,000	30	4.310×10^{-1}	4.680×10	1.604×10^{5}	1.932×10^{5}
	31	3.595×10^{-1}	3.921×10	1.659×10^{5}	1.991×10^{5}
	32	2.880×10^{-1}	3.162×10	1.714×10^{5}	2.051×10^{5}
	33	2.165×10^{-1}	2.403×10	1.769×10^{5}	2.110×10^{5}
	34	1.450×10^{-1}	1.644×10	1.824×10^{5}	2.169×10^{5}
	35	1.143×10^{-1}	0.327×10	1.888×10^{5}	2.238×10^{5}
	36	9.446×10^{-2}	1.109×10	1.955×10^{5}	2.310×10^{5}
	37	7.462×10^{-2}	8.916	2.022×10^{5}	2.383×10^{5}
	38	5.883×10^{-2}	7.170	2.091×10^{5}	2.457×10^{5}
	39	4.968×10^{-2}	6.131	2.164×10^{5}	2.536×10^{5}
	40	4.053×10^{-2}	5.093	2.237×10^{5}	2.615×10^{5}
	41	3.438×10^{-2}	4.404	2.313×10^{5}	2.697×10^{5}
	42	3.014×10^{-2}	3.880	2.390×10^{5}	2.780×10^{5}
	43	2.569×10^{-2}	3.356	2.467×10^{5}	2.863×10^{5}
	44	2.125×10^{-2}	2.832	2.544×10^{5}	2.947×10^{5}
	45	1.789×10^{-2}	2.430	2.623×10^{5}	3.032×10^{5}
	46	1.567×10^{-2}	2.155	2.704×10^{5}	3.119×10^{5}
	47	1.346×10^{-2}	1.880	2.784×10^{5}	3.205×10^{5}
	48	1.157×10^{-2}	1.644	2.865×10^{5}	3.293×10^{5}
	49	1.041×10^{-2}	1.490	2.946×10^{5}	3.380×10^{5}
	50	9.239×10^{-3}	1.335	3.028×10^{5}	3.468×10^{5}
	51	8.072×10^{-3}	1.180	3.109×10^{5}	3.557×10^{5}
	52	6.905×10^{-3}	1.025	3.190×10^{5}	3.644×10^{5}

Table 7.15 (Continued)

T	ΔS/R	ρ/ρ_0	p/p_0	E/R	H/R
20,000	24	1.140×10	1.611×10^3	1.975×10^5	2.277×10^5
	25	7.603	1.085×10^3	2.065×10^5	2.491×10^5
	26	5.761	8.449×10^2	2.121×10^5	2.561×10^5
	27	3.749	5.554×10^2	2.305×10^5	2.745×10^5
	28	2.994	4.492×10^2	2.377×10^5	2.849×10^5
	29	2.550	3.908×10^2	2.424×10^5	2.901×10^5
	30	1.852	2.989×10^2	2.498×10^5	2.983×10^5
	31	1.327	2.161×10^2	2.635×10^5	3.124×10^5
	32	1.017	1.668×10^2	2.755×10^5	3.254×10^5
	33	8.650×10^{-1}	1.426×10^2	2.860×10^5	3.374×10^5
	34	7.127×10^{-1}	1.184×10^2	2.965×10^5	3.493×10^5
	35	5.694×10^{-1}	9.429×10	3.070×10^5	3.612×10^5
	36	4.081×10^{-1}	6.961×10	3.176×10^5	3.732×10^5
	37	3.314×10^{-1}	5.849×10	3.244×10^5	3.803×10^5
	38	2.825×10^{-1}	5.147×10	3.300×10^5	3.855×10^5
	39	2.363×10^{-1}	4.477×10	3.346×10^5	3.915×10^5
	40	2.173×10^{-1}	4.136×10	3.410×10^5	3.989×10^5
	41	1.982×10^{-1}	3.795×10	3.474×10^5	4.062×10^5
	42	1.791×10^{-1}	3.454×10	3.538×10^5	4.135×10^5
	43	1.600×10^{-1}	3.112×10	3.601×10^5	4.209×10^5
	44	1.410×10^{-1}	2.771×10	3.665×10^5	4.282×10^5
	45	1.219×10^{-1}	2.430×10	3.729×10^5	4.355×10^5
	46	1.028×10^{-1}	2.089×10	3.793×10^5	4.429×10^5
	47	8.372×10^{-2}	1.748×10	3.857×10^5	4.502×10^5

Table 7.15 (Continued)

T	ΔS/R	ρ/ρ_0	p/p_0	E/R	H/R
20,000	48	6.465×10^{-2}	1.406×10	3.920×10^{5}	4.576×10^{5}
	49	5.690×10^{-2}	1.261×10	4.003×10^{5}	4.626×10^{5}
	50	5.064×10^{-2}	1.142×10	4.089×10^{5}	4.720×10^{5}
	51	4.439×10^{-2}	1.023×10	4.174×10^{5}	4.814×10^{5}
	52	3.814×10^{-2}	9.045	4.260×10^{5}	4.909×10^{5}
	53	3.188×10^{-2}	7.857	4.345×10^{5}	5.003×10^{5}
	54	2.563×10^{-2}	6.669	4.431×10^{5}	5.097×10^{5}
	55	2.423×10^{-2}	5.765	4.510×10^{5}	5.226×10^{5}
	56	2.145×10^{-2}	5.134	4.584×10^{5}	5.307×10^{5}
	57	1.867×10^{-2}	4.503	4.658×10^{5}	5.388×10^{5}
	58	1.589×10^{-2}	3.872	4.731×10^{5}	5.470×10^{5}
	59	1.311×10^{-2}	3.241	4.805×10^{5}	5.508×10^{5}
	60	1.080×10^{-2}	2.706	4.873×10^{5}	5.625×10^{5}
	61	9.206×10^{-3}	2.322	4.930×10^{5}	5.689×10^{5}
	62	7.614×10^{-3}	1.938	4.988×10^{5}	5.752×10^{5}
	63	6.370×10^{-3}	1.632	5.038×10^{5}	5.808×10^{5}
	64	5.241×10^{-3}	1.352	5.086×10^{5}	5.860×10^{5}
	65	4.316×10^{-3}	1.120	5.128×10^{5}	5.906×10^{5}
	66	3.533×10^{-3}	0.921	5.165×10^{5}	5.962×10^{5}
25,000	25	8.838	1.755×10^{3}	2.367×10^{5}	2.953×10^{5}
	30	3.234	6.975×10^{2}	2.840×10^{5}	3.498×10^{5}
	35	2.186	4.783×10^{2}	3.363×10^{5}	4.084×10^{5}
	40	1.139	2.813×10^{2}	3.885×10^{5}	4.671×10^{5}
	45	2.677×10^{-1}	7.513×10	4.398×10^{5}	5.246×10^{5}

Table 7.15 (Continued)

T	ΔS/R	ρ/ρ_0	p/p_0	E/R	H/R
25,000	50	1.216×10^{-1}	3.663×10	4.865×10^5	5.769×10^5
	55	5.696×10^{-2}	1.782×10	5.237×10^5	6.186×10^5
	60	2.124×10^{-2}	6.948	5.525×10^5	6.507×10^5
	65	8.044×10^{-3}	2.691	5.773×10^5	6.778×10^5
	70	3.240×10^{-3}	1.111	6.082×10^5	7.038×10^5
30,000	30	6.283	1.885×10^3	4.114×10^5	5.005×10^5
	35	4.541	1.362×10^3	4.321×10^5	5.253×10^5
	40	1.621	5.361×10^2	4.909×10^5	5.947×10^5
	45	7.535×10^{-1}	2.700×10^2	5.316×10^5	6.420×10^5
	50	2.897×10^{-1}	1.110×10^2	5.782×10^5	6.895×10^5
	55	9.942×10^{-2}	3.964×10	6.022×10^5	7.219×10^5
	60	4.709×10^{-2}	1.916×10	6.406×10^5	7.637×10^5
	65	1.977×10^{-2}	8.352	6.888×10^5	8.158×10^5
	70	1.030×10^{-2}	4.516	7.488×10^5	8.805×10^5
	75	6.446×10^{-3}	2.912	8.177×10^5	9.546×10^5
	80	3.642×10^{-3}	1.726	8.885×10^5	1.031×10^6
	85	2.320×10^{-3}	1.142	9.614×10^5	1.109×10^6
	90	1.501×10^{-3}	7.647×10^{-1}	1.035×10^6	1.189×10^6
40,000	50	6.661×10^{-1}	3.628×10^2	7.168×10^5	8.815×10^5
	55	3.461×10^{-1}	1.956×10^2	7.861×10^5	9.581×10^5
	60	1.648×10^{-1}	9.844×10	8.605×10^5	1.040×10^6
	65	1.040×10^{-1}	6.421×10	9.448×10^5	1.133×10^6
	70	6.202×10^{-2}	4.009×10	1.030×10^6	1.226×10^6

Table 7.15 (Continued)

T	ΔS/R	ρ/ρ_0	p/p_0	E/R	H/R
40,000	75	4.105×10^{-2}	2.731×10	1.116×10^{6}	1.320×10^{6}
	80	2.271×10^{-2}	1.602×10	1.200×10^{6}	1.413×10^{6}
	85	1.441×10^{-2}	1.043×10	1.277×10^{6}	1.497×10^{6}
	90	8.558×10^{-3}	6.415	1.346×10^{6}	1.573×10^{6}
	95	4.772×10^{-3}	3.682	1.407×10^{6}	1.639×10^{6}
	100	2.549×10^{-3}	2.009	1.459×10^{6}	1.695×10^{6}
	105	1.385×10^{-3}	1.109	1.505×10^{6}	1.745×10^{6}
50,000	45	5.023	3.333×10^{3}	8.501×10^{5}	1.054×10^{6}
	50	2.393	1.638×10^{3}	9.389×10^{5}	1.155×10^{6}
	55	6.998×10^{-1}	5.595×10^{2}	1.104×10^{6}	1.345×10^{6}
	60	5.143×10^{-1}	3.870×10^{2}	1.172×10^{6}	1.419×10^{6}
	65	3.123×10^{-1}	2.388×10^{2}	1.242×10^{6}	1.499×10^{6}
	70	1.385×10^{-1}	1.498×10^{2}	1.319×10^{6}	1.592×10^{6}
	75	1.023×10^{-1}	9.558×10	1.380×10^{6}	1.662×10^{6}
	80	6.142×10^{-2}	5.884×10	1.436×10^{6}	1.725×10^{6}
	85	3.767×10^{-2}	3.709×10	1.487×10^{6}	1.782×10^{6}
	90	1.904×10^{-2}	1.983×10	1.537×10^{6}	1.838×10^{6}
	95	1.293×10^{-2}	1.472×10	1.576×10^{6}	1.882×10^{6}
	100	6.988×10^{-3}	9.618	1.619×10^{6}	1.929×10^{6}
	105	4.455×10^{-3}	4.762	1.729×10^{6}	2.050×10^{6}
	110	2.922×10^{-3}	3.198	1.809×10^{6}	2.137×10^{6}
	115	2.000×10^{-3}	2.242	1.893×10^{6}	2.229×10^{6}
	120	1.380×10^{-3}	1.586	1.979×10^{6}	2.324×10^{6}

Table 7.15 (Continued)

T	ΔS/R	ρ/ρ_0	p/p_0	E/R	H/R
50,000	125	9.677×10^{-4}	1.139	2.066×10^{6}	2.419×10^{6}
71,000	55	5.730	6.781×10^{3}	1.495×10^{6}	1.860×10^{6}
	60	3.259	3.864×10^{3}	1.636×10^{6}	2.022×10^{6}
	65	1.784	2.146×10^{3}	1.785×10^{6}	2.189×10^{6}
	70	9.689×10^{-1}	1.236×10^{3}	1.962×10^{6}	2.383×10^{6}
	75	4.579×10^{-1}	6.487×10^{2}	2.104×10^{6}	2.541×10^{6}
	80	3.505×10^{-1}	4.846×10^{2}	2.205×10^{6}	2.663×10^{6}
	85	2.236×10^{-1}	3.348×10^{2}	2.247×10^{6}	2.711×10^{6}
	90	1.621×10^{-1}	2.467×10^{2}	2.345×10^{6}	2.820×10^{6}
	95	7.389×10^{-2}	1.194×10^{2}	2.553×10^{6}	3.046×10^{6}
	100	5.280×10^{-2}	8.740×10	2.728×10^{6}	3.233×10^{6}
	105	3.669×10^{-2}	6.113×10	2.899×10^{6}	3.416×10^{6}
	110	2.720×10^{-2}	4.733×10	3.059×10^{6}	3.591×10^{6}
	115	1.872×10^{-2}	3.353×10	3.219×10^{6}	3.766×10^{6}
	120	1.264×10^{-2}	2.349×10	3.370×10^{6}	3.930×10^{6}
	125	9.964×10^{-3}	1.879×10	3.508×10^{6}	4.080×10^{6}
	130	7.290×10^{-3}	1.409×10	3.646×10^{6}	4.229×10^{6}
	135	5.514×10^{-3}	1.087×10	3.722×10^{6}	4.387×10^{6}
	140	4.199×10^{-3}	8.409	3.942×10^{6}	4.548×10^{6}
	145	2.940×10^{-3}	6.050	4.089×10^{6}	4.709×10^{6}
	150	2.315×10^{-3}	4.815	4.231×10^{6}	4.861×10^{6}
	155	1.691×10^{-3}	3.580	4.373×10^{6}	5.014×10^{6}
	160	1.217×10^{-3}	2.626	4.511×10^{6}	5.160×10^{6}
	165	8.823×10^{-4}	1.933	4.640×10^{6}	5.298×10^{6}

Table 7.15 (Continued)

T	ΔS/R	ρ/ρ_0	p/p_0	E/R	H/R
71,000	170	6.514×10^{-4}	1.445	4.759×10^{6}	5.425×10^{6}
	175	4.552×10^{-4}	1.023	4.873×10^{6}	5.547×10^{6}
101,430	70	5.266	1.172×10^{4}	2.741×10^{6}	3.409×10^{6}
	80	2.149	5.104×10^{3}	3.137×10^{6}	3.854×10^{6}
	90	1.130	2.781×10^{3}	3.502×10^{6}	4.270×10^{6}
	100	3.581×10^{-1}	9.747×10^{2}	3.860×10^{6}	4.678×10^{6}
	110	2.074×10^{-1}	5.912×10^{2}	4.247×10^{6}	5.118×10^{6}
	120	9.353×10^{-2}	2.882×10^{2}	4.710×10^{6}	5.645×10^{6}
	130	5.127×10^{-2}	1.631×10^{2}	5.077×10^{6}	6.033×10^{6}
	140	3.549×10^{-2}	1.152×10^{2}	5.232×10^{6}	6.214×10^{6}
	150	2.059×10^{-2}	6.897×10	5.585×10^{6}	6.596×10^{6}
	160	8.667×10^{-3}	3.023×10	6.269×10^{6}	7.342×10^{6}
	170	4.312×10^{-3}	1.583×10	6.786×10^{6}	7.888×10^{6}
	180	3.234×10^{-3}	1.202×10	7.026×10^{6}	8.148×10^{6}
	190	2.156×10^{-3}	8.201	7.267×10^{6}	8.408×10^{6}
	200	1.363×10^{-3}	5.186	7.547×10^{6}	8.710×10^{6}
	210	7.499×10^{-4}	2.964	7.837×10^{6}	9.023×10^{6}
	220	4.352×10^{-4}	1.104	8.043×10^{6}	9.243×10^{6}
140,000	80	7.282	2.646×10^{4}	4.214×10^{6}	5.305×10^{6}
	85	4.884	1.830×10^{4}	4.438×10^{6}	5.564×10^{6}
	90	3.335	1.286×10^{4}	4.743×10^{6}	5.904×10^{6}
	95	2.315	9.166×10^{3}	5.007×10^{6}	6.199×10^{6}
	100	1.651	6.727×10^{3}	5.293×10^{6}	6.526×10^{6}

Table 7.15 (Continued)

T	$\Delta S/R$	ρ/ρ_0	p/p_0	E/R	H/R
140,000	105	1.308	5.420×10^{3}	5.600×10^{6}	6.883×10^{6}
	110	9.654×10^{-1}	4.113×10^{3}	5.906×10^{6}	7.240×10^{6}
	115	7.598×10^{-1}	3.328×10^{3}	6.089×10^{6}	7.454×10^{6}
	120	4.109×10^{-1}	2.085×10^{3}	6.483×10^{6}	7.906×10^{6}
	125	2.732×10^{-1}	1.698×10^{3}	6.734×10^{6}	8.189×10^{6}
	130	2.553×10^{-1}	1.256×10^{3}	6.975×10^{6}	8.261×10^{6}
	135	1.837×10^{-1}	9.168×10^{2}	7.298×10^{6}	8.807×10^{6}
	140	1.210×10^{-1}	6.179×10^{2}	7.585×10^{6}	9.192×10^{6}
	145	9.706×10^{-2}	5.039×10^{2}	7.836×10^{6}	9.401×10^{6}
	150	8.150×10^{-2}	4.256×10^{2}	7.995×10^{6}	9.576×10^{6}
	155	6.594×10^{-2}	3.474×10^{2}	8.154×10^{6}	9.751×10^{6}
	160	5.037×10^{-2}	2.691×10^{2}	8.312×10^{6}	9.926×10^{6}
	165	3.747×10^{-2}	2.031×10^{2}	8.472×10^{6}	1.010×10^{7}
	170	2.852×10^{-2}	1.557×10^{2}	8.623×10^{6}	1.027×10^{7}
	175	1.967×10^{-2}	1.088×10^{2}	8.776×10^{6}	1.043×10^{7}
	180	1.467×10^{-2}	8.154×10	8.901×10^{6}	1.057×10^{7}
	185	1.005×10^{-2}	5.863×10	9.020×10^{6}	1.070×10^{7}
180,000	95	5.437	2.994×10^{4}	6.214×10^{6}	7.866×10^{6}
	100	3.836	2.168×10^{4}	6.551×10^{6}	8.248×10^{6}
	105	2.845	1.640×10^{4}	6.871×10^{6}	8.614×10^{6}
	110	1.928	1.148×10^{4}	7.188×10^{6}	8.978×10^{6}
	115	1.291	8.052×10^{3}	7.417×10^{6}	9.343×10^{6}
	120	8.252×10^{-1}	5.483×10^{3}	7.685×10^{6}	9.706×10^{6}
	125	6.440×10^{-1}	4.323×10^{3}	8.058×10^{6}	1.007×10^{7}

Table 7.15 (Continued)

T	ΔS/R	ρ/ρ_0	p/p_0	E/R	H/R
180,000	130	4.628×10^{-1}	3.163×10^{3}	8.430×10^{6}	1.042×10^{7}
	135	3.608×10^{-1}	2.436×10^{3}	8.633×10^{6}	1.064×10^{7}
	140	2.764×10^{-1}	1.947×10^{3}	8.860×10^{6}	1.094×10^{7}
	145	1.979×10^{-1}	1.410×10^{3}	9.018×10^{6}	1.111×10^{7}
	150	1.503×10^{-1}	1.077×10^{3}	9.165×10^{6}	1.130×10^{7}
	155	1.027×10^{-1}	7.432×10^{2}	9.311×10^{6}	1.148×10^{7}
	160	7.850×10^{-2}	5.699×10^{2}	9.422×10^{6}	1.161×10^{7}
	165	5.609×10^{-2}	4.091×10^{2}	9.529×10^{6}	1.172×10^{7}
	170	3.700×10^{-2}	2.684×10^{2}	9.628×10^{6}	1.183×10^{7}
	175	2.647×10^{-2}	1.916×10^{2}	9.701×10^{6}	1.191×10^{7}
	180	1.725×10^{-2}	1.276×10^{2}	9.764×10^{6}	1.198×10^{7}

Table 7.16

PROPERTIES OF AIR ALONG THE ADIABATICS

$\Delta S/R$	ρ/ρ_0	$\gamma - 1$
20	0.0414	0.15421
	0.8074	0.15693
	1.858	0.16146
	3.841	0.16866
	6.6489	0.17623
	11.47	0.18983
21	0.0396	0.15068
	0.6125	0.15364
	1.3916	0.15889
	2.699	0.16647
	4.576	0.17436
	8.527	0.18866
	11.07	0.19864
22	0.0378	0.14781
	0.4542	0.15132
	1.785	0.16467
	3.104	0.17286
	5.103	0.18755
	10.72	0.21001
23	0.0360	0.14575
	0.3355	0.14934
	1.230	0.16334
	1.817	0.17154
	3.723	0.18677
	7.935	0.20356
	10.55	0.21231
24	0.0342	0.14428
	0.2732	0.14582
	1.083	0.17056
	2.253	0.18582
	4.914	0.20175
	10.39	0.21450
25	0.0325	0.14152
	0.2138	0.14296

$\Delta S/R$	ρ/ρ_0	$\gamma - 1$
25	0.7984	0.17115
	1.4513	0.18611
	2.4864	0.22263
	10.23	0.21717
26	0.0307	0.14252
	0.1545	0.14133
	0.5711	0.16903
	2.000	0.22055
	5.761	0.20745
	10.10	0.22526
27	0.0288	0.14212
	0.0999	0.14210
	0.3240	0.16604
	1.157	0.21923
	3.749	0.19280
	9.974	0.23514
28	0.0271	0.14195
	0.0741	0.14063
	0.2154	0.16479
	0.7862	0.21125
	2.994	0.18935
	9.849	0.24506
29	0.0253	0.14202
	0.0484	0.13994
	0.1313	0.16399
	0.5551	0.20783
	2.550	0.18965
	3.794	0.23586
	9.736	0.24390
30	0.0235	0.14383
	0.0296	0.13980
	0.0832	0.16328
	0.4310	0.21209
	1.8519	0.19384

Table 7.16 (Continued)

$\Delta S/R$	ρ/ρ_0	$\gamma - 1$
30	3.2337	0.22784
	9.639	0.23813
35	0.01384	0.15522
	0.1143	0.17455
	0.5694	0.16182
	2.786	0.19514
	4.541	0.20829
	9.292	0.23991
40	0.01166	0.14301
	0.04054	0.16851
	0.2173	0.16751
	1.139	0.19073
	1.621	0.20210
	9.068	0.24677
45	0.009491	0.13902
	0.01789	0.15532
	0.1219	0.16042
	0.2677	0.19145
	0.7535	0.20220
	5.023	0.23418
	9.000	0.24542
50	0.007318	0.13879
	0.009239	0.14314
	0.05064	0.16547
	0.1216	0.18571
	0.2896	0.19882
	0.6661	0.22796
	2.393	0.21866
	9.000	0.24793
55	0.006112	0.14085
	0.02423	0.15823
	0.05696	0.17921
	0.09942	0.19867
	0.34612	0.21565
	0.6998	0.21726
55	5.730	0.24439
	9.054	0.24361
60	0.005043	0.14508
	0.01080	0.15428
	0.02124	0.17760
	0.04709	0.19059
	0.1647	0.20867
	0.5143	0.21118
	3.259	0.23552
	9.132	0.24741
65	0.003975	0.15058
	0.004316	0.15176
	0.008044	0.17383
	0.01977	0.18402
	0.1040	0.19877
	0.3123	0.20696
	1.784	0.22552
	9.195	0.24336
70	0.003030	0.16633
	0.003243	0.16890
	0.01030	0.17568
	0.06202	0.19037
	0.1385	0.20660
	0.9689	0.21445
	5.266	0.23146
	9.157	0.24245
75	0.002667	0.16169
	0.006446	0.16572
	0.04105	0.18308
	0.1023	0.20377
	0.4579	0.20794
	3.707	0.22005
	9.118	0.24490
80	0.002386	0.15669
	0.003642	0.16008

Table 7.16 (Continued)

$\Delta S/R$	ρ/ρ_0	$\gamma - 1$
80	0.02271	0.17703
	0.06142	0.20111
	0.3505	0.20756
	2.149	0.21573
	7.282	0.24571
	8.974	0.25006
85	0.002105	0.15383
	0.002320	0.15349
	0.01441	0.17212
	0.03767	0.19855
	0.2236	0.20659
	1.640	0.20650
	4.884	0.24060
	8.730	0.25781
90	0.001878	0.15328
	0.008558	0.16811
	0.01904	0.19603
	0.1621	0.20249
	1.130	0.20034
	3.335	0.24467
	8.489	0.26697
95	0.001678	0.15428
	0.004772	0.16486
	0.01293	0.19381
	0.07389	0.19376
	0.7440	0.20578
	2.315	0.23800
	5.437	0.26589
	8.296	0.27342
100	0.001479	0.15624
	0.002549	0.16211
	0.006988	0.19141
	0.05280	0.18497
	0.3581	0.21753
	1.651	0.23297
	3.836	0.25911
100	8.102	0.28119
105	0.00128	0.15868
	0.001384	0.15963
	0.004455	0.18554
	0.03569	0.17827
	0.2828	0.20496
	1.308	0.22927
	2.845	0.25380
	6.817	0.27818
	7.854	0.29239
110	0.001167	0.16074
	0.002922	0.18154
	0.02720	0.17380
	0.2074	0.20530
	0.9654	0.22588
	1.928	0.24909
	4.837	0.27368
	7.544	0.30627
115	0.001072	0.16304
	0.002	0.17773
	0.01872	0.16979
	0.1505	0.20173
	0.7598	0.22408
	1.291	0.25977
	3.385	0.28395
	6.030	0.31294
	7.177	0.32699
120	0.000977	0.16559
	0.001380	0.17420
	0.01264	0.16619
	0.09353	0.19845
	0.4109	0.21953
	0.8252	0.25303
	2.204	0.27801
	4.184	0.31071
	6.761	0.35124

Table 7.16 (Continued)

$\Delta S/R$	ρ/ρ_0	$\gamma - 1$
125	0.000881	0.16840
	0.000968	0.17118
	0.009964	0.16295
	0.07240	0.19326
	0.2732	0.21609
	0.6440	0.23741
	1.684	0.26524
	2.966	0.30950
	6.184	0.37243
	6.412	0.36854
130	0.000818	0.16757
	0.00729	0.15993
	0.05127	0.18848
	0.2552	0.21170
	0.4628	0.23103
	1.249	0.26333
	1.947	0.31137
	4.295	0.37115
	6.503	0.35884
135	0.000776	0.15719
	0.005514	0.15701
	0.04338	0.18816
	0.1837	0.20676
	0.3608	0.23236
	0.8144	0.26758
	1.5463	0.31059
	3.0599	0.36754
	6.594	0.35344

Table 7.17

RATE OF CHANGE OF SHOCK PRESSURE WITH ENTROPY

$\Delta S/R$	$[d \ln (p_s/p_0)]/d(\Delta S/R)$
0.1	4.4458
0.2	2.3603
0.3	1.7583
0.4	1.4474
0.5	1.2385
0.6	1.0816
0.7	1.0021
0.8	0.9226
0.9	0.8553
1.0	0.8169
1.5	0.6723
2.0	0.5843
2.5	0.5134
3.0	0.4680
3.5	0.4347
4.0	0.4115
4.5	0.3842
5	0.3481
6	0.2877
7	0.2657
8	0.2583
9	0.2163
10	0.1992
11	0.1691
12	0.1537
13	0.1474
14	0.1351
15	0.1238
16	0.1210
17	0.1079
18	0.09789
19	0.09037
20	0.09471
21	0.10195
22	0.10750
23	0.11305
24	0.11217
25	0.11028
26	0.10840
27	0.10656
28	0.10429
29	0.10330
30	0.10065
35	0.07265
40	0.06484
45	0.06027
50	0.05456
55	0.04885
60	0.04396
65	0.04025
70	0.03654
75	0.03437
80	0.03252
85	0.03103
90	0.03044
95	0.02984
100	0.02970
105	0.02970
110	0.0297
125	0.0298
130	0.0299
135	0.02961
140	0.02902
145	0.02843
150	0.02784

$$X = a(S)\frac{\rho}{\rho_0} \tag{7.88}$$

Here a, b, g, and h are functions of the entropy. Alternatively they can be considered as functions of the shock pressure, which raised the air to the given entropy.

The IBM run was started when the shock pressure had dropped to about 80 atm. This pressure raises the entropy by 5.4 R. In the interior we have mass elements at lower pressures (down to 39 atm) and higher entropies, and we require the adiabatics for these entropies from the given pressure down to somewhat below 1 atm. The constants a and b were therefore chosen in such a way as to get a good fit in this region. a and b as functions of the entropy were still rough and had to be smoothed considerably.

For shock pressures below 80 atm, we require the adiabatics only from the shock pressure down to somewhat below 1 atm. Hirschfelder and Magee used the following scheme to determine the constants. According to the Hugoniot relationship between shock pressure and shock density

$$\gamma = \left(\frac{p_s/p_0 - 1}{p_s/p_0 + 1}\right)\left(\frac{\rho_s/\rho_0 + 1}{\rho_s/\rho_0 - 1}\right) \tag{7.89}$$

From the tables of Brinkley, Kirkwood, and Richardson, they computed the value of gamma for different values of the shock pressure. This procedure was satisfactory except for small values of the shock pressure where the above equation becomes essentially indeterminate. For these small values of shock pressure, gamma is very close to 1.4 and it was sufficiently accurate to assume that gamma varies linearly with ρ_0/ρ_s between $\gamma = 1.3966$ at $\rho_0/\rho_s = 0.52$ (or $p_s/p_0 = 2.578$) and standard conditions. They checked this assumption by determining gamma independently from the shock temperature and the thermochemical properties of air. The agreement was quite good. The values of gamma obtained in this way were quite smooth and needed only the slightest changes to eliminate small fluctuations. Having obtained gamma as a function of ρ_0/ρ_s, they obtained the constant a by asserting that to a good approximation

$$p/p_0 = (g + h)(\rho/\rho_0)^{\gamma} \tag{7.90}$$

Expanding $(\rho/\rho_0)^{\gamma}$ in the vicinity of $p/p_0 = 1$

$$p/p_0 = (g + h)\ \{2(\gamma - 1)(\rho/\rho_0)^{1.5} + [1 - 2(\gamma - 1)]\ (\rho/\rho_0)\} \tag{7.91}$$

so that

$$\frac{g}{h} = \frac{2(\gamma - 1)}{1 - 2(\gamma - 1)}$$

But p/p_0 can also be written

$$p/p_0 = b[a^{1.5}\ (\rho/\rho_0)^{1.5} + a(\rho/\rho_0)] \tag{7.92}$$

and

$$a = \left(\frac{g}{h}\right)^2 = \left[\frac{2(\gamma - 1)}{1 - 2(\gamma - 1)}\right]^2 \tag{7.93}$$

Keeping ρ_0/ρ_s as the independent variable, we can express the shock pressure in the form

$$p_s p_0 = \frac{\left[1/\gamma + \dfrac{1 - \rho_0/\rho_s}{1 + \rho_0/\rho_s}\right]}{\left[\dfrac{1 - \rho_0/\rho_s}{1 + \rho_0/\rho_s} - 1/\gamma\right]} \tag{7.94}$$

Then the constant b is determined by the equation

$$b = (p_s/p_0)/[a^{1.5}\ (\rho_s/\rho_0)^{1.5} + a(\rho_s/\rho_0)] \tag{7.95}$$

The values of the constants are given in Table 7.18.

In using this formulation for the equation of state, the velocity of sound c can be expressed in terms of the normal velocity of sound, $c_0 = 3.472 \times 10^4$ cm/sec, by the relation

$$c/c_0 = \sqrt{(15/14\ ab)}\quad \sqrt{X^{1/2} + 2/3} \tag{7.96}$$

Table 7.18

SMOOTHED EQUATION OF STATE OF AIR

p_s/p_0	ρ_0/ρ_s	$\Delta S/R$	T_s	γ	$1/a$	b
1.00000	1.000	0	300.0	1.40000	0.06250	0.012500
1.00704	0.995	0	300.6	1.39996	0.06256	0.012516
1.01469	0.990	0.0000005	301.2	1.39993	0.06261	0.012531
1.02138	0.985	0.0000006	301.8	1.39989	0.06267	0.012547
1.02869	0.980	0.0000012	302.4	1.39986	0.06272	0.012562
1.03608	0.975	0.0000052	303.1	1.39982	0.06278	0.012578
1.04356	0.970	0.0000086	303.7	1.39979	0.06283	0.012593
1.05114	0.965	0.0000127	304.3	1.39975	0.06289	0.012609
1.05881	0.960	0.0000179	304.9	1.39972	0.06294	0.012624
1.06658	0.955	0.0000288	305.6	1.39968	0.06300	0.012640
1.07445	0.950	0.0000386	306.2	1.39965	0.06305	0.012655
1.08242	0.945	0.0000501	306.9	1.39961	0.06311	0.012671
1.09049	0.940	0.0000680	307.5	1.39958	0.06317	0.012686
1.09866	0.935	0.0000841	308.2	1.39954	0.06322	0.012702
1.10695	0.930	0.0001066	308.8	1.39950	0.06328	0.012718
1.11534	0.925	0.0001320	309.5	1.39947	0.06333	0.012733
1.12384	0.920	0.0001631	310.2	1.39943	0.06339	0.012749
1.13246	0.915	0.0001966	310.9	1.39940	0.06345	0.012764
1.14119	0.910	0.0002358	311.5	1.39936	0.06350	0.012780
1.15004	0.905	0.0002779	312.2	1.39933	0.06356	0.012796
1.15900	0.900	0.0003275	312.9	1.39929	0.06361	0.012812
1.16810	0.895	0.0003812	313.6	1.39926	0.06367	0.012827
1.17731	0.890	0.0004435	314.3	1.39922	0.06373	0.012843
1.18666	0.885	0.0005111	315.1	1.39919	0.06378	0.012859
1.19613	0.880	0.0005867	315.8	1.39915	0.06384	0.012875
1.20574	0.875	0.0006692	316.5	1.39912	0.06389	0.012891
1.21548	0.870	0.0007593	317.2	1.39908	0.06395	0.012907
1.22537	0.865	0.0008569	318.0	1.39904	0.06401	0.012923
1.23539	0.860	0.0009631	318.7	1.39901	0.06406	0.012939
1.24556	0.855	0.0010792	319.5	1.39897	0.06412	0.012955
1.25588	0.850	0.0012057	320.2	1.39894	0.06417	0.012971
1.26635	0.845	0.0013432	321.0	1.39890	0.06423	0.012987
1.27697	0.840	0.0014905	321.8	1.39887	0.06429	0.013003
1.28776	0.835	0.0016500	322.6	1.39883	0.06434	0.013019
1.29870	0.830	0.0018216	323.4	1.39880	0.06440	0.013036

Table 7.18 (Continued)

p_s/p_0	ρ_0/ρ_s	$\Delta S/R$	T_s	γ	$1/a$	b
1.30981	0.825	0.0020054	324.2	1.39876	0.06446	0.013052
1.32109	0.820	0.0022025	325.0	1.39873	0.06451	0.013068
1.33254	0.815	0.0024135	325.8	1.39869	0.06457	0.013085
1.34417	0.810	0.0026396	326.6	1.39865	0.06463	0.013102
1.35598	0.805	0.0028801	327.5	1.39862	0.06468	0.013118
1.36798	0.800	0.0031363	328.3	1.39858	0.06474	0.013135
1.38017	0.795	0.0035907	329.2	1.39855	0.06480	0.013152
1.392549	0.790	0.0037013	330.0	1.39851	0.06485	0.013169
1.405130	0.785	0.0040108	330.9	1.39848	0.06491	0.013186
1.417915	0.780	0.0043146	331.8	1.39844	0.06497	0.013203
1.430910	0.775	0.0046872	332.7	1.39841	0.06502	0.013220
1.444119	0.770	0.0050563	333.6	1.39837	0.06508	0.013237
1.457548	0.765	0.0054475	334.5	1.39834	0.06514	0.013254
1.471205	0.760	0.0058666	335.4	1.39830	0.06519	0.013272
1.485088	0.755	0.0063001	336.4	1.39827	0.06525	0.013289
1.499210	0.750	0.0067621	337.3	1.39823	0.06531	0.013307
1.513575	0.745	0.0072484	338.3	1.39819	0.06537	0.013325
1.528190	0.740	0.0077638	339.3	1.39816	0.06542	0.013343
1.543061	0.735	0.0083064	340.2	1.39812	0.06548	0.013361
1.558195	0.730	0.0089052	341.2	1.39809	0.06554	0.013379
1.573598	0.725	0.0094804	342.3	1.39805	0.06559	0.013398
1.589278	0.720	0.0101136	343.3	1.39802	0.06565	0.013416
1.605244	0.715	0.01107816	344.3	1.39798	0.06571	0.013435
1.621502	0.710	0.0114826	345.4	1.39795	0.06577	0.013454
1.638061	0.705	0.0122209	346.4	1.39791	0.06582	0.013473
1.654928	0.700	0.0129951	347.5	1.39788	0.06588	0.013492
1.672114	0.695	0.0138420	348.6	1.39784	0.06594	0.013512
1.689626	0.690	0.0146616	349.8	1.39781	0.06600	0.013531
1.707474	0.685	0.0155567	350.9	1.39777	0.06605	0.013551
1.725669	0.680	0.0164959	352.0	1.39773	0.06611	0.013571
1.744220	0.675	0.0174865	353.2	1.39770	0.06617	0.013592
1.763137	0.670	0.0185367	354.4	1.39766	0.06623	0.013612
1.782432	0.665	0.0195931	355.6	1.39763	0.06628	0.013633
1.802117	0.660	0.0207265	356.8	1.39759	0.06634	0.013654
1.822203	0.655	0.0219128	358.1	1.39756	0.06640	0.013675

Table 7.18 (Continued)

p_s/p_0	ρ_0/ρ_s	$\Delta S/R$	T_s	γ	$1/a$	b
1.842702	0.650	0.0231549	359.3	1.39752	0.06646	0.013697
1.863627	0.645	0.0244848	360.6	1.39749	0.06651	0.013719
1.884994	0.640	0.0258153	361.9	1.39745	0.06657	0.013741
1.906813	0.635	0.0272371	363.2	1.39742	0.06663	0.013764
1.929101	0.630	0.0287266	364.6	1.39738	0.06669	0.013787
1.951874	0.625	0.0302825	366.0	1.39734	0.06675	0.013810
1.975146	0.620	0.0319103	367.4	1.39730	0.06680	0.013834
1.998934	0.615	0.0336113	368.8	1.39727	0.06686	0.013858
2.023256	0.610	0.0353892	370.3	1.39724	0.06692	0.013882
2.048130	0.605	0.0372486	371.7	1.39720	0.06698	0.013907
2.073576	0.600	0.0391917	373.2	1.39717	0.06704	0.013932
2.099611	0.595	0.0412199	374.8	1.39713	0.06709	0.013958
2.126259	0.590	0.0433891	376.3	1.39710	0.06715	0.013985
2.153540	0.585	0.0456708	377.9	1.39706	0.06721	0.014012
2.181478	0.580	0.0478674	379.6	1.39703	0.06727	0.014039
2.210096	0.575	0.0502831	381.2	1.39699	0.06733	0.014067
2.239420	0.570	0.0528108	382.9	1.39696	0.06739	0.014095
2.269476	0.565	0.0554426	384.7	1.39692	0.06744	0.014125
2.300292	0.560	0.0581956	386.4	1.39688	0.06750	0.014154
2.331897	0.555	0.0610700	388.3	1.39685	0.06756	0.014185
2.364321	0.550	0.0640718	390.1	1.39681	0.06762	0.014216
2.397598	0.545	0.0672062	392.0	1.39678	0.06768	0.014248
2.431761	0.540	0.0704810	393.9	1.39674	0.06773	0.014281
2.466845	0.535	0.0738457	395.9	1.39671	0.06780	0.014314
2.502890	0.530	0.0774729	398.0	1.39667	0.06786	0.014349
2.539934	0.525	0.0811402	400.0	1.39664	0.06791	0.014384
2.578021	0.520	0.0850969	402.2	1.39660	0.06797	0.014420
2.617909	0.515	0.0898540	404.5	1.39656	0.06803	0.014458
2.657494	0.510	0.0934026	406.6	1.39653	0.06809	0.014497
2.698979	0.505	0.0978513	408.9	1.39649	0.06816	0.014538
2.741698	0.500	0.1025353	411.2	1.39645	0.06822	0.014580
2.785708	0.495	0.1073368	413.7	1.39641	0.06829	0.014623
2.831067	0.490	0.1124028	416.2	1.39637	0.06835	0.014669
2.877839	0.485	0.1176608	418.7	1.39633	0.06842	0.014716
2.926090	0.480	0.1232320	421.4	1.39629	0.06849	0.014766
2.975892	0.475	0.1290190	424.1	1.39624	0.06856	0.014817

Table 7.18 (Continued)

p_s/p_0	ρ_0/ρ_s	$\Delta S/R$	T_s	γ	$1/a$	b
3.027320	0.470	0.1350707	426.9	1.39620	0.06863	0.014870
3.080454	0.465	0.1414009	429.7	1.39615	0.06871	0.014926
3.135380	0.460	0.1480221	432.7	1.39611	0.06879	0.014984
3.192190	0.455	0.1549506	435.7	1.39606	0.06887	0.015045
3.250984	0.450	0.1622031	438.9	1.39601	0.06896	0.015109
3.311865	0.445	0.1697973	442.1	1.39596	0.06904	0.015176
3.374948	0.440	0.1777438	445.5	1.39590	0.06913	0.015246
3.440355	0.435	0.1860712	449.0	1.39585	0.06922	0.015319
3.508211	0.430	0.1947959	452.6	1.39579	0.06932	0.015396
3.578655	0.425	0.2039431	456.3	1.39573	0.06942	0.015477
3.651833	0.420	0.2136190	460.1	1.39567	0.06953	0.015563
3.727903	0.415	0.2277592	464.4	1.39560	0.06964	0.015656
3.807035	0.410	0.2341280	468.3	1.39553	0.06977	0.015755
3.889405	0.405	0.2454080	472.6	1.39544	0.06991	0.015862
3.975215	0.400	0.2568153	477.0	1.39535	0.07006	0.015977
4.064681	0.395	0.2690200	481.7	1.39525	0.07024	0.016101
4.158038	0.390	0.2818436	486.5	1.39514	0.07042	0.016235
4.255542	0.385	0.2932255	491.5	1.39502	0.07063	0.016380
4.357409	0.380	0.3094965	496.7	1.39488	0.07087	0.016541
4.463938	0.375	0.3239	502.2	1.39472	0.07114	0.016720
4.575454	0.370	0.3391	507.9	1.39454	0.07145	0.016916
4.692314	0.365	0.3549	513.8	1.39434	0.07179	0.017131
4.814908	0.360	0.3715	520.0	1.39412	0.07217	0.017366
4.943583	0.355	0.3890	526.5	1.39387	0.07261	0.017627
5.078802	0.350	0.4073	533.3	1.39359	0.07309	0.017918
5.221069	0.345	0.4266	540.4	1.39328	0.07364	0.018234
5.370947	0.340	0.4469	547.8	1.39294	0.07423	0.018584
5.529059	0.335	0.4683	555.7	1.39257	0.07489	0.018963
5.696101	0.330	0.4910	563.9	1.39217	0.07560	0.019384
5.872843	0.325	0.5150	572.6	1.39174	0.07637	0.019840
6.060152	0.320	0.5403	581.8	1.39128	0.07720	0.020336
6.258999	0.315	0.5673	591.5	1.39079	0.07810	0.020876
6.470481	0.310	0.5960	601.8	1.39027	0.07905	0.021463
6.695832	0.305	0.6265	612.7	1.38972	0.08007	0.022102
6.936290	0.300	0.6591	624.3	1.38913	0.08118	0.022803
7.193415	0.295	0.6940	636.6	1.38850	0.08237	0.023573

Table 7.18 (Continued)

p_s/p_0	ρ_0/ρ_s	$\Delta S/R$	T_s	γ	1/a	b
7.468993	0.290	0.7314	649.8	1.38783	0.08365	0.024419
7.765072	0.285	0.7715	663.9	1.38712	0.08502	0.025345
8.084018	0.280	0.8147	679.1	1.38637	0.08649	0.026364
8.428321	0.275	0.8614	695.3	1.38557	0.08808	0.027494
8.801106	0.270	0.9120	712.9	1.38472	0.08979	0.028745
9.206045	0.265	0.9656	731.9	1.38382	0.09162	0.030134
9.647125	0.260	1.0225	752.5	1.38286	0.09361	0.031688
10.129009	0.255	1.0841	774.9	1.38183	0.09578	0.033437
10.657185	0.250	1.1498	799.3	1.38072	0.09816	0.035419
11.238590	0.245	1.2222	826.0	1.37953	0.10075	0.037669
11.880092	0.240	1.3021	855.4	1.37823	0.10365	0.040261
12.589677	0.235	1.3848	887.6	1.37679	0.10693	0.043286
13.377246	0.230	1.4754	923.0	1.37519	0.11066	0.046846
14.253156	0.225	1.5736	962.1	1.37339	0.11498	0.051089
15.229965	0.220	1.676	1005.2	1.37136	0.11999	0.056194
16.323461	0.215	1.790	1052.9	1.36908	0.12538	0.062373
17.550159	0.210	1.915	1105.7	1.36652	0.13263	0.069909
18.935429	0.205	2.049	1164.5	1.36366	0.14056	0.079371
20.505376	0.200	2.193	1230.3	1.36050	0.14974	0.090301
22.292772	0.195	2.344	1304.1	1.35700	0.16042	0.104804
24.335644	0.190	2.516	1387.1	1.35316	0.17287	0.122639
26.681095	0.185	2.699	1480.8	1.34893	0.18743	0.145230
29.384061	0.180	2.904	1586.7	1.34430	0.20450	0.174111
32.511013	0.175	3.121	1706.8	1.33924	0.22456	0.211371
36.139438	0.170	3.359	1843.1	1.33373	0.24823	0.259893
40.358840	0.165	3.620	1997.8	1.32774	0.27625	0.323653
45.268966	0.160	3.888	2172.9	1.32126	0.30955	0.408141
50.975052	0.155	4.176	2370.3	1.31427	0.34929	0.520926
57.57373	0.150	4.483	2590.8	1.30675	0.39693	0.674805
65.131941	0.145	4.811	2833.2	1.29868	0.45431	0.876315
73.646167	0.140	5.164	3093.1	1.29007	0.52391	1.151158
94.73	7.684	6	3606		0.7937	2.3797
124.89	8.374	7	4248		1.2270	5.0657
161.17	9.134	8	4812		1.6667	8.8022
224.49	9.753	9	5451		2.0000	14.3488
250.79	10.258	10	6021		2.3256	18.3394

Table 7.18 (Continued)

p_s/p_0	ρ_0/ρ_s	$\Delta S/R$	T_s	γ	1/a	b
301.03	10.700	11	6648		2.5641	23.7077
352.63	11.060	12	7050		2.6316	27.5087
410.00	11.395	13	7530		2.5316	29.1810
491.11	11.703	14	8001		2.2727	29.1733
532.50	11.885	15	8475		2.0408	26.7892
602.14	12.033	16	8838		1.7699	24.5515
671.14	12.083	17	9537		1.4925	21.5594
747.86	11.984	18	10254		1.2658	19.3758
820.07	11.777	19	11004		1.0417	16.6271
899.17	11.473	20	12012		0.8658	14.6232
993.0	11.068	21	13392		0.6944	12.4802
1094.0	10.72	22	14920		0.5435	10.1931
1248.6	10.55	23	16486		0.4132	8.0798
1408.3	10.39	24	18083		0.3384	7.0126
1568.1	10.23	25	19680		0.2890	6.3749
1763.0	10.10	26	21253		0.2513	5.9750
1966.8	9.974	27	22821		0.2247	5.7834
2170.5	9.849	28	24389		0.2033	5.6264
2412.2	9.736	29	26081		0.1866	5.6207
2678.2	9.629	30	27854		0.1736	5.7164
4039.3	9.292	35	36929		0.1300	5.9799
5688.0	9.068	40	46600		0.1048	6.3829

and the Riemannian variable $\sigma = \left[\int_{p_0}^{p} \frac{dp}{c\rho}\right]_{s=\text{constant}}$ is given by the equation

$$\sigma/c_0 = 4\sqrt{(15/14)\,ab}\left\{\sqrt{X^{1/2} + 2/3} - \sqrt{X_0^{1/2} + 2/3}\right.$$

$$\left. - \frac{2}{\sqrt{6}}\ln\left(\frac{\sqrt{X^{1/2} + 2/3} + \sqrt{2/3}}{\sqrt{X_0^{1/2} + 2/3} + \sqrt{2/3}}\right) + \frac{1}{2\sqrt{6}}\ln\left(\frac{X}{X_0}\right)\right\} \qquad (7.97)$$

Here X_0 is the value of X when $p/p_0 = 1$, keeping the entropy constant, or X_0 is the solution to the equation

$$X_0^{3/2} + X_0 = \frac{1}{b} \qquad (7.98)$$

7.6 Approximate Form Used for IBM Run of HE Explosion

It was necessary to begin this calculation immediately after the blast wave left the explosive charge, when the shock pressure was about 575 atm. It was felt that the approximate form described in the last section was not quite good enough at these higher shock pressures; for this reason, and to remove some irregularities in the low-pressure region, new calculations using a different form of approximation were made by Skyrme.

The primary data used were taken from the report of Brinkley, Kirkwood, and Richardson;[3] however the derived tables (Hugoniot curve and adiabatics) given in that report were not used. The equation of state

$$pV = (1 + \alpha)\,RT \qquad (7.99)$$

was used throughout, combined with the values of α and E/RT given by the above authors.

At temperatures $T < 1800°K$, $\alpha = 0$ and E is a function only of T independent of the density, in a sufficiently good approximation. The data given could be represented by the empirical formula

$$\frac{E}{RT} = 2.5 + 0.0444\,(\ln x)^2 + 0.0464\,(\ln x)^3 \qquad (7.100)$$

where $x = T/T_0$, $T_0 = 300°K$. Combined with the equation $pV = RT$ this leads to the following expression for the entropy

$$\frac{S}{R} = \left(\ln \frac{V}{V_0}\right) + 2.5 \ln x + 0.0444 (\ln x)^2 + 0.0612 (\ln x)^3 + 0.0116 (\ln x)^4 \quad (7.101)$$

The Hugoniot curve was recalculated from the primary data. For shock pressures less than 35 atm, Eq. 7.100 holds and the shock conditions lead to the equations

$$\left(\frac{p_s}{p_0}\right)\left(\frac{V_s}{V_0}\right) = \frac{T_s}{T_0} = x$$

$$\frac{1}{2}\left(\frac{p_s}{p_0} + 1\right)\left(1 - \frac{V_s}{V_0}\right) = 2.5(x - 1) + 0.0444 (\ln x)^2 + 0.0464 \times (\ln x)^3 \quad (7.102)$$

Above 35 atm the Hugoniot curve was determined by quadratic interpolation from the primary data in Brinkley, Kirkwood, and Richardson. The results, for shock pressures between 35 and 750 atm, were represented by the empirical formula

$$\frac{V_s}{V_0} = 0.171128 - 0.0463787 z + 0.0191332 z^2 - 0.003176683 z^3 + 0.02322615 z^4 - 0.007111593 z^5 + 0.000800185 z^6 \quad (7.103)$$

$$z = \ln\left(\frac{p_s}{35} p_0\right) \quad (7.104)$$

This newly determined Hugoniot curve does not differ significantly from that obtained from Table 7.18.

The equations of the adiabatics were fitted into the form

$$p = A(S)\rho^{1.4} + B(S)\rho^{1.3} + C(S)\rho^{1.2} \quad (7.105)$$

or the equivalent form

$$\frac{p}{p_0} = y^{-1.4}\left[1 - \alpha(1 - y^{0.1}) - \beta(1 - y^{0.1})^2\right] \tag{7.106}$$

$$\frac{1}{y} = \delta\frac{\rho}{\rho_0} \tag{7.107}$$

where A, B, C, α, β, and δ are functions of the entropy. These three constants of entropy were determined for each adiabatic by the conditions

(a) $p = p_s$ when $V = V_s$ (correct at shock pressure)

(b) $p = p_0$ when $V = V_1$ (correct at normal pressure)

(c) $\int_{V_s}^{V_1} pdV = E_s - E_1$ (correct energy change)

where the subscript 1 refers to values at a pressure of 1 atm. These conditions were chosen with regard to the particular problem on hand. The coefficients α and β were determined by calculating their values from the above conditions for a number of values of p_s/p_0 (an expansion was used for $p_s/p_0 \approx 1$ when the conditions lead to indeterminate equations), and then interpolating graphically; it was found that $\alpha = 0$ was a sufficiently good approximation for $p_s/p_0 < 5$. The value of δ, which is less sensitive than α and β, was found by applying condition (a) to Eqs. 7.106 and 7.107 with the values of α and β already determined.

A condensed table of the values of V_s/V_0, α and β as functions of p_s/p_0 is given in Table 7.19. All other quantities used were derived from these to ensure consistency.

Table 7.19

VALUES OF V_s/V_0, α, AND β AS FUNCTIONS OF p_s/p_0

p_s/p_0	V_s/V_0	α	β
1.00	1.00000	0	0.2845
1.25	0.85289	0	0.3261
1.50	0.74984	0	0.3667
1.75	0.67362	0	0.4052
2.00	0.61494	0	0.4421
2.25	0.56837	0	0.4777
2.50	0.53049	0	0.5121
2.75	0.49907	0	0.5457
3.00	0.47258	0	0.5792
3.25	0.44994	0	0.6125
3.50	0.43036	0	0.6453
3.75	0.41326	0	0.6777
4.00	0.39818	0	0.7096
4.25	0.38479	0	0.7409
4.50	0.37281	0	0.7716
4.75	0.36202	0	0.8017
5.00	0.35226	0	0.8310
7.5	0.28895	0.0122	1.071
10.0	0.25579	0.0368	1.275
12.5	0.23495	0.0639	1.443
15.0	0.22039	0.0929	1.573
17.5	0.20948	0.1241	1.668
20.0	0.20089	0.1576	1.728
22.5	0.19387	0.1919	1.772
25.0	0.18798	0.2268	1.804
27.5	0.18293	0.2620	1.818
30.0	0.17852	0.2975	1.824
32.5	0.17462	0.3330	1.819
35.0	0.17113	0.3685	1.807
37.5	0.16801	0.4030	1.7910
40.0	0.16521	0.4370	1.7722
42.5	0.16264	0.4702	1.7529
45.0	0.16026	0.5015	1.7335
47.5	0.15803	0.5315	1.7144
50.0	0.15592	0.5608	1.6948

Table 7.19 (Continued)

p_s/p_0	V_s/V_0	α	β
75	0.13900	0.814	1.448
100	0.12699	1.055	1.102
125	0.11819	1.348	0.638
150	0.11160	1.712	+0.035
175	0.10656	2.128	–0.930
200	0.10260	2.628	–2.280
225	0.09943	2.728	–2.655
250	0.09682	2.702	–2.521
275	0.09464	2.673	–2.402
300	0.09279	2.645	–2.299
325	0.09120	2.617	–2.212
350	0.08981	2.591	–2.137
375	0.08860	2.566	–2.075
400	0.08753	2.545	–2.029
425	0.08659	2.528	–1.995
450	0.08577	2.515	–1.973
475	0.08506	2.510	–1.972
500	0.08446	2.523	–2.008
525	0.08395	2.554	–2.075
550	0.08353	2.585	–2.142
575	0.08321	2.608	–2.191
600	0.08298	2.624	–2.224
625	0.08285	2.635	–2.243
650	0.08281	2.638	–2.252
675	0.08286	2.634	-2.251
700	0.08300	2.620	–2.238
725	0.08323	2.596	–2.216
750	0.08356	2.564	–2.188